UNIVERSITY OF SOUTHAMPTON

"Post-larval development in deep-sea echinoderms"

Paulo Yukio Gomes Sumida

Doctor of Philosophy

SCHOOL OF OCEAN AND EARTH SCIENCE

October 1998

DECLARATION

This thesis is a result of work done wholly whilst registered under postgraduate candidature at the University of Southampton. No part of this work has been submitted for another degree.

UNIVERSITY OF SOUTHAMPTON

ABSTRACT

FACULTY OF SCIENCE
SCHOOL OF OCEAN AND EARTH SCIENCE

Doctor of Philosophy

POST-LARVAL DEVELOPMENT IN DEEP-SEA ECHINODERMS

Paulo Yukio Gomes Sumida

The post-larval phase is an essential period in the life history of marine invertebrates; vulnerable to high mortality, it ultimately influences the distribution and abundance of adult populations. The post-metamorphic ontogenesis of thirty species of deep-sea echinoderms, belonging to three classes (Ophiuroidea, Asteroidea and Echinoidea), is described using scanning electron microscopy. The life history of *Ophiocten gracilis* is also examined as a case study for future research on post-larval organisms.

The analysis of development in ophiuroids reveals that species can be identified from a very early post-metamorphic stage, even in congeneric species, contrary to the findings of other authors. The ontogeny of homologous structures is similar within related groups, but may give rise to different adult structures in different taxa. The mouth papillae within the ophiurids are serially homologous, originating from the jaw, but the fourth mouth papilla may have a different origin. In the families Ophiactidae, Ophiacanthidae and Amphilepididae examined, the mouth papillae have different origins, as, for instance, the adoral shield spine or tentacle scale. Data on the post-larval development of *Ophiura affinis* suggest that this species is more closely related to the genus *Ophiocten* and a change in the generic status is proposed.

Ophiocten gracilis is a bathyal brittle star occurring on both sides of the North Atlantic and its life history is studied in the eastern side of the North Atlantic. In this area, *O. gracilis* spawns in February/March of each year producing a large number of eggs. Fecundity is estimated to be around 40,000 eggs ind^{-1}, with the population of the Hebridean Slope being able to produce probably up to 16 million eggs m^{-2}. Post-larvae start settling in May and numbers settling reached over 3,200 post-larvae m^{-2}. The settling speed of post-larvae in the water column is estimated to be around 500 m day^{-1}, settling faster in warmer than colder water. Settling speeds appear to be similar for post-larvae ranging from 0.6 to 0.9 mm in disk diameter. Size at settlement is around 0.6 mm in disk diameter and 5-6 arm segments. The settlement of post-larval *O. gracilis* on the bottom of the Hebridean Slope also represented a considerable fraction of the particulate organic carbon (POC) flux in the area, reaching over 7% of the total daily flux. This is likely to have a considerable impact in the benthic community as competition and predation and as an additional food source for demersal and benthic organisms. The occurrence of post-larvae of *O. gracilis* in sediment traps also represented a large problem for POC flux measurements, with ophiuroids consuming part of the flux. In future works with sediment traps, such errors must be taken into account and ophiuroids must be included in the total POC flux.

The deep-sea juvenile asteroids of the NE Atlantic could be distinguished to species level from a very early stage of development. The ontogenesis of *Porcellanaster ceruleus* shows that this species is likely to undergo a shift in habitat and diet during the juvenile phase. This is evidenced by the appearance of the epiproctal cone, the changing of the furrow and apical spines, the early development of the cribriform organ adjacent to the madreporite and the appearance of sediment in the stomach. *P. ceruleus* is probably a predator on meiofauna and small macrofaunal organisms during the early stages of life, changing to a burrowed life style ingesting sediment particles. Most juvenile sea stars analysed during the present study showed wider bathymetric distribution than their adult counterparts, suggesting that events occurring during the early stages of life are important for the maintenance of the local population structure and diversity in the deep NE Atlantic.

The post-metamorphic development of three deep-sea spatangoid echinoids is very similar, but the morphology and formation of fascioles facilitate the distinction of the species examined. Whereas in *Hemiaster expergitus and Spatangus raschi* the fascioles present in the post-larvae develop to form the adult fascioles, in *Brissopsis lyrifera* post-larvae there is a juvenile fasciole, which disappears during ontogenesis giving way to the adult fascioles. The function of the juvenile fasciole is unknown in *B. lyrifera*. The development of the periproct in all spatangoids examined is similar to that described by other authors, with the periproct being initially endocyclic and migrating towards the rear of the animal as development progresses. Post-larvae of the genus *Echinus* could not be separated into different species, which may be linked to the recent diversification of the genus in the North Atlantic.

The widespread settlement of echinoderm post-larvae reported in the present thesis and in other works is thought to have been very important for the colonization of the deep-sea through the supply of stages to deeper areas and selection of pressure adapted animals and subsequent speciation.

CONTENTS

CHAPTER ONE - GENERAL INTRODUCTION AND AIMS

CHAPTER TWO - MATERIAL AND METHODS

CHAPTER THREE - POST-LARVAL DEVELOPMENT IN SHALLOW AND DEEP-SEA OPHIUROIDS (ECHINODERMATA: OPHIUROIDEA) OF THE NE ATLANTIC OCEAN

CHAPTER FOUR - EARLY JUVENILE DEVELOPMENT OF DEEP-SEA ASTEROIDS OF THE NE ATLANTIC OCEAN, WITH NOTES ON THE JUVENILE BATHYMETRIC DISTRIBUTION

CHAPTER FIVE - POST-LARVAL DEVELOPMENT OF SOME DEEP-SEA ECHINOIDS OF THE NE ATLANTIC OCEAN

CHAPTER SIX - REPRODUCTION, DISPERSAL, SETTLEMENT AND CARBON DEMANDS OF THE BATHYAL OPHIUROID *OPHIOCTEN GRACILIS* IN THE NE ATLANTIC

CHAPTER SEVEN - GENERAL DISCUSSION

REFERENCES

Acknowledgements

This work would not have been possible without the help of a number of people, to whom I am deeply grateful. I would like to thank Prof. Paul A. Tyler for his constant supervision, friendship and enthusiasm, which have always taught us never to lose that thrill for science. Financial support was provided by the "Coordenadoria de Aperfeiçoamento de Pessoal de Nível Superior" (CAPES – Ministry of Education, Brazil) through grant No 0900/94-1 to whom I am indebted.

A large amount of additional supervision and support were provided by Prof. John Gage (SAMS), Dr Richard Lampitt (SOC), Dr David Billett (SOC), Dr Gordon Paterson (BMNH), Dr Gordon Hendler (LA County Museum), Miss Ailsa Clark and Dr Thomas Brey (AWI). It has been a pleasure and an honour to work with you all!

My thanks to Dr Arne Nørrevang (Kaldbak Marine Biological Laboratory, Faroe Islands), Prof. John Gage, Dr David Billett, Dr Richard Lampitt, Mr Michael Thurston (SOC) and Dr Els Flach (NIOO/CEMO) and their respective Institutions for providing the benthic samples examined during the present study.

Thanks also to Mr Robin Harvey (SAMS) for help with samples; Dr Barbara Cressey (SOC) for the use of the electron microscope facilities at SOC; and the library staff for their patience and support. Assistance with art work was provided by Mrs Kate Davis (SOC). Dr Craig Young made possible the dream of knowing the deep-sea *in situ*, which I will treasure forever in my memory.

Many thanks to all my friends in Southampton for making so pleasant my stay in England and in special my Brazilian mates Alexandre, Ronald and Antônio. Our research group, including Jon, Cathy, Eva R., Eva G., Maria, Lus and Dawn has been fantastic throughout. You are a great team!!! Finally, all my love to my wife Andréia and my family in Brazil, for their unconditional support and love throughout my time in England.

To my wife Andréia and to my parents,

Issamu and Rosa... always

Para se ter o direito de possuir para sempre, é preciso querer pacientemente e por muito tempo

E.L.

Chapter One - General introduction and aims

1.1. The deep-sea

The image of the deep-sea as a huge and inaccessible environment is present ever since scientists set out to explore that area, and probably much earlier. It is interesting to note that, even though the deep-sea is today still a mysterious and relatively poorly known environment, its exploration began even before the events that marked the beginning of the science of Oceanography itself. If the circumnavigation of the British ship *H.M.S. Challenger* (1872-76) marks the dawn of Oceanography, some years before the cruises of the also British ships *Lightning* (1868) and *Porcupine* (1869-70) (section 1.2.1) proved beyond doubt that organisms thrived in the deep-sea. This was probably the first great event in the history of the biological exploration of the deep-sea.

Other important events mark the 130 years of this exploration. After a first half of the 20th century marked by the great expeditions, which collected abundant material for a large inventory of the fauna, the early 1960's brought the invention of the submersible technology, allowing *in situ* exploration of the deep-sea bed, as well as the possibility of experimentation (Sibuet *et al.*, 1990). The invention of improved sampling gear and the use of fine meshes revealed a extremely high diversity environment, composed by a large number of small-sized specimens (Sanders *et al.*, 1965).

The 1970's were marked by the discovery of the hydrothermal vents in the volcanic active locations of the Meso-oceanic Ridges (Ballard, 1977), with an astonishing fauna and autochtonous source of organic matter driven by geochemical energy (Jannasch & Wirsen, 1979). Later, similar environments were discovered on continental slope areas and called cold seeps, with production being fuelled by hydrocarbon/methane/sulphide seeping from the sediments (Kennicutt *et al.*, 1985).
In the beginning of the 1980's, seasonal pulses of phytodetritus originating from the euphotic layers were detected in deep-sea areas of the North Atlantic (Deuser & Ross, 1980; Deuser *et al.*, 1981; Billett *et al.*, 1983; Deuser, 1986). Such pulses of food are thought to drive seasonal processes in deep-sea animals (Rokop, 1974, 1977; Tyler, 1988; Tyler *et al.*, 1992). Before these events, the deep-sea was

considered a tranquil environment, with constant physical variables and a continuous, low supply of food.

Nowadays, the deep-sea is considered diverse and dynamic, with a multitude of different environments and difficult to be considered a single unit. Slope areas with a highly dynamic and, sometimes, unstable sediments (Jenkins & Keene, 1992); abyssal areas affected by seasonal pulses of food (Rice *et al.*, 1986) and those food-poor under the large oceanic gyres (Rowe, 1983*b*); hydrothermal vents and cold seeps, with a high productivity and biomass; and the relatively unknown oceanic trenches form this vast domain, characterized by the crushing pressures and complete absence of solar light.

1.1.1. The Physical Environment

As already discussed, the deep-sea environment is far from being constant, despite the view of a 'stable' environment, where the physical and biological processes are slow and unchanged over large time-scales. This is probably true for some of the physical variables, *e.g.* temperature and salinity, but not for other events (see Tyler, 1995).

A series of unpredictable events occur in certain areas of the ocean bed, causing effects in the sediment community. Benthic storms associated with the global pattern in eddy kinetic energy are highly erosive events occurring at the bottom during few days to weeks (Richardson *et al.*, 1993; Kontar & Sokov, 1994) and can be important as a disturbing factor in the local benthos (Aller, 1989, 1997). Areas such as the HEBBLE Site (High Energy Benthic Boundary Layer Experiment) on Nova Scotia Rise (NW Atlantic Ocean) are highly energetic, opposing sluggish currents found elsewhere in the deep-sea (Weatherly & Kelley, 1985; Gross *et al.*, 1988). Other unpredictable events include sediment slides and slumps occurring on the continental slopes and hadal trenches, sometimes moving enormous quantities of sediment downslope either to the continental rise and abyssal plain or to the deepest parts of trenches. Turbidity currents may also occur on slopes and submarine canyons carrying a mixture of sediments and water downslope (Gage & Tyler, 1991).

Although such events occur at variable time-scales and are unpredictable over time, some episodes can be highly predictable and recurrent. 'Seasonal' and annual

periodicity events, such as the pulses of organic matter arriving at the bottom may be detected at some areas (section 1.1).

1.1.1.1. Hydrothermal Vents and Deep-Sea Cold Methane/Sulphide Seeps

Hydrothermal vent systems are unique environments associated commonly with tectonic plate boundaries in spreading centres, subduction zones, fracture zones and back-arc basins (German *et al.*, 1995). The temperature at these environments can be as hot as 380°C close to black smokers or cooler as warm fluids (5-250°C) from diffuse emissions from crevices in the basaltic rocks (Gage & Tyler, 1991). Despite such high temperatures existing at vent sites, the overlying seawater temperature remains close to that of the surrounding deep-ocean (~ 2°C).

At those sites, water percolates in the system where it acquires a variety of different minerals, as metals and others, which together with hydrogen sulphide and methane are expelled in the surrounding water column as a hydrothermal plume. Some minerals are deposited near the chimneys as metalliferous sediments and Fe-Mn crusts and the hydrogen sulphide and methane (highly toxic for life in general) are used as a substrate (energy source) for chemosynthetic bacteria, which form the basis of the hydrothermal vent trophic web (Tunnicliffe, 1991; Van Dover & Fry, 1994; Van Dover, 1995).

In deep-sea cold methane/sulphide seeps, physical conditions are more like non-vent deep-sea areas, with the exception of the methane and sulphide that seeps from inside the Earth's crust, serving as energy source to chemosynthetic bacteria, supporting a fauna similar to that found in hydrothermal vent systems (Hecker, 1985; Gage & Tyler, 1991).

1.2. The North-east Atlantic

1.2.1. Historic background

The deep NE Atlantic Ocean is probably one of the best sampled deep-sea areas of the world's oceans. The first biological survey in the area was made by the British ship *H.M.S. Lightning*, which covered the region of the Hebridean Slope, Faroe Bank, Faroe-Shetland Channel and the north of Feni Ridge. The *Lightning* sailed on the summer of 1868, sampling 17 stations at depths down to 1200 m (Fig. 1.1;

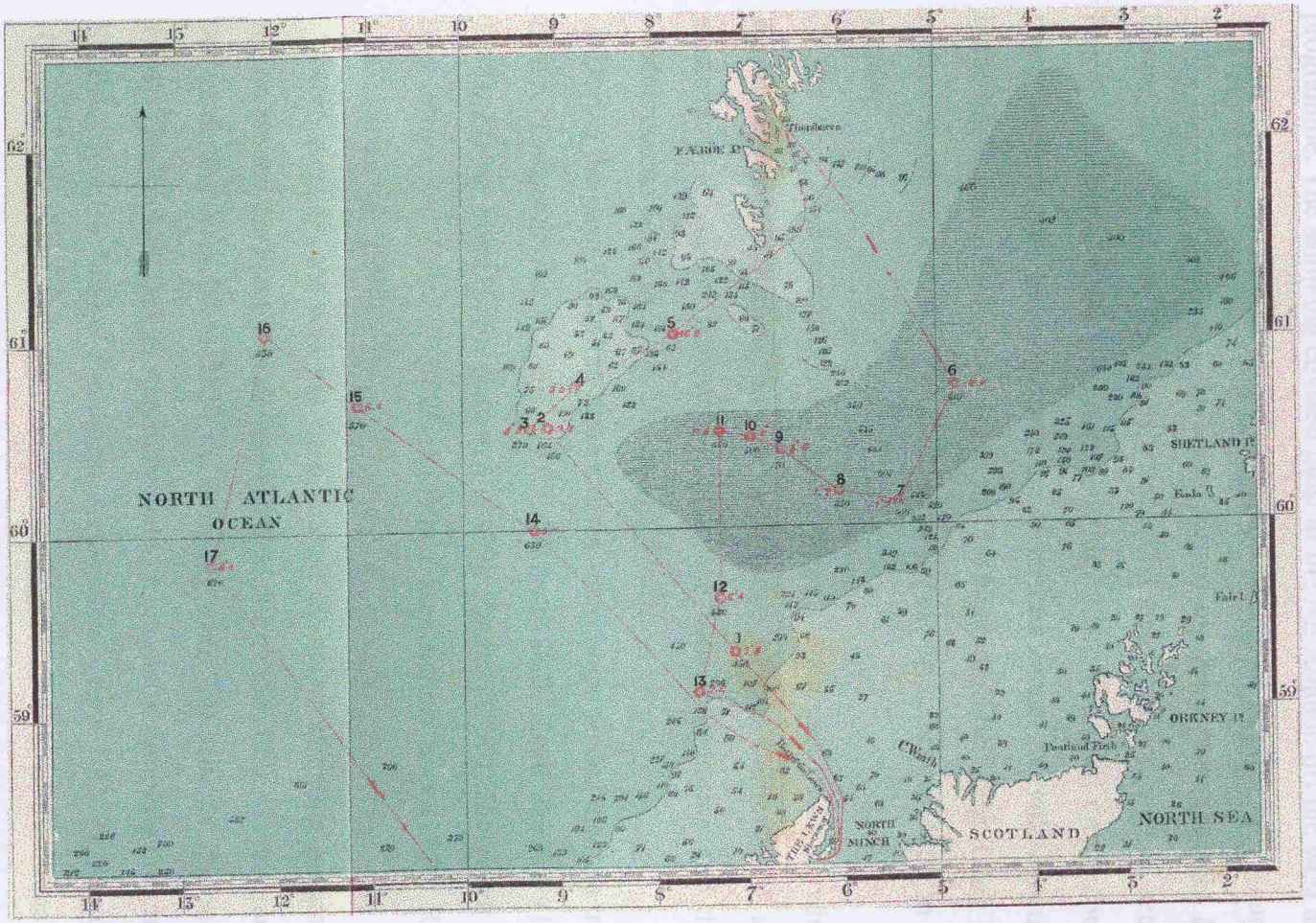

Figure 1.1. Map showing the station locations of the cruise of the *HMS Lightning* during the summer of 1868 in the NE Atlantic (From Thomson, 1874*a*).

Thomson, 1874*a*). In the following summer, the British *H.M. Surveying-vessel Porcupine* was used for three cruises in a much more comprehensive sampling programme. The sampling covered most of the NE Atlantic off the west and north of the British Isles. The first cruise surveyed the area of the Rockall Trough, Rockall Bank, Porcupine Bank and the north part of the Porcupine Seabight (Fig. 1.2*a*). During the second cruise, the Celtic Shelf, Goban Spur and a small section of the Porcupine Abyssal Plain were sampled (Fig. 1.2*b*). The third cruise comprised the more northern part, encompassing the Hebridean Slope, Wyville-Thomson Ridge, Faroe Shelf, Faroe-Shetland Channel and the Shetlands Shelf (Fig. 1.2*c*). Those three cruises surveyed a total of 90 stations at depths up to almost 4500 m (Thomson, 1874*a*).

The *Porcupine* would be used again during the summer of 1870, when a fourth cruise sampled 9 stations on the south edge of the Celtic Shelf and headed southwards to explore the west coast of the Iberian Peninsula and the southern Mediterranean Sea (Fig. 1.2*d*; Thomson, 1874*a*).

During the years following these cruises, many ships visited the area including the *H.M.S. Knight-Errant* (1880), *H.M.S. Triton* (1882), *Lord Bardon* (1885, 1886, 1888), *Flying Fox* (1889), *Research* (1889), *Fingal* (1890), *Harlequin* (1891), the Irish *Helga* and *Helga II* (1901-1914) and the *Michael Sars* (1910) (Gage *et al.*, 1983; Rice *et al.*, 1991).

More recently, the area has been studied by major sampling programmes. The region around the Faroe Islands was sampled during the BIOFAR programme (1987-90) at depths from 20 to 2420 m, sampling over 750 stations (Nørrevang *et al.*, 1994). The Rockall Trough was subjected to a long-term sampling programme by the SMBA (Scottish Marine Biological Association - now SAMS), starting in 1973 (Gage *et al.*, 1980) and also explored during the cruises of the French ship *Jean Charcot* in 1969 (Cherbonnier & Sibuet, 1973) and 1976 (INCAL expedition; Gage, 1986). More to the south, the areas comprising the Porcupine Seabight and Porcupine Abyssal Plain were studied by the IOS (Institute of Oceanographic Sciences - now at the SOC) sampling programme (1977-86), also including some areas of the Porcupine Bank and Goban Spur (Rice *et al.*, 1991). The Bay of Biscay was surveyed by the French programme BIOGAS (**BIO**logie **GAS**cogne - 1972-74/1978-81)

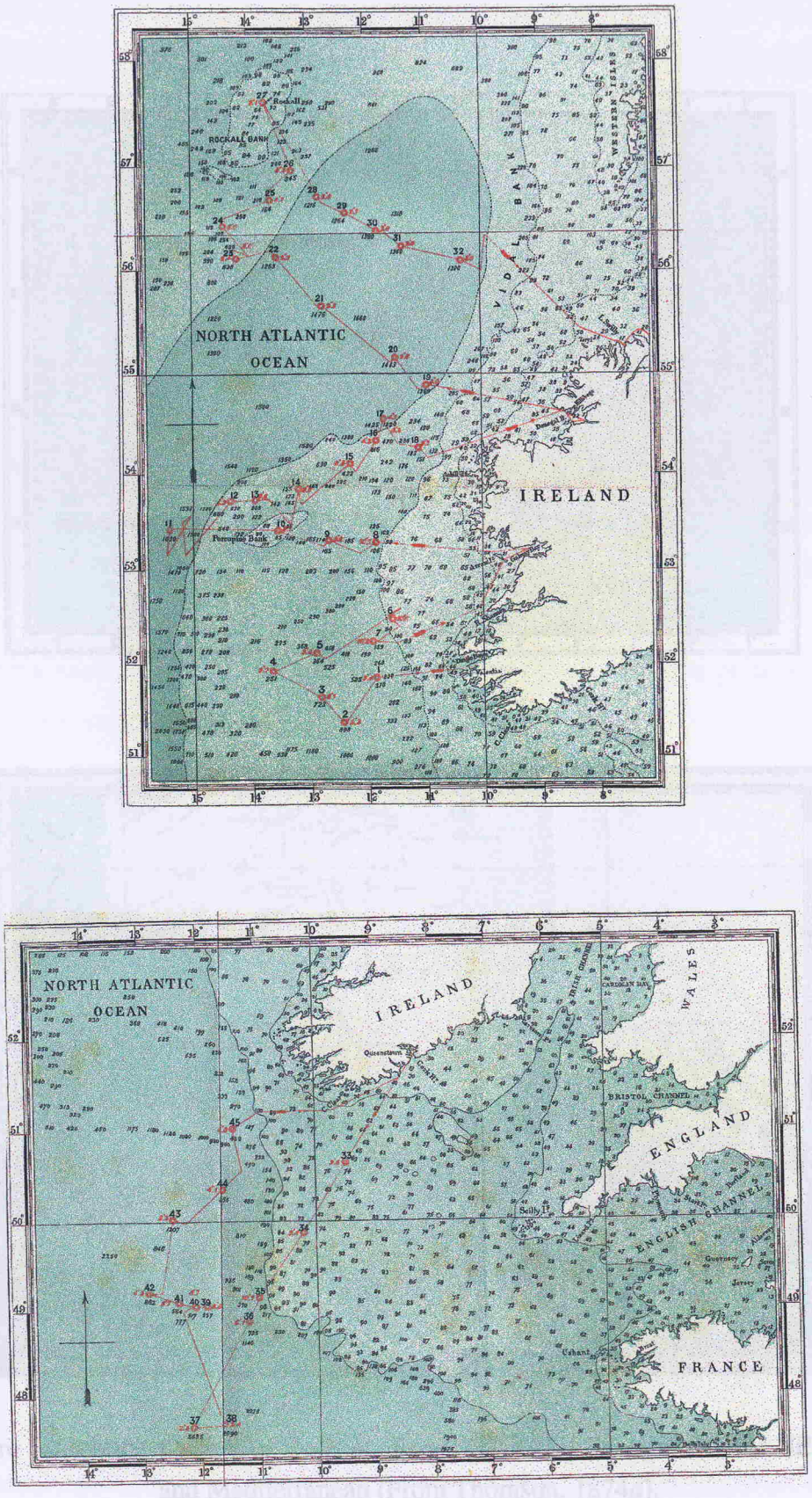

Figure 1.2. Map showing the station locations of the four cruises (A-D) of the *H.M. Surveying-vessel Porcupine* during the summers of 1869-70 in the NE Atlantic and Mediterranean (From Thomson, 1874*a*).

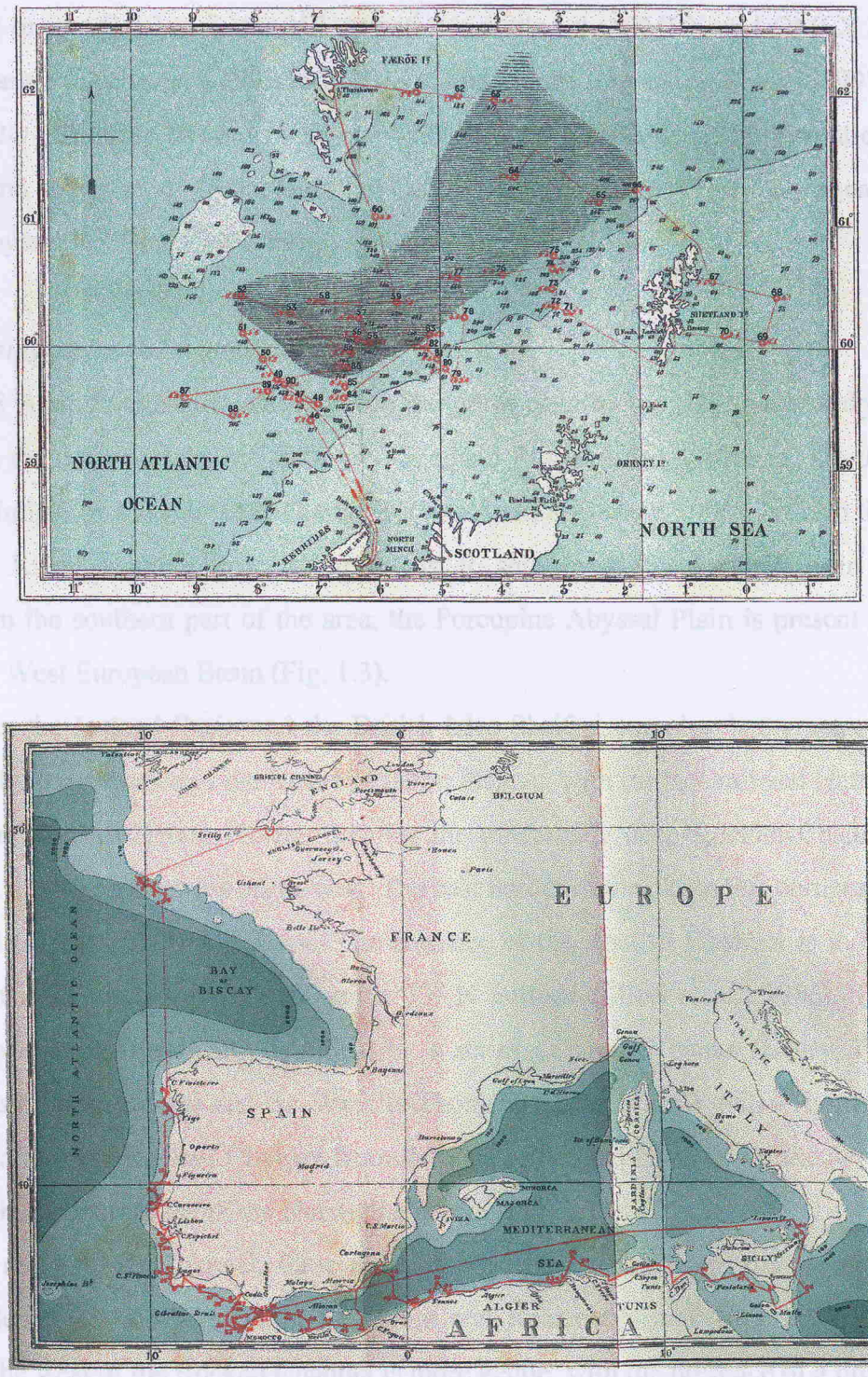

Figure 1.2 (cont.). Cruises of the *H.M. Surveying-vessel Porcupine* in the NE Atlantic and Mediterranean (From Thomson, 1874*a*).

(Laubier & Monniot, 1985). Several short term sampling programmes are still being carried out or just finished in the NE Atlantic, including the OMEX and OMEX II (**O**cean **M**argin **EX**change - 1993-99), LOIS (**L**and **O**cean **I**nteraction **S**tudy - 1991-96), BENBO (**BEN**thic **BO**undary layer - 1997-99) and BENGAL (High resolution temporal and spatial study of the **BEN**thic biology and **G**eochemistry of a north-east **A**tlantic abyssal **L**ocality - 1996-99).

1.2.2. Physiography and sediments

The NE Atlantic Ocean is delimited on the north-west by the Reykjanes Ridge, Iceland on the north and the Iceland-Faroe-Scotland Ridge on the north-east. On the east, it is limited by the European Continent (Van Aken & Becker, 1996). Next to the Reykjanes Ridge, running from the north-east to south-west, the Iceland Basin is present. On the southern part of the area, the Porcupine Abyssal Plain is present as part of the West European Basin (Fig. 1.3).

Between the Iceland Basin and the British Isles Shelf, a complex bathymetry is generated by the presence of the Rockall-Hatton Plateau, with the Rockall and Hatton Banks. The Rockall-Hatton Plateau delimits the moderately deep Rockall Channel (Rockall Trough) on the west-north-west. The east border of the channel is composed by the British Isles Shelf and Slope. The entrance of the Rockall Channel is in the south-west at depths of about 3500 m in 53° N latitude (Ellett *et al.*, 1986). The northern part is shallower and delimited by a series of smaller banks (Lousy, Bill Bailey's and Faroe Banks) and the Wyville-Thomson Ridge. The Wyville-Thomson Ridge separates the Rockall Channel from the Faroe-Shetland Channel on the north-east, which is connected with the Norwegian Basin (Fig. 1.3).

Inside the Rockall Channel, three major topographic features are the Hebrides Terrace Seamount, Anthon Dohrn Seamount and Rosemary Bank (Fig. 1.3). The slope on the west of the Rockall Channel is more gentle, with the presence of a broad sediment drift called Feni Ridge (Roberts, 1975). On the east border, the slope is relatively narrower and steeper, following the relatively broad continental shelf of the British Isles (Roberts, 1975, 1979). Close to the Hebrides Terrace Seamount, however, the slope is gentler owing to the presence of the Barra and Donegal deep-sea fans to the north and south of the Hebrides Terrace Seamount, respectively. The

upper slope on both sides of the Rockall Channel is composed by terrigenous sediments (Faugeres *et al.*, 1981) and recent evidence suggests that a large number of rock outcrops are present, mainly in the southern part of the channel (Tyler & Zibrowius, 1992; Neil Kenyon, personal communication). Gage (1986) points out that sediments collected with box core and anchor dredge in a transect in the Rockall Trough from 200-700 m depth showed muddy sand with pebbles, cobbles and some boulders. Below 700 m the sediment is made up of an increased proportion of calcareous particles of pelagic origin (Gage, 1986).

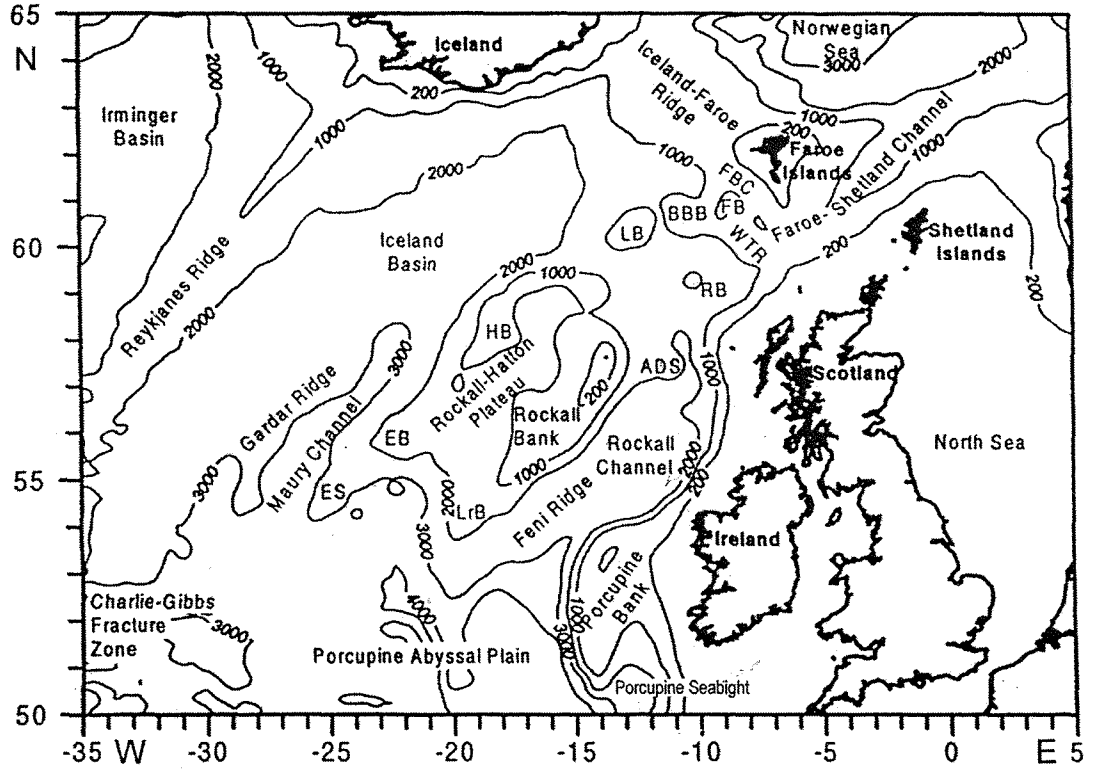

Figure 1.3. Map of the NE Atlantic showing the main topographic features. ADS=Anton Dohrn Seamount; BBB=Bill Bailey's Bank; EB=Edoras Bank; ES=Eriador Seamount; FB=Faroe Bank; FBC=Faroe Bank Channel; HB=Hatton Bank; LB=Lousy Bank; LrB=Lorien Bank; RB=Rosemary Bank; WTR=Wyville-Thomson Ridge (Modified from Van Aken & Becker, 1996)

Towards the south-west of the British Isles Shelf, the Porcupine Bank is present and a large embayment in the slope adjacent to it, the Porcupine Seabight, which leads, on the south-west, to the Porcupine Abyssal Plain (Fig. 1.3). The Porcupine Seabight is characterized by the presence of coarse carbonate sediments and rock outcrops (Faugeres *et al.*, 1981). The slopes on the west of the Porcupine Bank and Porcupine Seabight are characterized by the few number of canyons, which reflect the limited sediment supply available (Roberts, 1975; Rice *et al.*, 1991). The opposite is true for the eastern slope of the Porcupine Seabight and the southern part of the Celtic Shelf slope, where there are numerous canyons and channel systems (Rice *et al.*, 1991). The sediments of the centre of the Seabight are a coccolith-foraminiferan marl (Lampitt *et al.*, 1986). Rock and mineral debris, including clinker and drop stones, are also present (Kidd & Huggett, 1981), serving as substrata for sessile organisms (Rice *et al.*, 1991).

1.2.3. Water masses and circulation

The subsurface layers of the NE Atlantic are formed by the Subpolar Mode Water (SPMW - see McCartney & Talley, 1982), which may also bear different names in the literature (Subarctic Intermediate Water - SAIW, Bubnov, 1968; Eastern North Atlantic Water - ENAW, Harvey, 1982; North Atlantic Water - NAW, Dooley & Meincke, 1981; Modified North Atlantic Water - MNAW, Hansen, 1985; Rockall Channel Mode Water - RCMW, Arhan *et al.*, 1994) (Van Aken & Becker, 1996). This variety of names is related to the number of modifications that the SPMW is subjected, mainly owing to its transport and seasonal variation, with temperatures varying from 8-12°C. Van Aken & Becker (1996) state that the SPMW forms the bulk of 'warm' Atlantic water entering the Norwegian Sea between Iceland and Scotland. The SPMW is formed by cooling and freshening of water from the North Atlantic Current (NAC) in winter as a result of a deep convection driven by the heat loss at the sea surface (Van Aken & Becker, 1996).

Below the SPMW, a layer of salinity minimum water is present at around 1600-1900 m depth, comprising the Labrador Sea Water (LSW - see Talley & McCartney, 1982). In the Rockall Channel and in the Porcupine area close to the British Isles, there is a layer of salinity maximum and low oxygen formed by the Mediterranean

Water (MW; also Gibraltar Water - GW, Ellett & Martin, 1973; Ellett *et al.*, 1986; Lonsdale & Hollister, 1979) between 800-1200 m depth.

The deep layer north of the Rockall Channel and Iceland Basin is formed by waters resulting from the overflow of Norwegian Sea Deep Water (NSDW) through the Iceland-Faroe Ridge into the Iceland Basin and through the Wyville-Thomson Ridge into the Rockall Channel and Faroe Bank Channel (Lee & Ellett, 1965; Ellett & Roberts, 1973; Mauritzen, 1996). The NSDW interacts with the SPMW during the overflow forming the Iceland-Scotland Overflow Water (ISOW; also called North-east Atlantic Deep Water - NEAD, Ellett & Roberts, 1973). The ISOW is a saline water mass, with temperatures around 2.5°C. The ISOW is gradually mixed with less dense waters along its journey south on the west side of the Rockall-Hatton Plateau, forming a modified water mass called North-east Atlantic Deep Water (NEADW).

The NEADW is found in a salinity maximum at around 2600 m depth (Van Aken & Becker, 1996). In the south of the Iceland Basin, Porcupine Abyssal Plain and Southern Rockall Channel the NEADW is found between the LSW above and another water mass, the Lower Deep Water (LDW), below. The LDW (<2.5°C) occurs at depths below 3000 m in the Porcupine Abyssal Plain and at around 2500 m in the southern part of the Rockall Channel (Van Aken & Becker, 1996).

The surface circulation pattern in the NE Atlantic shows an overall trend towards the transport of Subpolar Mode Water north-eastwards into the Norwegian Sea (Fig. 1.4*a*). The SPMW is transported by the NAC from the south, passing on the west of the Rockall-Hatton Plateau and on the east into the Rockall Channel, entering the Norwegian Sea over the Iceland-Faroe and Wyville-Thomson Ridges (Van Aken & Becker, 1996). More to the west, over the Iceland Basin, part of the SPMW is diverted into the western North Atlantic over the Reykjanes Ridge (Fig. 1.4*a*).

The deep circulation is more complicated, with the overflow of NSDW (in the form of ISOW) through the Iceland-Faroe Ridge flowing south-westwards on the west-north-west part of the Iceland Basin, next to the Reykjanes Ridge (Fig. 1.4*b*). The overflow through the Wyville-Thomson Ridge flows into the Rockall Channel, with part of it being diverted into the Faroe Bank Channel, subsequently meeting the ISOW flowing through the Iceland Basin.

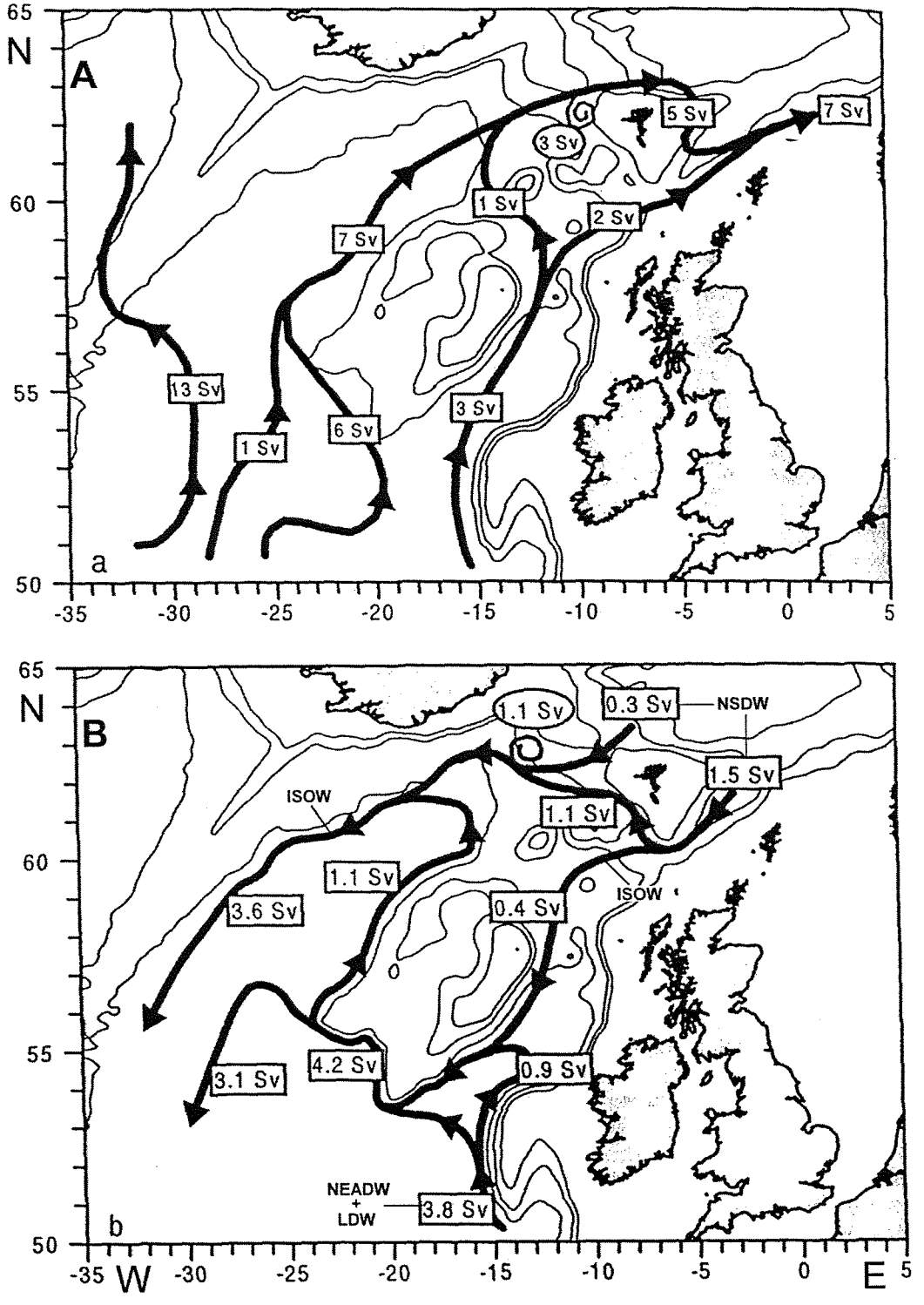

Figure 1.4. Map showing the circulation in the NE Atlantic and the estimated geostrophic transport (1 Sv=10^6 m^3 s^{-1}). A. surface circulation; B. bottom circulation. Abbreviations of water current names are according to the text (Modified from Van Aken & Becker, 1996).

In the south, next to the Porcupine Bank, the LDW and NEADW flow northwards, dividing into two branches. One follows the contours of the Porcupine Bank until the contours change to an east-west direction. At this point, the LDW and NEADW divert to the north-west and then to the south-west, recirculating along the South Feni Ridge, where they meet the waters flowing from the north of the Rockall Channel (Fig. 1.4*b*). The second branch of LDW and NEADW diverts earlier in the Porcupine Bank to the west, meeting the first branch just south of the Lorien Bank. Then, the waters follow the contours of the south-western part of the Rockall-Hatton Plateau until the Edoras Bank, where they divide again. One branch flows to the south, where it either recirculates again in the eastern North Atlantic or leaves the area through the Charles-Gibbs Fracture Zone, flowing into the western North Atlantic. The other branch flows north-eastwards along the west part of the Rockall-Hatton Plateau and at around 60°N it recirculates, joining the ISOW flowing south-westwards. This branch may also recirculate or leave the eastern North Atlantic through the Charles-Gibbs Fracture Zone (Fig. 1.4*b*; Van Aken & Becker, 1996).

1.2.4. Primary productivity and input of organic matter to the sediments

The NE Atlantic region is subject to the seasonal bloom of phytoplankton during the spring and summer (Lochte *et al.*, 1993). This bloom drives an export of carbon, as well as other biogenic and detrital material, from the surface ocean to deeper layers (Newton *et al.*, 1994). However, the arrival of this material on the bottom was only detected relatively recently (Billett *et al.*, 1983; Rice *et al.*, 1986). The amount of the primary production that arrives on the bottom is generally around 2-4% of the surface productivity (Turley *et al.*, 1995) and may vary spatially and temporally (Lampitt, 1985; Newton *et al.*, 1994; Rice *et al.*, 1994). The majority of the flux is in the form of fast sinking (~60-500 m day^{-1} - Turley *et al.*, 1995) aggregated particles commonly called 'marine snow' (Aldredge & Silver, 1988; Lampitt *et al.*, 1993*a*, *b*). Evidence also suggests that once on the bottom, this material may be resuspended back to the water column (Lampitt, 1985). The phytodetritus arriving on the seabed may serve as a food source for marine invertebrates living in the deep NE Atlantic (Thiel *et al.*, 1988; Campos-Creasey, 1994).

1.2.5. Benthic community composition

The benthic fauna of the deep NE Atlantic is composed by a large number of species, of which the echinoderms are some of the most conspicuous (Gage *et al.*, 1983, 1985). The zonation of the fauna in the Rockall Trough is described by Gage (1986) and seems to be similar to that found in the Bay of Biscay and Porcupine Seabight (LeDanois, 1948; Sibuet, 1977). The fauna on the west side of the Rockall Trough is richer in number of species than that of the east side (Gage *et al.*, 1983), with a large number of suspension feeders.

On the east side, the upper slope down to 700 m depth is characterized by coral banks of *Lophelia pertusa* and *Madrepora oculata*, and the echinoderms *Cidaris cidaris*, *Spatangus raschi*, *Stichopus tremulus* and *Luidia sarsi*. Other echinoderms with wider bathymetric distributions also occur at these sites, such as *Gorgonocephalus caputmedusae*, *Pseudarchaster parelli* and *Ophiacantha abyssicola* (Gage, 1986).

From 700 to 1300 m depth, on the Hebrides-Donegal slope, a richer megafauna is found composed mainly by the sea urchin *Echinus acutus* var. *norvegicus* and the crustaceans *Nematocarcinus ensifer*, *Pontophilus norvegicus*, *Geryon tridens* and *Nephropsis atlantica*. The echinoderms *Ophiocten gracilis*, *Calveriosoma hystrix*, *Bathyplotes natans*, *Laetmogone violacea*, *Benthogone rosea*, *Psilaster andromeda* and *Plutonaster bifrons* are also present. A number of ahermatypic corals and the pycnogonid *Collosendeis clavata* also inhabit this area, as well as deeper ones (Gage, 1986).

A large number of echinoderms inhabit the zone between 1400 and 2000 m depth, including *Echinus alexandri*, *E. affinis*, *Persephonaster patagiatus*, *Plinthaster dentatus*, *Bathybiaster vexillifer*, *Zoroaster fulgens*, *Ophiacantha bidentata*, *Ophiomusium lymani*, *Ophiura ljungmani* and *Phormosoma placenta*. *Munidopsis curvirostra*, *Polycheles sculptus*, *Neolithodes grimaldi*, *Colus jeffreysianus* and *Troschelia bernicensis* are among the other species that live at those depths (Gage, 1986).

In the upper abyssal, *Hymenaster pellucidus*, *Dytaster insignis*, *Porcellanaster ceruleus*, *Echinosigra phiale*, *Ypsilothuria bitentaculata*, *Peniagone azorica*,

Hygrosoma petersii, *Benthothuria funebris* and *Oneirophanta mutabilis* figure among the echinoderms present (Gage, 1986).

In the slope areas rich in rock outcrops to the western part of the Porcupine Bank, Tyler & Zibrowius (1992) describe a rich suspension feeding fauna, mainly composed by sponges, cnidarians, stalked and comatulid crinoids, and brisingid asteroids, among others (see also Tyler & Lampitt, 1988).

The factors affecting the benthic distribution in the NE Atlantic are probably related to the hydrography and dynamics of water masses in the area. The depth of winter mixing is around 600 m (Ellett & Martin, 1973) and may influence the presence of the 'mud line' (Gage & Tyler, 1991), where Gage (1986) reported a maximum in rate of faunal change at around 1000 m depth (Gage *et al.*, 1984).

In terms of biomass and abundance, the general pattern appears to be a decrease of both parameters with increasing depth, for both the megafauna (Laubier & Sibuet, 1979; Sibuet, 1984; Lampitt *et al.*, 1986) and macrofauna (Flach & Heip, 1996; Cosson *et al.*, 1997). Lampitt *et al.* (1986) found that the biomass of the megabenthos in the Porcupine Seabight is dominated by suspension feeders and crustaceans in the upper slope, whereas in the middle and lower slope the biomass is dominated by echinoderms. Recent observations on the Porcupine Abyssal Plain revealed a dramatic change in the relative abundance of megafaunal species, mainly in the elasipodid holothurian *Amperima rosea* (David Billett, personal communication).

The megabenthic biomass appears to be more sensitive to changes in food input than the macrofauna (Lampitt *et al.*, 1986; Flach & Heip, 1996). On the other hand, the seasonal input of organic matter appears to affect the density of the macrofauna (Flach & Heip, 1996). The meiofauna is also affected by food pulses, with individuals being larger in size during food-rich periods (Soltwedel *et al.*, 1996).

Diversity also appears to decrease with depth. Sibuet (1977) points out that asteroid diversity decreases with increasing depth in the Bay of Biscay. Paterson & Lambshead (1995) show that polychaetes have a parabolic distribution in species richness, with peak at 1800 m depth in the Rockall Trough. Data collected on the benthos of the NE Atlantic appear to be in concert with data found elsewhere (Rowe, 1983*a*).

1.3. Reproduction and development in deep-sea invertebrates

Throughout history the deep-sea has being marked by untested hypotheses, most of which were subsequently discarded. One of the most famous was the concept of an 'azoic zone' below 600 m depth (Forbes, 1844), which was formulated even though the first animal to be retrieved from the deep-sea, the ophiuroid *Gorgonocephalus caputmedusae* (as *Astrophyton linkii*), was collected much earlier in 1818 (Tyler, 1988). During the first half of the 20th century, another important untested hypothesis, stating that deep-sea organisms should not undergo pelagic development was being erected (see Young, 1994).

Two works were remarkably important in consolidating those ideas on the development of deep-sea organisms. The first was suggestion by Orton (1920) that animals living in a temperature-stable environment, as the deep-sea and polar regions, should breed continuously. The second was the comprehensive paper written by Thorson (1936), which supports that deep-sea and polar animals should develop directly, without a larval stage.

Despite the early evidence present in the literature (Prouho, 1888; Shearer *et al.*, 1914; Mortensen, 1921), only by the late 1960s and 1970s these ideas were found to flawed. Rokop (1977) reported that the deep-sea brachiopod *Frieleia halli* and the scaphopod *Cadulus californicus* reproduce seasonally and that the most obvious factor influencing breeding was probably periodicity in food supply (for *F. halli*). The same was earlier put forward by Schoener (1968), who found seasonality in two species of deep-sea ophiuroids and probably the presence of a free-living larval stage for those species. Those findings were important not only as an evidence for pelagic development, but that seasonality was also present in deep-sea organisms (see also George & Menzies, 1967, 1968; and Tyler, 1988 for a review). Later on, during the 1980s, seasonal cues and events were discovered for different deep-sea areas in the form of particulate organic material falling to the seabed (Deuser & Ross, 1980; Deuser *et al.*, 1981; Billett *et al.*, 1983; Deuser, 1986).

It seems that only a minority of the deep-sea species studied so far have a seasonal reproduction, with the presence of a planktotrophic larva. In the Rockall Trough region (NE Atlantic, ~ 2000 m depth), where much work have been done on the reproductive biology of echinoderms, Tyler *et al.* (1982*c*) show that the ophiuroids

Ophiura ljungmani and *Ophiocten gracilis*, the seastars *Plutonaster bifrons* and *Dytaster grandis* (formerly identified as *D. insignis* - Tyler *et al.*, 1990) and the sea urchin *Echinus affinis* produce seasonally a large number of small eggs, indicating probably the presence of planktotrophic larval development (see also Tyler & Gage, 1979; Gage & Tyler, 1981*a*; Tyler & Pain, 1982*a*; Tyler *et al.*, 1993). In addition to *Echinus affinis*, Tyler & Gage (1984*a*) note that the closer related species *E. alexandri* and *E.acutus* var. *norvegicus* also possessed a planktotrophic development based on the egg size, fecundity and the presence of larvae (Shearer *et al.*, 1914; Hagström & Lønning, 1961; Gage *et al.*, 1986). The same was found for the cidarid sea urchin *Cidaris cidaris* (Tyler & Gage, 1984*b*), which already had a known larva (Prouho, 1888, as *Dorocidaris papillata*). Young (1991) working in the Bahamian continental slope found that all the 21 different species of echinoids collected presented a long-lived planktonic larvae, with the majority being planktotrophic. Young *et al.* (1989) raised larvae of the bathyal urchin *Aspidodiadema jacobyi* and found that they were obligate planktotrophs, but with an extended pre-feeding lecithotrophic stage. Unfed larvae remained alive for 80 days at 12°C and their mouth did not open until 3 weeks after fertilization! Young & Cameron (1989) also report planktotrophic development for *Linopneustes longispinus*, a bathyal irregular sea urchin from the Bahamas.

Other deep-sea groups also show planktotrophic development. Muirhead *et al.* (1986) note that two species of *Epizoanthus* (*E. paguriphilus* and *E. abyssorum*) from the deep-sea have planktotrophic development mainly owing to the specialized commensal lifestyle, despite the latter possessing oocytes with only one quarter of the volume of that of *E. paguriphilus* (see also Tyler *et al.*, 1985*b*). Van Praët (1990) reports seasonality in the deep-sea anemone *Paracalliactis stephensoni* (see also Van Praët *et al.*, 1990 for *Phelliactis*). Bronsdon *et al.* (1993) also found reproductive seasonality in the deep-sea epizoic anemone *Amphianthus inornata*. Data on deep-sea pennatulids reveals that the development is likely to be lecithotrophic (Rice *et al.*, 1992; Tyler *et al.*, 1995*b*).

Data based on the embryonic and larval shells reveal that planktotrophy is present amongst deep-sea gastropods (Bouchet & Warén, 1979*a*). Rex & Warén (1982) found an increase in planktotrophic prosobranchs with increasing depth and

suggested this may be linked to the ability to track patch prey. In the Rockall Trough, Colman *et al.* (1986*a*) estimate that 43% of the 14 neogastropods examined showed shell morphologies indicative of planktotrophic development.

Evidence cited above showed that Thorson's Rule (named by Mileikovsky, 1971) was not true, since planktotrophy, although not dominant, is common amongst deep-sea species. Moreover, the statement that direct development would be the main type of development proved also not to be true, since direct development appears to be rare in the deep-sea and a lecithotrophic pelagic development is probably most common in that environment (Pearse, 1994).

Table 1.1 shows the probable mode of development for some of the deep-sea species and higher taxa. The mode of development is inferred from egg size and fecundity, shell morphology or cultured larvae (or information on more than one approach). Data on the development of some hydrothermal vent and cold seep invertebrates are also included.

Table 1.1. Modes of development in deep-sea species. Hydrothermal vents and cold seeps section modified from Cann *et al.* (1994) and Copley (1998).

Taxon	Egg Diameter	Development	Source
'Normal' Deep-Sea			
Cnidaria			
Epizoanthus paguriphilus	Up to 280 µm	Planktotrophic	Muirhead *et al.*, 1986
Epizoanthus abyssorum	Up to 180 µm	Planktotrophic	Muirhead *et al.*, 1986
Kophobelemnon stelliferum	Up to 800 µm	Lecithotrophic, 'continuous'	Rice *et al.*, 1992
Umbellula lindahli	Up to 800 µm	Lecithotrophic	Tyler *et al.*, 1995*b*
Paracalliactis stephensoni	Up to 180 µm	Seasonal	Van Praët, 1990
Phelliactis hertwigi	Up to 180 µm	Seasonal	Van Praët *et al.*, 1990
Phelliactis robusta	Up to 210 µm	Seasonal	Van Praët *et al.*, 1990
Amphianthus inornata	Up to 205 µm	Seasonal	Bronsdon *et al.*, 1993
Kadosactis commensalis	Up to 150 µm	'Continuous'	Bronsdon *et al.*, 1993
Mollusca			
Gastropoda			
Colus jeffreysianus	Up to 170 µm	Lecithotrophic, 'continuous'	Colman *et al.*, 1986*a,b*
Calliotropis ottoi	150-260 µm	Lecithotrophic, 'continuous'	Colman & Tyler, 1988
Benthonella tenella		Planktotrophic	Bouchet & Warén, 1979*a*
Benthomangelia macra		Planktotrophic	Bouchet & Warén, 1979*a*
Tacita danielsseni		Lecithotrophic, contained	Bouchet & Warén, 1979*b*
Tacita abyssorum		Lecithotrophic	Colman *et al.*, 1986*a*
Mohnia mohni		Lecithotrophic, contained	Bouchet & Warén, 1979*b*
Oenopota ovalis		Lecithotrophic, contained	Bouchet & Warén, 1979*b*; Colman *et al.*, 1986*a*
Oenopota graphica		Lecithotrophic	Colman *et al.*, 1986*a*
Anachis haliaeeti		Planktotrophic	Bouchet & Warén, 1979*a*; Colman *et al.*, 1986*a*
Trophon sp.		Lecithotrophic	Colman *et al.*, 1986*a*
Typhlomangelia sp.		Lecithotrophic	Colman *et al.*, 1986*a*

Gymnobela frielei		Planktotrophic	Colman *et al.*, 1986*a*
Gymnobela subaraneosa		Planktotrophic	Colman *et al.*, 1986*a*
Pleurotomella packardi		Planktotrophic	Bouchet & Warén, 1979*a*; Colman *et al.*, 1986*a*
Pleurotomella lottae		Planktotrophic	Bouchet & Warén, 1979*a*
Taranis moerchi		Lecithotrophic	Colman *et al.*, 1986*a*
Lusitanops sp.A		Planktotrophic	Colman *et al.*, 1986*a*
Turridae sp.A		Planktotrophic	Colman *et al.*, 1986*a*
Belomitra quadruplex		Lecithotrophic	Colman *et al.*, 1986*a*
Iphitella tuberata		Planktotrophic	Bouchet & Warén, 1979*a*
Epitonium formosissimum		Planktotrophic	Bouchet & Warén, 1979*a*
Bivalvia			
Malletia cuneata	Up to 240 μm	Lecithotrophic, 'continuous'	Tyler *et al.*, 1992
Ledella pustulosa	Up to 120 μm	Lecithotrophic, seasonal	Tyler *et al.*, 1992
Ledella messanensis	Up to 109 μm	Lecithotrophic, seasonal	Lightfoot *et al.*, 1979
Yoldiella jeffreysi	Up to 120 μm	Lecithotrophic, seasonal	Lightfoot *et al.*, 1979; Tyler *et al.*, 1992
Scaphopoda			
Cadulus californicus	Up to 240 μm	Lecithotrophic or direct, seasonal	Rokop, 1977
Echinodermata			
Ophiuroidea			
Ophiura ljungmani	Up to 110 μm	Planktotrophic, seasonal	Tyler & Gage, 1979, 1980; Gage & Tyler, 1981*b*
Ophiomusium lymani	Up to 450 μm	Lecithotrophic, 'continuous', but seasonality in recruitment	Gage & Tyler, 1982*c*
Ophiocten gracilis		Planktotrophic, seasonal	Gage & Tyler, 1981*a*; Tyler & Gage, 1982*b*
Ophiacantha bidentata	Up to 650 μm	Lecithotrophic, 'continuous'	Tyler & Gage, 1982*a*
Echinoidea			
Echinus affinis	Up to 110 μm	Planktotrophic, seasonal	Tyler & Gage, 1984*a*
Echinus alexandri	Up to 110 μm	Planktotrophic, seasonal	Tyler & Gage, 1984*a*
Echinus acutus var. *norvegicus*	Up to 110 μm	Planktotrophic, seasonal	Tyler & Gage, 1984*a*, Gage *et al.*, 1986
Echinus elegans	Up to 60 μm	Planktotrophic, seasonal	Gage *et al.*, 1986
Phormosoma placenta	1100-1500 μm	Lecithotrophic, 'continuous'	Tyler & Gage, 1984*b*
Calveriosoma hystrix	1100-1500 μm	Lecithotrophic, continuous	Tyler & Gage, 1984*b*
Araeosoma fenestratum	1100-1500 μm	Lecithotrophic, 'continuous'	Tyler & Gage, 1984*b*
Sperosoma grimaldii	1100-1500 μm	Lecithotrophic, 'continuous'	Tyler & Gage, 1984*b*
Hygrosoma petersii	1100-1500 μm	Lecithotrophic, 'continuous'	Tyler & Gage, 1984*b*
Poriocidaris purpurata	1100-1500 μm	Lecithotrophic, 'continuous'	Tyler & Gage, 1984*b*
Cidaris cidaris	Up to 110 μm	Planktotrophic, seasonal	Tyler & Gage, 1984*b*
Stylocidaris lineata		Planktotrophic, seasonal	Young *et al.*, 1992
Pourtalesia jeffreysi	Up to 225 μm	Lecithotrophic	Harvey & Gage, 1984
Pourtalesia miranda	173-357 μm	Lecithotrophic, 'continuous'	Harvey & Gage, 1984
Echinosigra phiale	250-335 μm	Lecithotrophic, 'continuous'	Harvey & Gage, 1984
Aspidodiadema jacobyi	Up to 98 μm	Planktotrophic, seasonal	Young *et al.*, 1989
Linopneustes longispinus	Up to 109 μm	Planktotrophic, seasonal	Young & Cameron, 1989
Asteroidea			
Hymenaster pellucidus	Up to 1100 μm	Lecithotrophic, 'continuous'	Pain *et al.*, 1982*a* (as *H. membranaceus*)
Hymenaster gennaeus	Up to 1200 μm	Lecithotrophic, 'continuous'	Pain *et al.*, 1982*a*
Brisinga endecacnemos	Up to 1250 μm	Lecithotrophic, 'continuous'	Tyler *et al.*, 1984*b*
Brisingella coronata	Up to 1250 μm	Lecithotrophic, 'continuous'	Tyler *et al.*, 1984*b*
Freyella spinosa	Up to 1250 μm	Direct demersal, 'continuous'	Tyler *et al.*, 1984*b*
Zoroaster fulgens	Up to 950 μm	Lecithotrophic, (seasonal?)	Tyler *et al.*, 1984*b*
Dytaster grandis	Up to 120 μm	Planktotrophic, seasonal	Tyler & Pain, 1982*a*; Tyler *et al.*, 1990
Plutonaster bifrons	Up to 120 μm	Planktotrophic, seasonal	Tyler & Pain, 1982*a*

Psilaster andromeda	Up to 950 μm	Lecithotrophic, 'continuous'	Tyler & Pain, 1982*a*
Benthopecten simplex	Up to 950 μm	Lecithotrophic, 'continuous'	Pain *et al.*, 1982*b*
Pectinaster filholi	Up to 850 μm	Lecithotrophic, 'continuous'	Pain *et al.*, 1982*b*
Pontaster tenuispinis	Up to 800 μm	Lecithotrophic, 'continuous'	Pain *et al.*, 1982*b*
Bathybiaster vexillifer	Up to 1000 μm	Lecithotrophic, 'continuous'	Tyler *et al.*, 1982*a*
Pseudarchaster parelli	Up to 900 μm	Direct, 'continuous'	Tyler & Pain, 1982*b*
Paragonaster subtilis	Up to 900 μm	Direct, 'continuous'	Tyler & Pain, 1982*b*
Holothuroidea			
Ypsilothuria bitentaculata	Up to 350 μm	Lecithotrophic, 'continuous'	Tyler & Gage, 1983 (as *Y. talismani*)
Laetmogone violacea	Up to 400 μm	Lecithotrophic, 'continuous'	Tyler *et al.*, 1985*c*
Benthogone rosea	Up to 750 μm	Direct, 'continuous'	Tyler *et al.*, 1985*c*
Peniagone azorica	Up to 300 μm	Lecithotrophic	Tyler *et al.*, 1985*a*
Peniagone diaphana	Up to 300 μm	Lecithotrophic	Tyler *et al.*, 1985*a*
Cherbonniera utriculus	Up to 200 μm	Lecithotrophic	Tyler *et al.*, 1987
Molpadia blakei	Up to 200 μm	Lecithotrophic	Tyler *et al.*, 1987
Deima validum	Up to 700 μm	Lecithotrophic	Tyler *et al.*, 1984*a*
Oneirophanta mutabilis	Up to 950 μm	Lecithotrophic	Tyler *et al.*, 1984*a*
Bathyplotes natans	Up to 280 μm	'Continuous'	Tyler *et al.*, 1994*b*
Benthodites sordida	> 1000 μm	Direct	Tyler & Billett, 1987
Psychropotes longicauda	Up to 4400 μm	Direct	Hansen, 1975; Tyler & Billett, 1987
Psychropotes depressa	Up to 1800 μm	Direct	Tyler & Billett, 1987
Psychropotes semperiana	Up to 3000 μm	Direct	Tyler & Billett, 1987
Brachiopoda			
Frieleia halli	Up to 112 μm	Planktotrophic, seasonal	Rokop, 1977
Hydrothermal Vents and Cold Seeps			
Crustacea			
Ventiella sulfuris		Direct	France *et al.*, 1992
Bythograea thermydron	480-540 μm	Planktotrophic	Van Dover *et al.*, 1985
Munidopsis sp.	2.2-2.3 mm	No planktotrophic stage	Van Dover *et al.*, 1985
Alvinocaris lusca	340-500 μm	Planktotrophic	Williams & Chace, 1982
Rimicaris exoculata	Up to 600 μm	Planktotrophic?, 'continuous'	Copley, 1998
Polychaeta			
Alvinella	> 250 μm	Short larval dispersal or direct development	Desbruyeres & Laubier, 1991
Paralvinella pandorae	215-275 μm	Short larval dispersal or direct development (possible offspring brooding)	McHugh, 1989; Desbruyeres & Laubier, 1991
Paralvinella palmiformis	215 μm	Brooding?, 'continuous' or semi-continuous	McHugh, 1989
Paralvinella grasslei	275 μm	Direct benthic, periodic recruitment?	Zal *et al.*, 1995
Paralvinella sulfincola	Up to 250 μm	Lecithotrophic, asynchronous	Copley, 1998
Amphisamytha Galapagensis	Large yolky eggs	Short larval development (possibly demersal)	Zottoli, 1983; McHugh & Tunnicliffe, 1994
Mollusca			
Gastropoda			
Alvinoconcha		Planktotrophic	Warén & Bouchet, 1993
Bivalvia			
Bathymodiolus Thermophilus	Small eggs	Planktotrophic, 'continuous' recruitment	Lutz *et al.*, 1980, 1984
Calyptogena magnifica	150-310 μm	Short larval dispersal	Lutz *et al.*, 1984, 1988

Vestimentifera			
Riftia pachyptila	Up to 80 μm	Planktotrophic	Jones & Gardiner, 1985; Cary *et al.*, 1989
Ridgeia piscesae	Up to 90 μm	Short larval dispersal?	Southward, 1988; Southward & Coates, 1989
Lamellibrachia sp.	Up to 105 μm	Lecithotrophic	Young *et al.*, 1996*b*
Escarpia sp.	Up to 115 μm	Lecithotrophic	Young *et al.*, 1996*b*

Data on echinoderm egg size and gametogenic cycles from Rockall Trough show that most asteroids, with the exception of *Plutonaster bifrons* and *Dytaster grandis* cited above, reproduce all year round (Tyler *et al.*, 1993) and a pelagic lecithotrophic larva is probably present (Tyler & Pain, 1982*a*; Tyler *et al.*, 1982*b*; Pain *et al.*, 1982*b*; Tyler *et al.*, 1984*b*). The same seems to be true for holothurians (Tyler & Gage, 1983; Tyler *et al.*, 1984*a*; Tyler *et al.*, 1985*a, c*; Tyler *et al.*, 1987). Amongst echinoids, a large number of planktotrophs are found (cited above) and many lecithotrophs are also present (Harvey & Gage, 1984; Tyler & Gage, 1984*b*; Tyler *et al.*, 1984*a*; Young, 1991).

In molluscs, Lightfoot *et al.* (1979) reported that the deep-sea bivalves *Ledella messanensis* and *Yoldiella jeffreysi* present a synchronous seasonal cycle in gametogenesis, spawning in early spring and producing probably a free-swimming lecithotrophic larva. In contrast, *Malletia cuneata* shows a continuous breeding cycle, presenting also lecithotrophic development (Tyler *et al.*, 1992). In gastropods, some mesogastropods and all archaeogastropods are lecithotrophs, with the latter being probably phylogenetically constrained to such development (Rex & Warén, 1982; Bouchet & Warén, 1994). In neogastropods, Colman *et al.* (1986*a*) calculated that 57% of the examined species presented nonplanktotrophic development based on shell morphology (see also Colman & Tyler, 1988). For more information on the reproduction of deep-sea benthic molluscs, see Scheltema (1994).

1.3.1. Hydrothermal Vents and Cold Seeps

Dispersal in highly isolated, ephemeral habitats is supposed to be of great importance in maintaining community structure. Lutz (1988) argues that for the sessile invertebrates, which make up most of the hydrothermal vent community, a pelagic larval stage for dispersal is present (the same must be true for sessile seep organisms) (see also Van Dover *et al.*, 1988). Actually, lecithotrophy is probably the

dominant kind of development in hydrothermal vents, although some species with planktotrophic development are present (Lutz *et al.*, 1980; Lutz *et al.*, 1984; Berg & Van Dover, 1987; Lutz, 1988).

Lutz *et al.* (1984) report that from 18 species of Mollusca, 10 limpets and 6 trochoids are probably nonplanktotrophic, with a free-swimming larval stage and two turrids are planktotrophic. *Calyptogena magnifica* has also a nonplanktotrophic stage inferred from the egg size (see also Gustafson & Lutz, 1994).

Among the Crustacea, Lutz *et al.* (1984) cite two nonplanktotrophic galatheids and two planktotrophic brachyurans. The predominance of nonplanktotrophs is probably related to phylogenetic constraints on vent taxa than to the nature of the vent habitat itself (Berg, 1985; Turner *et al.*, 1985; Van Dover *et al.*, 1985; Van Dover *et al.*, 1988).

The dispersal of larval stages is thought to occur in many different ways. Larvae of hydrothermal vent organisms have been captured in deep-water zooplankton tows at and near the vents (Berg & Van Dover, 1987; Wiebe *et al.*, 1988; Mullineaux *et al.*, 1996). Such larvae probably entrain into rising plumes of hydrothermal fluid, being carried through the water column (Kim *et al.*, 1994; Mullineaux, 1994; Mullineaux *et al.*, 1995). It is of interest to note that lecithotrophic larvae have been captured in plumes (Berg & Van Dover, 1987) suggesting that this larval type can have a high dispersal potential. Mullineaux *et al.* (1995) argue that the presence of lecithotrophic larvae in the water column, at a distance of thousands of meters away from potential source populations, support the supposition by Lutz (1988) that vent larvae may disperse much farther than previously expected. These data together with the occurrence of large post-metamorphic individuals in the water column (Wiebe *et al.*, 1988) suggests that the dispersal potential of vent organisms (and probably non-vent deep-sea organisms) is high. Lutz *et al.* (1980) suggests that dispersal could also occur in surface waters and by swimming or crawling near the bottom (by means of a demersal planktotrophic larvae).

Lutz *et al.* (1984) argue that planktotrophy in such habitats is, maybe, disadvantageous, since it could carry larvae away from suitable sites and that nonplanktotrophy would allow a rapid exploitation of the resources available, owing to the early competency and that delayed metamorphosis in cold water would be

advantageous in a deteriorating habitat (allowing the larvae to exploit new "healthier" sites). However, as cited above, dispersal of organisms may be high through the entrainment into vent plumes. Perhaps such dispersal stages are likely to colonise new vent sites, keeping the genetic flow amongst populations.

Data on deep-sea cold methane/sulphide seeps shows similarities with hydrothermal vents. Gustafson & Lutz (1994) stress that the archaeogastropods present in those habitats are evolutionary constrained to nonplanktotrophy.

Recently, Young *et al.* (1996*b*) cultured, for the first time, embryos and larvae of two deep-sea cold methane/sulphide seep vestimentiferans (*Lamellibrachia* sp. and *Escarpia* sp.), showing that they possess lecithotrophic trochophores, although the authors argue that it is not known whether larvae will require planktonic food later in the development. Young *et al.* (1996*b*) found that the eggs of both species were able to float up into the water column and could disperse at least for several weeks. Floating lecithotrophic eggs are common amongst marine invertebrates, owing to the increased lipid content present, making them less dense than the seawater. Young & Cameron (1987) report floating lecithotrophic eggs for the deep-sea urchin *Phormosoma placenta*, with an average flotation rate of 0.42 cm s^{-1}. With this value, an egg released from 800 m depth should reach the surface in only 2.2 days! The presence of floating eggs could then increase substantially the dispersal potential of lecithotrophic larvae in addition to other factors previously discussed (see also Young, 1991; Cameron *et al.*, 1988).

1.3.2. Post-larval development in deep-sea invertebrates

As already seen above, the adult and larval phases of the life history in deep-sea invertebrates are relatively well-known. Despite being less understood than adult biology and ecology, larval studies still encompass a number of works with deep-sea species but it is much better understood in shallow water species. One area still poorly examined is the post-larval development (Fig. 1.5) and it will be discussed in chapters 3, 4 and 5.

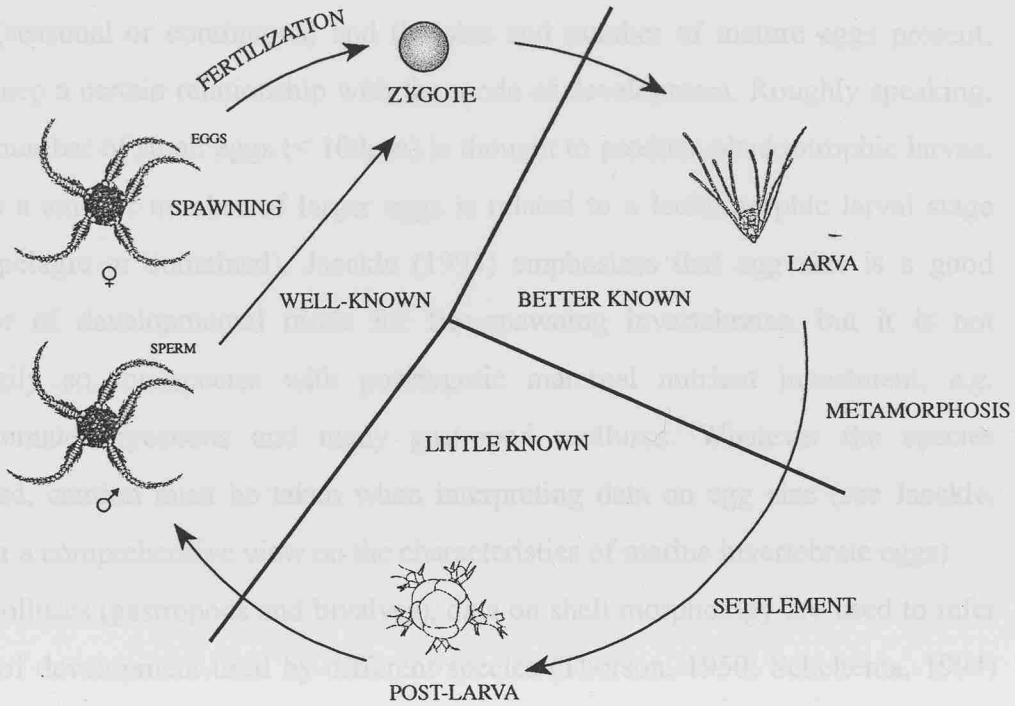

Figure 1.5. Complex life cycle of an ophiuroid (and may be generalized for a large number of echinoderm species), showing the relative knowledge of the different phases of the life cycle.

1.3.3. Approaches Used to Infer Modes of Development

The inference of modes of development in deep-sea invertebrates is not easily achieved and most studies employ indirect methods. The only direct method available, where the development is known for sure, is the induction of spawning (or dissection of gonads) of specimens collected from deep-sea areas (either by remotely operated sampling gears or submersibles), in order to obtain gametes for fertilization and further raising of embryos and larvae. Although this method is straightforward, it has been used for very few species, generally larger ones (in comparison with the huge diversity of small forms found in the deep-sea sediments) and, sometimes, very difficult to accomplish.

Concerning indirect methods, the most widely used is probably the study of the reproductive biology of the species through samples collected periodically from a particular site (Tyler & Pain, 1982*a*; Harvey & Gage, 1984; Tyler *et al.*, 1985*c*). The analysis of the gametogenic cycles reveals the periodicity by which reproduction

occurs (seasonal or continuous) and the size and number of mature eggs present, which keep a certain relationship with the mode of development. Roughly speaking, a large number of small eggs (< 100μm) is thought to produce planktotrophic larvae, whereas a smaller number of larger eggs is related to a lecithotrophic larval stage (either pelagic or contained). Jaeckle (1995) emphasizes that egg size is a good indicator of developmental mode for free-spawning invertebrates, but it is not necessarily so for species with postzygotic maternal nutrient investment, *e.g.* cheilostomate bryozoans and many gastropod molluscs. Whatever the species examined, caution must be taken when interpreting data on egg size (see Jaeckle, 1995 for a comprehensive view on the characteristics of marine invertebrate eggs).

In molluscs (gastropods and bivalves), data on shell morphology are used to infer modes of development used by different species (Thorson, 1950; Scheltema, 1994) and much work has been done in the deep-sea (Bouchet & Warén, 1979*a*; Rex & Warén, 1982; Colman *et al.*, 1986*a*; Colman & Tyler, 1988) and hydrothermal vents and cold seeps (Lutz *et al.*, 1980; Lutz *et al.*, 1984; Gustafson & Lutz, 1994). In gastropods, the embryonic (protoconch I) and larval (protoconch II) shells are different in planktotrophic and lecithotrophic species. Rex & Warén (1982) cite that in prosobranch gastropods, species with planktotrophic development have shells with high spires, numerous whorls, brown coloration and fine sculpture. The protoconch I is present at the apex, being deposited before hatching. The protoconch II is larger, consisting of subsequent whorls grown during the planktonic phase (and presenting a sinusigerous lip - Scheltema, 1994). In lecithotrophs, the shell has a blunter apex, fewer and larger initial whorls (usually just one), which comprise the whole larval shell; coloration is similar to the adult shell (white or gray), and generally lacks visible sculpture. There is no change between pre- and post-hatching larval shell (absence of a sinusigerous lip - Scheltema, 1994).

In bivalves, species with a planktotrophic larva and long planktonic life bear a small prodissoconch I (embryonic shell) (between 70-150 μm in length) and a large prodissoconch II (larval shell), indicative of a long planktonic life. Lecithotrophic bivalves, with short planktonic lives, possess a prodissoconch I between 135-230 μm and a narrow prodissoconch II, indicating a brief planktonic life. In direct developers,

without a planktonic development, the embryonic shell is large (230-500 μm) (Scheltema, 1994).

Another confirmation of the site of development, in the case of shell data, is the analysis of the isotopic composition of the shell carbonate (ratio of the oxygen stable isotopes ^{16}O and ^{18}O, expressed as $\delta^{18}O$, and of the carbon ^{12}C and ^{13}C, as $\delta^{13}C$), which reveals whether a particular carbonate was deposited in warm or cold waters, yielding distinct results (Killingley & Rex, 1985).

Analysis of the population structure can also give some information on the mode of development of species. Presence of a large number of post-larvae during specific times of the year can be indicative of seasonal recruitment of juveniles (Schoener, 1968, 1972; Lightfoot *et al.*, 1979; Tyler & Gage, 1980; Gage & Tyler, 1981*a*; Gage, 1994). Nevertheless, data on age structure must be used as an additional evidence and is generally clearer for seasonally breeders (as in the case of *Ophiura ljungmani* - see references above). For non-seasonally breeding species, the size and composition of post-larval population remains unclear (Gage, 1994).

Finally, larvae of deep-sea animals can be collected in the water column and cultured until metamorphosis. The post-metamorphic stages can, then, be identified by comparing with known post-larvae (Tyler & Fenaux, 1994).

1.5. Aims of the present work

Following what was stressed in section 1.3.2, the present thesis has as its primary aim to produce a comprehensive understanding of the general morphology and its ontogenetic changes during the early post-metamorphic period of deep-sea echinoderms (Ophiuroidea, Asteroidea and Echinoidea) and how they are related among species and higher taxa. This study also intends to help in the identification of early juvenile stages collected in the deep-sea areas to the west of the British Isles. The study of the functional morphology of the post-larvae is explored in order to understand the biology and ecology of the studied species. It is also intended to explore possible phylogenetic affinities among different species based on post-larval morphology. In chapter 6, the life cycle of *Ophiocten gracilis* is used as a case study, where the aim is the study of settlement and recruitment processes, as well as the reproductive biology of this bathyal ophiuroid.

Chapter Two - Material and methods

2.1. Sampling Material

The echinoderm fauna collected during the present study was obtained in the areas from the Faroe Islands to the Porcupine Abyssal Plain. Figure 2.1 shows most of the stations and which echinoderm class was obtained. The station details are given in the tables shown below.

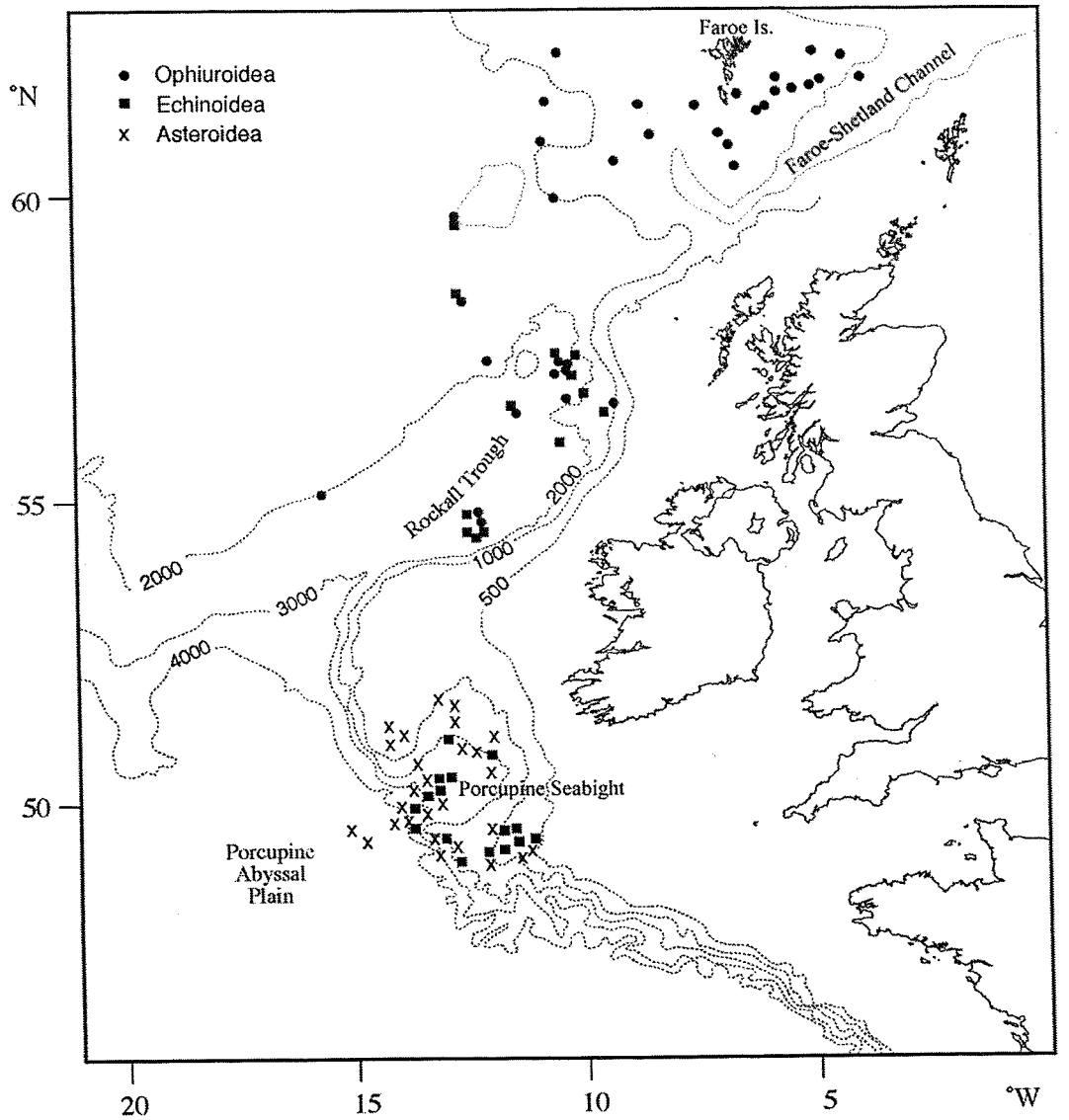

Figure 2.1. Map of the NE Atlantic showing study area. Different symbols represent the stations were the different echinoderm classes were collected during the Biofar, SAMS and IOS programmes.

2.1.1. Ophiuroid post-larvae

Deep-sea ophiuroid post-larvae were sorted out from samples of two research programs: the Biofar (Investigations on the Marine Benthic Fauna of the Faroe Islands), organized by the Nordic Council of Marine Biology and the long-term SAMS (Scottish Association for Marine Science, former SMBA) Programme in the Rockall Trough (NE Atlantic Ocean) (Gage *et al.*,1980).

During the Biofar Programme a large number of ophiuroid species were collected, between 1986 and 1990 (at over 700 stations), on the Faroe Shelf and Slope, Faroe Bank and Faroe-Shetland Channel (Emson *et al.*, 1994). Some of these stations yielded a large number of ophiuroid post-larvae, which are described in the present work. A total of 13 species of post-larva were found but only 11 are described. The remaining species did not yield enough numbers to allow good descriptions. Specimens were collected at depths between 77 and 1319 m, using several different sampling gears. They include a modified Rothlisberg & Pearse epibenthic sampler (Brattegard & Fosså, 1991), a detritus sledge, a scallop sledge and a heavy triangular dredge (Table 2.1). For more information on Biofar stations, see Nørrevang *et al.* (1994).

Table 2.1. List of stations where ophiuroid post-larvae were collected during the BIOFAR Programme. RP=Modified Rothlisberg & Pearse Epibenthic Sampler; DS=Detritus Sledge; SS=Scallop Sledge; 3S=Heavy Triangular Dredge.

Station	Date	Lat. (°N)	Long. (°W)	Depth (m)	Gear	Ophiuroid Post-larvae
10	17.07.87	62°31	05°02	430	RP	*Ophiura sarsi, Ophiocten gracilis*
19	18.07.87	62°12	04°25	276	DS	*Ophiacantha bidentata, O. abyssicola*
27	18.07.87	61°54	05°03	225	RP	*Ophiacantha abyssicola*
29	18.07.87	61°49	05°25	170	RP	*Ophiura sarsi, Ophiocten gracilis, O. affinis, Ophiopholis aculeata*
32	18.07.87	61°41	05°47	354	RP	*Ophiura sarsi*
51	19.07.87	61°24	06°10	235	RP	*Ophiopholis aculeata, Ophiocten gracilis, Ophiura sarsi, Ophiacantha abyssicola*
56	20.07.87	61°54	06°28	77	RP	*Ophiura carnea, Ophiura albida*
65	20.07.87	61°35	08°05	322	DS	*Ophiura sarsi, O. carnea, Ophiocten gracilis*
73	21.07.87	61°14	08°29	185	RP	*Ophiocten affinis*
80	22.07.87	60°39	08°28	678	DS	*Ophiactis abyssicola*
82	22.07.87	60°31	08°25	732	RP	*Ophiactis abyssicola*
90	22.07.87	60°33	06°32	252	SS	*Ophiactis balli*

95	23.07.87	60°42	05°19	803	DS	*Ophiocten gracilis*
98	23.07.87	60°54	06°15	150	RP	*Ophiocten affinis, Ophiactis abyssicola*
100	24.07.87	61°34	06°17	283	RP	*Ophiura sarsi, Ophiocten gracilis, Ophiopholis aculeata, Ophiacantha bidentata, O. abyssicola*
132	05.05.88	61°30	07°41	225	DS	*Ophiacantha abyssicola*
137	05.05.88	61°02	07°11	542	RP	*Ophiacantha bidentata*
345	22.07.88	62°31	08°11	358	3S	*Ophiacantha abyssicola*
381	27.05.89	62°12	03°59	402	DS	*Ophiura sarsi, Ophiocten gracilis, Ophiopholis aculeata, Ophiacantha bidentata, O. abyssicola*
496	24.07.89	60°33	09°35	515	DS	*Ophiomyces grandis, Ophiura carnea*
504	25.07.89	60°37	08°38	404	3S	*Ophiopholis aculeata*
601	11.04.90	61°56	05°58	140	DS	*Ophiura albida*
605	12.04.90	61°49	06°19	100	DS	*Ophiopholis aculeata*
609	12.04.90	62°05	06°20	90	3S	*Ophiura albida*
694	12.05.90	60°57	10°59	624	RP	*Ophiura sarsi, Ophiomyces grandis*
696	13.05.90	61°35	10°46	1319	RP	*Ophiactis abyssicola*
719	28.09.90	61°07	05°02	610	DS	*Ophiura sarsi*
726	29.09.90	60°39	06°54	400	DS	*Ophiopholis aculeata*
737	01.10.90	62°04	10°22	850	DS	*Ophiactis abyssicola*
747	03.10.90	62°43	05°56	394	3S	*Ophiacantha abyssicola*

Material from the Rockall Trough Programme was collected at depths of 1000-3000 m using a Woods Hole Oceanographic Institution (WHOI)-pattern epibenthic sledge. Only three species of post-larva were described in the present thesis of a total of 6 (Table 2.2). The additional species were either in poor condition or could not be identified.

Samples from both programmes were fixed in buffered seawater formalin and transferred to 70% isopropanol for long-term storage.

Table 2.2. List of stations where ophiuroid post-larvae were collected during the SAMS Programme. ES=Epibenthic Sledge.

Station	Date	Lat (°N)	Long (°W)	Depth (m)	Ophiuroid Post-larvae
ES 12	03.07.73	56°49	10°15	2076	*Ophiura ljungmani*
ES 18	22.09.73	56°44	09°20	1392	*O. ljungmani*
ES 34	10.05.75	56°36	11°30	2515	*Amphilepis ingolfiana*
ES 99	09.07.76	60°00	10°35	1160	*Ophiura ljungmani*
ES 112	25.10.76	55°12	15°50	1900	*O. ljungmani*
ES 197	19.08.81	57°21	10°29	2200	*O. ljungmani, Amphilepis*

					ingolfiana
ES 244	25.07.83	57°23	10°20	2150	*A. ingolfiana*
ES 255	31.07.83	58°26	12°42	1595	*Ophiura scomba*
ES 261	01.08.83	57°24	12°05	1824	*O. scomba*
ES 283	15.04.85	54°39	12°15	2946	*Amphilepis ingolfiana*
ES 401	10.09.90	54°40	12°16	2900	*A. ingolfiana*
ES 402	11.09.90	54°40	12°16	2905	*A. ingolfiana*
ES 405	12.09.90	54°40	12°20	2910	*A. ingolfiana*
ES 412	17.02.91	57°18	10°18	2195	*A. ingolfiana*
ES 446	08.03.93	54°42	12°18	2846	*Ophiura ljungmani*

2.1.2. Sediment trap ophiuroid post-larvae

Samples of *Ophiocten gracilis* post-larvae were obtained using two PARFLUX Mark 7G-21 time-series sediment traps moored in 1496 m water depth in the Hebridean slope (56°72'N, 09°46'W). The trap has an opening of 0.5 m^2 and is covered by a honeycomb baffle of 2.5 cm diameter/6.5 cm depth cells and 0.5 mm thick walls. The array consisted of one trap at 1000 m and another at 1400 m depth. The mooring was deployed on the 22/04/96 and recovered on the 02/08/96, with a sampling interval of 7 days. Sampling cups were filled prior to deployment with preservative fluid of 2% borax buffered formaldehyde and 5 ppt excess NaCl. The animals entering the cups were assumed to have been killed immediately. On recovery, 1ml of concentrated Aristar grade formaldehyde was added prior to storage at 4°C.

During the analysis of particulate material it was noticed that a large number of post-larval ophiuroids were present and were later identified as *Ophiocten gracilis* (see chapter 3). The animals were picked out by forceps under stereomicroscope. Disk diameter (dd) and arm length were measured under stereomicroscope using a digitizing tablet driven by a microcomputer.

2.1.3. Adult Ophiocten gracilis

Adult individuals for reproductive biology studies (see below) were collected in the Rockall Trough area using one of three sampling gears: a WHOI-pattern epibenthic sledge (ES), a Semi-Balloon Otter Trawl (OTSB) and an Agassiz Trawl (AT) (Table

2.3). Samples were fixed in 4% sea water formalin and preserved in 70% alcohol for long-term storage.

Table 2.3. List of stations of the adult *Ophiocten gracilis* used for reproductive biology studies. ES=Epibenthic Sledge; OTSB=Semi-Balloon Otter Trawl; AT=Agassiz Trawl.

Station	Date	Lat (°N)	Long (°W)	Depth (m)	Gear
23	23.09.73	56°37	09°10	704	ES
13/83/6	22.09.83	56°36	09°17	980-1005	OTSB
9/84/2	02.11.84	56°34	09°16	910-960	OTSB
3/85/10	17.04.85	56°31	09°13	795-805	OTSB
75/91/1	16.02.91	56°24	09°14	725-870	OTSB
583	04.08.95	56°29.90	09°09.70	678	AT

2.1.4. Asteroidea juveniles

Juvenile asteroids were collected on the Porcupine Seabight and Porcupine Abyssal Plain areas on the South-west of Ireland at depths between 400 and 4565 m (Table 2.4) as part of the Institute of Oceanographic Sciences (IOS) Programme in the Porcupine area. Sampling was undertaken using an IOS epibenthic sledge (Aldred *et al.*, 1982) or a semi-balloon otter trawl. For further information on the sampling gear used see Rice *et al.* (1991).

A total of 4013 specimens were collected in 53 stations. Twelve different species belonging to 8 families were identified, representing 6 of the 7 orders of the Class Asteroidea.

Table 2.4. List of stations of the juvenile asteroids collected during the IOS Program in the Porcupine area (SW Ireland). OTSB14=Semi-Balloon Otter Trawl; BN1.5/3M=Epibenthic Sledge.

		Position - Start		Position – End			
Station	**Date**	**°N**	**°W**	**°N**	**°W**	**Depth (m)**	**Gear**
9638#2	09.11.77	49°50.2	14°07.3	49°50.3	14°12.6	4043-4104	OTSB14
9640#1	13.11.77	50°03.2	13°50.6	50°08.0	13°52.7	3749-3757	OTSB14
9753#7	08.04.78	50°54.5	12°10.9	50°54.8	12°11.4	1942-1942	BN1.5/3M
9754#3	09.04.78	51°08.4	12°01.5	51°09.5	12°01.8	1484-1484	BN1.5/3M
9756#9	13.04.78	49°47.1	14°01.5	49°48.5	14°02.0	4039-4069	BN1.5/3M
9756#14	15.04.78	54°04.0	13°55.6	50°04.3	13°53.2	3680-3697	BN1.5/3M
9774#1	21.04.78	51°04.4	11°59.3	51°05.2	12°03.4	1494-1572	OTSB14
9775#3	22.04.78	50°56.8	12°22.4	50°55.7	12°19.2	2012-2019	BN1.5/3M
9776#2	23.04.78	49°22.7	11°36.0	49°21.5	11°35.6	770-785	BN1.5/3M
9779#1	24.04.78	49°22.3	12°49.1	49°20.7	12°49.5	1398-1404	BN1.5/3M
50510	03.06.79	51°05.3	13°04.5	51°06.5	12°59.5	1925-1960	OTSB14
50515#1	06.06.79	49°43.9	15°04.6	49°46.9	15°08.2	4505-4515	OTSB14
50518#1	07.06.79	49°27.3	13°21.1	49°30.1	13°26.8	2045-2110	OTSB14
50519#1	08.06.79	49°29.5	12°48.9	49°29.9	12°43.6	1465-1431	OTSB14
50523#1	09.06.79	49°31.6	11°23.9	49°29.0	11°23.9	455-490	OTSB14
50602#2	01.07.79	51°01.0	13°05.9	51°01.1	13°08.4	1955-1980	BN1.5/3M
50602#3	01.07.79	51°06.8	13°16.7	51°06.9	13°24.4	1817-1930	OTSB14
50603#1	02.07.79	49°46.2	14°01.5	49°44.4	14°00.5	4000-4000	BN1.5/3M
50604#1	04.07.79	50°06.1	13°53.0	50°06.4	13°49.9	3490-3550	BN1.5/3M
50605#1	05.07.79	50°11.6	13°32.4	50°11.2	13°29.0	2820-2930	BN1.5/3M
50606#5	06.07.79	50°43.1	13°56.1	50°42.7	13°57.0	1120-1140	BN1.5/3M
50607#1	07.07.79	51°01.7	14°12.1	51°01.4	14°07.3	700-712	OTSB14
50607#2	07.07.79	51°01.4	14°06.4	51°01.4	14°07.5	700-700	BN1.5/3M
50608#2	07.07.79	51°19.3	14°22.3	51°19.3	14°24.3	510-510	BN1.5/3M
50715	21.10.79	51°19.5	12°57	---	---	1635-1720	OTSB14
10108#1	05.09.79	49°20.6	12°49.2	49°19.6	12°48.7	1385-1390	BN1.5/3M
10109#8	07.09.79	49°11.7	12°19.4	49°10.0	12°18.5	1120-1130	BN1.5/3M
10111#8	09.09.79	49°32.6	13°07.1	49°33.5	13°05.9	1630-1640	BN1.5/3M
10112#1	09.09.79	50°25.0	13°19.1	50°26.4	13°17.6	2640-2660	BN1.5/3M
10112#2	09.09.79	50°25.2	13°20.3	50°25.7	13°20.4	2640-2650	BN1.5/3M
10112#3	10.09.79	50°19.1	13°25.8	50°19.9	13°26.9	2740-2755	BN1.5/3M
10113#1	10.09.79	50°16.1	13°31.6	50°16.3	13°32.3	2755-2760	BN1.5/3M
10114#1	10.09.79	49°45.6	14°08.2	49°45.0	14°08.0	4040-4060	BN1.5/3M
10115#1	11.09.79	49°46.3	13°56.0	49°45.6	13°56.6	3900-3950	BN1.5/3M
10120#1	13.09.79	49°27.5	11°21.7	49°27.9	11°21.2	400-400	BN1.5/3M
50913	12.11.80	50°11.9	13°39.8	50°11.3	13°41.3	3000-3040	BN1.5/3M
51103#5	21.05.81	51°47.0	13°13.1	51°47.6	13°13.8	950-930	BN1.5/3M
51110#3	28.05.81	50°16.4	13°30.9	50°15.4	13°30.6	2785-2800	BN1.5/3M
51403#1	25.03.82	51°37.7	12°59.8	51°36.6	13°00.0	1292-1314	BN1.5/3M
51403#2	25.03.82	51°37.4	12°59.2	51°36.9	12°59.2	1317-1325	BN1.5/3M
51403#3	25.03.82	51°36.8	12°59.1	51°36.4	12°59.3	1319-1325	BN1.5/3M
51403#4	26.03.82	51°36.7	12°59.6	51°36.0	12°59.8	1319-1333	BN1.5/3M
51403#5	26.03.82	51°37.8	12°58.9	51°37.3	12°59.0	1289-1297	BN1.5/3M
51403#6	26.03.82	51°37	12°59	---	---	1278-1295	BN1.5/3M
51403#7	26.03.82	51°36.4	12°59.6	51°39.2	12°58.8	1330-1255	OTSB14
51416#1	31.03.82	50°16.8	13°31.4	50°16.9	13°30.7	2780-2770	BN1.5/3M
51417	01.04.82	50°10.3	13°22.3	50°10.1	13°21.2	2790-2770	BN1.5/3M
51420#1	02.04.82	51°37.3	12°58.6	51°36.9	12°58.6	1326-1328	BN1.5/3M
51420#2	02.04.82	51°37.2	12°59.1	51°36.9	12°59.1	1304-1309	BN1.5/3M
51420#3	02.04.82	51°38.3	12°58.9	51°38.0	12°59.0	1293-1298	BN1.5/3M

51420#4	02.04.82	51°37.9	12°59.5	51°37.5	12°59.6	1279-1287	BN1.5/3M
52215#1	22.06.85	49°30.3	14°49.0	49°30.6	14°51.3	4561-4565	BN1.5/3M
11907#1	20.08.89	49°40.3	12°08.2	49°37.8	12°08.8	1315-1295	OTSB14

2.1.5. Echinoidea juveniles

Samples of post-larval sea urchins were taken from three major research programmes: the SAMS programme on the Rockall Trough; the IOS programme on the Porcupine area; and the OMEX (Ocean Margin EXchange) programme in the Goban Spur area, South-west Ireland. Stations positions and sampling gear used are summarised in Table 2.5. Samples from the IOS and SAMS programmes were treated in the same way as described above for ophiuroids and asteroids.

During the OMEX programme samples were obtained using two circular box cores with diameters of 30 and 50 cm. Samples were fixed in 4% formaldehyde and preserved in 70% ethanol.

Four species of echinoids were identified among the juveniles. Individuals of the genus *Echinus* were also collected.

Table 2.5. List of stations of juvenile echinoid samples collected during three different sampling programmes. OMEX=Ocean Margin Exchange; SAMS=Scottish Association for Marine Science; IOS=Institute of Oceanographic Sciences. CBC-30 and 50=Circular Box Cores with diameters 30 and 50 cm, respectively; ES and BN1.5/3M=Epibenthic Sledge; OTSB14=Semi-Balloon Otter Trawl.

Station	Date	Lat. (°N)	Long. (°W)	Depth (m)	Gear	Programme
A	26.10.93	49°28.98	11°07.97	208	CBC	OMEX
A	23.05.94	49°29.7	11°08.4	208	CBC-30	OMEX
A	18.08.95	49°28.52	11°12.45	231	CBC-30	OMEX
B	20.10.93	49°21.99	11°48.09	1034	CBC-50	OMEX
B	24.05.94	49°22.4	11°45.1	1034	CBC-50	OMEX
B	20.08.95	49°22.00	11°47.99	1021	CBC-50	OMEX
I	19.10.93	49°24.72	11°31.86	670	CBC-50	OMEX
I	23.05.94	49°24.9	11°31.4	670	CBC-30	OMEX
I	19.08.95	49°24.70	11°31.86	693	CBC-50	OMEX
II	21.10.93	49°11.20	12°49.18	1425	CBC-50	OMEX
II	26.05.94	49°11.3	12°49.7	1425	CBC-50	OMEX

II	21.08.95	49°11.19	12°49.17	1457	CBC-50	OMEX
4	03.06.73	56°52	10°01	1993	ES	SAMS
15	03.07.73	56°44	09°28	1632	ES	SAMS
34	10.05.75	56°36	11°30	2515	ES	SAMS
99	09.07.76	60°00	10°35	1160	ES	SAMS
118	28.01.77	54°39	12°14	2910	ES	SAMS
122	29.01.76	54°31	12°31	2951	ES	SAMS
137	22.02.78	54°34	12°19	2900	ES	SAMS
147	02.06.78	54°36	12°19	2921	ES	SAMS
169	28.02.80	54°40	12°17	2910	ES	SAMS
176	28.05.80	57°15	10°26	2245	ES	SAMS
185	10.04.81	54°44	12°15	2907	ES	SAMS
190	16.08.81	54°41	12°18	2898	ES	SAMS
197	19.08.81	57°21	10°29	2200	ES	SAMS
200	06.02.82	57°20	10°32	2220	ES	SAMS
204	12.05.82	54°40	12°20	2904	ES	SAMS
218	03.08.82	57°22	10°24	2175	ES	SAMS
232	19.05.83	57°17	10°16	2195	ES	SAMS
244	25.07.83	57°23	10°20	2150	ES	SAMS
250	28.07.83	59°43	12°33	1270	ES	SAMS
255	31.07.83	58°26	12°42	1595	ES	SAMS
283	15.04.85	54°39	12°15	2946	ES	SAMS
285	15.04.85	54°39	12°14	2906	ES	SAMS
289	21.04.85	57°19	10°25	2190	ES	SAMS
402	11.09.90	54°40	12°16	2905	ES	SAMS
405	12.09.90	54°40	12°20	2910	ES	SAMS
412	17.02.91	57°18	10°18	2195	ES	SAMS
9753#7	08.04.78	50°54.5	12°10.9	1942-1942	BN1.5/3M	IOS
9776#2	23.04.78	49°22.7	11°36.0	770-785	BN1.5/3M	IOS
9779#1	24.04.78	49°22.3	12°49.1	1398-1404	BN1.5/3M	IOS
50511	04.06.79	50°32.4	13°01.4	2435-2405	OTSB14	IOS
50602#2	01.07.79	51°01.0	13°05.9	1955-1980	BN1.5/3M	IOS
50604#1	04.07.79	50°06.1	13°53.0	3490-3550	BN1.5/3M	IOS
50606#5	06.07.79	50°43.1	13°56.1	1120-1140	BN1.5/3M	IOS
50607#2	07.07.79	51°01.4	14°06.4	700-700	BN1.5/3M	IOS
50609#1	08.07.79	51°39.7	14°16.5	400-400	BN1.5/3M	IOS
50913	12.11.80	50°11.9	13°39.8	3000-3040	BN1.5/3M	IOS
51217#1	30.09.81	50°36.1	10°19.0	150	BN1.5/3M	IOS

51403#1	25.03.82	51°37.7	12°59.8	1292-1314	BN1.5/3M	IOS
51403#2	25.03.82	51°37.4	12°59.2	1317-1325	BN1.5/3M	IOS
51403#3	25.03.82	51°36.8	12°59.1	1319-1325	BN1.5/3M	IOS
51403#4	26.03.82	51°36.7	12°59.6	1319-1333	BN1.5/3M	IOS
51403#5	26.03.82	51°37.8	12°58.9	1289-1297	BN1.5/3M	IOS
51420#1	02.04.82	51°37.3	12°58.6	1326-1328	BN1.5/3M	IOS
51420#3	02.04.82	51°38.3	12°58.9	1293-1298	BN1.5/3M	IOS
52204#1	16.06.85	51°37.07	12°59.96	1295-1310	BN1.5/3M	IOS
10108#1	05.09.79	49°20.6	12°49.2	1385-1390	BN1.5/3M	IOS
10109#8	07.09.79	49°11.7	12°19.4	1120-1130	BN1.5/3M	IOS
10111#8	09.09.79	49°32.6	13°07.1	1630-1640	BN1.5/3M	IOS
10112#2	09.09.79	50°25.2	13°20.3	2640-2650	BN1.5/3M	IOS
10112#3	10.09.79	50°19.1	13°25.8	2740-2755	BN1.5/3M	IOS
10113#1	10.09.79	50°16.1	13°31.6	2755-2760	BN1.5/3M	IOS
10115#1	11.09.79	49°46.3	13°56.0	3900-3950	BN1.5/3M	IOS

2.2. Study of the Post-larval Development in Echinoderms

All three groups of echinoderms studied received a similar treatment for examination under scanning electron microscope (SEM). All ophiuroids and most of the echinoids and asteroids were air-dried. Ophiuroids and asteroids were dried straight from the 70% alcohol, whereas the echinoids were first dehydrated in increasing grades of acetone for 5 minutes each (30, 50, 70, 90, 95 and 100%) and twice at 100%, leaving at this concentration overnight. After that the echinoids were left to dry in the air. This process was adopted in order to avoid the higher surface tensions of the alcohol and water, which can cause the delicate tests of the sea urchins to collapse. In the case of the acetone, surface tension is smaller and therefore the evaporation of the liquid present in the sea urchin body is less damaging.

In some cases (for asteroids and echinoids), the animals were critical point dried. In this technique the animals are dehydrated in acetone (as described earlier) and taken into a pressure chamber (the critical point drier), which is then filled with liquid CO_2. The acetone is flushed out of the chamber and the CO_2 is allowed to replace the acetone. This process takes approximately 1 hour. During this phase, the chamber is kept at temperatures below 14°C in order to maintain the CO_2 in its liquid state. After that the temperature of the chamber is gradually increased, making the

pressure to increase also. When the temperature and pressure attain a specific threshold (31.5°C and 75 bar) the CO_2 passes directly into the gaseous state without problems with surface tension of the liquid. This makes the shrinkage of the soft tissues of the animal to be minimal, allowing the examination of the soft parts. After all CO_2 have passed into the gaseous phase, the gas is gently flushed out of the chamber and the specimens put into a dessicator.

Although a better preservation of the material is achieved using the critical point drier, the air drying techniques described above were preferred, since they allow a better analysis of the calcareous skeleton of the specimens. In critical point dried animals, the skin is preserved covering the internal skeleton of the echinoderms, making the description of the specimens very difficult.

After drying the species were arranged in ontogenetic series and mounted in stubs using a double-sided adhesive tape. All animals were examined under a low-vacuum SEM (JEOL JSM-5300LV). This equipment does not require the specimens to be gold-coated when working on the low-vacuum mode. However, it also allows the use of the high-vacuum mode with gold-coated specimens. Because the use of the low-vacuum mode in this instrument requires an optimum working distance (the distance between the specimen and the point source of the beam of electrons) of around 15 mm, the minimum magnification achieved is 50 times. For all the ophiuroids examined, this magnification was enough to have a complete view of the disk. However, for the larger asteroids and echinoids (with long spines) a larger working distance was necessary. For this reason, all ophiuroids were examined without a gold-coating and in the low-vacuum mode and asteroids and echinoids were gold-coated and subsequently examined under the high-vacuum mode, which allows higher working distances. The gold-coating was undertaken using a Hummer IV Sputter Coater. The animals were coated in the pulse mode for 9 minutes. In this mode, pulses of gold coating of 5 seconds collide with the specimens. This mode was preferred over the continuous coating because it is better for coating surfaces with a complex relief. In this mode, the time lag between the pulses allows the thin gold layer over the specimen to spread covering better all the surface of the specimen.

Ophiuroid micrographs were made using roll film and the disk diameters were measured using the SEM scalebar. During the course of this work, the Department

acquired a new frame store for the low-vacuum SEM, which allows pictures to be stored in a digital format. Therefore, asteroid and echinoid micrographs were stored on a CD-ROM and measurements were performed using an image analysis software. Asteroid measurements include arm ray (R), which is the distance between the centre of the disk and the tip of the arm, and the disk ray (r), representing the distance between the centre of the disk and the edge of the disk in the interradius. The ratio between the two rays is given as R/r. Echinoid measurements include the diameter of the test in regular echinoids and the length of the test in irregular echinoids.

Fourteen species of ophiuroid post-larvae are described including *Ophiacantha abyssicola, O. bidentata, Ophiomyces grandis, Ophiura sarsi, O. carnea, O. ljungmani, O. albida, O. scomba, Ophiocten affinis* (comb. nov.), *O. gracilis, Amphilepis ingolfiana, Ophiactis abyssicola, O. balli* and *Ophiopholis aculeata*. The asteroids include 11 predominantly deep-sea species: *Luidia sarsi sarsi, Bathybiaster vexillifer, Psilaster andromeda andromeda, Hyphalaster inermis, Porcellanaster ceruleus, Benthopecten simplex simplex, Pectinaster filholi, Plinthaster dentatus, Hymenaster pellucidus, Zoroaster fulgens* and *Brisingella coronata*. Sea urchins were the least abundant of the groups and yield only 4 species: *Phormosoma placenta, Spatangus raschi, Brissopsis lyrifera and Hemiaster expergitus*. Post-larvae of the genus *Echinus* are also described.

2.3. Reproductive Biology of *Ophiocten gracilis*

A total of 75 adults were used for reproductive studies (Table 2.3). They were decalcified in Bouins solution and dehydrated in increasing grades of isopropanol (70, 90, 100%) for two hours each and twice at 100%. After this treatment the individuals were cleared in Histoclear overnight and embedded in paraffin wax blocks and sectioned at 5 μm. The sections were stained with hematoxylin/eosin and examined under compound microscope for the study of reproductive stages. These were represented as a maturity index of the gonads (M.I.) (Patent, 1969). The stages of gonad development followed that given by Fenaux (1970) for *Amphiura chiajei* and Tyler (1977) for the genus *Ophiura*.

The presence of gametogenic tissues in post-larvae and juveniles were examined through sectioning of the whole animal, following the same method described above.

Samples were taken from the Rockall Trough (19 specimens), Faroe Islands (18 specimens) and sediment traps (19 specimens).

Fecundity was estimated for 4 females of different sizes (6.72, 7.53, 8.19 and 8.24 mm dd) (Table 2.3). The number of eggs was counted in 3 different gonads within the same animal under compound microscope after a smear slide preparation. The mean number of eggs was multiplied by the total number of gonads present. The resulting number represented the fecundity of the determined animal. The eggs in each animal were measured using an image analysis software in order to estimate the mean oocyte size, which was represented by the feret diameter. The feret diameter represents the diameter of a circle of area equal to the area of the oocyte projected in a two-dimensional plane (video image).

2.4. Settling Rates Experiment

Settling rates of post-larvae were measured using fixed animals from sediment traps. Three sets of 10 animals belonging to 3 different size classes (dd=0.63±0.02, 0.79±0.02 and 0.91±0.01 mm) and with arms intact were dropped into an isothermal water column (at 2, 5, 10 and 15°C) in a 500 ml measured cylinder in a constant temperature room. Prior to the experiment, animals were put in sea water at room temperature to avoid adverse effects of the preservative. The settling times were measured using a digital chronometer. Settling times of animals falling close or touching the walls of the measured cylinder were discarded. The mean feret diameter of the animals was used.

2.5. Estimation of Carbon Demands of *Ophiocten gracilis* Growing in Deep-Sea Sediment Traps

Section 2.1.2 describes the sampling of the post-larval *Ophiocten gracilis* in two deep-sea sediment traps. During the study period, post-larvae were observed to grow and the carbon demands required to achieve such a growth were estimated in the present work. In order to calculate the carbon demand of post-larvae, 50 intact animals of a wide variety of sizes were individually measured and dried at 60°C for 24 h. The animals were weighed (DW) and then burned in a muffle furnace for 18 h,

in order to estimate the ash-free dry weight (AFDW). The relationship between AFDW and disk diameter (dd) was

$$AFDW = 0.0082e^{1.78dd} \ (r^2 = 0.7851),$$

and this was used to calculate AFDW for the remaining specimens.

50% of the AFDW was assumed to be organic carbon (Salonen *et al.*, 1976).

Weight-specific respiration rates were calculated for each individual. The calculations were based on a formula described by Mahaut *et al.* (1995) for deep-sea animals living in temperatures of 2-4°C:

$R = 0.0074\ OC^{-0.24}$, where R=individual respiration rate (mg organic C/mg body organic C/day) and OC=individual organic content (mgC).

The respiratory demand (R_D, in mgC ind^{-1} day^{-1}) was then calculated by multiplying the organic carbon content by the weight-specific respiration rate. From the respiratory demand, the somatic production (P, in mgC ind^{-1} day^{-1}) was estimated assuming a growth efficiency of 30% (P/R_D=3/7) (Piepenburg and Schmid, 1997). As discussed later, the growth term is not a loss of material as long as the specimens are included in the flux.

Assimilation (A, in mgC ind^{-1} day^{-1}) was assumed to equal the sum of the respiratory demand and somatic production ($A = R_D+P$). From assimilation, carbon demand (D, in mgC ind^{-1} day^{-1}) was estimated assuming an efficiency of 80%. Therefore, D = A/0.8 (Piepenburg and Schmid, 1997).

A second and alternative method of estimating somatic production was based on the observed increase in mean body weight of the collected specimens.

$$P_{t1\text{-}t2} = \Delta AFDW_{t1\text{-}t2}/\Delta t = AFDW_{t2} - AFDW_{t1}/t_2\text{-}t_1, \text{ where:}$$

$P_{t1\text{-}t2}$ = Somatic production between time t_1 and t_2

$AFDW_{t1}$ = Mean ash-free dry weight of the population at time t_1

$AFDW_{t2}$ = Mean ash-free dry weight of the population at time t_2

Carbon demand was then calculated from production assuming a growth efficiency of 30% and assimilation efficiency of 80%.

The main assumption, used for the calculation of the population respiratory demand, was that all ophiuroids arrived at the same time in the trap, that all were collected by the cups during the study period, that they were randomly sampled

during each sampling interval and that they were not subject to any pressure of predation. These can obviously not be tested retrospectively.

2.6. Stomach Content Analysis of Post-larval *Ophiocten gracilis*

Stomach contents of all post-larval *Ophiocten gracilis* collected in the sediment trap (described above) were analysed under stereomicroscope. The contents were classified qualitatively by observing the material through the mouth or through the transparent body wall. Soft, amorphous material were classified as detritus. *O. gracilis* often showed empty stomachs and were classified as 'Empty'.

Chapter Three - Post-larval development in shallow and deep-sea ophiuroids (Echinodermata: Ophiuroidea) of the NE Atlantic Ocean

3.1. Introduction

Studies on the post-larval development in ophiuroids are not abundant in the literature. Two small specimens of *Hemipholis cordifera* showing the primary plates and first appearance of the radial shields are depicted in the work of Lyman (1882) on the Ophiuroidea of the *Challenger* Expedition. Subsequently, post-larval growth in five species of brittlestar from South America was described by Ludwig (1899). Later, Mortensen (1912) described the development of *Asteronyx loveni*. Clark (1914) was the first researcher to be really concerned with the lack of studies on post-larval growth, followed by Campbell (1922). The main aim of Clark and Campbell was to find a natural classification for the group, solving the taxonomic problems existing at that time.

Although at the first half of this century some species had already been described, the main problem was the poor illustrations exhibited in such publications, which made accurate identification of post-larvae difficult (Fig. 3.1). In the deep-sea, sampling was extremely difficult and relatively infrequent. The sampling gear used mesh that was too coarse to collect the small fraction of the fauna. While in shallow waters the collection of species that brood their young helped the study of early brittlestar stages, in the deep-sea the rarity of brooding (most of the species having a lecithotrophic development - see Pearse, 1994; chapter 1), and the lack of a proper sampling apparatus prevented in a certain extent the study of deep-sea forms.

After the invention of improved sampling equipment (see Hessler & Sanders, 1967), smaller species and post-larval forms were retrieved. Schoener (1967) described the growth stages of juvenile ophiuroids and traced back from the identified adults the respective post-larvae of each particular species. Schoener (1967) cited that at least two species of the same genus could be identified from the very early stages of growth, unlike Mortensen (1920) who found it impossible to recognise differences between the post-larvae of two species of the genus *Amphiura*. In a subsequent study, Schoener (1969) again concluded it was possible to

distinguish between congeneric species soon after the metamorphosis. Other species from shallow water were added to this list (see Muus, 1981; Webb & Tyler, 1985).

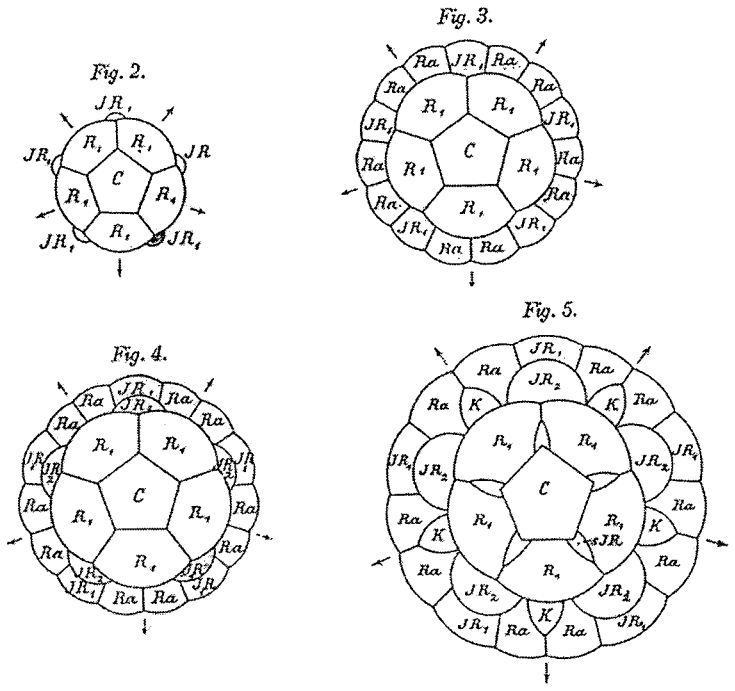

Figure 3.1. Post-larval development of *Ophiactis asperula* described by Ludwig (1899). Specimens are depicted by simple lines, which do not reflect the complex morphological characters found in such organisms.

The papers cited above were the first to deal with deep-water species and despite all the importance related to identification of the deep-sea ophiuroid post-larvae, few papers followed Schoener's work. Gage & Tyler (1981*a*) compare the post-larvae of the deep-sea species *Ophiura ljungmani* and *Ophiocten gracilis* using the Scanning Electron Microscope (SEM) and emphasise that they could also be recognised under low-power microscopes. Webb & Tyler (1985) give a good description and plates of the post-metamorphic growth stages of three shallow water species, among which *Ophiura albida*, although rarely, can also be found in deeper water. Tyler & Fenaux (1994) infer the adult of *Ophiopluteus compressus* by analysing the post-larval forms of a variety of species and the geographical distribution of the possible adults, matching it with the larval distribution. This last paper shows the importance of a knowledge of the very early post-metamorphic specimens, which could be useful to

assign the adults of unknown ophioplutei that can be reared to metamorphosis and therefore to the young post-larva. Tyler *et al.* (1995*c*) describe the post-larva of a new species of brittlestar (*Ophioctenella acies*) from the hydrothermal vents of the Mid-Atlantic Ridge comparing it with *Ophiura ljungmani*, a common non-vent deep-sea species. Other papers were published concerning this subject, mainly with shallow water inhabitants (see Stancyk, 1973; Turner, 1974; Hendler, 1978; Turner & Dearborn, 1979; Muus, 1981; Turner & Miller, 1988; Byrne, 1991), but few show good plates. One of the exceptions is Hendler (1988) on the post-larval ontogeny of amphiurids. Hendler identifies significant morphological characters and follows their growth changes, correlating them in closely related species. Based on these data, Hendler argues that the ontogenesis in post-larvae may be a reliable indicator of systematic relationships (Hendler, 1988). Recently, Hendler (1998) compares the ontogenetic changes in the oral papillae and other structures in some post-larval ophiuroids.

The lack of important taxonomic characters in the post-larvae makes identification of specimens collected in benthic samples difficult, and most frequently post-larvae are ignored in benthic ecology studies (Turner & Miller, 1988). In the deep-sea, post-larval ophiuroids have been collected in large quantities at certain times of the year, representing a significant proportion of the total population (Tyler & Gage, 1980; Gage & Tyler, 1981*a*). Gage (1994) noted that post-larval bivalves are not significant in terms of biomass, but they can dominate populations numerically. The same is true for brittlestars (Flach & Heip, 1996). In view of this problem, it is important to be able to recognise the different species of post-larvae when adults live sympatrically in benthic communities. In addition, such descriptions help in phylogenetic determination (Hendler, 1988) as well as on the assessment of growth rates on early stages of development. Gage & Tyler (1982*a*) showed that growth strategies can be different in different deep-sea ophiuroid species. The early stages of growth are particularly important as they reveal different survival strategies among species. Rapid early growth may be a strategy for predator avoidance whereas a slow growth rate may be determined by energy availability. The knowledge of post-larvae would also help in brittlestar settlement and recruitment studies (Gage & Tyler, 1981*b*, 1982*b*). Moreover, before assuming an adult life style, the post-larvae must spend

some time in the meiobenthic environment, where they might be an important component. All these factors should affect the rates of mortality and survivorship and, consequently, the maintenance of the deep-sea brittlestar populations.

In this chapter the early post-metamorphic development of 14 species of ophiuroids from the shallow and deep NE Atlantic Ocean is described. The species were chosen based on the relative abundance of different growth stages and individuals. *Ophiura sarsi*, *O. ljungmani* and *Amphilepis ingolfiana* had already been previously described (Schoener, 1967, 1969). However, the line drawings presented in those papers do not allow an accurate identification and their development is re-described in the present paper. The early growth stages of *Ophiura albida* (<1 mm disk diameter) are also described, complementing the work done by Webb & Tyler (1985), who described the development of specimens larger than 1mm in disk diameter. The aim is to produce, primarily, good descriptions of the ontogenetic development of the early growth stages of these species, showing the general aspect, as well as particular characteristics of the metamorphosed ophiuroid. It is also intended to investigate possible phylogenetic affinities using the morphological characters of the post-larvae.

3.2. Post-larval development

The main morphological characteristics in the early ophiuroid post-larvae are shown in figure 3.2.

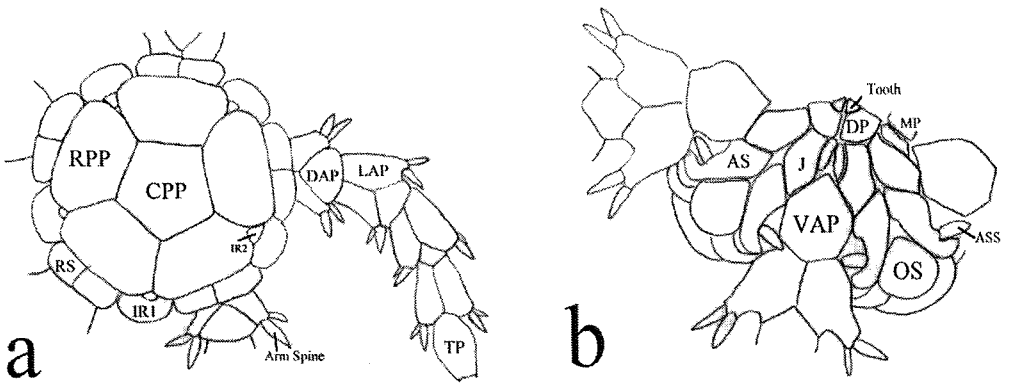

Figure 3.2. Main structures found in the early ophiuroid post-larvae. a) Dorsal view; b) Ventral view. CPP=Central Primary Plate; RPP=Radial Primary Plate; RS=Radial Shield; IR=Interradial Plate; DAP=Dorsal Arm Plate; LAP=Lateral Arm Plate; TP=Terminal Plate; VAP=Ventral Arm Plate; OS=Oral Shield; AS=Adoral Shield; ASS=Adoral Shield Spine; J=Jaw; DP=Dental Plate; MP=Mouth Papilla.

Subclass Ophiuridea Gray, 1840

Order Ophiurida Müller & Troschel, 1840

Suborder Ophiurina Müller & Troschel, 1840

Family Ophiacanthidae Perrier, 1891

Subfamily Ophiacanthinae Paterson *et al.*, 1982

Ophiacantha abyssicola G.O. Sars, 1871

Post-larvae of this species were found in the samples from Biofar. The earliest post-larva found measured 0.4 mm disk diameter (dd) and possessed 5 arm segments. The dorsal part of the disk is formed by the central primary plate (CPP), the 5 radial primary plates (RPP), the radial shields (RS), the first interradial plate (IR1) and the k-plate (k). The k-plate is a small plate present between the proximal end of the radial shields and the RPPs (Ludwig, 1899). The CPP is strongly pentagonal, with the borders filled with several small fenestrations and a solid edge. The central part of the plate is almost imperforate, bearing few small fenestrations. Each corner of the plate has a big trifid spine pointing outwards in a total of five spines, which are sometimes missing owing to losses during the sample acquisition. When missing, the places where these spines are attached can be recognized by the larger fenestrations

Figure 3.3. *Ophiacantha abyssicola* post-larval development (A-D). A and D, dorsal view; B and D, ventral view. A. 0.4 mm; B. 0.4 mm; C. 0.9 mm. Note the pentagonal central primary plate in the centre of the disk; D. 2.0 mm. Three spine-like mouth papillae (MP) are present (the distal-most being the former ASS). See Fig. 3.2 for explanation. k = k-plates. Sizes represent the disk diameter.

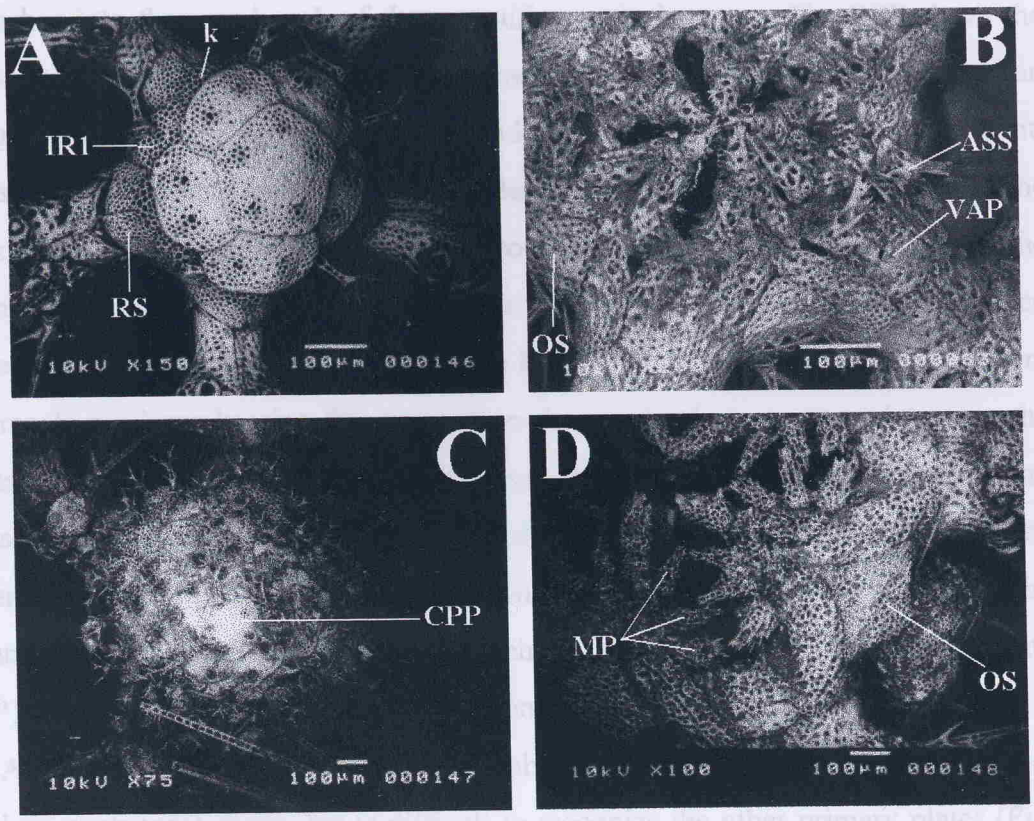
A
k
IR1
RS
10kV X150
100µm 000146
B
ASS
VAP
OS
100µm
C
CPP
10kV X75
100µm 000147
D
MP
OS
10kV X100
100µm 000148

present on the plate (Fig. 3.3A). The main stem of these spines is fenestrated and branches into three and each of these ramifies again into two. The RPPs have the same fenestration pattern, but only two spines are present. The RSs are broader than long and overlap the proximal arms. Besides the former plates, an IR1 is present, possessing one single spine. As an individual grows, each dorsal plate added to the disk bears just one spine. The spines also begin to erode probably owing to the animal's activity. The k-plate, together with the IR1, bears large rounded fenestrations. No spines are present on the k-plates or the RSs (Fig. 3.3A). The arm segments are large bearing three spines on the proximal segments and two on the distal ones. The spines of the proximal segments are large, with large spinelets, and those of the distal ones are smaller with spinelets distributed along their edges. The lateral arm plates (LAP) are contiguous dorsally throughout their length, leaving the rounded dorsal arm plates (DAPs) on their distalmost portion. The terminal plate (TP) is bulb-shaped with several fenestrations.

At 0.9 mm dd the CPP is still recognizable by the number of spines present on it and its pentagonal shape, but is difficult to recognize the other primary plates (Fig. 3.3C). The number of dorsal plates increases with size and they are hardly distinguishable, with a precise description of the dorsal plates almost impossible.

On the ventral side, the oral armature is well formed with strong and spinose teeth. No mouth papillae (MP) are present yet and the dental plate (DP) is small and broader than long. The adoral shield spines (ASS) are strong and spinose. The first ventral arm plate (VAP) is bell-shaped with a convex distal end. This plate is almost solid, bearing only few fenestrations on the lateral parts. The 2nd tentacle pore (TPo) is well concealed by the ASS in the smallest post-larvae examined (Fig. 3.3B). At a disk diameter of 0.66 mm the 1st MP is present as a spine-like structure at the distal part of the jaw, near the base of the DP. Reaching 2.0 mm dd three large MP are present and a groove is present on the oral shield (OS), indicating the identity of this species (Fig. 3.3D).

Ophiacantha bidentata (Retzius, 1805)

Individuals at 0.5 mm dd were collected on Biofar samples, being very similar to *O. abyssicola*. However, a careful examination of the dorsal plates of *O. bidentata*

Figure 3.4. *Ophiacantha bidentata* post-larval development (A-D). A and D, dorsal view; B and D, ventral view. A. 0.5 mm. Note the arrangement of the dorsal plates; B. 0.8 mm; C. 1.2 mm; D. 3.0 mm. See Fig. 3.2 for explanation. Sizes represent the disk diameter.

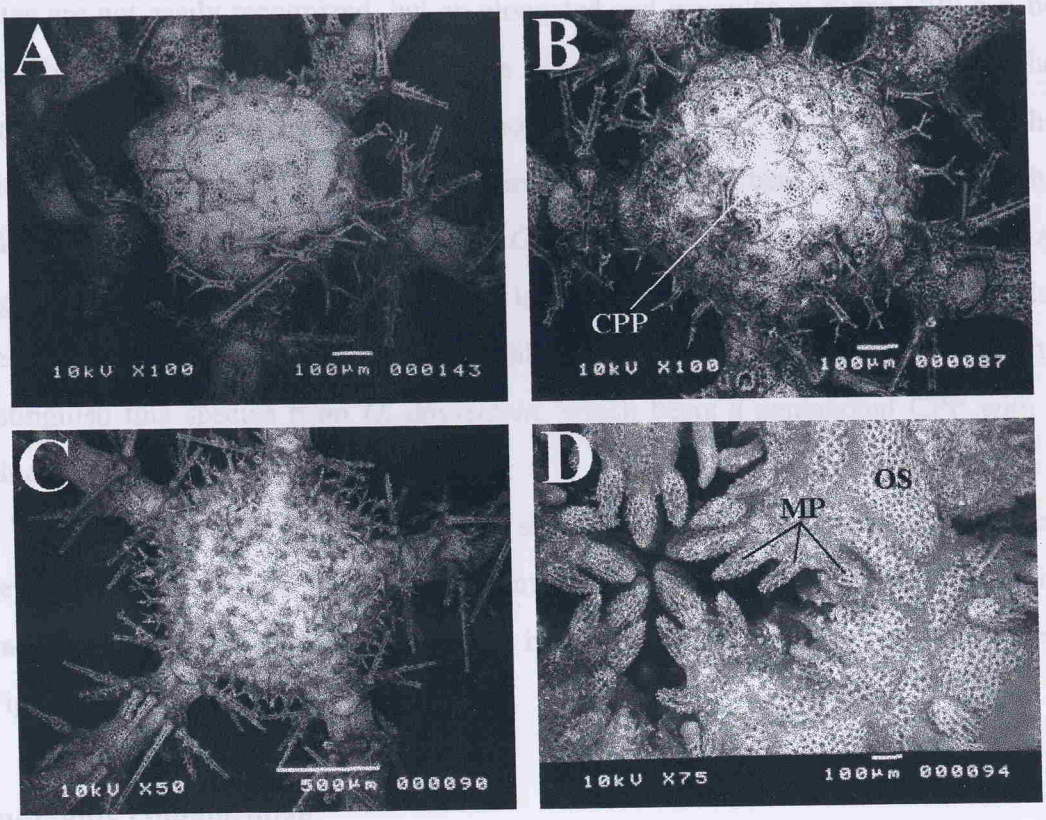
A
10kV X100
100µm 000143
B
CPP
10kV X100
100µm 000087
C
10kV X50
500µm 000090
D
OS
MP
10kV X75
100µm 000094

reveals significant differences in the shape of the plates. In this species the primary plates are not easily recognized, but an elongated and irregular in shape CPP can be seen, bearing two spines similar to those described earlier for *O. abyssicola*. The dorsal plates have scattered tiny fenestrations and larger ones on the areas below the spines. The dorsal plates are all irregular in shape and most bear just one spine. The RSs are similar to those described for *O. abyssicola*. The arms possess several segments (> 4) with large spines, bearing large spinelets (Fig. 3.4A). At 0.8 mm dd, the irregular CPP (bearing 2 spines) is still visible (Fig. 3.4B) and can be used to distinguish this species from *O. abyssicola*, which bears a pentagonal CPP with 5 spines (Fig. 3.4C).

The early ventral development is very similar to that of *O. abyssicola*. However, they are easily distinguished when the animal attains a larger size by the shape of the oral shields (OS), which in *O. bidentata* is broader than long and no groove is present (Fig. 3.4D).

Subfamily Ophiohelinae

Ophiomyces grandis Lyman, 1878

The smaller specimen of *O. grandis* shows a sac-like disk formed by several scales, some of which bear large smooth spines. The scales of the central part of the disk are largest, becoming smaller toward the edges (Fig. 3.5A). The teeth are bulb-shaped with a pointed end mounted on a large dental plate (DP). Several mouth papillae (MP) are present, all of which have an elongated shape. Two infradental papillae (IP) lie on the DP, three MP on each edge of the jaw and three supplementary papillae on its innermost part and finally one larger papilla is present on the adoral shields. The 2nd tentacle pore (TPo) opens close to the oral slit (Fig. 3.5B).

One long tentacle scale (TS) is present on each TPo of the arms (Fig. 3.5C) when the individual attained a larger size. The distalmost MP has now a wide flattened end. The oral shields (OS) appear as a somewhat diamond-shaped plate (Fig. 3.5D). Further development involves growth and broadening of the papillae and spines (Fig. 3.5E).

Figure 3.5. Some stages of the post-metamorphic development of *Ophiomyces grandis* (A-E). A and C, lateral view; B, D and E, ventral view. T = tooth; IP = infradental papilla; MP = mouth papilla; TPo = tentacle pore; DP = dental plate. See Fig. 3.2 for explanation.

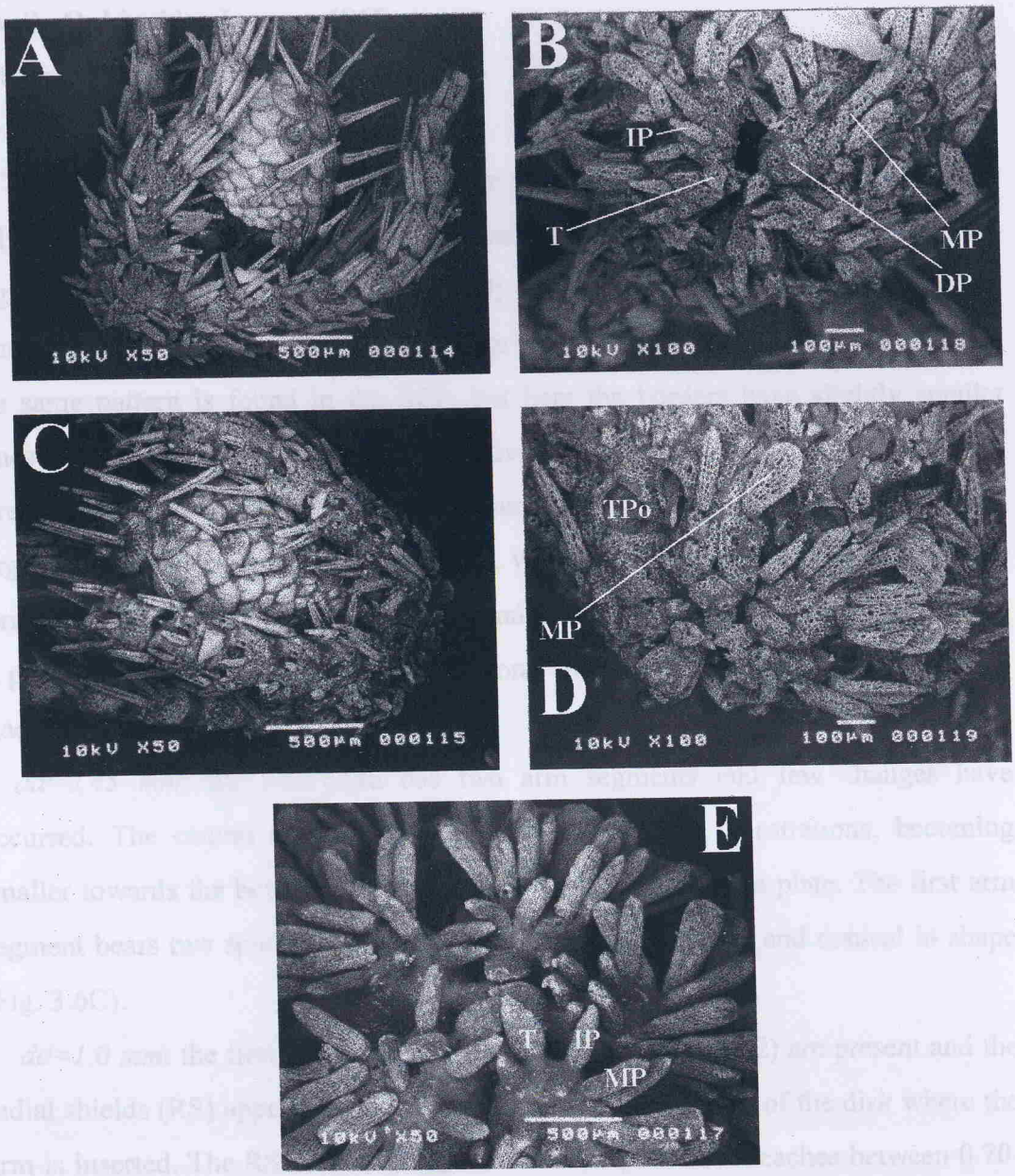
A
10kV X50
500µm 000114
B
IP
T
MP
DP
10kV X100
100µm 000118
C
10kV X50
500µm 000115
TPo
MP
D
10kV X100
100µm 000119
E
T
IP
MP
10kV X50
500µm 000117

Infraorder Chilophiurina Matsumoto, 1915

Family Ophiuridae Lyman, 1865

Subfamily Ophiurinae Lyman, 1865

Ophiura sarsi Lütken, 1858

The smallest individuals examined were about 0.37 mm dd (Fig. 3.6A), bearing only the CPP, the five RPPs on the dorsal side and the TP of the arms. The first arm segment is only visible ventrally (Fig. 3.6B). The CPP has a pentagonal shape and its fenestrations are round, numerous and large throughout the plate and edges. Almost the same pattern is found in the RPP, but here the borders have slightly smaller fenestrations (Fig. 3.6A). The TPs are relatively large, with the distal part possessing three large spines, being regularly fenestrated throughout its length (Fig. 3.6A). A large adoral shield spine (ASS) is present, which is visible dorsally in the smallest forms, as it is directed radially. It is stout and bears many small spinelets (Fig. 3.6B). A protuberance can be seen in one of the oral shields (OS), which distinguishes the madreporite (M) from the remaining OSs.

dd=0.45 mm: the post-larva has two arm segments and few changes have occurred. The central part of the CPP has large round fenestrations, becoming smaller towards the borders and larger again on the edge of the plate. The first arm segment bears two spines and the second, one. They are small and conical in shape (Fig. 3.6C).

dd=1.0 mm: the first and second interradial plates (IR1 and 2) are present and the radial shields (RS) appear as a squared structure on the borders of the disk where the arm is inserted. The RSs begin to appear when the post-larva reaches between 0.70-0.80 mm dd, but they are very small and difficult to observe. The post-larva has already developed several arm joints and the first ventral arm plate (VAP) assumed a pentagonal aspect, with a slightly convex distal edge. The ASSs are not visible dorsally. The first two dorsal arm plates (DAP) are broad and fan-shaped and contiguous, whereas the subsequent DAPs are smaller and non-contiguous (Fig. 3.6E). Three spines are present on the proximal arm joints and two on the distal ones.

dd=2.7 mm: the k-plates (k) were added to the dorsal side, as well as secondary plates among the CPP and RPPs. The outer arm comb (OAC) is well formed on the

Figure 3.6. *Ophiura sarsi* post-larval development (A-H). A, C, E and G, dorsal view; B, D, F and H, ventral view. A. 0.37 mm; B. 0.37 mm. Note the oral shields (OS) on the interradial area; C. 0.45 mm; D. 0.45 mm. Note the appearance of the 1st mouth papilla (the buccal scale - BS) and the massive dental plates (DP); E. 1.0 mm; F. 1.0 mm; G. 2.7 mm; H. 1.5 mm. TPo = tentacle pore; M = madreporite; MP2 = 2nd mouth papilla; k = k-plate; SIR = secondary interradial plates; OAC = outer arm combs. See Fig. 3.2 for further explanation. Sizes represent the disk diameter.

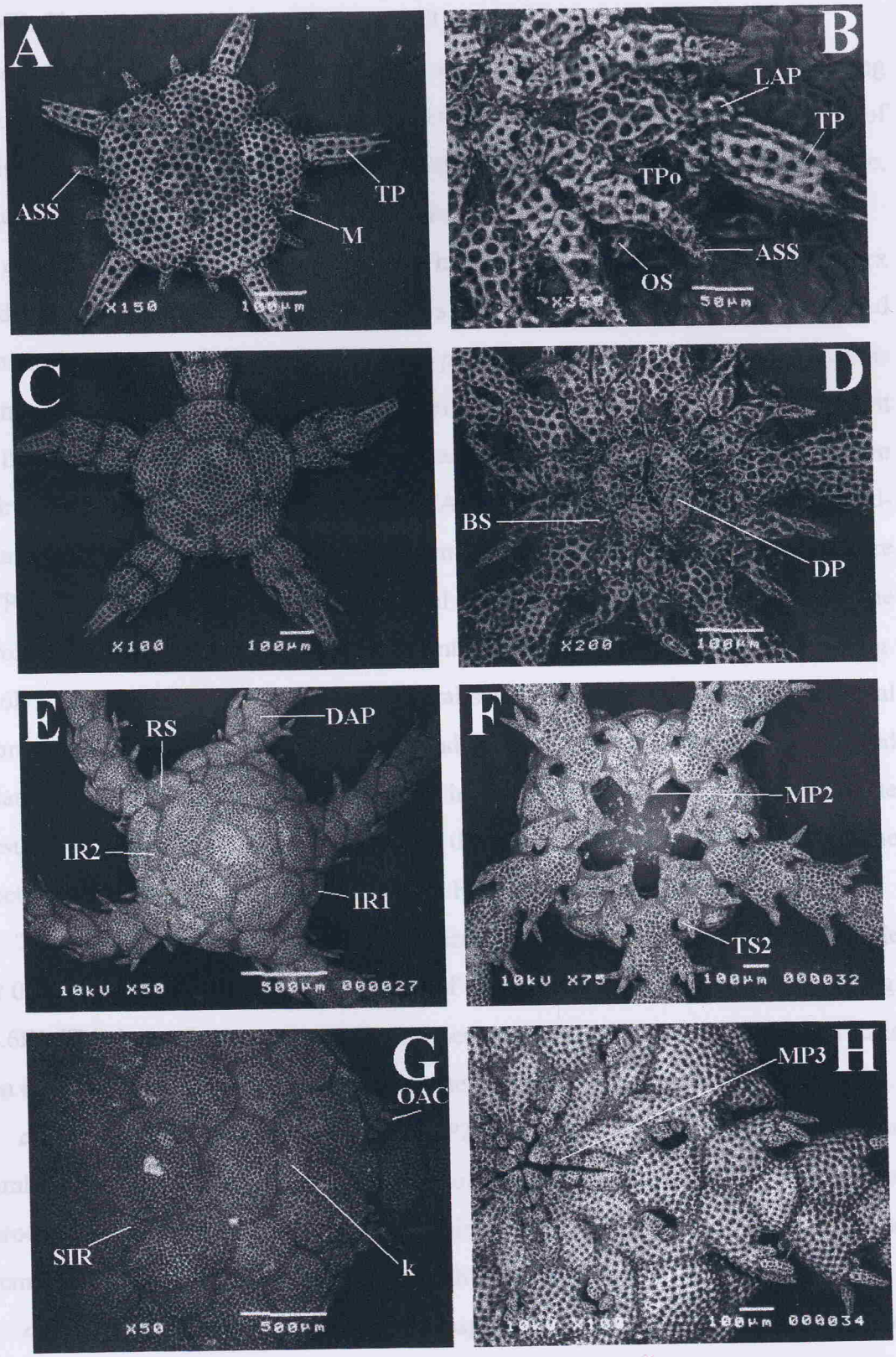
A
ASS
TP
M
X150
100µm
B
LAP
TP
TPo
ASS
OS
X350
50µm
C
X100
100µm
D
BS
DP
X200
100µm
E
RS
DAP
IR2
IR1
10kV X50
500µm 000027
F
MP2
TS2
10kV X75
100µm 000032
G
OAC
SIR
k
X50
500µm
H
MP3
100µm 000034

genital plate and the DAP can be seen intruding between them into the disk (Fig. 3.6G). The secondary interradial plates (SIR) are also seen.

dd=3.8 mm: the arm combs resemble those of the adult, with the comb extending into the disk, as well as the first DAP, which is inserted between the distal end of paired RSs. The RSs are "hexagonal" in shape, with a continuous mid-line suture. Intermediate interradial plates are present on the dorsal side.

dd=0.37 mm: on the oral side, the tooth has a triangular shape with a pointed apex and some accessory spinelets on the borders. The dental plate is large and fenestrated mounted on somewhat rectangular oral plates. Each pair of the oral plates is connected by an interdigitation on the proximal side and no mouth papilla is present at this size. The adoral shields are longer than broad, bearing a spine that is about two thirds its size. The 1st ventral arm plate (VAP) is regularly fenestrated and diamond-shaped, with a small notch resulting from the presence of the 2nd tentacle pore (TPo). The first appearance of the lateral arm plates (LAP) can be seen on the proximal side of the terminal plates. No tentacle scales are present at this stage (Fig. 3.6B). Also visible in this stage are the oral shields (OS), present on the interradial portion, between the distal corners of the adoral shields, as slightly oval, fenestrated plates (Fig. 3.6B). The presence of OSs in the earliest post-larva agree with the results of several authors, who reported the appearance of this plate during the metamorphosis of the larva (Fewkes, 1887; Fell, 1941; Hendler, 1978).

The dental plate (DP) has increased in size and a small buccal scale (BS) is visible at 0.45 mm dd on the proximal outer part of the jaw, occupying its entire length (Fig. 3.6D). This is the first mouth papilla to appear in this species, arising as a small scale on the proximal portion of the oral plate when the animal is around 0.39 mm in dd.

dd=1.0 mm: the 2nd mouth papilla (MP2) is present on the proximal side of the oral plate and the 2nd tentacle scale (TS) of the 2nd tentacle pore (TPo) is a broad process placed next to the adoral shield spine (ASS) (which forms the 1st TS). The remaining TPo of the arms bear one TS each (Fig. 3.6F).

dd=1.5 mm: the genital slits become conspicuous on each side of the arm base, the distal edge of the 1st VAP is straight and a 3rd TS is added to the 2nd TPo, opposite to the other two. The ASS assumes a form of a scale, covering partially the 2nd TPo.

The 3rd mouth papilla (MP3) has also appeared on each side of the dental plate and the tooth is a stronger structure (Figs. 3.6H).

dd=3.8 mm: the three MPs are well developed, with the third being somewhat elongated, about half the size of the tooth. The 1st VAP is almost triangular in shape and the 2nd TPo is elongated, with 6 scales in total on its edges. The oral shields are broad and teardrop-shaped, with a constriction on the proximal third.

Ophiura carnea Lütken, 1858

The smallest post-larvae found in the Biofar samples are around 0.6 mm dd. At this stage, the post-larva has a pentagonal CPP and the five RPPs. Also present are the RSs and the IR1s. A dorsal view reveals the presence of the adoral shield spines (ASS) (Fig. 3.7A). The fenestration pattern in this species is characteristic, the central part of the CPP bears regularly spaced medium-sized circular fenestrations, while the borders have small and more numerous round holes (Fig. 3.7A). The ASSs in *O. carnea* are quite smooth and delicate (Fig. 3.7B), differing from the stout and spinose spines of *O. sarsi* (Fig. 3.6B).

dd=1.2 mm: the IR1s and RSs are much larger in size and the IR2 is already present. The RSs are almost square in shape (Fig. 3.7C). The relative size of the CPP is much smaller in this species at this stage than that of *O. sarsi*.

dd=1.8 mm: the interradial plates are well developed, the RSs begin to elongate and the k-plate (k) is present, but small (Fig. 3.7E). The outer arm combs (OAC) are visible on the genital plates (Fig. 3.7E).

dd=2.9 mm: the animal has the adult characteristics. The outer and inner combs grow towards the interior of the disk and the dorsal arm plate intrudes into the disk with an elongated shape. The k-plate attained a large size, being broad triangular in shape. Adjacent to the k-plate are intermediate interradial plates (IIR). Secondary interradial plates (SIR) can be seen among the primary plates (Fig. 3.7G).

On the ventral side, the individual at 0.6 mm dd bears a fully developed mouth papilla (= buccal scale), which is present on the oral plate throughout the oral slit. Its outer part possesses small spinelets on the border. The tooth is triangular in shape, spinulose, bearing large fenestrations. The dental plate is large and trapezoidal (Fig. 3.7B). The ASS is a quite long and slender process with squared fenestrations and

pointed radially. The 1st VAP is arrow-shaped with a slight notch on each of its distal lateral sides, where the 2nd tentacle pores are inserted. A very small OS can be seen among the distal of the adoral shields and the IR1 (Fig. 3.7B).

dd=1.3 mm: the OSs have a teardrop shape and the ASSs changed in form to a small scale-like structure forming the tentacle scales of the 2nd tentacle pores. The genital slits are clearly visible. The small 2nd mouth papilla (MP) lies on the proximal part of the first one (Fig. 3.7D). The 3rd MP is present when the individual is 1.8 mm dd. At this stage, the tentacle pore begins to elongate, possessing 2 tentacle scales on each side (Fig. 3.7F).

dd=2.9 mm: the oral frame is well formed with large teeth and a 4th MP. The second tentacle pore is very elongated with four tentacle scales on each side, almost inside the oral slit. The outer arm comb is clearly visible on the genital plate and the oral shields are more elongated (Fig. 3.7H).

Ophiura ljungmani (Lyman, 1878)

dd=0.52 mm: the dorsal side bears a pentagonal CPP and 5 RPPs, which have large fenestrations in the centre and smaller in the borders (Fig. 3.8A). Some fenestrations are irregular in shape and some are round. The disk is slightly pentagonal with a notch on the outer part of the junction between the RPPs. Three arm segments are present with two spines on each side and the TPs. Those are large and strong, with rows of fenestrations running along their length (Fig. 3.8A).

dd=0.6 mm: only the primary plates are present, but larger in size and with larger fenestrations on the centre of the plate and smaller ones on the edges. The notch between the RPPs is less pronounced. The arm spines are relatively small and slender, bearing very small spinelets.

dd=1.0 mm: the IR1 can be seen from above, as well as a slight signal of the radial shields on the sides of the arm, alongside the disk edge. The stereom structure of the plates remains the same, although the plates are bigger in size (Fig. 3.8E).

dd=1.5 mm: individuals have well-developed primary plates, the IR1 and 2 plates and radial shields. The dorsal arm plates are bell-shaped, with the 1st being broader than the subsequent ones. The shape of the CPP is more round on the corners (Fig. 3.8G).

Figure 3.7. *Ophiura carnea* post-larval development (A-H). A, C, E and G, dorsal view; B, D, F and H, ventral view. A. 0.6 mm; B. 0.6 mm; C. 1.2 mm; D. 1.3 mm; E. 1.8 mm; F. 1.8 mm; G. 2.9 mm; H. 2.9 mm. OAC = outer arm combs; k = k-plates; M = madreporite; MP2-4 = 2nd-4th mouth papilae; SIR = secondary interradial plates; IIR = intermediate interradial plates. See Fig. 3.2 for further explanation. Sizes represent the disk diameter.

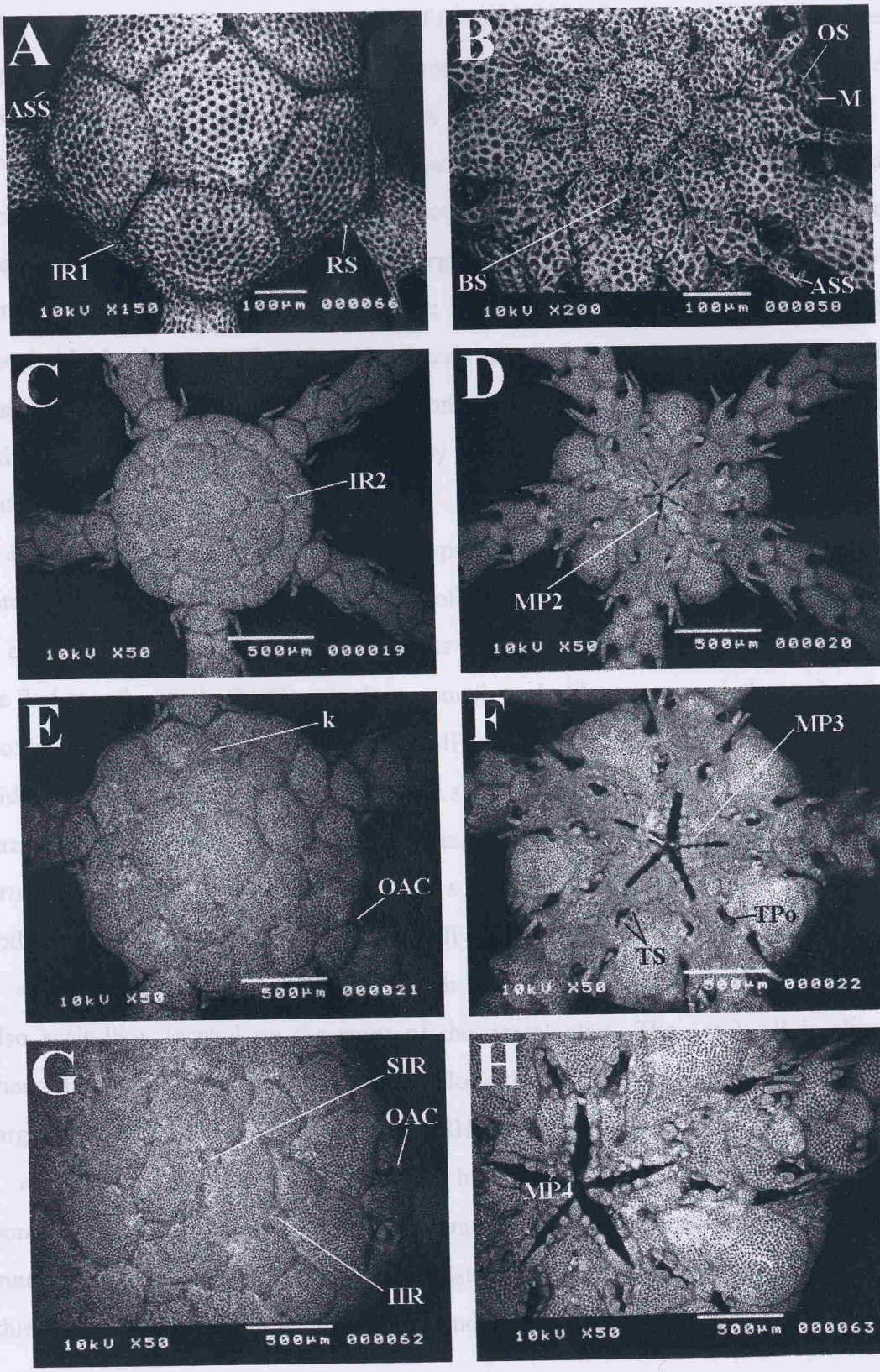
A
ASS
IR1
RS
10kV X150
100µm 000066
B
OS
M
BS
ASS
10kV X200
100µm 000058
C
IR2
10kV X50
500µm 000019
D
MP2
10kV X50
500µm 000020
E
k
OAC
10kV X50
500µm 000021
F
MP3
TP6
TS
10kV X50
500µm 000022
G
SIR
OAC
IIR
10kV X50
500µm 000062
H
MP4
10kV X50
500µm 000063

dd=2.7 mm: the CPP assumed an almost circular outline and secondary interradial scales are present on the point of contact of the CPP and RPPs. The radial shields are longer, and a relatively large k-plate is present between the proximal portions of the RSs, separating almost half of their mid-line suture.

Ventrally, the early 0.52 mm dd post-larva is very similar to the other *Ophiura* species described above. The tooth is broadly triangular and pointed, with some small spinelets and the dental plate is a large, fenestrated structure, with a v-shaped distal edge. A large and block-like mouth papilla is present (= buccal scale). The adoral shield spine is small and stubby, bearing some small spinelets along its edge. The first VAP is pointed proximally and convex distally. The oral shields are present and the madreporite (M) is distinguished by a protuberance in one of the sides of the plate (Fig. 3.8B).

dd=0.6 mm: the first VAP changes shape, having a straight distal portion and a notch on each side, related to the presence of the second tentacle pore (Fig. 3.8D).

dd=1.0 mm: the mouth structure presents a much stronger and spinulose tooth and the 2nd mouth papilla (MP2), which is a small, scale-like structure, is located at the proximal end of the 1st mouth papilla (MP). The 1st VAP distal portion is much wider with numerous, regularly distributed small fenestrations, whereas the proximal three quarters presents larger fenestrations, arranged in a more complex stereom structure. The ASS forms the 1st tentacle scale of the 2nd tentacle pore (TPo), and both oral shields and IR1 are visible ventrally (Fig. 3.8F).

dd=1.5 mm: a 3rd MP is formed, which is slightly smaller than the 2nd MP and also scale-like, located on the sides of the dental plate. The 1st VAP is almost triangular and the 2nd TPo bear 3 scales along their outer edge. The oral shields are large, resembling a broad teardrop (Fig. 3.8H).

dd=2.7 mm: the oral structure is more heavily calcified and the second tentacle pore is enlarged and is almost inside the mouth, bearing an additional scale on the inner edge. The 1st VAP has a convex distal edge pointed in the middle. The oral shield is broader with a pointed proximal and rounded distal portion.

Figure 3.8. Post-larval development of *Ophiura ljungmani* (A-H). A, C, E and G, dorsal view; B, D, F and H, ventral view. A. 0.4 mm. Note the shape and fenestration pattern of the primary plates and the elongated terminal plates (TP); B. 0.4 mm; C. 0.6 mm; D. 0.6 mm; E. 1.0 mm; F. 1.0 mm. Note the fenestration pattern of the 1st ventral arm plate; G. 1.5 mm; H. 1.5 mm. M = madreporite; MP2-3 = 2nd and 3rd mouth papillae. See Fig. 3.2 for further explanation. Sizes represent the disk diameter.

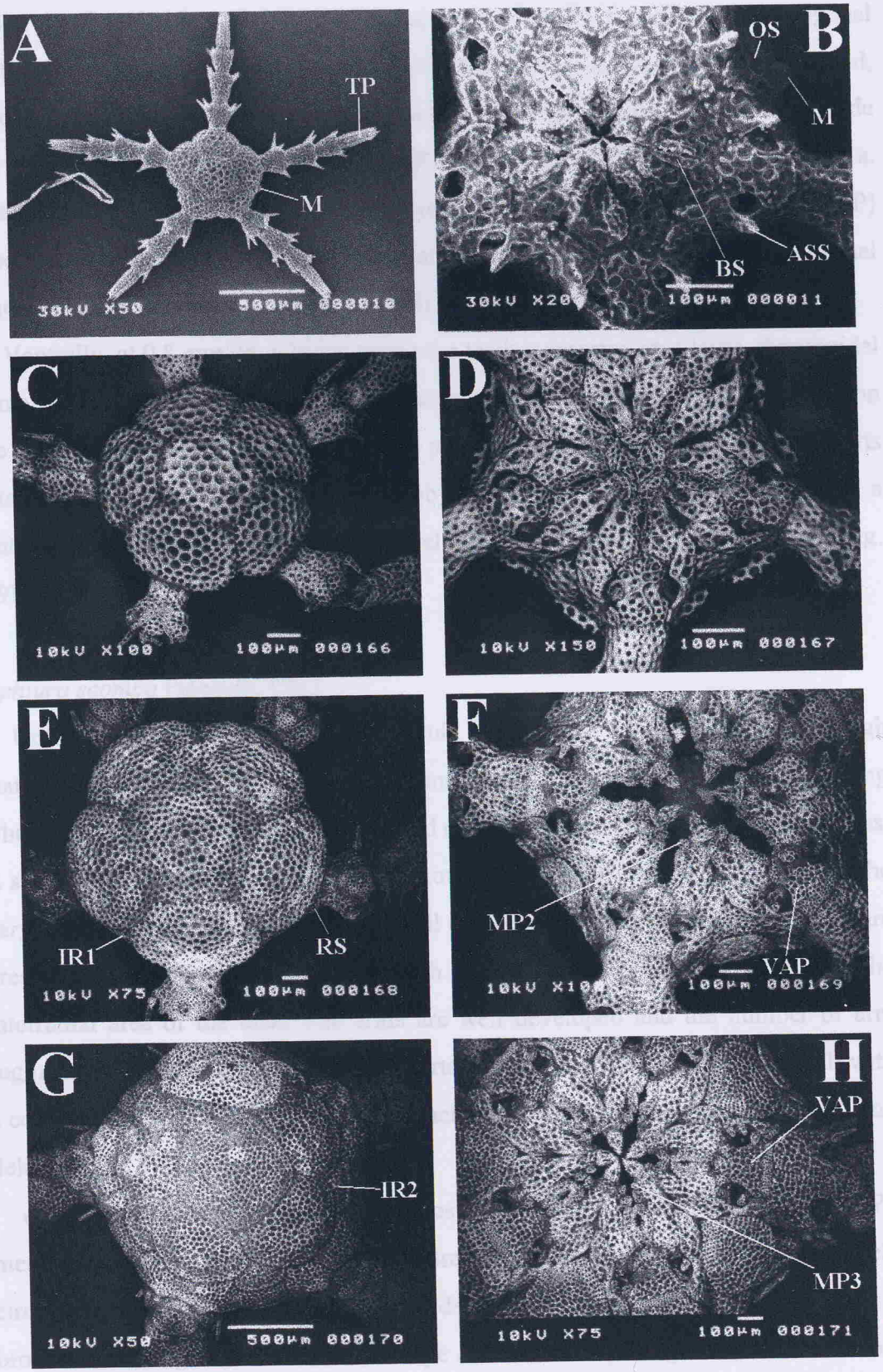
A
TP
M
30kV X50
500µm 000010
B
OS
M
BS
ASS
30kV X20
100µm 000011
C
10kV X100
100µm 000166
D
10kV X150
100µm 000167
E
IR1
RS
10kV X75
100µm 000168
F
MP2
VAP
10kV X10
100µm 000169
G
IR2
10kV X50
500µm 000170
H
VAP
MP3
10kV X75
100µm 000171

Ophiura albida (Forbes, 1839)

On the dorsal side at 0.6 mm dd the specimen has the 5 RPP and a pentagonal CPP, with a complex stereom structure, but apparently the original plate bears round, medium-sized fenestrations on the centre and smaller ones on the borders. Alongside the edge of the disk, strongly rectangular RSs are present and very pronounced IR1s. The arms are quite broad and strong (4 joints), with the dorsal arm plates (DAP) much broader than long. Two arm spines are present on each arm joint. The terminal plates (TP) are somewhat bulb-shaped with several fenestrations (Fig. 3.9A).

Ventrally, at 0.8 mm dd, a broad triangular teeth is inserted on a large, rhomboidal dental plate. Only one large, block-like mouth papilla (= buccal scale) is present on the side of the oral plates. The 1st VAP is pentagonal in shape and on its lateral parts a tentacle pore is present, with one stubby adoral shield spine (ASS) placed as a tentacle scale. The oral shield (OS) is well developed, resembling a teardrop (Fig. 3.9B).

Ophiura scomba Paterson, 1985

Unfortunately only few specimens could be obtained from the Rockall Trough material. The smallest post-larva is 1.0 mm dd and bears the primary plates, among which the CPP is pentagonal with rounded corners and has large, ovoid fenestrations. A second layer of stereom is deposited throughout the CPP, with the exception of the very edges of the plate. The RPPs are well conformed with the arms and the RSs are present on the borders of the disk, on each side of the arm. The IR1 is visible on the interradial area of the disk. The arms are well developed and the number of arm segments could not be determined, but certainly exceeds 3. The DAPs are small with a convex distal line and separated from each other; the arm spines are very small and delicate (Fig. 3.10A).

dd=1.5 mm: secondary interradial scales are present on the corners where the CPP meets the adjacent RPPs. The CPP is more circular in shape now and is completely circular at 2.6 mm dd. The IR2 is well developed and the RSs grew larger and is broader than long now. The outline shape of the disk is pentagonal and the stereom structure did not change (Fig. 3.10C).

Figure 3.9. Early stages of the post-larval development of *Ophiura albida* (A-B). A. Dorsal view of a 0.8 mm specimen; B. Ventral view of a 0.8 mm specimen. See Fig. 3.2 for explanation. Sizes represent the disk diameter.

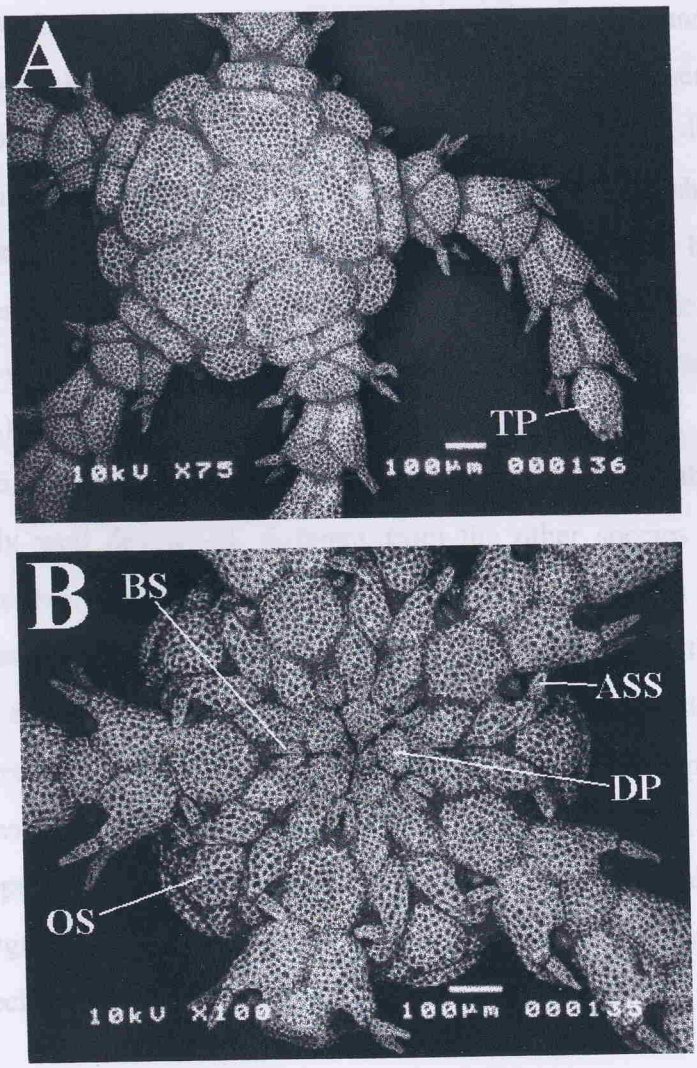
A
TP
10kV X75
100µm 000136
B
BS
ASS
DP
OS
10kV X100
100µm 000135

Ventrally, the structure of the body is very similar to those of the other *Ophiura* species examined so far. At 1.0 mm dd the tooth is a strong process and 3 MP are present, a large block-like papilla that covers most of the oral slit; a second small, scale-like papilla on the proximal side of the jaw; and a third spine-like papilla, which is best seen in figure 3.10B. The 1st VAP has a double-arrowed shape and the fenestrations do not differ in size like in *O. ljungmani*. Its lateral sides bear a notch owing to the presence of the 2nd tentacle pores, which have one scale (the adoral shield spine). The oral shield is present on the interradial area, between the adoral shields (Fig. 3.10B).

dd=1.5 mm: the mouth papillae are much better formed, with the third papillae being exceptionally well developed, different from the other species of *Ophiura* studied here at this size. The 2nd tentacle pore now has 3 broad scales on the outer and 1 on the inner edge, and is closer to the oral slit. As a result, the 1st VAP changed in shape showing a much broader distal portion, with its middle portion pointed and a narrower proximal side. The oral shield is well developed, with the shape of a broadened teardrop. The 3rd tentacle pore has 2 broad scales (Fig. 3.10D).

Further development could not be depicted, since the specimens did not yield good electromicrographs, however, no larger differences in the development from the other *Ophiura* species occurred up to 2.6 mm dd.

Ophiocten affinis (Lütken, 1858) comb. nov.

Individuals with a disk diameter of 0.68 mm were obtained from the Biofar samples. On the dorsal surface the CPP is pentagonal and five RPPs are present at 0.8 mm dd. The RSs are much broader than long and between paired RSs the IR1 and 2 are clearly seen. Among the primary plates a small plate, the secondary interradial plate (SIR), is present. The arms are well developed, bearing two medium-sized spines. The spines are smoother in smaller animals (Fig. 3.11B) and become slightly thicker in the larger ones (Fig. 3.11A). The first dorsal arm plate (DAP) is broad and short, and the subsequent plates are longer and fan-shaped (Fig. 3.11A).

dd=1.3 mm: several secondary scales (ss) surround the primary plates, but these are still very conspicuous. The RSs are larger and the k-plate (k) is present on the suture line between paired RSs. The intermediate interradial plate lies between that

Figure 3.10. Two stages of the post-larval development of *Ophiura scomba* (A-D). A and C, dorsal view; B and D, ventral view. A and B. 1.0 mm; C and D. 1.5 mm. SIR = Secondary interradial plate; ss = secondary scales; TS = tentacle pore scale. See Fig. 3.2 for explanation. Sizes represent the disk diameter.

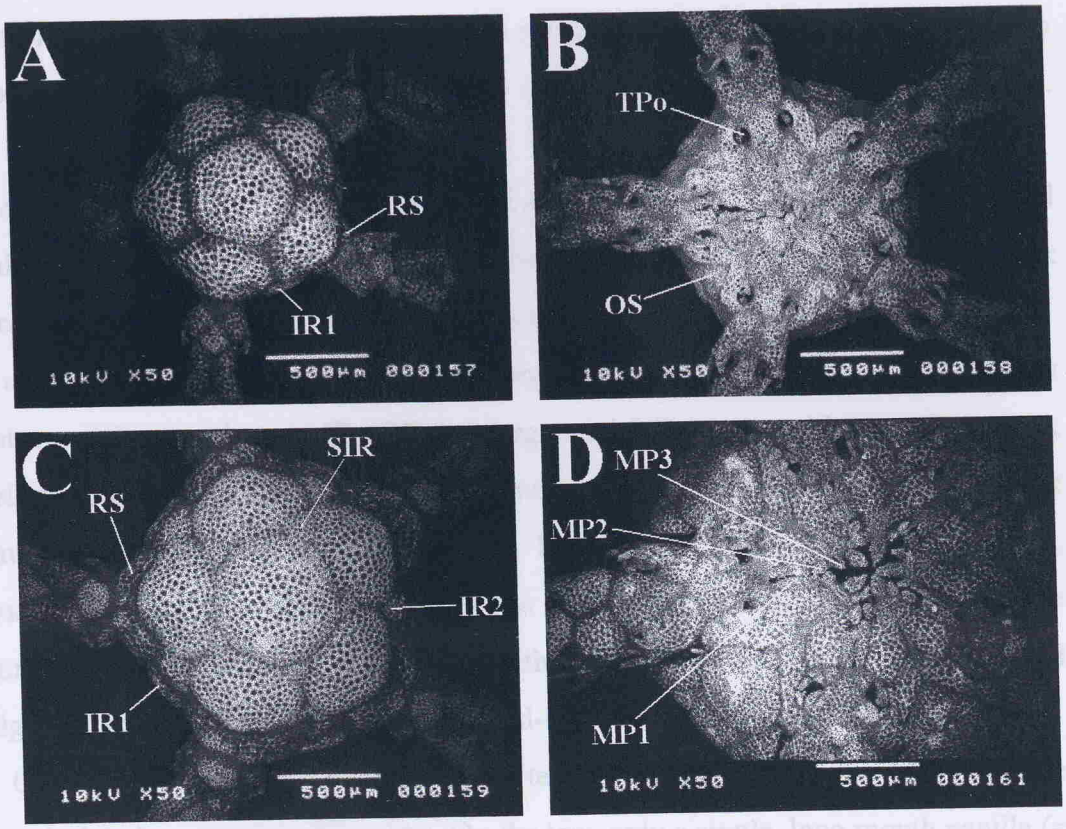
A
RS
IR1
10kV X50
500µm 000157
B
TPo
OS
10kV X50
500µm 000158
C
SIR
RS
IR2
IR1
10kV X50
500µm 000159
D
MP3
MP2
MP1
10kV X50
500µm 000161

and the RS. The DAPs are now contiguous and elongated, with the exception of the first plate, which is much smaller than the subsequent ones. The arm combs start to appear on each side of the arm as a small spine on the outer edge of the RSs (Fig. 3.11C).

dd=2.0 mm: all the plates on the dorsal side of the disk are surrounded by small scales. The disk is circular in shape and only a very slight notch is present on the disk borders over the arm bases. The arm combs are more developed (Fig. 3.11E).

dd=3.0 mm: a larger number of secondary scales are present, although the primary plates remain conspicuous. The RSs are larger and fully separated by small scales. A well-pronounced notch in the disk edge is now present over the arm bases. The outer comb is well developed, bearing small, blunt spines. The first DAP is small, possessing small spinelets arranged in a row (V-shaped) forming the inner comb. The remaining DAPs are broader than long, with the distal border convex and a rounded ridge running along the arm axis on the mid-line of the plate (Fig. 3.11G).

On the ventral side at 0.68 mm dd, the teeth are triangular, thin and pointed. The dental plate is somewhat ellipsoidal. On the jaw, only a single, long mouth papilla (= buccal scale) is present, covering the entire length of the oral gap. The adoral shields are longer than broad, bearing a relatively small spine beside the 2nd tentacle pore (TPo). The oral shields (OS) are large triangular structures. The 1st VAP is a broad arrow-shaped plate with a straight distal end. The arm spines are relatively large and slender, nearly two thirds the size of the arm joint (Fig. 3.11B).

dd= 1.0 mm: the 2nd mouth papilla (MP) is present and the first sign of the apppearance of the 3rd MP is noticed (Fig. 3.11D). The 1st VAP, although with the same shape, has now two distinct fenestration patterns, with distal portion bearing small, regularly distributed fenestrations, whereas in the rest of the plate the fenestrations are larger and irregularly distributed. The adoral shield spine starts to change in form to a scale-like structure. The bursal slit is well developed at that stage (Fig. 3.11D).

dd=2.0 mm: all the three MP are well formed and the OSs assume the elongated shape found in the adult. The 1st VAP is almost rectangular in shape and the tentacle pores bear one scale (Fig. 3.11F).

Figure 3.11. Post-larval development of *Ophiocten affinis* comb. nov. (A-H). A, C, E and G, dorsal view; B, D, F and H, ventral view. A. 0.8 mm; B. 0.68 mm; C. 1.3 mm. Note the secondary scales (ss) surrounding the primary plates; D. 1.0 mm; E. 2.0 mm. Note the slight notch in the disk over the bases of the arms; F. 2.0 mm; G. 3.0 mm; H. 3.0 mm. MP1-4 = 1st-4th mouth papillae; SIR = secondary interradial plates; IR3 = interradial plate 3; k = k-plate; OAC = outer arm combs; TPo = 2nd tentacle pore; TS = tentacle scale. See Fig. 3.2 for further explanation. Sizes represent the disk diameter.

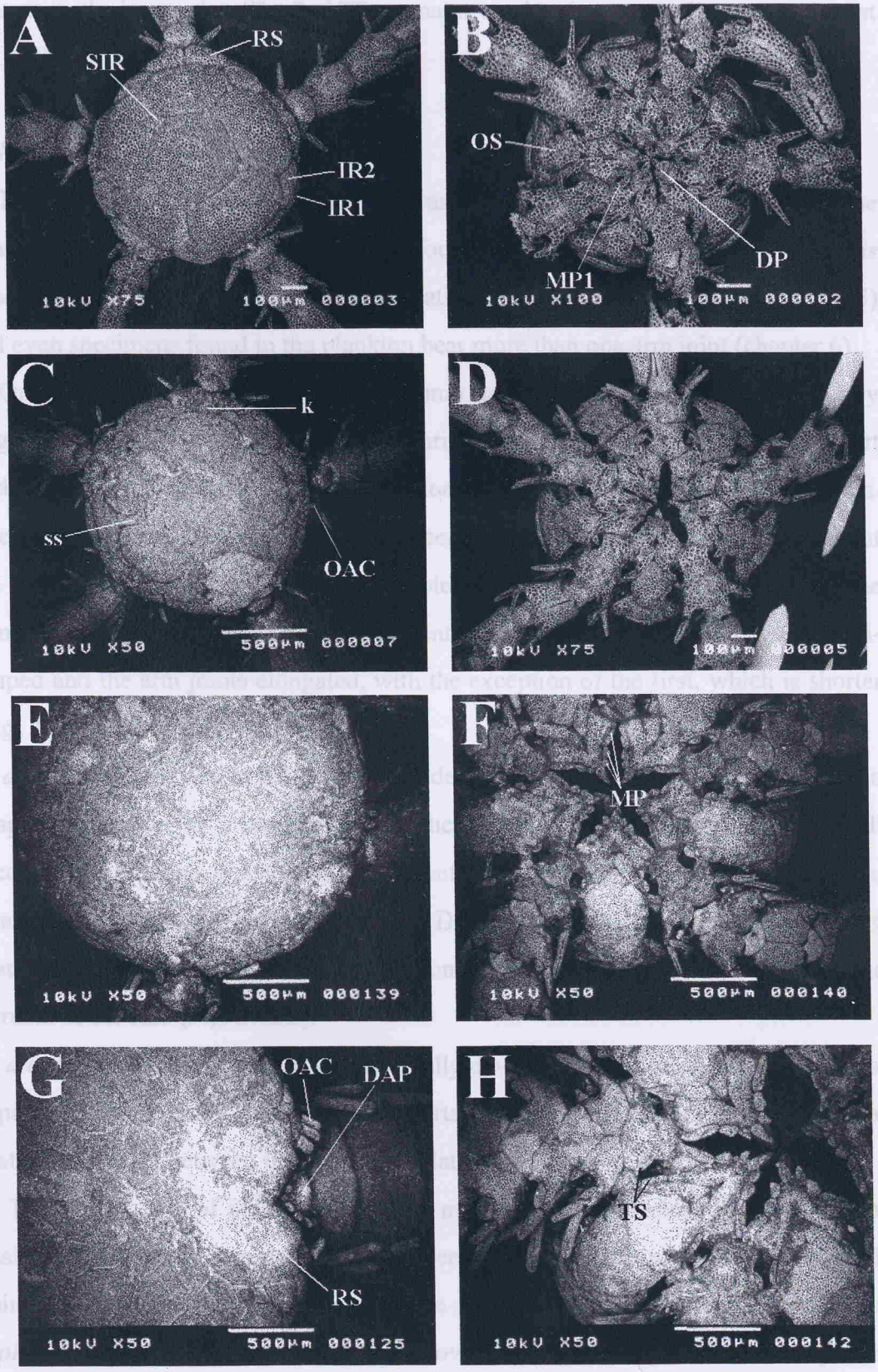
A
SIR
RS
IR2
IR1
10kV X75
100µm 000003
B
OS
MP1
DP
10kV X100
100µm 000002
C
k
ss
OAC
10kV X50
500µm 000007
D
10kV X75
100µm 00005
E
10kV X50
500µm 000139
F
MP
10kV X50
500µm 000140
G
OAC
DAP
RS
10kV X50
500µm 000125
H
TS
10kV X50
500µm 000142

dd=3.0 mm: the outer scale of the 2nd TPo is elongated and an additional scale is present on the inner edge. The 2nd TPo remains outside the mouth slit, next to the 1st VAP (Fig. 3.11H).

Ophiocten gracilis (G.O. Sars, 1871)

This is a common species in the Northeast Atlantic (Paterson *et al.*, 1982). In the Biofar material the smallest post-larvae found measured 0.48 mm dd. *O. gracilis* appears to settle on the sediment with a relatively high number of arm segments (~5) and even specimens found in the plankton bear more than one arm joint (chapter 6).

On the dorsal side, specimens at 0.65 mm dd have five broad RPPs and a very large pentagonal CPP with a solid edge bearing tiny fenestrations and the central part with irregularly distributed small fenestrations, becoming larger towards the borders. The RPPs have a similar border, but the central fenestrations are larger throughout the plate. The IR1 is present but not visible dorsally. The RSs are very small. The arms bear two large spines on each segment. The dorsal arm plates (DAP) are bell-shaped and the arm joints elongated, with the exception of the first, which is shorter (Fig. 3.12A).

dd=1.2 mm: the IR1 and IR2 are well developed and the RSs are rectangular in shape. The k-plate (k) is present between the RSs. Among the primary plates a small secondary interradial plate (SIR) is present. The arm spines are longer and 3 in number on the proximal segments. The 1st DAP is short and broad and the remaining plates are very elongated. The outer arm combs (OAC) first appear as a spine on the borders of the RSs (Fig. 3.12C).

dd=1.5 mm: the arm combs are more fully developed, the k-plate is larger, almost separating the adjacent RSs. The IR3 starts to appear and intermediate interradial plates are present between the interradial plates and RSs (Fig. 3.12E).

The ventral side of individuals at 0.48 mm dd is well developed and all ventral ossicles have large fenestrations. The teeth are pointed, triangular with small spinelets on each side. The dental plate is ellipsoidal, very similar to that of *Ophiocten affinis*. A large mouth papilla covers the whole length of the outer part of the oral plate. The 1st VAP is arrow-shaped, but its proximal edge is strongly convex and its distal edge is slightly convex; on each side a deep notch leaves a way for the

Figure 3.12. Post-metamorphic development of *Ophiocten gracilis* (A-F). A, C and E, dorsal view; B, D and F, ventral view. A. 0.65 mm; B. 0.48 mm. Note the ellipsoid dental plate; C. 1.2 mm; D. 0.45 mm. Note the fenestration pattern of the 1st ventral arm plate; E. 1.5 mm; F. 1.6 mm. MP1-4 = 1st-4th mouth papillae; SIR = secondary interradial plates; IR3 = interradial plate 3; OAC = outer arm combs; k = k-plate. See Fig. 3.2 for further explanation. Sizes represent the disk diameter.

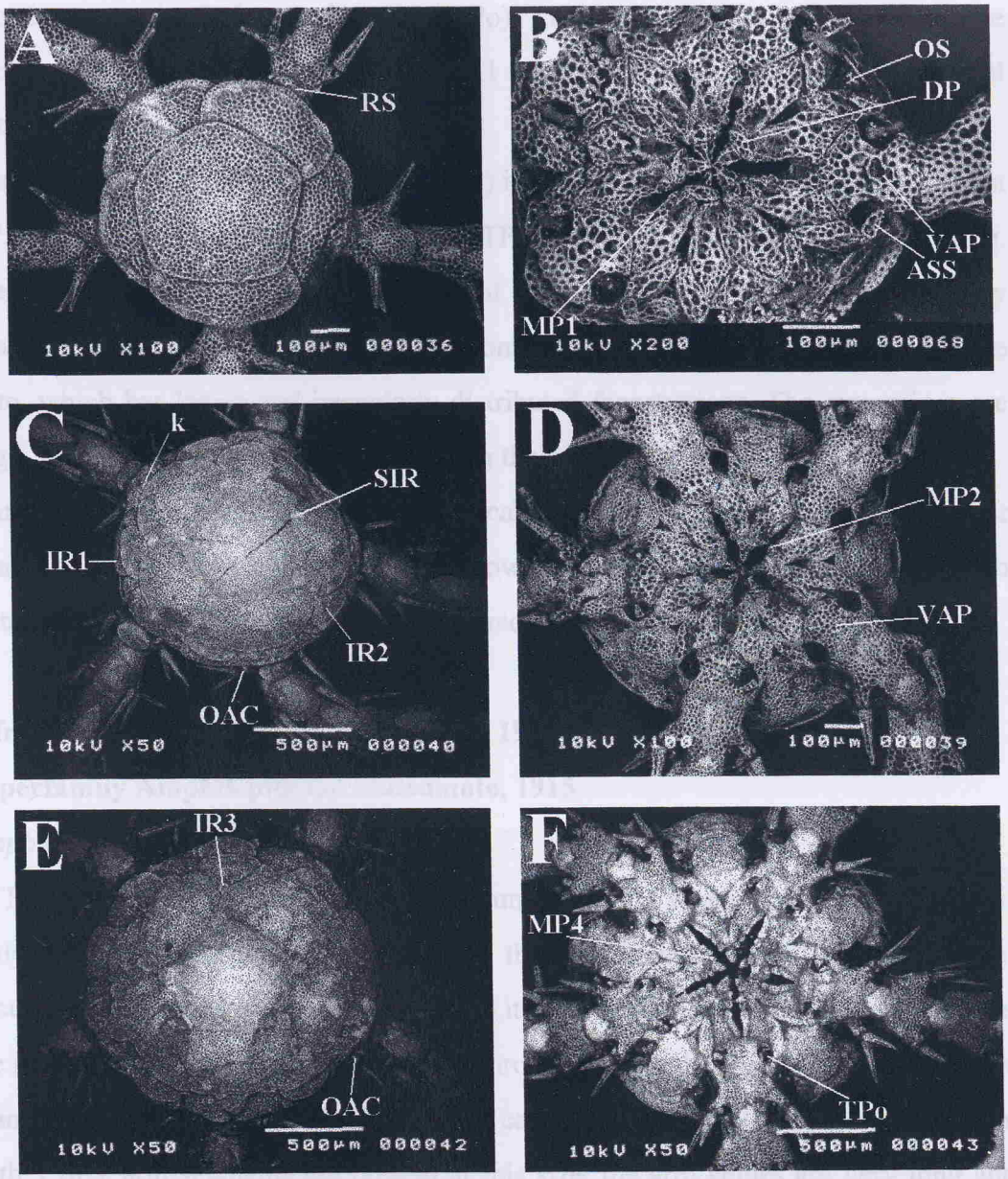
A
RS
10kV X100
100µm 000036
B
OS
DP
VAP
ASS
MP1
10kV X200
100µm 000068
C
k
SIR
IR1
IR2
OAC
10kV X50
500µm 000040
D
MP2
VAP
10kV X100
100µm 000039
E
IR3
OAC
10kV X50
500µm 000042
F
MP4
TPo
10kV X50
500µm 000043

second tentacle pore. The adoral shield spine (ASS) is small with large fenestrations, placed next to the 2nd tentacle pores (TPo). The oral shield (OS) is a small plate among the adoral shields and IR1. The IR1 is larger, but not yet seen on the dorsal part (Fig. 3.12B).

dd=0.9 mm: the 2nd mouth papilla (MP) is present on the proximal side of the 1st MP. The ASS lies by the edge of the 2nd TPo forming a tentacle scale (Fig. 3.12D). The OSs are larger and the distal border of the 1st VAP become straight with very small and regularly distributed fenestrations, differing from the remainder of the plate, which has larger and irregularly distributed fenestrations. The arm spines are large, with small spinelets distributed along their edge (Fig. 3.12D).

dd=1.6 mm: the teeth are more heavily calcified, the 3rd MP is present as another small scale-like ossicle. The 1st VAP now is almost rectangular in shape. Two tentacle scales are present on the 2nd TPo and only one on the others (Fig. 3.12F).

Infraorder Gnathophiurina Matsumoto, 1915

Superfamily Amphilepididae Matsumoto, 1915

Amphilepis ingolfiana Mortensen, 1933

The smallest post-larva measured 0.6 mm dd and its shape is readily recognized. Only the primary plates are present in this specimen, the CPP is very large, occupying almost the entire dorsal side and its central part is raised. The fenestrations are medium-sized and evenly distributed throughout the plate. The RPPs are broader than long and the stereom structure of its central part is slightly denser. Specimens with 1 or 2 arm segments are present at this size; the arm spines are very long and slender, with rectangular fenestrations running along its length. The terminal plate (TP) is thin and larger than the arm segments (Fig. 3.13A).

dd=1.0 mm: the IR1s are visible on the interradial area and the elevation on the CPP almost disappeared. However, all six primary plates have a more solid stereom structure on their central parts. The dorsal arm plates (DAP) are fan-shaped and the arm spines are the same size of the arm segments, with the exception of the first (Fig. 3.13C).

Figure 3.13. Post-metamorphic development of *Amphilepis ingolfianal* (A-H). A, C, E and G, dorsal view; B, D, F and H, ventral view. A. 0.6 mm. Note the raised central portion of the central primary plate and the large terminal plates (TP); B. 0.6 mm; C. 1.0 mm; D. 1.0 mm; E. 1.5 mm; F. 1.5 mm; G. 3.5 mm; H. 3.5 mm. ASp = arm spines; MP2 = 2nd mouth papilla; k = k-plate. See Fig. 3.2 for further explanation. Sizes represent the disk diameter.

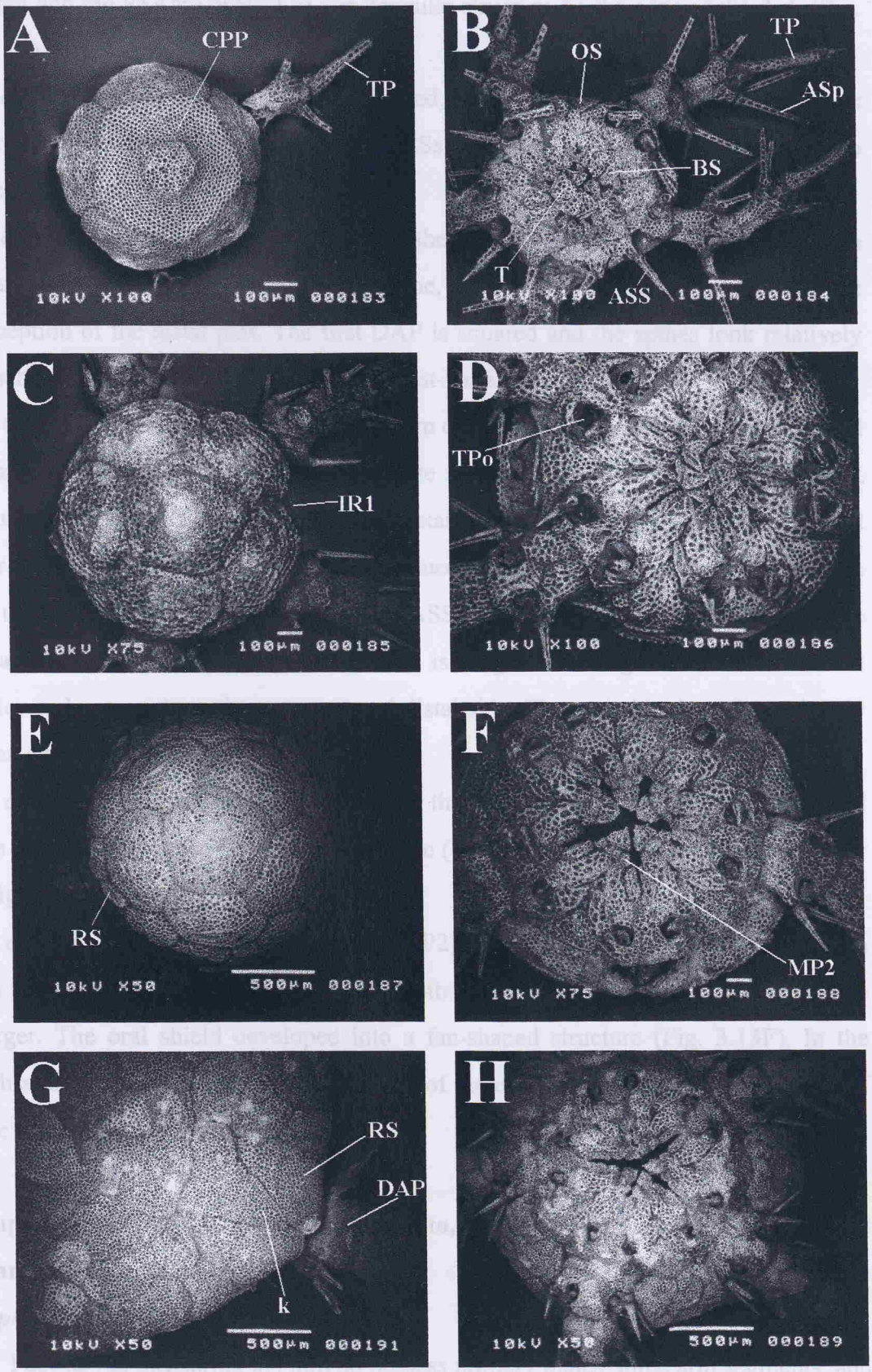
A
CPP
TP
10kV X100
100µm 000183
B
OS
TP
ASp
BS
T
ASS
10kV X100
100µm 000184
C
IR1
10kV X75
100µm 000185
D
TPo
10kV X100
100µm 000186
E
RS
10kV X50
500µm 000187
F
MP2
10kV X75
100µm 000188
G
RS
DAP
k
10kV X50
500µm 000191
H
10kV X50
500µm 000189

dd=1.5 mm: the RPPs bear a kind of scar almost in the centre. The IR1 is much larger and the RSs are present as a rectangular structure on the edge of the disk (Fig. 3.13E).

dd=2.0 mm: the IR2 has already appeared, as well as the k-plate (k), which stands between the proximal parts of the paired RSs. Intermediate interradial scales are also present.

dd=3.5 mm: more scales are added to the dorsal side and the RSs (triangular in shape now) are almost fully divided by the, now, long, triangular k-plate, with the exception of the distal part. The first DAP is squared and the spines look relatively much smaller than observed in the early post-larva (Fig. 3.13G).

On the ventral side, specimens at 0.6 mm dd present a very large, flat tooth, broad triangular in shape, bearing relatively large fenestrations. This kind of tooth is not found in any of the ophiuroid post-larvae examined. The dental plate is very thin and bar-shaped. A large block-like papilla (= buccal scale) is present covering the whole of the oral slit. The adoral shield spines (ASS) are very large and slender, about one quarter the size of the disk. The 1st VAP is long with a large notch on the lateral sides and convex both the proximal and distal side. The oral shields (OS) are barely seen on the interradial area (Fig. 3.13B).

dd=1.0 mm: the dental plate is thicker, the oral shield is triangular in shape and the ASS stands next to the 2nd tentacle pore (TPo). The first VAP is bell-shaped now (Fig. 3.13D).

dd=1.5 mm: a second mouth papilla (MP2) is present as a small scale-like process on the proximal side of the jaw. The tooth is much stronger and the dental plate larger. The oral shield developed into a fan-shaped structure (Fig. 3.13F). In the subsequent development, the enlargement of the disk and a slight increase in size of the MP2 takes place (Fig. 3.13H).

Superfamily Gnathophiuridea Matsumoto, 1915

Family Ophiactidae Matsumoto, 1915

Ophiactis abyssicola (M. Sars, 1861)

Post-larvae measuring 0.4 mm dd possess primary plates, three arm segments, and the terminal plates (TP). The fenestration pattern consists of large holes of varying

Figure 3.14. Post-larval development of *Ophiactis abyssicola* (A-L). A, C, E, G, I and K, dorsal view; B, D, F, H, J and L, ventral view. A. 0.4 mm. Note the fenestration pattern of the primary plates and the terminal plates (TP); B. 0.4 mm; C. 0.5 mm. Note the 'bridges' formed in the central fenestrations of the primary plates; D. 0.5 mm; E. 1.0 mm; F. 0.9 mm. k = k-plates; M = madreporite; TPo = 2nd tentacle pore; TS2 = 2nd tentacle pore scale. See Fig. 3.2 for further explanation. Sizes represent the disk diameter.

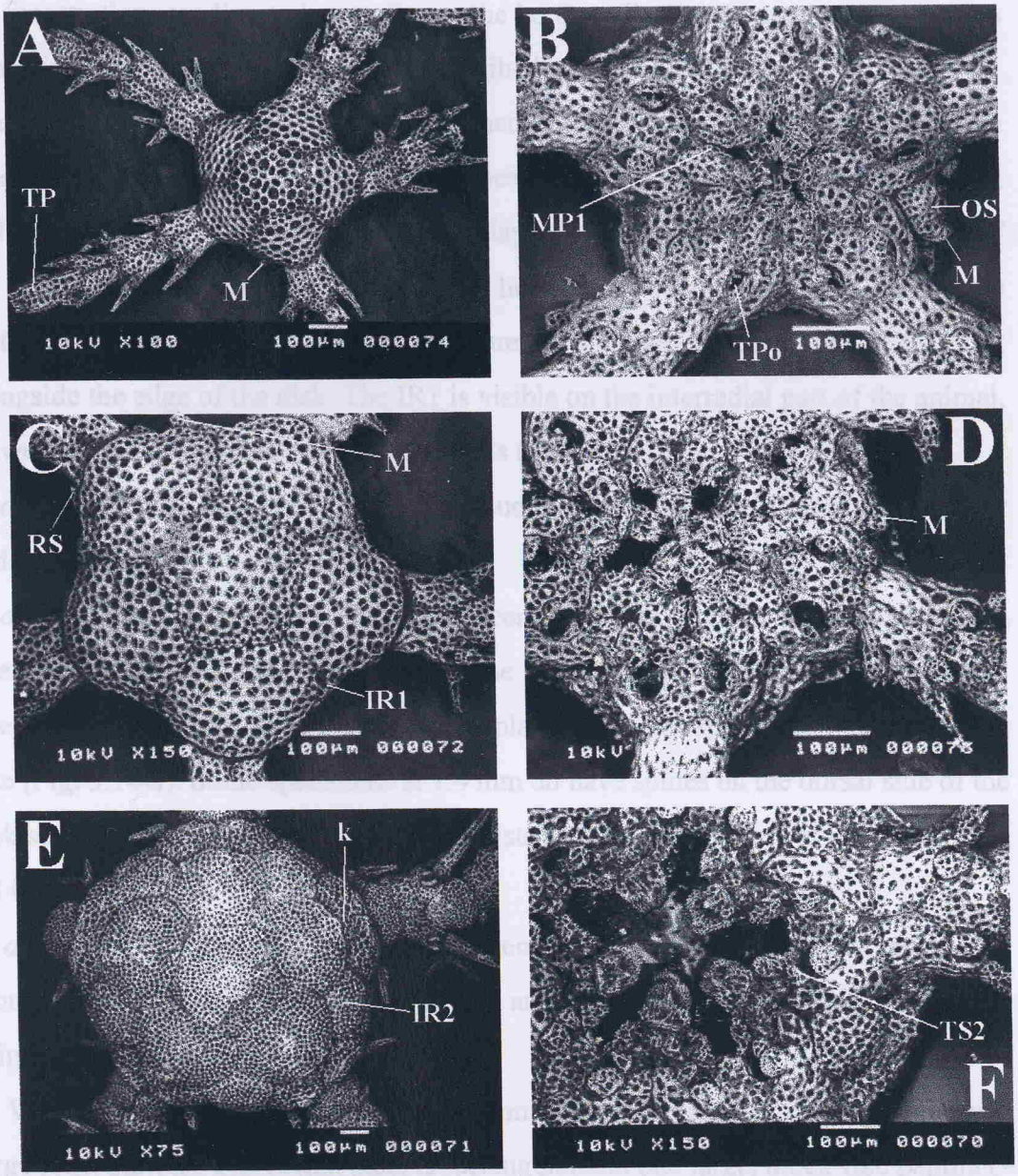
A
TP
M
10kV X100
100µm 000074
B
MP1
OS
M
TPo
100µm
C
M
RS
IR1
10kV X150
100µm 000072
D
M
100µm 000073
E
k
IR2
10kV X75
100µm 000071
TS2
F
10kV X150
100µm 000070

size and shape (from a circular to elipsoidal shape) spread throughout the plate, with the fenestrations tending to be smaller on the borders. Each arm segment possess two arm spines and the TP is fenestrated and bulb-shaped (Fig. 3.14A).

dd=0.5 mm: specimens possess a distinctive dorsal structure with respect to the fenestration pattern. The pentagonal CPP bears large fenestrations in the central part and smaller ones on the borders. A second layer is present over the central portion of the CPP, showing bridges that divide the holes into two or three parts. The same pattern is seen on the 5 RPPs. The RSs are small plates on each side of the arm, alongside the edge of the disk. The IR1 is visible on the interradial part of the animal, between the far corners of the adjacent RPPs (Fig. 3.14C).

dd=1 mm: both IR1 and IR2 are conspicuous on the disk, the RSs are much larger and the k-plate (k) is present (Fig. 3.14E).

dd=1.4 mm: additional scales have been added among the dorsal plates, the intermediate interradial plate between the k-plate and IR2, and the secondary interradial plate (SIR) among the primary plates. The arm spines are much larger in size (Fig. 3.14G). Some specimens at 1.4 mm dd have spines on the dorsal side of the disk surface, which are short and conical, distributed on the corners of the plates (Fig. 3.14I).

dd=1.8 mm: many more plates are present, mainly on the interradial region and around the RSs, which are well developed and begin to be separated by the k-plate (Fig. 3.14K).

Ventrally, the earliest post-larva at 0.4 mm dd bears a large, spinulose tooth, with large fenestrations. The dental plate is rectangular and one large, block-like papilla (= buccal scale) is present. The 1st VAP is arrow-shaped, narrowed laterally where the 2nd tentacle pore (TPo) is inserted. The 2nd TPo bears one broad scale, as do the remaining tentacle pores. The oral shield (OS) is present on each interradius and it is relatively large. The madreporite (M) is well visible and is distinguished by a protuberance (Fig. 3.14B).

dd=0.5 mm: not many changes occur from the former stage, only the teeth are more spinulose and crown-shaped (Fig 3.14D).

dd=0.9 mm: the strong spinulose inferior teeth are more conspicuous. The 1st mouth papilla (MP) is a prominent structure and the 2nd TPo is almost inside the oral

Figure 3.14 (cont.). Post-larval development of *Ophiactis abyssicola*. G. 1.4 mm. Note that no dorsal spine is present in this individual (compare with Fig. 12I); H. 1.1 mm; I. 1.4 mm. Note the dorsal spines; J. 1.4 mm; K. 1.8 mm; L. 2.6 mm. See Fig. 3.2 for further explanation. Sizes represent the disk diameter.

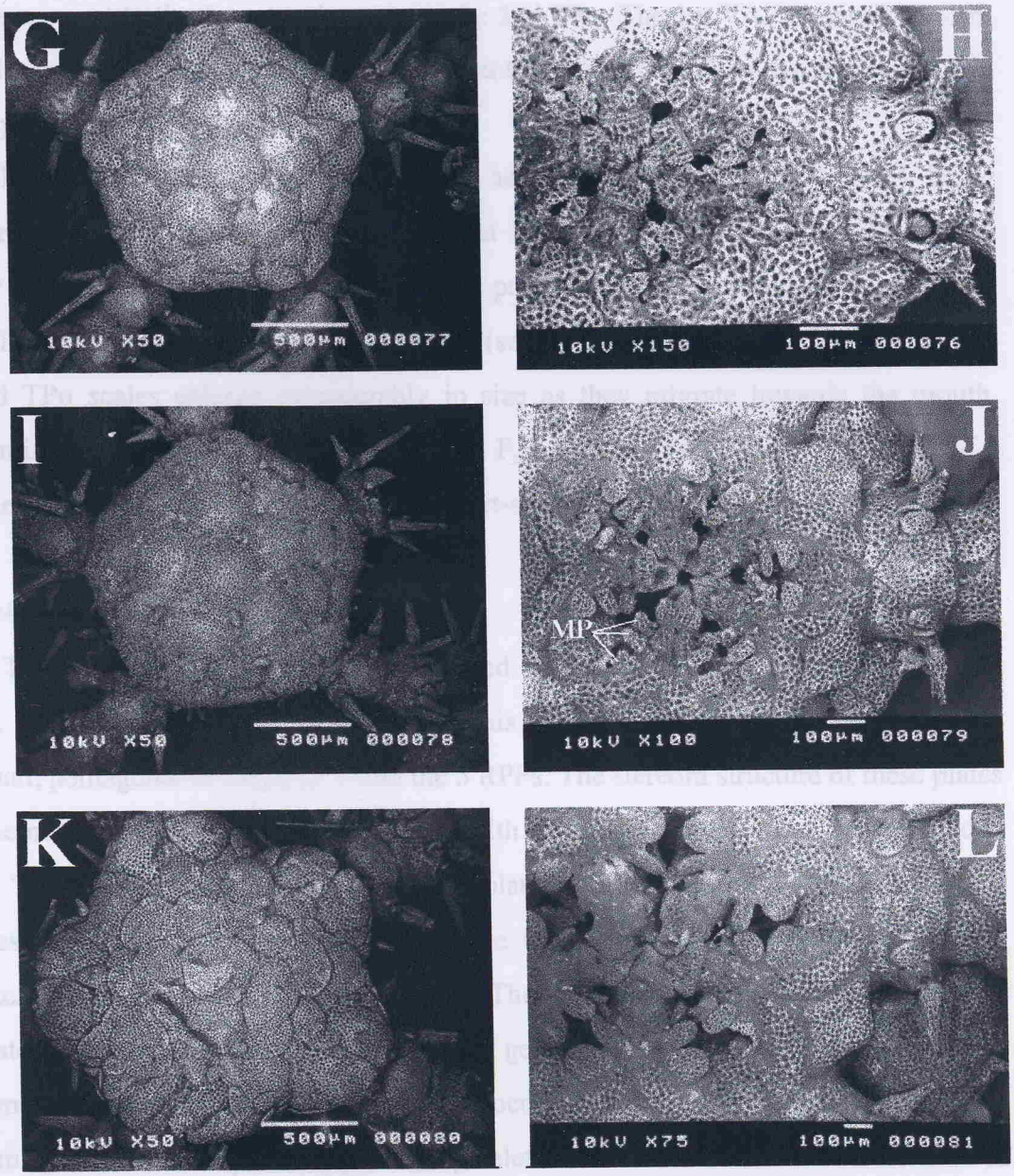
G
10kV X50 500µm 000077
H
10kV X150 100µm 000076
I
10kV X50 500µm 000078
J
MP
10kV X100 100µm 000079
K
10kV X50 500µm 000080
L
10kV X75 100µm 000081

slit, with its 1st tentacle scale covering it almost entirely. A second smaller scale can be seen next to the 1st tentacle scale of the 2nd TPo. The 1st VAP changed in form and has now a straight proximal and a pointed distal line. The OSs are rounded in shape (Fig. 3.14F).

The 2nd TPo gets closer to the mouth as the animal grows (Fig. 3.14H), being completely inside the mouth (Fig. 3.14J) at 1.4 mm dd. During this process the 1st MP change in form from a large scale-like process to a blunted finger-like structure, which is located deeper into the mouth slit (see Figs. 3.14 D, F, J and L). The 1st and 2nd TPo scales enlarge considerably in size as they migrate towards the mouth, forming the 2nd and 3rd MP (figs. 3.14 D, F, J and L). The OSs assume a form of a lozenge and the teeth the characteristic heart-shaped form (Fig. 3.14L).

Ophiactis balli (Thompson, 1840)

The smallest post-larva of *O. balli* sorted out from the Biofar samples is 1.0 mm dd. Many plates are present dorsally at this size, the primary plates, with a rather small, pentagonal in shape CPP and the 5 RPPs. The stereom structure of these plates resembles that of *Ophiactis abyssicola*, with the central fenestrations being divided by "bridges" of carbonate. Among these plates, the secondary interradial plates are present, but are not large in size. On the interradial area, the IR1, 2 and some intermediate interradial plates are present. The RSs are broader than larger and the k-plates almost divide them completely. The general shape of the disk is circular. The arms are well developed with broad DAPs occupying the entire width of the arm. The arm spines are stubby, bearing small spinelets and are 3 in number on each side of the arm joint in the proximal segments (Fig. 3.15A).

dd=1.5 mm: a large number of scales are present, but noticeably are the secondary interradial plates, which are much larger in size and triangular in shape, with one of the vertexes touching the IR3, both separating completely apart the adjacent radial primary plates. The RSs are now almost as broad as large (Fig. 3.15C).

dd=2.0 mm: the RSs are longer than broad and almost completely separated by the k-plate and other secondary plates. Several additional scales are present now (Fig. 3.15E).

Figure 3.15. *Ophiactis balli* post-larval development (A-F). A, C and E, dorsal view; B, D and F, ventral view. A. 1.0 mm; B. 1.0 mm; C. 1.5 mm; D. 1.5 mm. Note the spines in the interradial region; E. 2.0 mm; F. 2.0 mm. SIR = Secondary interradial plate; TPo = 2nd tentacle pore. See Fig. 3.2 for further explanation. Sizes represent the disk diameter.

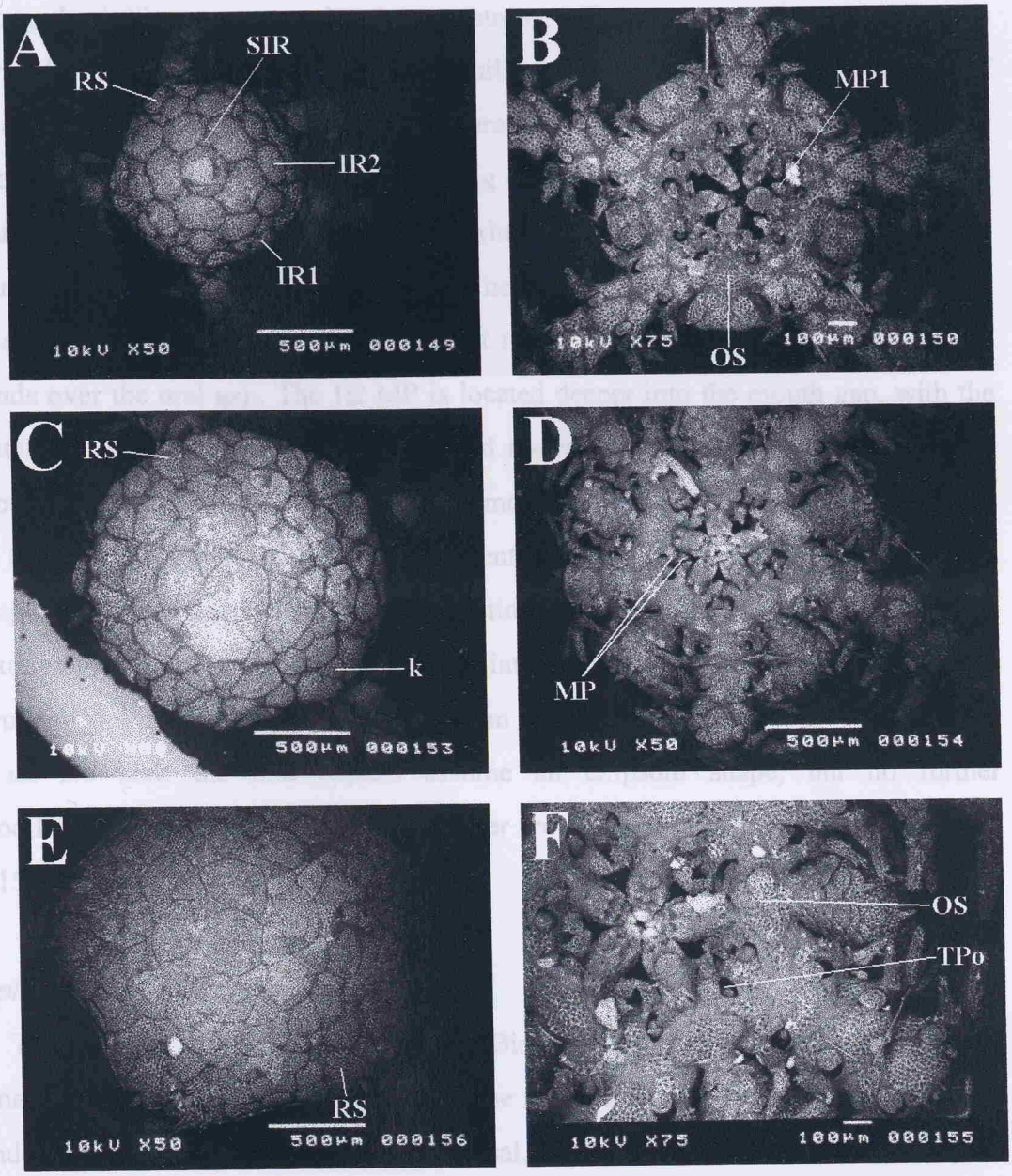
A
SIR
RS
IR2
IR1
10kV X50
500µm 000149
B
MP1
OS
10kV X75
100µm 000150
C
RS
k
500µm 000153
D
MP
10kV X50
500µm 000154
E
RS
10kV X50
500µm 000156
F
OS
TPo
10kV X75
100µm 000155

At the ventral side, when the animal is 1.0 mm dd, the tooth is already a very strong, bush-like process and only one strong MP is present, which is probably derived from a large block-like papilla, similar to that found in the early post-larva of *Ophiactis abyssicola*. The 2nd tentacle pore is located outside the mouth and bears one large tentacle scale, the same occurring on the remaining pores. The 1st VAP is diamond-shaped with the distal and proximal ends straight. The oral shields are small, broader than long and rhomboid in shape (Fig. 3.15B).

dd=1.5 mm: the tentacle pore is almost inside the oral slit and its tentacle scale bends over the oral gap. The 1st MP is located deeper into the mouth gap, with the distal part beneath the tentacle scale cited above. The tooth is more solid, with a tricuspid shape. The oral shield outline is more circular and some spinescan be seen on the interradial areas of the disk. The ventral arm plates are almost rectangular in shape. From this stage one can already distinguish some adult characters used in the taxonomic keys, *e.g.* the spines on the interradial areas of the disk, the mouth structure and tentacle scales, and ventral arm plates (Fig. 3.15D).

dd=2.0 mm: the oral shields assume an ellipsoid shape, but no further modifications appear to happen that differ from the former stage described (Fig. 3.15F).

Ophiopholis aculeata Linnaeus, 1758

The smallest individual found in the Biofar samples is 0.3 mm dd and is the smallest ophiuroid post-larva obtained. The specimen presented the primary rosette and 3 arm segments. The CPP is pentagonal, solid with almost no fenestrations, but some smaller ones scattered on the borders of the plate and a trifid spine on each corner. The 5 RPPs have similar structures, but with just one spine on each of the far corners, between the two adjacent RPPs, and the one on the mid-distal edge, right on the mid-line suture of the LAPs. It is worth noting that the dorsal spines on this species seem to be inserted not on a single plate but on the mid-line suture between two or more the plates, with each half inserted on each plate. The arm segments bear 2 spinulose spines on each side and the dorsal arm plates (DAP) possess a bifid spine in the form of an H (Fig. 3.16A).

Figure 3.16. *Ophiopholis aculeata* post-larval development (A-G). A-E, dorsal view; F-G, ventral view. A. 0.3 mm; B. 0.6 mm; C. 1.0 mm; D. 1.5 mm. Note the arrangement of the disk spines; E. Detail of the proximal arm segments and disk edge of a 3.0 mm post-larva; F. 0.7 mm; G. 2.0 mm. M = madreporite; T = tooth; Tpo = 2nd tentacle pore. See Fig. 3.2 for further explanation. Sizes represent the disk diameter.

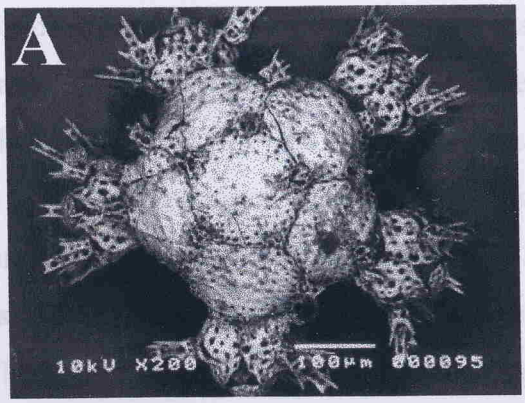
A
10kV X200
100µm 000095

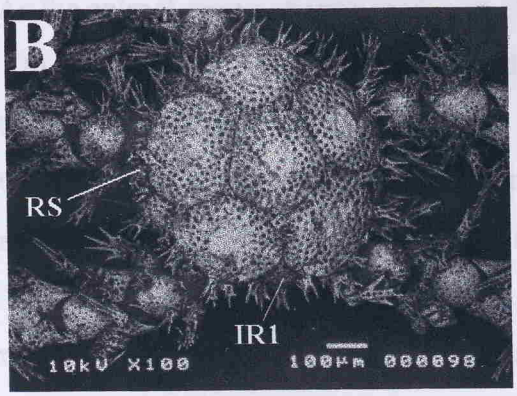
B
RS
IR1
10kV X100
100µm 000098

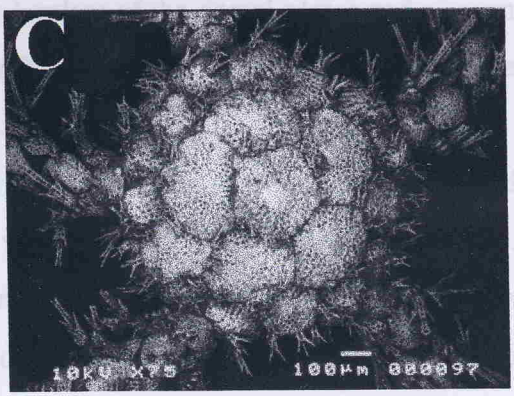
C
10kV X75
100µm 000097

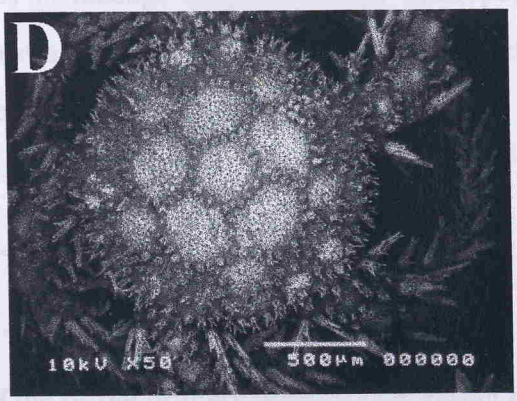
D
10kV X50
500µm 000000

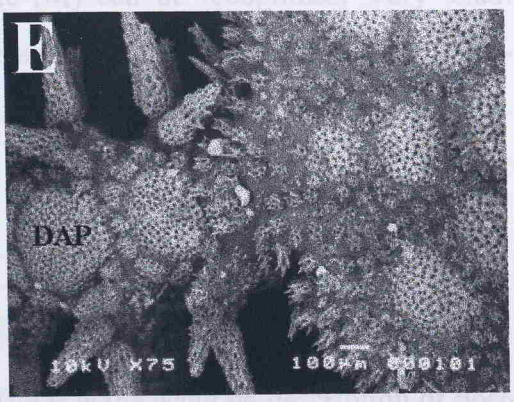
E
DAP
10kV X75
100µm 000101

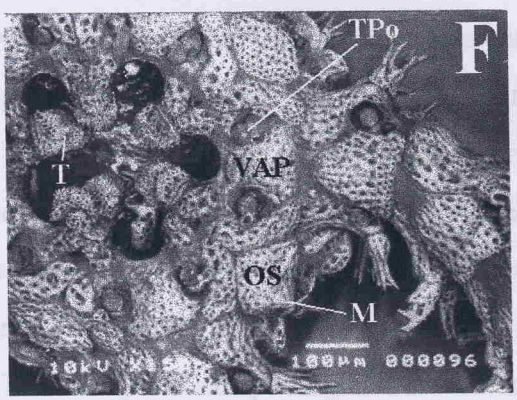
F
TPo
T
VAP
OS
M
10kV X150
100µm 000096


G
T
MP
10kV X100
100µm 000102

dd=0.6 mm: a deposition of a secondary layer of carbonate changes the stereom structure of the plate, forming some medium-sized fenestrations except in the very centre of the primary plates. The IR1 is present and bears 3 spines distributed evenly on the outer edge. On the arm, the 1st DAP has 4 spines on the distal edge and the adoral shields are much larger and spinulose. Between the arm and the disk lies the paired RSs which are small and rectangular, with 2 spines (Fig. 3.16B).

dd=1.0 mm: the RSs and IR1s are much larger and the plates are increasingly surrounded by spines. The IR2 appears on the interradial area (Fig. 3.16C).

As the animal grows, spines appear on the borders of the dorsal plates and also on the DAPs (Figs. 3.16D) and the spines of the DAPs become scale-like, bordering the distal and lateral edges of these plates (Fig. 3.16E).

On the ventral side, specimens at 0.7 mm dd show strong crown-shaped teeth and spinulose inferior teeth. The dental plate is very wide and short imperforated plate. No mouth papillae are present and the oral gap is strongly rounded. The 1st VAP is a somewhat bell-shaped with the proximal side shorter and straight. The oral shield (OS) is lozenge-shaped and the madreporite (M) can be recognized. Very small fenestrations are present on the ventral surface (Fig. 3.16F). At 2.0 mm dd 3 spine-like MP are present (Fig. 3.16G).

3.3. Discussion

3.3.1. General Comments

One of the primary aims of the present chapter is the accurate description of post-larval ophiuroids. Post-larval ophiuroids can be collected in large numbers in certain deep-sea areas at certain times of the year and many times they are put aside owing to the lack of expertise to match them to the respective adult. Most taxonomic keys are based on adult characters, which are not conspicuous or, more frequently, not well developed in the post-larvae. Thus, different features must be found in order to identify such organisms.

The study of morphological characteristics of early post-metamorphic stages revealed that the primary plates are very important specific features. The relative size of the central primary plate and its fenestration pattern and size are decisive in

distinguishing congeneric species (see taxonomic discussion). Some of the arm characteristics, as the size and shape of the adoral shield spines, dorsal arm plates and arm spines and the size, shape and fenestration pattern of the terminal plates can also be very useful (see *O. albida*). Other important characters include the dental plate, teeth, mouth papillae and first ventral arm plate, but these appear to be more conservative within genera. However, the dental plate and the first ventral arm plate showed a certain degree of variation within the genus *Ophiura*. This variation may be important in grouping closely related congeneric species.

Despite the fact that Mortensen (1920) could not recognise the post-larvae of two species of *Amphiura*, other authors detected that some congeneric species were distinguishable from a very early post-metamorphic stage (Schoener, 1967, 1969; Muus, 1981; Webb & Tyler, 1985). The present data show that more species may be added to this list and evidence suggests all the species studied here have a distinct and recognisable post-larva.

3.3.2. Taxonomic Discussion

Genus *Ophiacantha*

The mouth structure of *O. abyssicola* and *O. bidentata* is very similar in the smaller individuals. The shape and arrangement of the dorsal plates are very useful in the distinction of both species. *O. abyssicola* bears a pentagonal central primary plate (CPP) with five spines distributed on the corners of the plate, whereas *O. bidentata* possesses a irregular CPP (bean-shaped) with only two spines. As specimens get larger the dorsal structure becomes unclear and at this stage the oral shield (on the ventral side) is used for identification. In *O. abyssicola* the oral shield presents a groove in the median region of the plate, while in *O. bidentata* this structure is wide and plain, with no groove present.

Genus *Ophiura*

Post-larvae of *O. sarsi* and *O. carnea* are very similar under light microscopy. However, early stages of *O. carnea* can be distinguished under SEM by the fenestration pattern of the primary plates, which presents smaller fenestrations in the centre of the plate and much smaller on the edges. The central primary plate is

smaller relative to the disk diameter and the adoral shield spines are slender and smooth, as opposed to the stubby and rough spines of *O. sarsi*. The relative size of the central primary plate in *O. carnea* distinguishes it from *O. ljungmani*.

O. ljungmani can be distinguished from the former species by the much larger fenestrations in the central parts of the primary plates, the more elongated terminal plates, the somewhat ellipsoidal shape of the dental plate (as opposed to romboidal) and the fenestration pattern and shape of the first ventral arm plate (in larger specimens, >1 mm dd). Those characters and the relative larger central primary plate also distinguish this species from *O. albida*.

O. albida is separated mainly by the presence of a bulb-shaped terminal plate and the different stereom structure of the primary plates. The dorsal arm plates are also much wider than long in this species.

O. scomba is distinguished mainly by the different stereom structure of the primary plates.

Genus *Ophiocten*

O. gracilis is easily distinguished from all examined *Ophiura* species by the presence of a very large central primary plate, with a characteristic fenestration pattern composed of small fenestrations in the centre of the plate, which become larger towards the edges and then very small again on the very edge of the plate. The arm spines are much larger and the dorsal arm plates are more elongated.

Post-larvae of *O. affinis* can be distinguished from the former species of Ophiurinae by the different fenestration structure of the primary plates, the early appearance of the secondary interradial plate and by the presence of secondary scales surrounding the primary plates in individuals larger than 1 mm dd.

Genus *Ophiactis*

O. abyssicola can be distinguished from *O. balli* mainly by the larger arm spines, compared with the shorter and stubbier arm spines of *O. balli*. The radial shields are much larger in *O. abyssicola*. *O. balli* has a more rounded disk shape and it bears a larger number of plates on the dorsal surface of the disk.

3.3.3. *The Systematic Position of* Ophiura affinis

The relationship between the genera *Ophiura* and *Ophiocten* has been questioned by several authors (Mortensen, 1927*a*, 1933, 1936; Clark & Courtman-Stock, 1976), owing mainly to the characteristics exhibited by the species *Ophiura affinis*, which is, apparently, intermediate between both genera. Paterson *et al.* (1982) discuss such characters and, despite the fact that *Ophiura affinis* possesses only one major characteristic in common with other *Ophiura* species (a well developed notch on the disk margin above the arm bases), still consider the species as belonging to that genus. The characteristics found in *Ophiura affinis* and species of *Ophiocten*, when adult, include the emergence of the second oral tentacle pore outside the mouth, the shape of ventral arm plates and the tentacle pore and scales of the proximal arm segments. The only intermediate feature found in *Ophiura affinis* is the arm combs, which show an intermediate feature between both genera, which together with the notch over the arm bases, form the main characters that places *O. affinis* in the genus *Ophiura* (Table 3.1). Yet, Paterson *et al.* (1982) argue that the status of *O. affinis* needs to be checked after a revision is carried out for the genus *Ophiura*.

Table 3.1. Comparison of the main adult characters of *Ophiocten*, *Ophiura affinis* and *Ophiura* (modified from Paterson *et al.*, 1982). VAP = Ventral Arm Plate.

Characters	*Ophiocten*	*Ophiura affinis*	*Ophiura*
Second tentacle pore	**Away from the mouth slit**	**Away from the mouth slit**	Via furrow into mouth slit
Arm combs	Simple	Intermediate	Well developed
Disk margin above arm bases	Without a notch	**With a well developed notch**	**With a well developed notch**
Shape of the VAPs	**Proximal side produced, distal side rounded**	**Proximal side produced, distal side rounded**	Scallop-shaped, irregularly hexagonal but not as *Ophiocten*
Proximal tentacle pore and scales	**Large with only a small scale**	**Large with only a small scale**	Large with many, often large, tentacle scales

The well-developed notch over the arm bases and the arm combs considered typical of *Ophiura*, are subject to a great deal of variation within this genus and even within the species *Ophiura affinis*. In his description of this species, Mortensen (1927*a*) describes the notch present over the arm as a small structure, containing only

two small dorsal plates, whereas Paterson *et al.* (1982) point out a well-developed notch. Within the genus *Ophiura*, the notch can be well developed in species such as *Ophiura carnea*, *O. sarsi* and *O. ljungmani*, or non-existent as in *O. clemens*, *O. nitida* and *O. violainae* (see Paterson, 1985). The same degree of variation is found for the arm combs, which can assume several shapes and disposition. In the genus *Ophiocten*, there is, generally, no marked notch over the arm bases, but the same variation in the arm combs do occur. Mortensen (1927*a*) points out that in *Ophiocten* is present "...usually a continuous comb of papillae across the base of the arms". However, variation exists within the genus and some species show the arm combs continuous over the arm bases as in *Ophiocten sericeum* and *O. centobi* (Paterson *et al.*, 1982); arm combs confined to each side of the arms, as in *O. gracilis* (Paterson *et al.*, 1982) and *O. bisquamatum* (Mortensen, 1936); or arm combs reduced or absent as in *O. hastatum* (Paterson *et al.*, 1982). The characters observed in *Ophiura affinis* fall certainly within the range of variation found in both genera. Paterson *et al.* (1982) show the disposition of the arm combs in *Ophiocten abyssicolum* and argue that "the form of the papillae on the dorsal arm plates may suggest an affinity with *Ophiura affinis*". The range of variation in the shape and disposition of the arm combs is probably a good indicator of specific affinities, but not consistent enough to describe different genera within the Ophiurinae. Characters such as the emergence of the second tentacle pore and number of scales round this pore appear to be a reliable distinguishing feature between *Ophiura* and *Ophiocten.*

The study of homologous structures in the post-larvae of *Ophiura affinis* and *Ophiocten gracilis* showed that the similarity with *Ophiocten* is greater when comparing the early states of some important features. Characters such as the shape of the disk, tooth, dental plate and first ventral arm plate appear to be conservative within both genera. Comparing these characters with those found in *Ophiura sarsi* (Table 3.2), we found conspicuous differences, particularly in the shape of the dental plate. In *Ophiura sarsi* it is a large and robust rhomboidal plate, whereas in *Ophiocten gracilis* and *Ophiura affinis*, it is ellipsoidal and more delicate. The tooth is also clearly different, with that of *Ophiura sarsi* being broader at the base. The characteristics referred to *Ophiura sarsi* seem to agree with those of other post-larvae of *Ophiura* species, e.g. *Ophiura carnea* (present work), *O. ophiura* and *O. albida*

(Webb & Tyler, 1985; present work). *O. ljungmani* presents an intermediate dental plate morphology.

Table 3.2. Comparison of the main post-larval characters of *Ophiocten gracilis*, *Ophiura affinis* and *Ophiura sarsi*. VAP = Ventral Arm Plate.

Characters	*Ophiocten gracilis*	*Ophiura affinis*	*Ophiura sarsi*
Teeth	**long and slender**	**long and slender**	broad triangular
Dental plate	**ellipsoid**	**ellipsoid**	rhomboid
1st VAP shape	**convex proximally straight distally**	**convex proximally straight distally**	pointed proximally convex distally
1st VAP fenestration patern	**large fenestrations throughout the plate, but the distal part with small and regularly distributed fenestration**	**large fenestrations throughout the plate, but the distal part with small and regularly distributed fenestration**	fenestrations with the same size and distributed evenly throughout the plate
General shape of the disk and arms	**disk with a sharp edge, with the arms do not appearing of issuing from the dorsal side of the disk**	**disk with a sharp edge, with the arms do not appearing of issuing from the dorsal side of the disk**	margins of the disk not sharp arms appearing of issuing from the dorsal side of the disk

The first ventral arm plate in *Ophiura affinis* and *Ophiocten gracilis* are also very similar (as is the distal part of the 1st VAP in *O. ljungmani*), as well as the general shape of the disk, mainly on the margins over the arm bases. In *Ophiura sarsi*, this part is continuous with the dorsal side of the disk and in *Ophiura affinis* and *Ophiocten gracilis*, it is clearly detached. Mortensen (1927*a*) points out that feature as distinctive of *Ophiocten*, where "... the notch above the arms is feeble and the arms thus not having the appearance of issuing from the dorsal side". Ursin (1960) found it very easy to distinguish small specimens of *Ophiura affinis* from those of *Ophiura albida*, but could not discern *Ophiura ophiura* (= *O. texturata*) from *O. albida* and suggested that juveniles of both species were probably similar. In fact, small individuals of *Ophiura* are quite alike and difficult to recognize and the observations made by Ursin (1960) reinforces the proposal that *Ophiura affinis* does not belong to the genus *Ophiura*. Koehler (1897) described small individuals of *O. affinis* as a new species of *Ophiocten* (*O. scutatum*). Furthermore, the adult features in common with the *Ophiura* described above are, therefore, considered as within the range of variation found among congeners of *Ophiocten*. We propose that the post-

larval characteristics described above and the adult features known for the species are sufficient to consider *Ophiura affinis* as belonging to the genus *Ophiocten*.

3.3.4. Phylogenetic considerations

The ontogenesis of homologous structures in the ophiuroid post-larvae can be of good value in defining systematic and phylogenetic relationships among taxonomic groups (Hendler, 1988).

The development of the mouth papillae differed among the different genera studied. In the genera *Ophiura* and *Ophiocten* studied, the first mouth papilla (= buccal scale) is block-like and remains as a large block-like papilla on the distal part of the jaw in larger specimens. Additional mouth papillae are added in an unidirectional sequence, from distal to proximal along the jaw. The same pattern of development is observed for *Ophiura ophiura* (Webb & Tyler, 1985) and probably for *Ophiura scomba*. The mouth papilla in these species appears to be serially homologous. However, the fourth mouth papilla (and maybe the third) appears to originate from the dental plate, in which case it should be homologous with the teeth and not with the remaining mouth papillae. In this case we should consider it as an infradental papilla. Despite being formerly considered to be present exclusively in amphiurid species, Hendler (1998) found that an infradental papilla also occurs in the species *Ophiomusium lymani* (an Ophiuridae). It is possible that this papilla occurs all over the family Ophiuridae. However, a more careful examination of the ontogenesis of these papillae is needed before a definite conclusion is drawn. The general development of the oral frame within the family Ophiuridae seems to differ among different genera. Schoener (1967, 1969) presented the oral frames of five different genera of deep-sea species and they look very different from the *Ophiura*/*Ophiocten* examined.

The mouth papillae in both *Ophiacantha abyssicola* and *Ophiactis abyssicola* are not serially homologous. In *Ophiacantha abyssicola*, the first mouth papilla is formed by the adoral shield spine, which is serially homologous with the arm spines (see Hendler, 1988), whereas the second mouth papilla formed on the jaw (not shown).

In *Ophiactis abyssicola*, the first mouth papilla is the buccal scale and the second and third are the tentacle scales of the 2nd tentacle pore. The development of the buccal scale in this species (and in *Ophiactis balli*) is similar to that of some amphiurids. Hendler (1988) shows that in the *Amphiura*- and *Amphioplus*-groups the buccal scale are not resorbed as in the *Amphiodia*- and *Amphipholis*-groups. The buccal scale in those groups suffers an enlargement of the proximal end in a similar fashion to that of *Ophiactis abyssicola*. In *O. abyssicola*, the buccal scale develops further to form an elongated mouth papilla placed deep inside the mouth.

The appearance of the secondary interradial plates in the Ophiuridae is also interesting. In some species like *Ophiura ljungmani* (Schoener, 1967; present work), *O. scomba*, *Ophiura ophiura* (Webb & Tyler, 1985), *Ophiocten affinis* and *O. gracilis*, this plates appear earlier during the ontogenesis (< 1.5 mm dd). Later appearance occurs in *Ophiura sarsi*, *O. carnea* and *O. albida* (Webb & Tyler, 1985) (>2.5 mm dd).

Development of the oral frame in *Ophiocten* species appears to stop at an early stage, similar to early ontogenetic stages in *Ophiura*. Could this represent a paedomorphic feature in the evolution of the genus *Ophiocten*? How much these events reflect phylogenetic affinities among the groups is not known yet, but these characters could be useful data to test phylogenetic schemes of the Ophiuroidea, as for instance that of Smith *et al.* (1995). Nevertheless, we think more data should be gathered on the early development of ophiuroids in order to test such phylogenies.

3.3.5. Ecological Considerations

Gage (1994) emphasises that recruitment and age structure in deep-sea populations are important in understanding processes structuring the highly diverse communities found in the sediments and for the knowledge of rates of colonization to predict recovery times from perturbations (see also Gage, 1991). The early phases in the development of juveniles are then of great importance since such organisms are subject to high rates of mortality (Gage, 1984; Tyler *et al.*, 1991). Competition for resources can also be important.

Recently, Medeiros-Bergen (1996) related different types of tooth with micro- and macrophagous feeding habits in adult ophiuroids. The mouth structure of congeneric

post-larvae is very similar and conservative within the class. This suggests that congeneric species could compete for the same kinds of food (some specimens were observed to consume large food items, such as entire forams) and space, generating an intra- and interspecific competition. In habitats containing several congeneric species, settlement, recruitment and growth rates should be fundamental in structuring those communities, controlling the relative abundance and distribution of adult populations. Fast growth rates can be very important in avoiding predation by larger organisms. Tyler *et al.* (1993) report that juveniles of the deep-sea urchin *Hemiaster expergitus* are heavily preyed on by the seastar *Bathybiaster vexillifer*. Gage & Tyler (1982*c*) point out that the deep-sea ophiuroid *Ophiomusium lymani* grows rapidly to a larger size during the early post-metamorphic stages, probably to avoid predation. Post-larvae of *Ophiocten gracilis* also grow very fast and start gametogenesis very early during development (see chapter 6). As the animals grow larger, they probably become less susceptible to predators after attaining a certain size refuge. Gage (1984) points out that post-larvae and juveniles initially grow quickly, but are subjected to high mortality through predation and resource competition.

Chapter Four – Early juvenile development of deep-sea asteroids of the NE Atlantic Ocean, with notes on the juvenile bathymetric distribution

4.1. Introduction

The taxonomic literature on the Class Asteroidea is vast, going back to the 18th century (Linck, 1733; Linnaeus, 1758) though not really taking off until the 19th century (Sars, 1875; Sladen, 1889). Taxonomic accounts are mostly based on adult descriptions. Asteroid larvae (and echinoderm larvae in general) demand a completely separate description, since these stages are so different from the adults that they appear to be a completely different group (Mortensen, 1921; Strathmann, 1971).

Descriptions of juvenile forms are quite frequent among the main taxonomic papers (Fisher, 1940; Madsen, 1961, 1981; Walenkamp, 1976; Clark, 1981, 1982, 1984; Clark & Downey, 1992). In those papers, the aim was to emphasise some of the more important differences between juveniles and conspecific adults. Nevertheless, many juveniles of known species have been described as new species, causing taxonomic confusion (see Clark & Downey, 1992 for a series of Atlantic species synonymized).

In general, descriptions involve animals with an arm radius R>5 mm. The ontogenesis of very early juveniles (R<1 mm) has sometimes been described from specimens reared from larvae in the laboratory (Yamaguchi, 1973; Komatsu, 1975; Oguro *et al.*, 1976; McEdward, 1992). Such an approach was only made possible after the discovery of the hormone responsible for the maturation of oocytes, 1-methyladenine (Kanatani *et al.*, 1969). As expected, the development of many shallow water species are known, together with their recently metamorphosed juveniles. The knowledge of culturing asteroid larvae has also helped in a better understanding of juvenile ecology in allowing a positive identification of juveniles in the field. Keesing *et al.* (1993) stress the importance of experience in culturing methods for the distinction of different asteroid postlarvae in the field.

Few asteroid species from the deep-sea have had the early post-metamorphic development described (Sars, 1875; Sibuet & Cherbonnier, 1972). Juvenile ecology is unknown. The method employed by the cited authors is to study an increasing series of growth stages of specimens collected in deep-sea samples. This method is the most feasible in such areas, since the culturing of deep-sea species is not yet routine or practicable. Deep-sea asteroid embryos were obtained in few occasions (Young *et al.*, 1996*a*) and juveniles have never been reared in the laboratory.

The importance of juvenile stages of marine invertebrates has already been discussed in chapter 3. In shallow water, the juvenile development and ecology of some of the more common and important sea stars are known: *Asterias* (Orton & Fraser, 1930; Vevers, 1949; Barnes & Powell, 1951; Hancock, 1958; Loosanoff, 1964; Barker & Nichols, 1983; Nichols & Barker, 1984), *Pisaster* (Feder, 1970; Sewell & Watson, 1993), *Acanthaster* (Yamaguchi, 1974; Zann *et al.*, 1987; Johnson *et al.*, 1991; Keesing & Halford, 1992), *Mediaster* (Birkeland *et al.*, 1971), *Linckia* and *Culcita* (Yamaguchi, 1977*a*, *b*), *Coscinasterias* and *Stichaster* (Barker, 1977, 1979), *Asterina* (Rumrill, 1989) and *Patiriella* (Chen & Chen, 1992).

In this chapter the post-metamorphic ontogenesis of 10 deep-sea asteroid species collected during the Deep-Sea Benthic Ecology Programme of the Institute of Oceanographic Sciences (IOS) in the Porcupine Seabight and Abyssal Plain is described. They include the paxillosidans *Bathybiaster vexillifer*, *Psilaster andromeda andromeda*, *Hyphalaster inermis* and *Porcellanaster ceruleus*; the notomyotids *Benthopecten simplex simplex* and *Pectinaster filholi*; the valvatid *Plinthaster dentatus*; the velatid *Hymenaster pellucidus* (*sensu* Clark & Downey, 1992); and the forcipulatid *Zoroaster fulgens*. I also describe an early stage of *Plutonaster bifrons* not shown by Sibuet & Cherbonnier (1972) and redescribe the early development of the brisingid *Brisingella coronata*.

The taxonomy, distribution, abundance and importance of the deep-sea asteroids of the NE Atlantic Ocean have been dealt with in several papers (*e.g.* Farran, 1913; Cherbonnier & Sibuet, 1973; Sibuet, 1977, 1979, 1984; Gage *et al.*, 1983; Harvey *et al.*, 1988). The asterozoan fauna of the Porcupine region forms the dominant element of the megafauna. It is important also in structuring the benthic community. Rice *et*

al. (1991) note the importance of *Bathybiaster vexillifer* as a bioturbator of the sediment in its search for infaunal prey (see also Tyler *et al.*, 1993).

The species studied in the present chapter are conspicuous elements of the megafauna of the deep NE Atlantic. Gage *et al.* (1983) cite the ten most abundant sea stars in the Rockall Trough, from which the post-metamorphic development of eight is described below. A great deal of the reproductive biology and possible mode of development is also known for the species cited above, with the exception of *Plinthaster dentatus*. *Plutonaster bifrons* is a seasonal breeder (Tyler & Pain, 1982*a*), taking advantage of the seasonal pulse of phytodetritus in the NE Atlantic (Billett *et al.*, 1983) to fuel reproduction. Evidence also suggests that *P. bifrons* benefits from seasonal inputs of food falls of the blue whiting (*Micromesistius poutassou*) in the Rockall Trough area (Tyler *et al.*, 1993).

Although seasonal breeding occurs in another species of sea star, *Dytaster grandis* (Tyler *et al.*, 1990), the most common mode of development in this group appears to be lecithotrophic development, with an asynchronous reproduction throughout the year. All the other sea stars cited above are likely to exhibit lecithotrophic development including *Bathybiaster vexillifer* (Tyler *et al.*, 1982*a*), *Psilaster andromeda* (Tyler & Pain, 1982*a*), *Hyphalaster inermis* and *Porcellanaster ceruleus* (P.A. Tyler, unpublished data), *Benthopecten simplex* and *Pectinaster filholi* (Pain *et al.*, 1982*b*), *Hymenaster pellucidus* (Pain *et al.*, 1982*a*, as *H. membranaceus*) and *Brisingella coronata* (Tyler *et al.*, 1982*c*). In *Zoroaster fulgens* the inferred mode of development is also lecithotrophic, but this species may have a seasonal reproductive cycle (Tyler *et al.*, 1984*b*).

The primary aim of this chapter is to describe the early growth changes of the species involved, showing how the different structures appear and change through development. I also analyse the distribution of juveniles in the Porcupine area in relation to that known for the respective adults.

4.2. Juvenile Development in Sea Stars

The main structures of interest for the study of juvenile asteroids are shown in figure 4.1 and will be used in the descriptions given below.

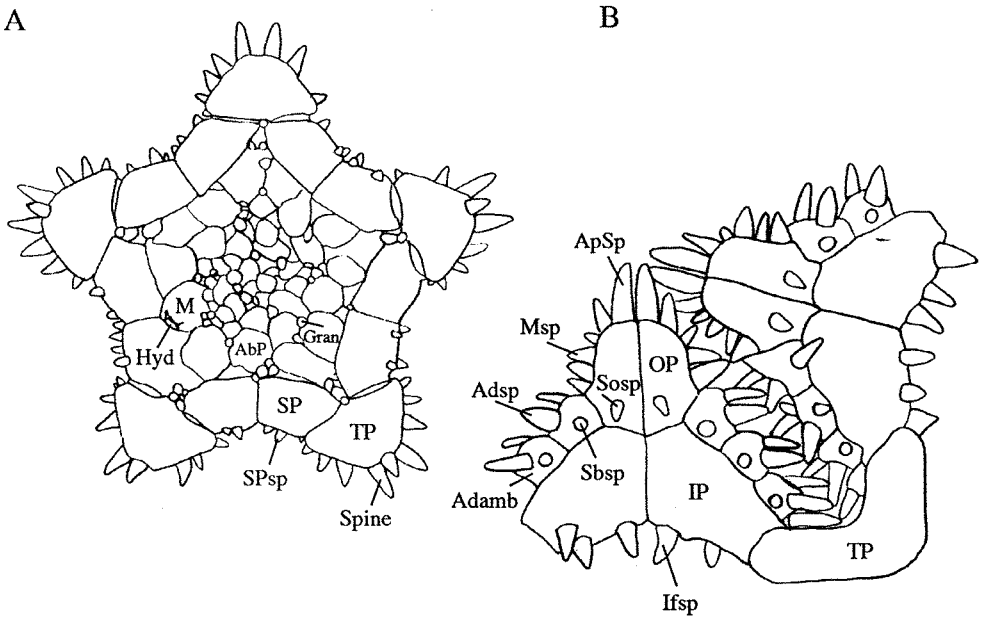

Figure 4.1. Morphological features of asteroid juveniles. A. Abactinal view; B. Actinal view. AbP = abactinal plate; Adamb = adambulacral plate; Adsp = adambulacral spine; ApSp = apical spine; Gran = granule; Hyd = hydropore; Ifsp = inferomarginal plate spine; IP = inferomarginal plate; M = madreporite; Msp = marginal spine; OP = oral plate; Sbsp = subambulacral spine; Smsp = superomarginal plate spine; Sosp = suboral spine; SP = superomarginal plate; TP = terminal plate;

Class Asteroidea Blainville, 1830

Order Paxillosida Perrier, 1884

Family Astropectinidae Gray, 1840

Bathybiaster vexillifer (Wyville Thomson, 1873)

R=0.84 mm (R/r=1.23): specimens have an overall body shape strongly pentagonal. The abactinal surface is formed by irregularly shaped imbricating paxillae, with one spine each. One superomarginal plate is present and in some of them one spine is present. A bar-like terminal plate is present bearing a large central spine with one small spine on each side. All spines are placed on a more dorsal position on the tip of the plate. On the ventral side of the terminals, there are 4 large spines, with the outer spines being the largest. A madreporite is visible on the abactinal surface, off the edge of the interradial area of the disk (Fig. 4.2A).

Figure 4.2. *Bathybiaster vexillifer* juvenile development (A-I). A-E, abactinal view; F-I, actinal view. A. 0.84 mm; B. 1.22 mm; C. 1.92 mm; D. 2.58 mm. Note the epiproctal cone (arrow); E. 4.06 mm. See Fig. 4.1 for explanation. Sizes represent the arm radius (R).

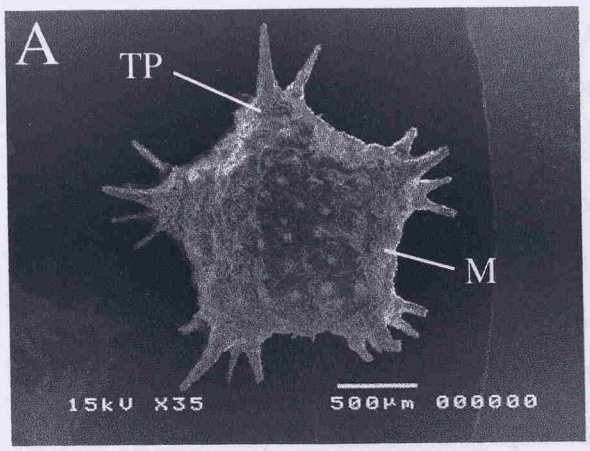
A
TP
M
15kV X35
500µm 000000

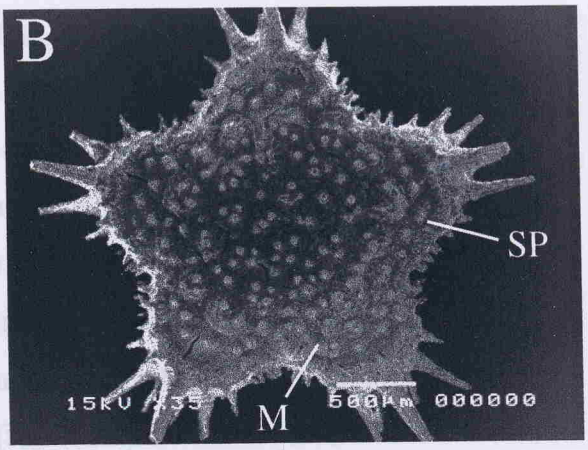
B
SP
M
15kV X35
500µm 000000

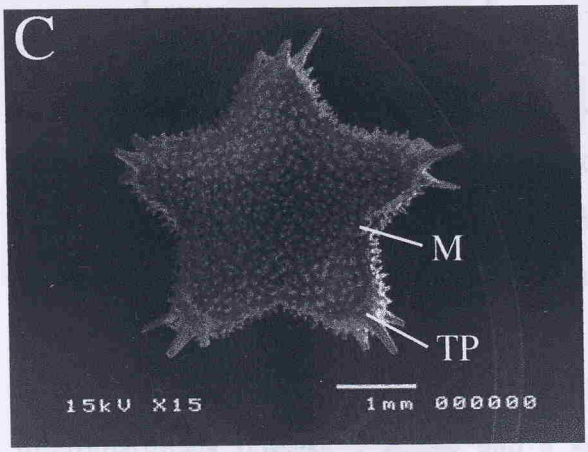
C
M
TP
15kV X15
1mm 000000

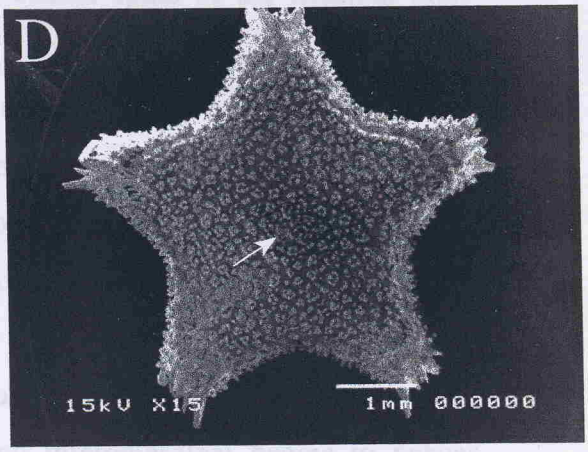
D
15kV X15
1mm 000000

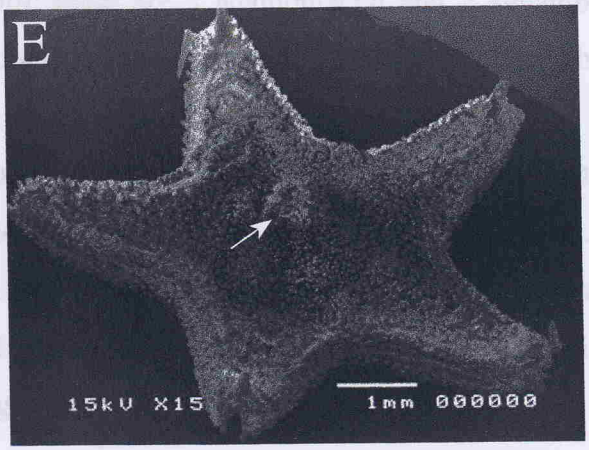
E
15kV X15
1mm 000000

R=1.22 mm (R/r=1.42): the individual is stellate and the abactinal paxillae bear 3-4 spines. The paxillar spines are small and spinulose and 3 in number. The madreporite is larger and is closer to the margin (Fig. 4.2B).

R=1.92 mm (R/r=1.57): there are 4 superomarginal spines and 3 spines in the terminal plates are conspicuously larger than the rest (Fig. 4.2C).

R=2.58 mm: the epiproctal cone is visible and the paxillar spines are arranged in groups of 3-5. The dorsal surface of the terminal plates bears small spines. The adambulacral spines are all short and spinulose (Fig. 4.2D).

R=4.06 mm: the epiproctal cone is very prominent and rows of spines can be seen on the supero- and inferomarginal plates. The central spine of the terminal plate points upwards (Fig. 4.2E).

On the actinal region, individuals at R=0.98 mm (R/r=1.34) possess a jaw longer than broad with 1 apical spine and one pair of marginal spines running in the furrow on the edge of the oral plate, with the distal-most being largest. Only 1 rather large adambulacral spine is present in most of the adambulacral plates, but some bear 2 (Fig. 4.2F).

R=1.20 mm (R/r=1.43): most adambulacral plates bear 2 spines. The inferomarginals possess 2 spines and a second inferomarginal begins to appear between the first one and the terminal plate, bearing 1 spine (Fig. 4.2G).

R=1.82 mm (R/r=1.50): there are 3 adambulacral and 2 subambulacral spines. Three marginal and 2 suboral spines are present in the oral plate. The fascioles are very conspicuous on the interradial areas (Fig.4.2H).

R=5.50 mm: the paxillar columns have up to 4 blunt spinelets, which look granuliform in appearance. The marginals are covered with granules. The spines of the inferomarginals and actinal areas merge. Those spines are somewhat flat at the top. Three adambulacral spines are present. The oral plate bears 2 apical, 5 marginal and 2 suboral spines (Fig. 4.2I).

Plutonaster bifrons (W. Thomson, 1873)

The post-metamorphic development of this species was described by Sibuet & Cherbonnier (1972), although their specimens were all R<0.85 mm. I describe below

Figure 4.2 (cont.). *Bathybiaster vexillifer* juvenile development. F. 0.98 mm; G. 1.20 mm; H. 1.82 mm; I. 5.50 mm. mo = mouth. See Fig. 4.1 for explanation. Sizes represent the arm radius (R).

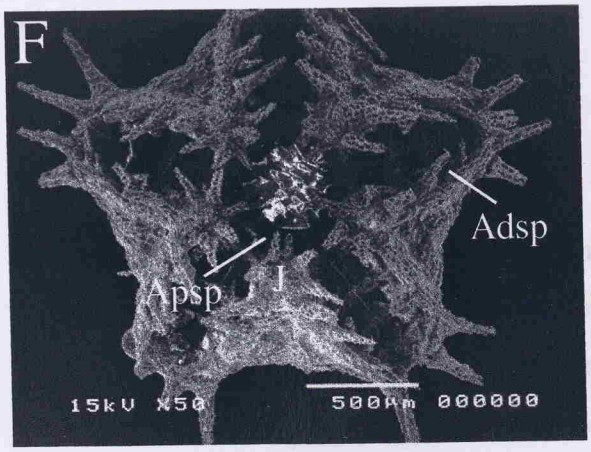
F
Adsp
Apsp
15kV X50
500µm 000000

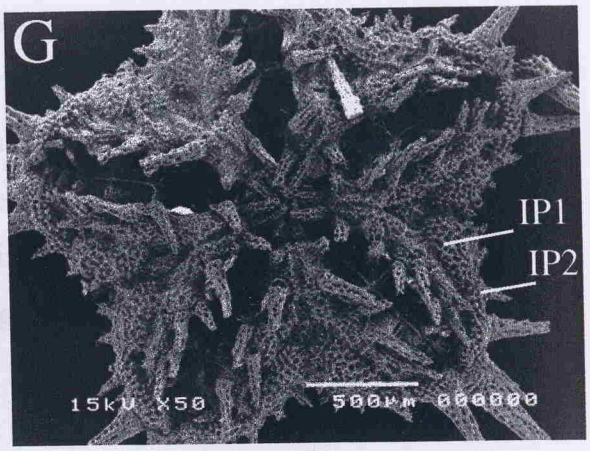
G
IP1
IP2
15kV X50
500µm 000000

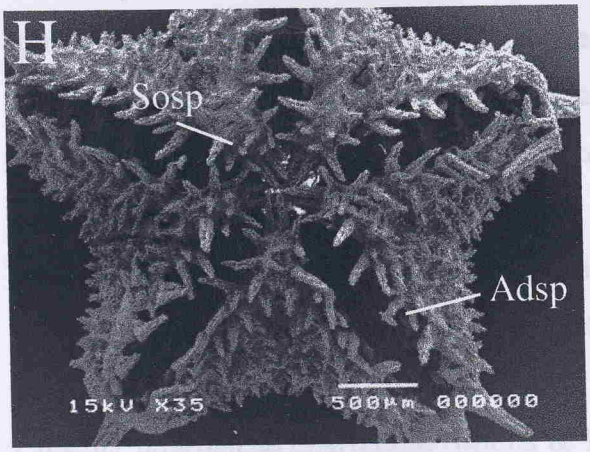
H
Sosp
Adsp
15kV X35
500µm 000000

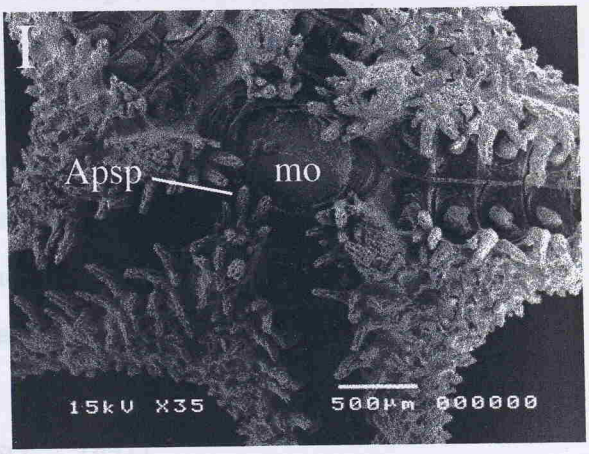
I
Apsp
mo
15kV X35
500µm 000000

specimens at an earlier stage of development (R=0.50 mm), which is the smaller size found in the sampling material.

At this stage, *Plutonaster bifrons* has a roughly rounded shape, with only the terminal plates forming the marginal frame. The terminals are broad, with a slightly concave proximal edge. They touch each other in the interradius, with the exception of the interradius where the madreporite is being formed. The madreporite is clearly visible in the interradius of the disk when R≥0.56 mm. At R≥0.56 mm the madreporite does not separate the two adjacent terminals. The rounded madreporite bears 5 spines, similar to the paxillar spines, arranged around the periphery. The terminal plates at R=0.50 mm are armed with rows of large, subequal and fenestrated spines running on the lateral part of the plate. A row of smaller spinulose spines run throughout the dorsal side of the plate. Abactinal paxillae have up to 4 spines, each spine dividing at the tip into several smaller branches (Fig. 4.3A).

Two adambulacral and 1 subambulacral spines are present on the actinal side. Each oral plate bears 1 apical, 3 marginal and 2 suboral spines. All spines are relatively elongated and spinulose. No actinal plates are present (Fig. 4.3B).

Psilaster andromeda andromeda (Müller & Troschel, 1842)

R=0.80 mm (R/r=1.32): specimens have a strongly pentagonal shape. The abactinal surface shows paxillae bearing at least 1 spine. However, individuals at this size were critical point dried, which preserved the epidermis preventing the examination of the abactinal paxillae in detail. Only 1 superomarginal is present, with 1 or 2 spines. The terminal plate bears 3 spines placed dorsally, with the central one being the largest, and 4 large spines ventrally, with the outer two being of a slightly larger size (Fig. 4.4A).

R=1.08 mm (R/r=1.39): the abactinal paxillae have 1-2 spines, whilst the body shape is slightly more stellate. The superomarginal have 3 spines and in the terminals, 1 pair of small spines is present on each side of the 3 large dorsal spines. The outer two ventral spines of the terminals are much enlarged and 1 additional spine is present on the outer side of the terminals (Fig. 4.4C).

R=1.49 mm (R/r=1.57): the arms are larger owing to the growth of the superomarginals and terminals. The abactinal paxillae bear 1 to 5 spines. The

Figure 4.3. *Plutonaster bifrons* juvenile development (A-B). A. 0.50 mm, abactinal view; B. 0.50 mm, actinal view. See Fig. 4.1 for explanation. Sizes represent the arm radius (R).

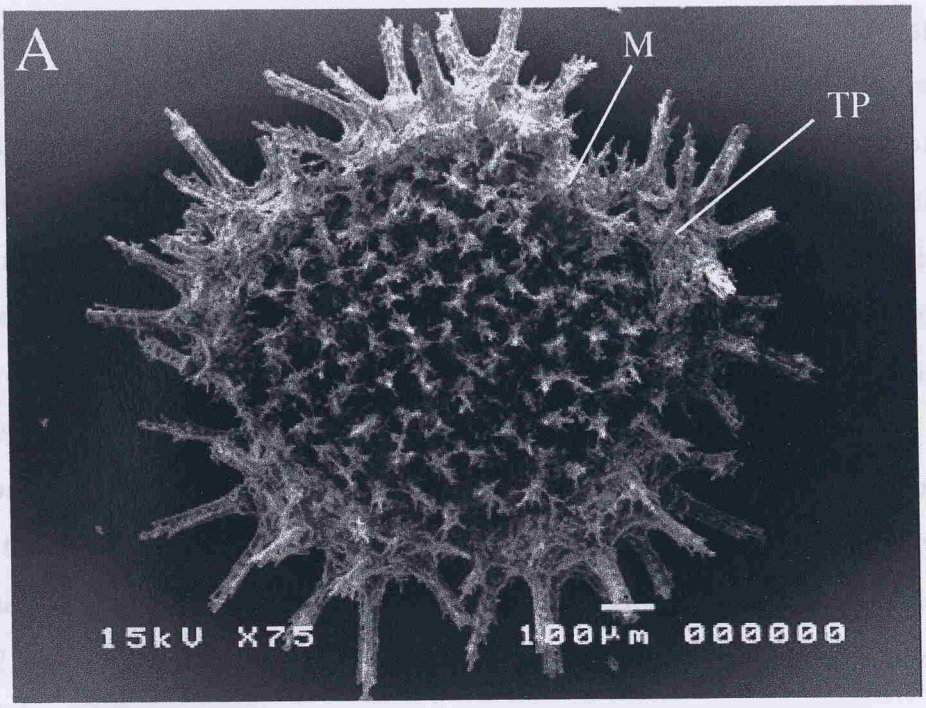
A
M
TP
15kV X75
100µm 000000

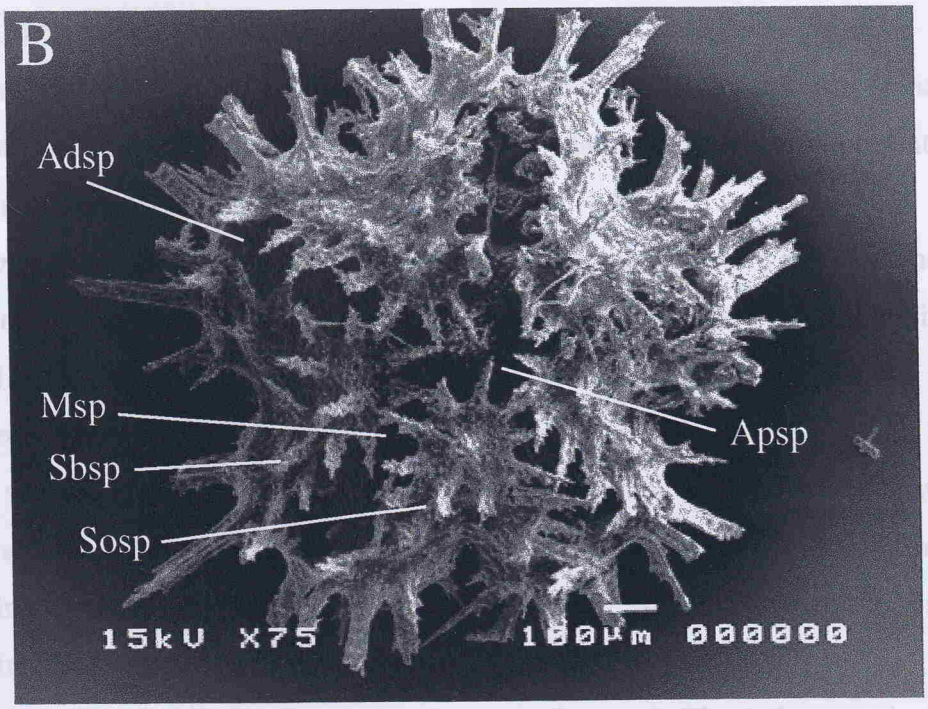
B
Adsp
Msp
Sbsp
Sosp
Apsp
15kV X75
100µm 000000

superomarginals possess 2 rows of 3 spines and the large spine of the 1st inferomarginal is easily seen on the interradial region. The terminals are more spinose with the addition of several new spines. There are 3 spines on each side of the 4 large ventral spines, and 2 spines in between the dorsal and the ventral terminal plate spines at the tip of the plate. A row of small spines is present, running through the proximal edge of the dorsal surface of the terminals. A large, rounded madreporite can be seen on the edge of the interradial area of the disk. The surface of the superomarginal and terminal plates is granular (Fig. 4.4E).

R=2.30 mm (R/r=1.73): there is a prominent epiproctal cone. Some papulae can be seen on the radial areas of the abactinal surface. The madreporite is relatively small and the arms are longer owing to the presence of the 2nd superomarginal. This plate bears 2 rows of 3 spines, whereas the 1st superomarginal plate possesses 2 rows of 4 spines (Fig. 4.4G).

R=4.55 mm (R/r=2.20): seven marginals are present, decreasing in size towards the tip of the arm. The terminals are much enlarged with a coarse granuliform aspect (Fig. 4.4H). Many papulae are present on the abactinal areas at the base of the arms.

The actinal surface of specimens at R=0.75 mm (R/r=1.26) shows 1 apical spine and 2 suboral spines on the oral plate. At least 1 large adambulacral spine is present. One inferomarginal plate is present, bearing 1 spine (Fig. 4.4B).

R=1.16 mm (R/r=1.42): three suboral and 3 adambulacral spines are present. The inferomarginal spine is much enlarged and 2 additional spines are present in this plate (Fig. 4.4D).

R=1.84 mm (R/r=1.66): the number of apical spines increases to 2. There are 2 rows of 4 suboral spines on the oral plate running parallel to each other. Five adambulacral and 3 subambulacral spines are present in the furrow region. A 2nd inferomarginal is present bearing 1 large spine and 2 smaller ones. The 1st inferomarginal has 3 large spine and several smaller ones (Fig. 4.4F).

R=4.26 mm (R/r=2.16): the 2 apical spines are flattened. The inferomarginals have a granuliform aspect and bear 1 larger and several smaller spines, with the exception of the 1st, which has 3 large spines (Fig. 4.4I).

R=14.20 mm: the 2 apical spines on the oral plate are spatulate and up to 7 adambulacral spines are present. The apical spines remain the same shape up to a size

Figure 4.4. *Psilaster andromeda andromeda* juvenile development (A-I). A, C, E, G and H, abactinal view; B, D, F and I, actinal view. A. 0.80 mm; B. 0.75 mm; C. 1.08 mm; D. 1.16 mm; E. 1.49 mm; F. 1.84 mm. Note the enlarged inferomarginal plate spine (arrow). See Fig. 4.1 for explanation. Sizes represent the arm radius (R).

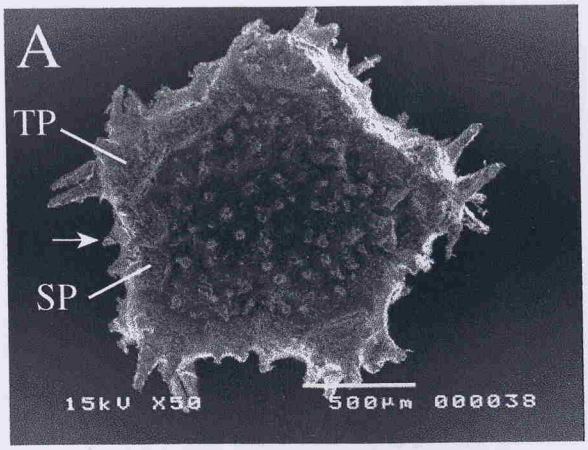
A
TP
SP
15kV X50
500µm 000038

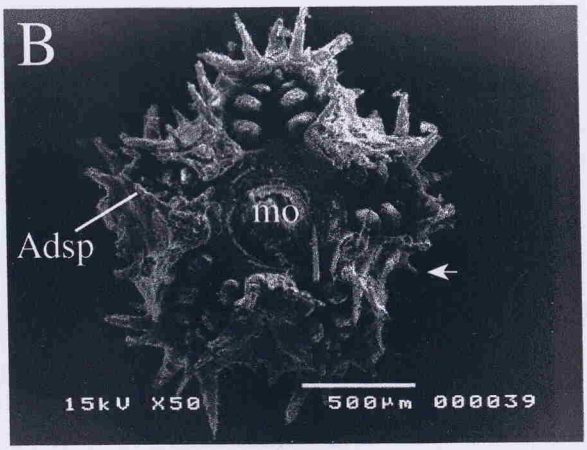
B
mo
Adsp
15kV X50
500µm 000039

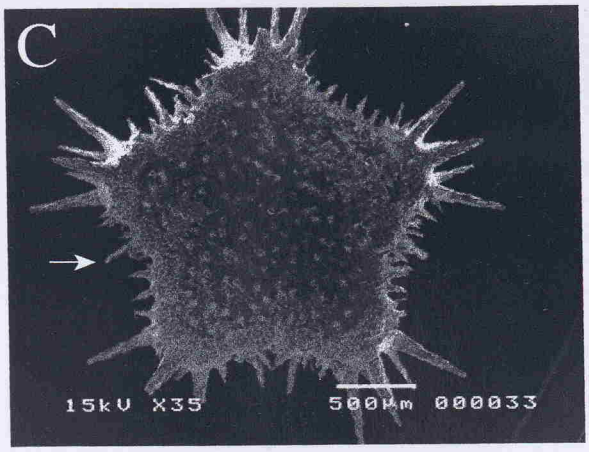
C
15kV X35
500µm 000033

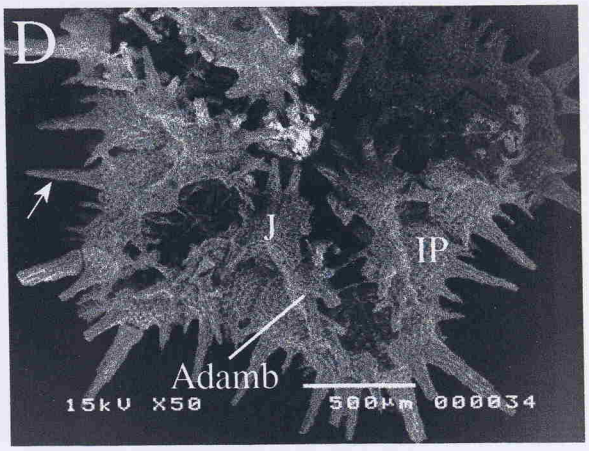
D
J
IP
Adamb
15kV X50
500µm 000034

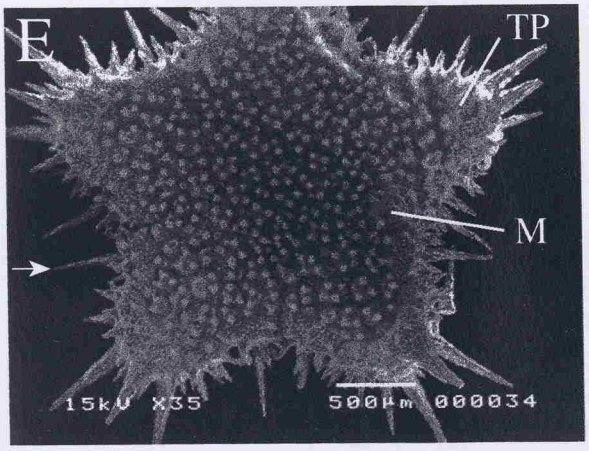
E
TP
M
15kV X35
500µm 000034


F
Sosp
15kV X35
500µm 000030

Figure 4.4 (cont.). *Psilaster andromeda andromeda* juvenile development. G. 2.30 mm; H. 4.55 mm; I. 4.26 mm. Note the enlarged inferomarginal plate spines (arrow). EC = epiproctal cone. Sizes represent the arm radius (R).

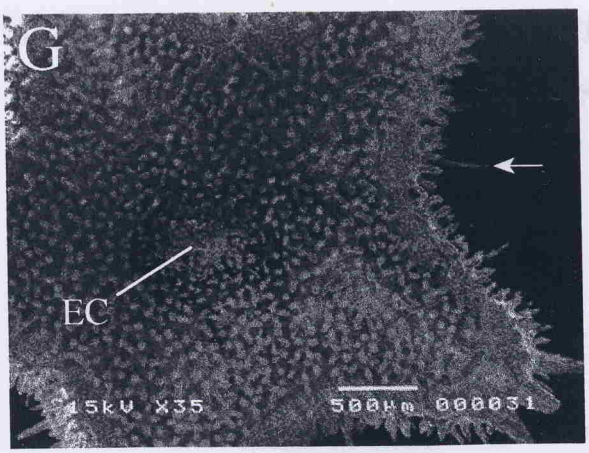
G
EC
15kV X35
500µm 000031

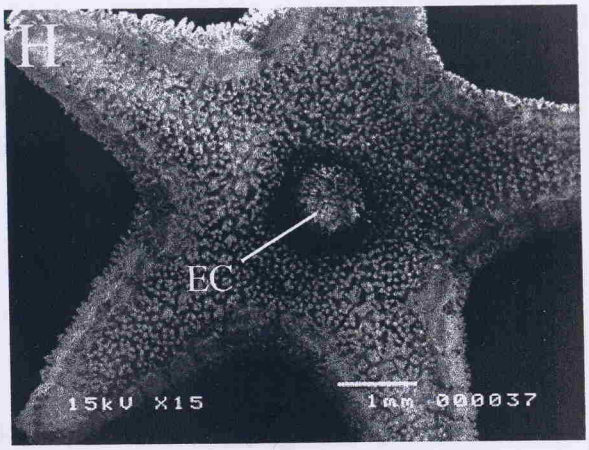
H
EC
15kV X15
1mm 000037


I
15kV X15
1mm 000039

of R=62.60 mm, only increasing in size. Clark & Downey (1992, Fig. 15a) depict much broadened apical spines. This probably happens later in the development, since specimens examined up to R ~ 62 mm show 4 distinct spatulate spines, but not to the degree shown by Clark & Downey (1992).

Family Porcellanasteridae Sladen, 1883

Hyphalaster inermis Sladen, 1883

Individuals of *Hyphalaster inermis* at R=1.35 mm (R/r=1.19) (Fig. 4.5A) have a strongly pentagonal and flattened body shape. The abactinal surface is large, with large polygonal and fenestrated plates, including the primary interradials, in the centre of the disk. The plates become smaller and rectangular in shape towards the edge of the disk. The arrangement of the abactinal plates is similar to that of tiles in a roof, with the plates imbricating. Only the 5 terminals are present on the edge of the disk, which are moderately thick and very elongated, with a concave proximal margin. The adjacent terminals meet in the interradial region. Each terminal plate bears a medium-size central spine pointing abradially and 3 smaller spines on each side on a more ventral position, 1 closer to the central spine and the other 2 closer to the interradius (see Fig. 4.5B). A hydropore is present on the edge of the abactinal region, next to the point of connection between 2 adjacent terminals (Fig. 4.5A).

R=3.74 mm (R/r=1.56): the primary interradials are still visible in the centre of the abactinal area, including a central plate. A row of small plates running on the interradia is present bearing one small spine. The abactinal surface of the arms is formed by small plates. All abactinal plates bear 1-2 short spines. Terminals, and their respective spines, are much enlarged, with 4 spines on each side ventrally. The most central plate is the largest. Two superomarginals are present, with the first being much larger and block-like. No spines are present in the superomarginals. Madreporite large and placed on the edge of the abactinal surface next to the 1st superomarginals (Fig. 4.5C).

R=4.38 mm (R/r=1.77): the central portion of the abactinal surface bears a cluster of small spines. Small plates can be seen scattered all over the surface among the larger plates. The interradial area with several small plates and small spines, gives a very rugose aspect to this area. Three superomarginals are present and a 4th is

Figure 4.5. *Hyphalaster inermis* juvenile development (A-E). A, C and E, abactinal view; B and D, actinal view. A. 1.35 mm; B. 1.43 mm; C. 3.74 mm. Note the central plate (arrow); D. 3.06 mm; E. 4.38 mm. crib = cribriform organ; EC = epiproctal cone; J = jaw. See Fig. 4.1 for further explanation. Sizes represent the arm radius (R).

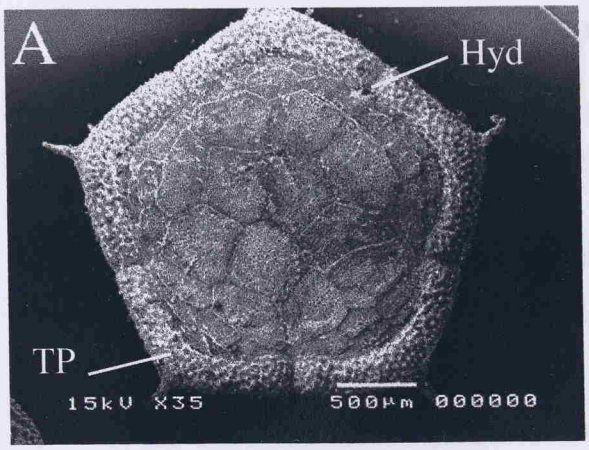
A
Hyd
TP
15kV X35
500µm 000000

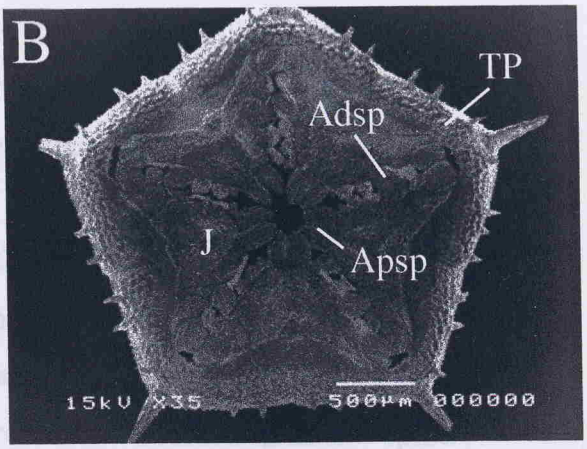
B
TP
Adsp
J
Apsp
15kV X35
500µm 000000

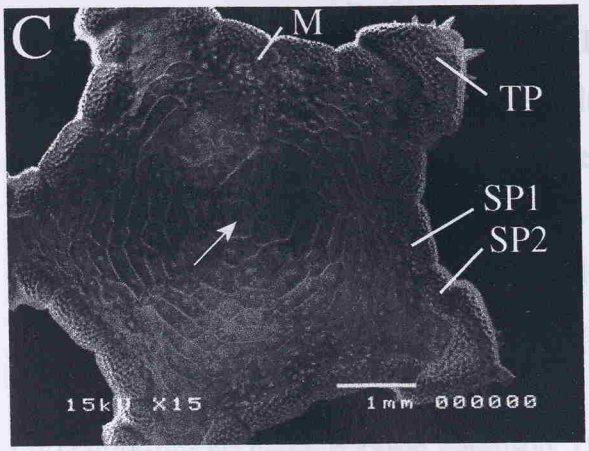
C
M
TP
SP1
SP2
15kV X15
1mm 000000

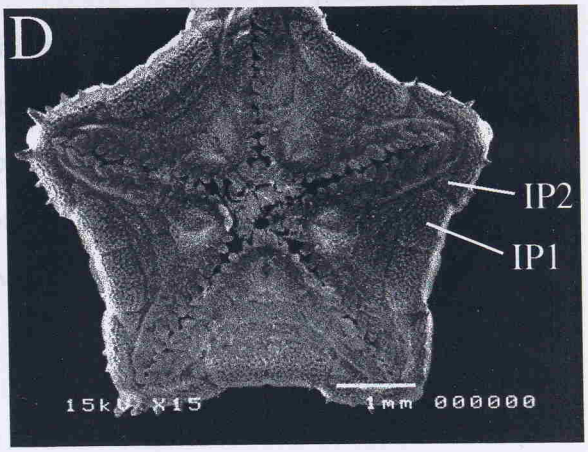
D
IP2
IP1
15kV X15
1mm 000000

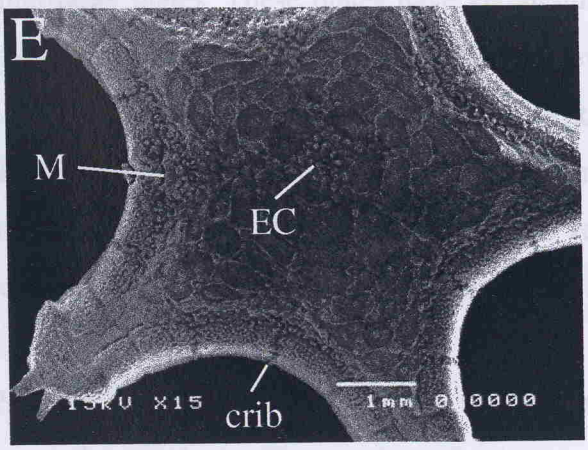
E
M
EC
15kV X15
crib
1mm 000000

beginning to form on the inner part between the terminal plate and the 3rd superomarginal. On the interradius, between the superomarginals, a row of spines is present on each side, possibly representing the primordia of the cribriform organ (Fig. 4.5E).

On the actinal surface at R=1.43 mm (R/r=1.23), all plates are flattened, with the exception of the broad jaws, which are raised in the central portion. Each oral plate bears a large and flattened apical spine and 2 smaller scale-like marginal spines on its lateral edge. Only 2 adambulacral plates are present, each with 2 flattened spines, with the distal-most the largest (Fig. 4.5B).

R=3.06 mm (R/r=1.34): four marginal and 3 adambulacral spines are present. All furrow spines appear more elongated. The 1st inferomarginal is large and bears 1 small spine. The 2nd inferomarginal is starting to appear in the inner part, between the 1st and the terminal. The actinal plates are rectangular in shape (Fig. 4.5D).

At a later stage (R=8.70mm), the arms are more elongated and the epiproctal cone is present. The cribriform organs are well-developed and 5 in number in each interradius. The apical spine is more elongated.

Porcellanaster ceruleus Wyville Thomson, 1877

R=0.47 mm (R/r=1.22): individuals are pentagonal in shape. The abactinal surface has 5 large developing interradial plates. These plates have an irregular shape with very large fenestrations. Some are still only fused bars. On the edge of the disk only the terminals are present. They are thin with a very thin and long central spine, with spinelets along its edge. Four small spines are found on each side of the central spine of the terminals. The terminals also bear two large spines at a more ventral position, so that when looking from above it is possible to see 3 long, thin spines in each radius (Fig. 4.6A).

R=0.54 mm (R/r=1.24): the abactinal plates assume a more round outline and fenestrations can be seen on the terminals. The number of spines on the terminals increases to up to 6 on each side. The hydropore is present in the interradial area (Fig. 4.6C).

R=0.92 mm (R/r=1.22): radial plates are added to the abactinal surface. The abactinal plates are rounded and the fenestrations are relatively smaller owing to the

Figure 4.6. *Porcellanaster ceruleus* juvenile development (A-J). A, C, E, G, I and J, abactinal view; B, D, F and H, actinal view. A. 0.47 mm; B. 0.52 mm; C. 0.54 mm; D. 0.53 mm; E. 0.92 mm; F. 1.05 mm. Note the presence of forams in B and D. inter = interradial plate. See Fig. 4.1 for further explanation. Sizes represent the arm radius (R).

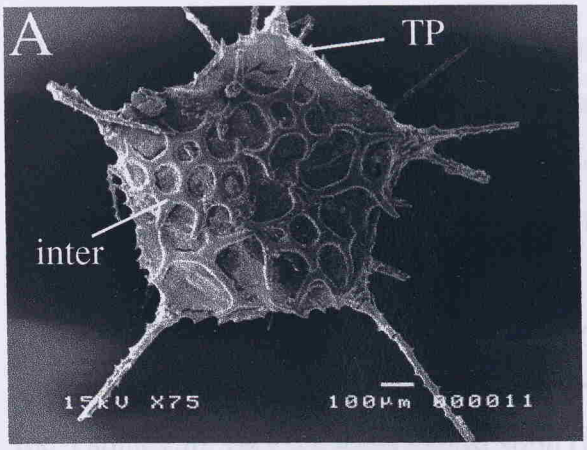
A
TP
inter
15kV X75
100µm 000011

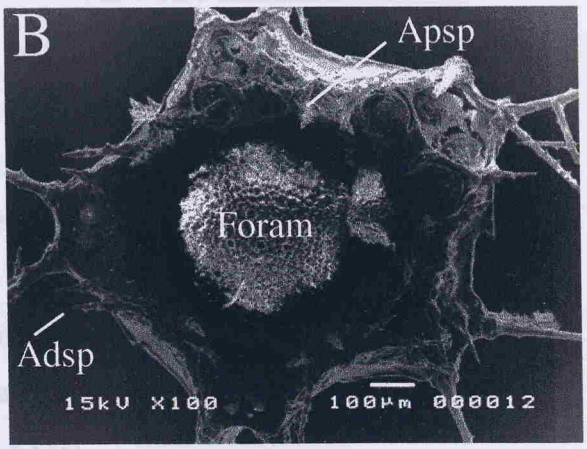
B
Apsp
Foram
Adsp
15kV X100
100µm 000012

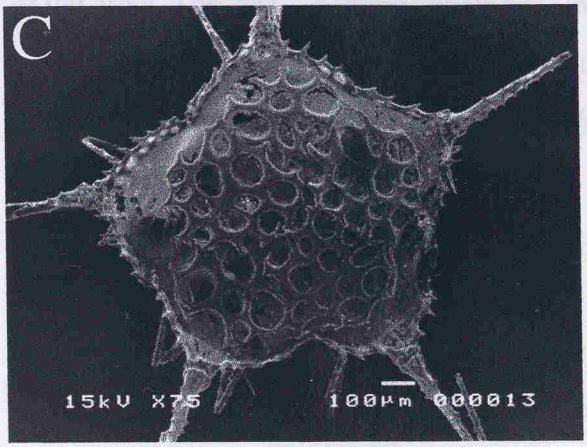
C
15kV X75
100µm 000013

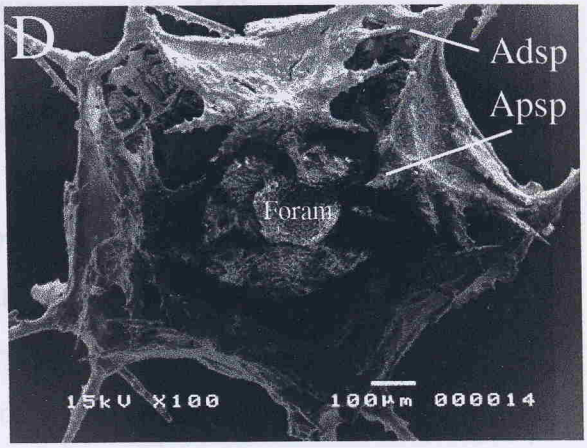
D
Adsp
Apsp
Foram
15kV X100
100µm 000014

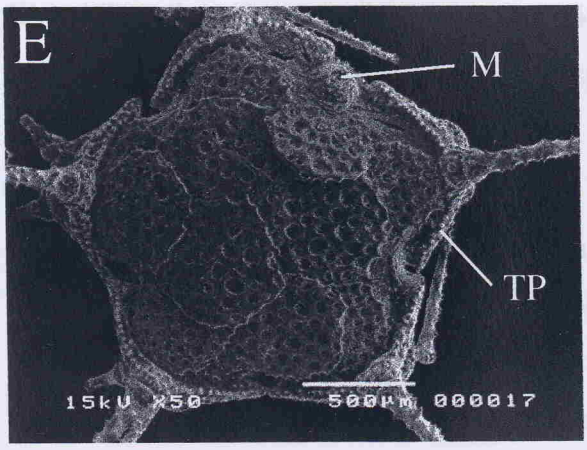
E
M
TP
15kV X50
500µm 000017

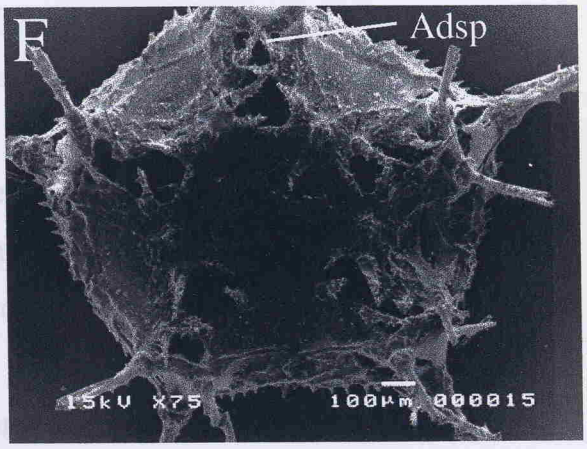
F
Adsp
15kV X75
100µm 000015

deposition of calcium carbonate. The terminals and spines are much enlarged and a round notch is present between adjacent terminals. The madreporite is large and placed between 2 terminals. The ventral side of the terminals is more protuberant with the place of insertion of the 2 ventral spines being easily seen from above (Fig. 4.6E).

R=1.40 mm (R/r=1.73): a central primary plate starts forming. The arms are larger owing to the presence of the 1st superomarginals. The terminals are very large and the 3 spines are very long and almost solid (Fig. 4.6G).

R=2.16 mm (R/r=1.96): animals have more plates added to the abactinal surface of the arms. The 2nd superomarginals are already present (Fig. 4.6I).

As the animals grow, new plates are added to the abactinal surface. In animals with stomachs full of sediment, the ratio R/r can be small even in larger specimens (compare Figs. 4.6I and K).

The actinal surface of individuals at R=0.52 mm (R/r=1.24) shows a single apical spine on the mid-line suture of 2 paired oral plates. In addition, each oral plate bears 2 marginal spines with the distal-most the largest. Only 1 adambulacral spine is present. All spines of the actinal surface are relatively long and thin, with small spinelets along their length (Figs. 4.6B and D).

R=0.70 mm (R/r=1.20): there are 2 adambulacral spines and at R=1.05 mm (R/r=1.41) all the furrow spines become thicker (Fig. 4.6F).

R=1.67 mm (R/r=2.18): the furrow spines are slightly flattened. The 1st inferomarginal is present (Fig. 4.6H).

R=4.40 mm: the epiproctal cone and the cribriform organs start forming. However, the cribriform organ present on the same interradius of the madreporite is already well-developed. The single apical spine of the jaws is thicker and 3 subequal and conical marginal spines are present.

R=6.00 mm: the epiproctal cone is more elongated and all 5 cribriform organs are fully-developed (one on each interradius).

Figure 4.6 (cont.). *Porcellanaster ceruleus* juvenile development. G. 1.40 mm; H. 1.67 mm; I. 2.16 mm; J. 2.31 mm. Note the central plate (arrow). See Fig. 4.1 for explanation. Sizes represent the arm radius (R).

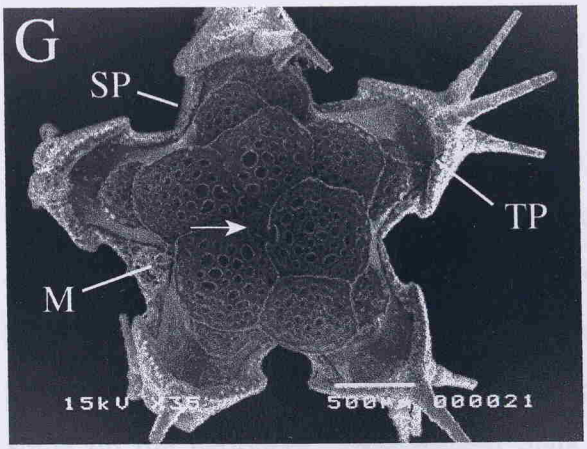
G
SP
TP
M
15kV X35
500µm 000021

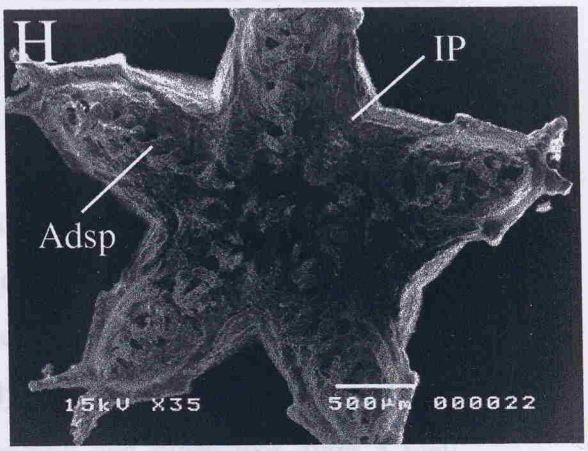
H
IP
Adsp
15kV X35
500µm 000022

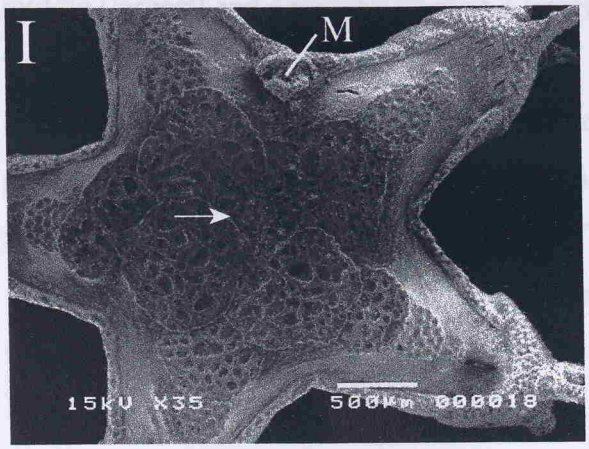
I
M
15kV X35
500µm 000018

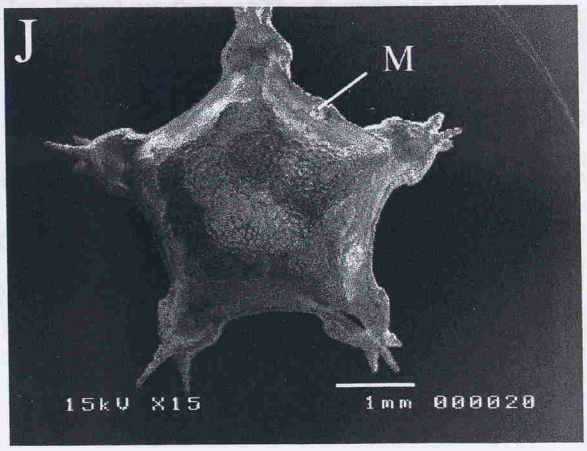
J
M
15kV X15
1mm 000020

Order Notomyotida Ludwig, 1910

Family Benthopectinidae Verrill, 1899

Benthopecten simplex simplex (Perrier, 1881)

R=0.83 mm (R/r=1.43): animals have a circular disk with the terminals issuing from it. The terminals do not meet in the interradial area. Instead, a large interradial plate is present bearing 1-2 spines. In the centre of the abactinal surface, a central primary plate is present possessing a moderately large central spine and a smaller spine on the periphery. The terminal plate is strong and block-like, with a well-developed spine armature composed of 3 spines located more dorsally, 2 in the middle (largest) and 4 ventrally (inner 2 larger). The dorsal surface of the terminals is very granular (Fig. 4.7A).

R=0.97 mm (R/r=1.44): new plates are added to the abactinal surface. The central primary plate bears a large central spine surrounded by 5 smaller ones. Primary interradials have 2 spines of different sizes. The remaining abactinal plates have only 1 spine. The terminals are larger, with a concave proximal margin and meet in the interradial area. An extra spine is present on the terminal plate on each side of the 2 largest (Fig. 4.7B).

R=1.41 mm (R/r=1.61): the arms are larger and the proximal margin of the terminals is strongly concave. A pair of spines is present between the 2 largest spines of the terminals, but in a slightly dorsal position. An odd superomarginal is present on the interradial area bearing a moderately small spine (Fig. 4.7C).

R=1.84 mm (R/r=1.91): the central primary plate is still visible bearing 1 central spine surrounded by 6 smaller ones. The spine on the odd superomarginal is very large in size (over 0.65 mm) and points upwards. Three additional smaller spines are present on the base of each odd superomarginal spine. The 2nd superomarginal bears 2 spines and the 3rd superomarginal is starting to appear between the 2nd and the terminal. The appearance of the marginals in this species is on the side of the arm and not internally as in other species (*e.g. Hyphalaster inermis*). The 3rd superomarginal possesses 1 spine at this stage (Fig. 4.7D).

R=5.86 mm (R/r=3.53): the large erect spines of the odd superomarginals are easily seen. The remaining superomarginals have 2 spines, one being larger and pointing abradially (Fig. 4.7E).

Figure 4.7. *Benthopecten simplex simplex* juvenile development (A-I). A-E, abactinal view; F-I, actinal view. A. 0.83 mm; B. 0.97 mm; C. 1.41 mm; D. 1.84 mm; E. 5.86 mm. Note the central plate (arrow). inter = interradial plate; SPsp = odd superomarginal plate spine. See Fig. 4.1 for further explanation. Sizes represent the arm radius (R).

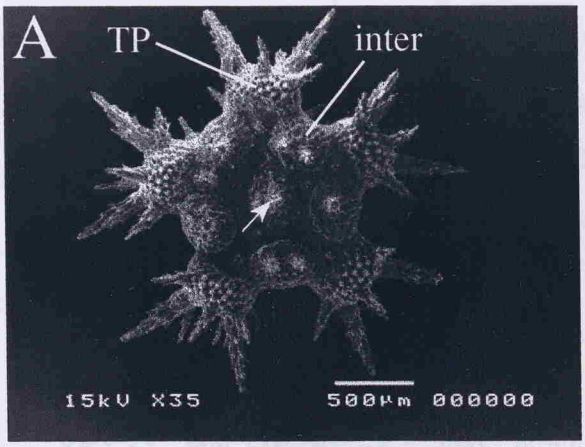
A
TP
inter
15kV X35
500µm 000000

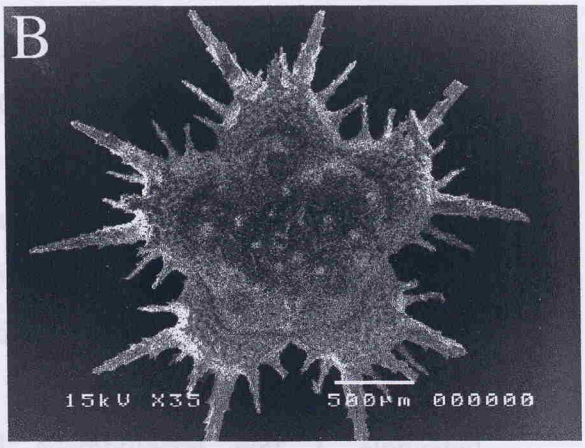
B
15kV X35
500µm 000000

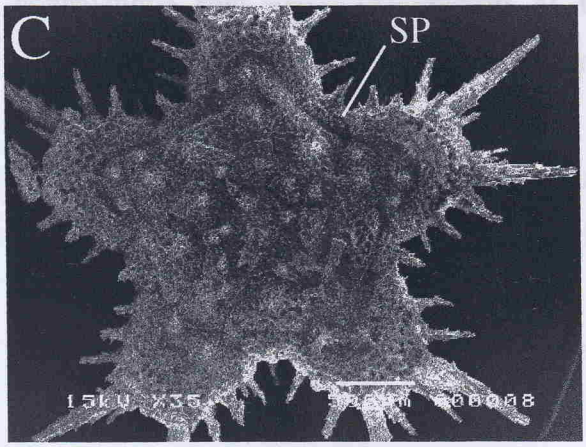
C
SP
15kV X35

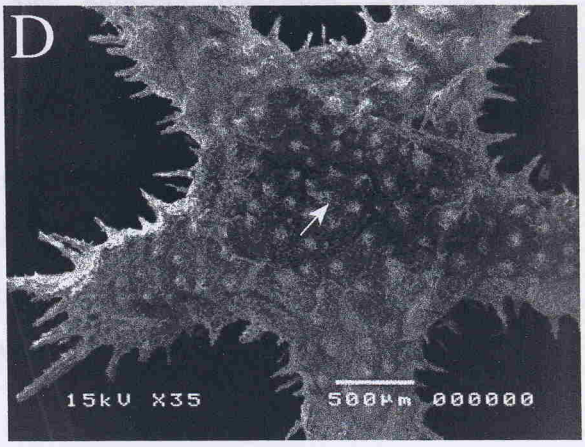
D
15kV X35
500µm 000000

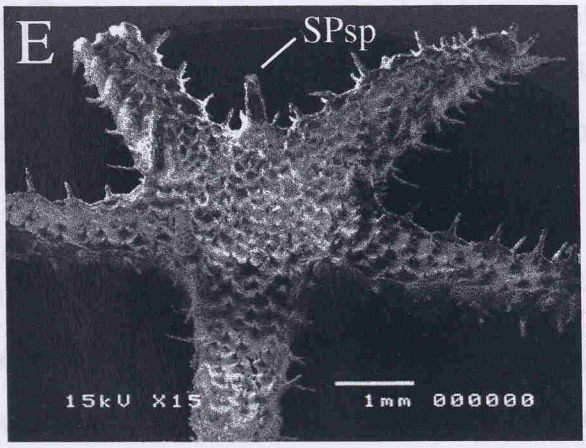
E
SPsp
15kV X15
1mm 000000

On the actinal surface at R=0.75 mm (R/r=1.39), the jaws are rectangular, with 1 apical and 2 marginal spines on each oral plate. Only 1 adambulacral spine is present. The furrow spines are rather large and spinulose (Fig. 4.7F).

R=1.02 mm (R/r=1.60): the apical spines are larger in size and cover the mouth. Three marginal spines are present on the furrow and 1 suboral spine on the distal margin of the oral plate. One adambulacral and 1 subambulacral spines are present (Fig. 4.7G).

R=3.25 mm (R/r=2.47): two elongated adambulacral and 1 elongated subambulacral spines are present. The suboral and subambulacral spines form a very conspicuous row along the margin of the disk pointing abradially. An odd inferomarginal bearing 3 spines is present on each interradius. The remaining inferomarginals have 2 spines (Fig. 4.7H).

R=6.12 mm (R/r=3.55): three to four marginal spines are present on the furrow and a 2nd suboral spine is found on the proximal edge of the oral plate, just above the apical spine. Adambulacral plates have 3 spines. Two subambulacral spines are present. The odd inferomarginal has 5 spines, while remaining inferomarginals have 2 spines (Fig. 4.7I).

When the animal attains a much larger size, R=14.00 mm, the abactinal plates have up to 3 spines and the supero- and inferomarginals bear 1 large spine. At R=17.50 mm, 4 adambulacral spines are present and the inferomarginals bear 1 large and 1 accessory spine. The odd inferomarginal has small spinelets. When R=36.00 mm, the accessory spine of the inferomarginals is ¼ of the main spine of the plate.

Pectinaster filholi Perrier, 1885

R=0.98 mm (R/r=1.47): the general shape of the body is similar to that of *Benthopecten simplex simplex* at a similar size. The disk is circular with a large rounded central plate bearing 4 small spines, and 5 large interradial plates bearing up to 5 small spines. Between the interradials, 1 or 2 radial plates are present, each possessing only 1 spine. The interradials touch the central plate in the proximal side and on the opposite side separate 2 adjacent terminals. The terminals are stubby and block-like, almost rectangular in shape bearing a strong spine armature on their tips,

Figure 4.7 (cont.). *Benthopecten simplex simplex* juvenile development. F. 0.75 mm; G. 1.02 mm; H. 3.25 mm; I. 6.12 mm. See Fig. 4.1 for explanation. Sizes represent the arm radius (R).

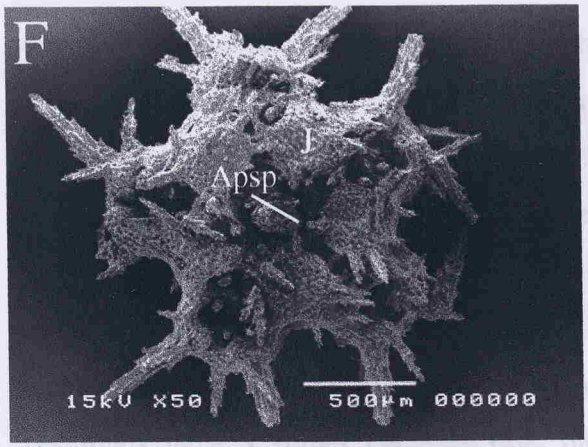
F
Apsp
15kV X50
500µm 000000

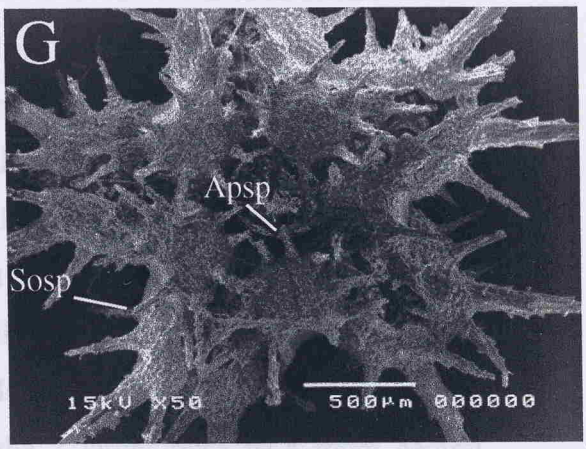
G
Apsp
Sosp
15kV X50
500µm 000000

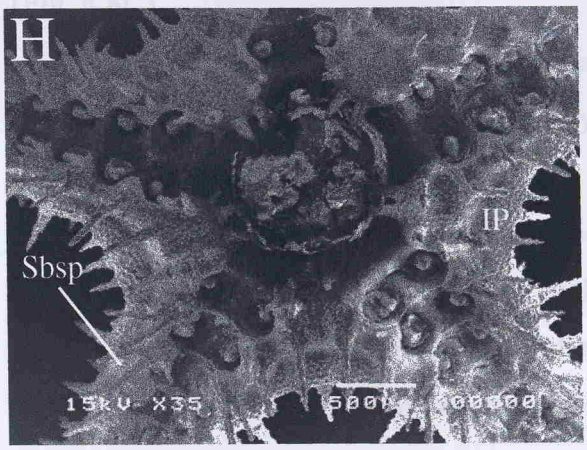
H
IP
Sbsp
15kV X35
500µm 000000

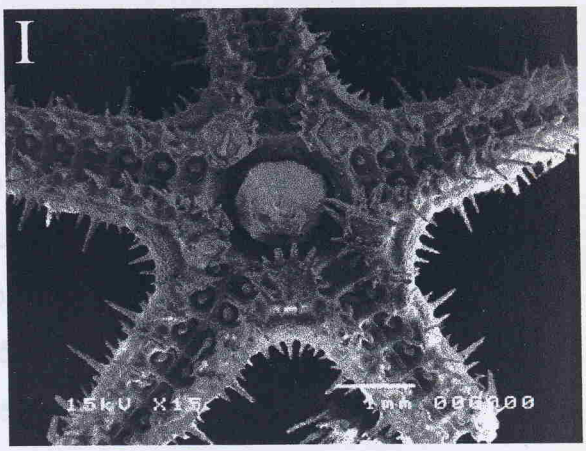
I
15kV X15
1mm 000000

with 4 medium-sized spines ventrally, 2 larger in the middle area and 4 on a more dorsal position. The dorsal surface of the terminals has a granular aspect (Fig. 4.8A).

R=1.83 mm (R/r=2.01): the central plate is still visible and it is ornamented with 1 central spine surrounded by up to 9 spines. The interradial plates still occupy a peripheral position separating the 2 adjacent 1st superomarginals. The distal-most spine of the interradial plate points abradially. The arms are larger, with one superomarginal bearing a spine and the terminals having a concave proximal margin. Terminals have 3 spines on each side, plus the 2 larger ones in a more central position. Smaller spines, on the sides and the centre of the plate, are also present (Fig. 4.8C).

R=3.60 mm (R/r=2.68): the abactinal paxillae are rounded and slightly convex and bear a larger central spine surrounded by smaller ones. The interradial plates still occupy the edge of the disk, but they do not separate the 2 adjacent 1st superomarginals, which now touch in the middle of the interradial area (Fig. 4.8E).

R=4.30 mm (R/r=2.91): the structure of the paxillae and superomarginals is easily seen. Five superomarginals are found, with the 5th being issued on the lateral part of the arm, between the terminal and the 4th superomarginal. Superomarginals bear 3 spines, with the central one the largest and 2 rather small ones (Fig. 4.8G).

On the actinal side at R=1.82 mm (R/r=1.90), the oral plates have 1 apical, 4 marginal and 1 suboral spines. The suboral spines are placed proximally and distally on the oral plate. In the furrow, 3 adambulacral and 1 subambulacral spines are present. Only 1 inferomarginal plate is present bearing 2 spines, the distal one the largest. Adjacent inferomarginals do not touch in the middle of the interradial area (Fig. 4.8B).

R=2.79 mm (R/r=2.14): three suboral spines are present, but in some oral plates a 4th spine may also be present. The adambulacral plates bear up to 4 spines. First inferomarginals touch in the middle of the interradial area, each possessing 3 spines, with the central the largest. The second interradial has 1 spine (Fig. 4.8D).

R=5.56 mm (R/r=3.41): five marginal and up to 5 adambulacral spines are present. There are 4 suboral spines, with the 2nd nearest to the distal margin the largest. The surface of the inferomarginals has a granular aspect. First inferomarginal bears 4 spines and several smaller spines on the surface (Fig. 4.8F).

Figure 4.8. *Pectinaster filholi* juvenile development (A-G). A, C, E and G, abactinal view; B, D and F, actinal view. A. 0.98 mm; B. 1.82 mm; C. 1.83 mm; D. 2.79 mm; E. 3.60 mm; F. 5.56 mm; G. 4.30 mm. cp = central plate; inter = interradial plate; J = jaw; mo = mouth; rad = radial plate; SPsp = superomarginal plate spine. See Fig. 4.1 for further explanation. Sizes represent the arm radius (R).

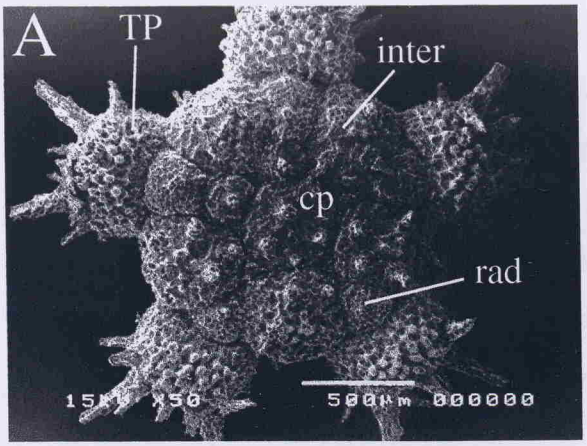
A
TP
inter
cp
rad
15kV X50
500µm 000000

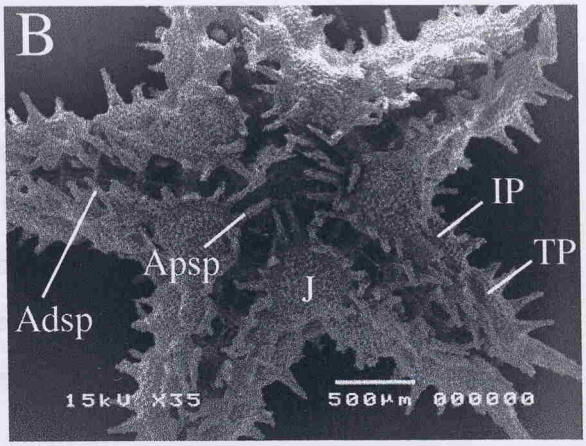
B
IP
TP
Apsp
J
Adsp
15kV X35
500µm 000000

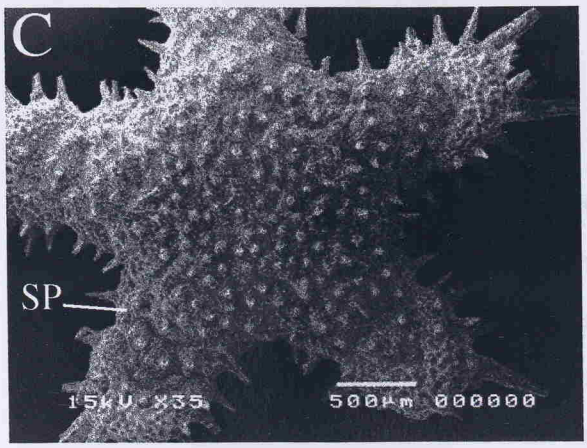
C
SP
15kV X35
500µm 000000

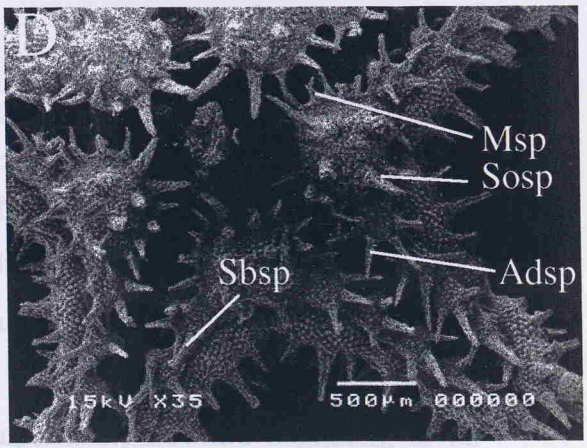
D
Msp
Sosp
Sbsp
Adsp
15kV X35
500µm 000000

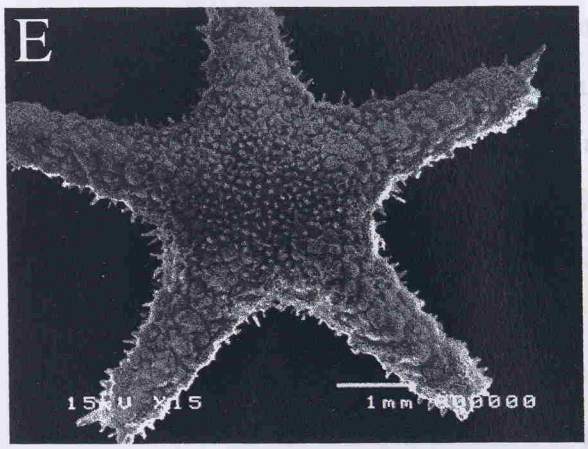
E
15kV X15
1mm 000000

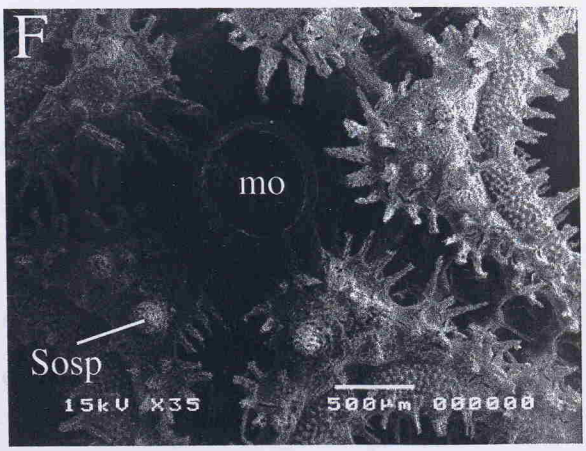
F
mo
Sosp
15kV X35
500µm 000000

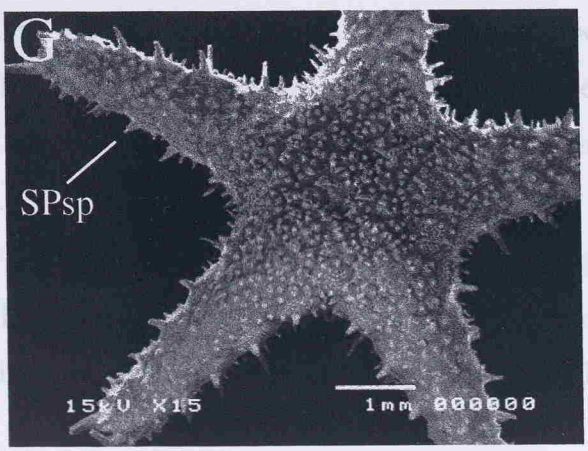
G
SPsp
15kV X15
1mm 000000

When R=8.00 mm, the five primary interradials are still visible on the edge of the abactinal area. At R=11.00 mm, these plates are located more to the centre of the disk owing to the addition of new abactinal plates between the primary interradials and the marginals. These are 9 in number and bear a single large spine, plus small spinelets. Only 1 subambulacral spine is present. At R=13.00 mm the number of adambulacral spines increases to 5.

Order Valvatida Perrier, 1884

Family Goniasteridae Forbes, 1841

Plinthaster dentatus (Perrier, 1884)

R=1.05 mm (R/r=1.50): animals bear several abactinal plates from which the central one is conspicuous, although the interradials are not easily distinguished. The terminals are stubby with a convex distal margin and 4 thick, triangular spines placed ventrally and a single smaller central spine at a more dorsal position. The terminals do not meet in the interradial area. The 1st superomarginals are beginning to be formed next to the terminals (Fig. 4.9A).

R=2.28 mm (R/r=1.52): the abactinal plates are enlarged and bear a small raised area in their centre. A number of small granules are present surrounding some of the abactinal plates. The madreporite occupies an interradial position and bears a long furrow. The 1st superomarginal is large with 2 small, knobby spines and a granular surface. The 2nd superomarginal is beginning to form in the middle of the area between the terminal plate and the 1st superomarginal. The terminal is a strong, triangular plate with 4 large spines on each side on the actinal side, increasing in size outwards. A central spine is present on the tip of the terminal plate (Fig. 4.9C).

R=3.60 mm (R/r=1.66): the central plate is still visible. The abactinal plates, mainly in the central portion, are surrounded by granules. The madreporite develops another furrow and now has a cross shape. The 1st superomarginal bears 3 knobby spines and the second 2. The 3rd superomarginal is present as a small plate (Fig. 4.9E).

On the actinal side at R=1.19 mm (R/r=1.49), the jaws are rectangular in shape. Each oral plate bears a large, triangular apical spine and smaller marginal spines running in the furrow, increasing in size distally. Only 1 adambulacral plate is

Figure 4.9. *Plinthaster dentatus* juvenile development (A-E). A, C and E, abactinal view; B and D, actinal view. A. 1.05 mm; B. 1.19 mm; C. 2.28 mm; D. 2.27 mm; E. 3.60 mm. J = jaw. See Fig. 4.1 for further explanation. Sizes represent the arm radius (R).

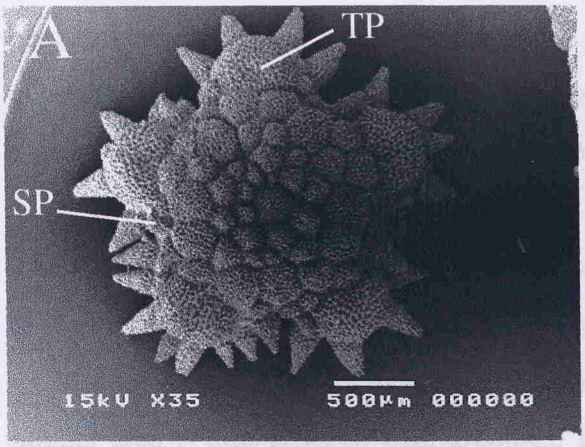

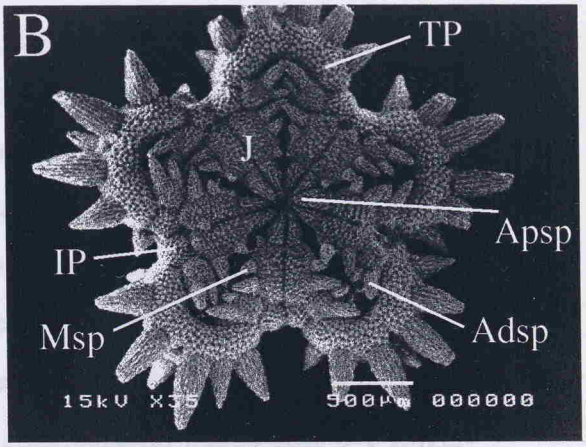

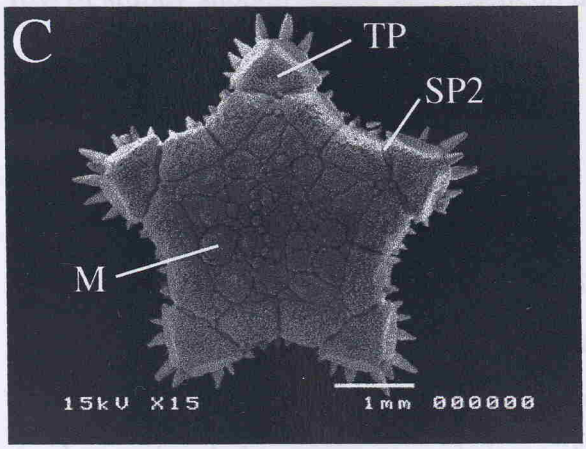

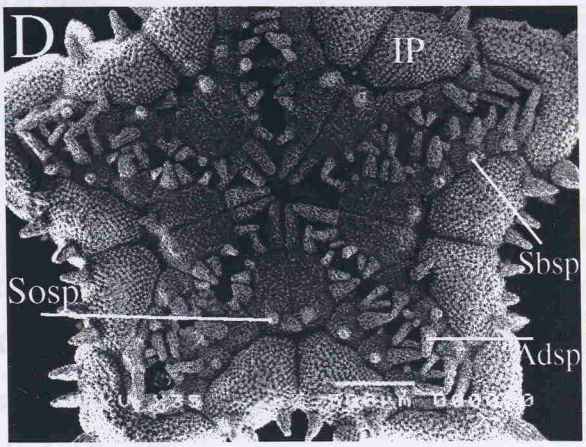

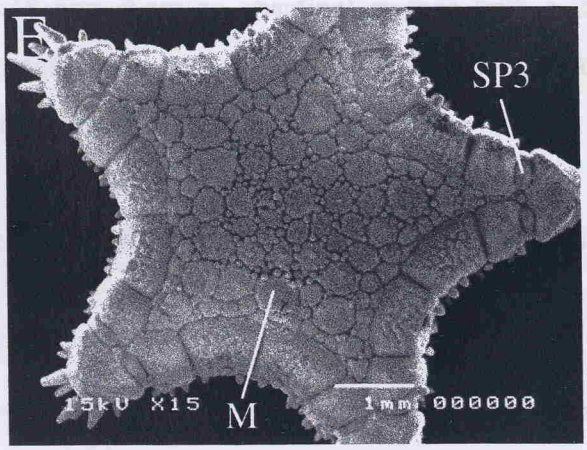

present bearing 2 spines, with the distal one the largest. The 1st inferomarginal plate is present in the interradial area. The terminals are fused on the ventral side and only a small orifice is present between the two most central spines (Fig. 4.9B).

R=2.27 mm (R/r=1.65): the oral plates bear 5 marginal and 1 suboral spines. Three adambulacral and 1 subambulacral spines are present. The 1st inferomarginal is very large bearing 3 medium-size stubby spine (Fig. 4.9D).

At a later stage, R=7.60 mm, all marginals bear a cluster of knobby granules. The actinal area is also covered with granules. The adambulacral plates bear 3-4 finger-like spines, 1 main subambulacral spine and a number of subambulacral granules. A row of stubby suboral spines are present on the oral plate.

Order Velatida Perrier, 1893

Family Pterasteridae Perrier, 1875

Hymenaster pellucidus Thomson, 1873

The presence of a thin supradorsal membrane and large spines on the abactinal surface made the description of this species rather difficult. The description of the abactinal plates was not possible. Also, at fixation, *Hymenaster pellucidus* specimens tend to curl and change the general shape of the body. For this reason, measurements of the body are estimates and some could not be measured.

Individuals with r=0.48 mm show an abactinal surface with a thin supradorsal membrane and 1 paxillar column in each ray bearing at least 7 large, thin spines with a solid structure. These form the osculum (Fig. 4.10A).

The structure of the tip of the arm can be seen in figure 4.10c. The individual (r=0.65 mm) has a large terminal plate with a concave proximal margin bearing a group of large spines, similar to the paxillar spines. Each side of the terminals possess at least 5 spines (Fig. 4.10C).

At R=1.57 mm (R/r=1.98), the structure of the abactinal plates can be seen in the centre of the plate. They are rounded and bear many fenestrations (Fig. 4.10E).

The actinal side at R=1.02 mm (R/r=2.24) show the oral plates bearing 1 large and acute apical spine. Only 1 acute adambulacral spine is present. The number of actinolateral spines is at least 6, with the size increasing from the proximal to the middle and then decreasing in size again towards the tip of the arm (Fig. 4.10B).

Figure 4.10. *Hymenaster pellucidus* juvenile development (A-F). A, C and E, abactinal view; B, D and F, actinal view. A. r=0.48 mm; B. R=1.02 mm; C. r=0.65 mm; D. R=2.43 mm; E. R=1.57 mm. Note the abactinal plate (arrow); F. r=1.09 mm. mo = mouth; PC = paxillar column; SM = supradorsal membrane; sp = spine; tf = tube foot. See Fig. 4.1 for explanation.

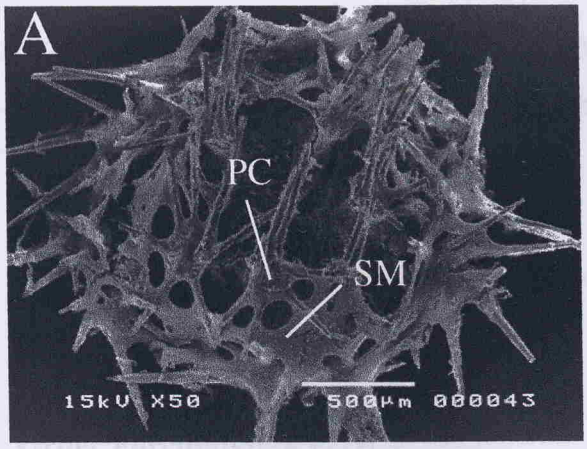
A
PC
SM
15kV X50
500µm 000043

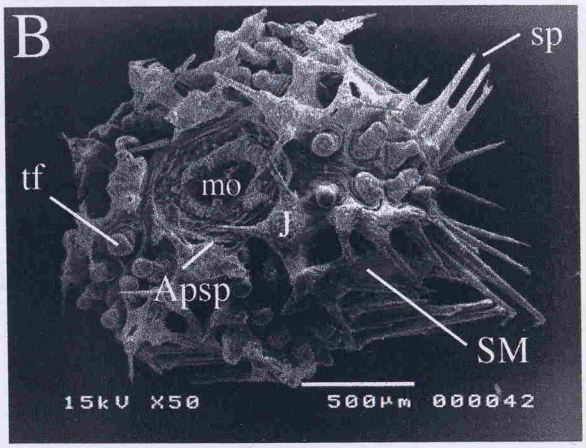
B
sp
tf
mo
J
Apsp
SM
15kV X50
500µm 000042

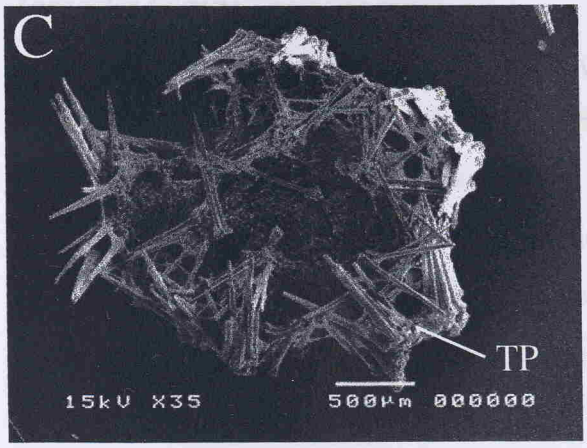
C
TP
15kV X35
500µm 000000

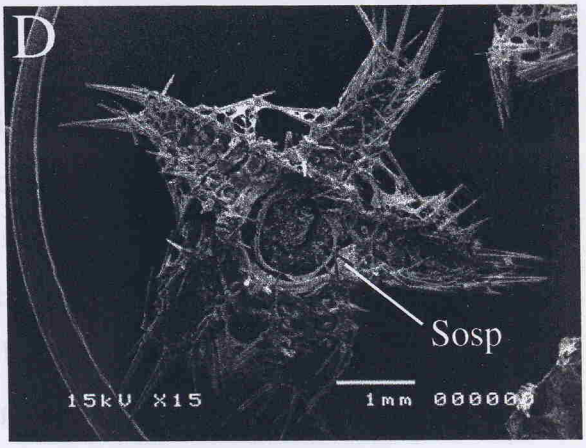
D
Sosp
15kV X15
1mm 000000

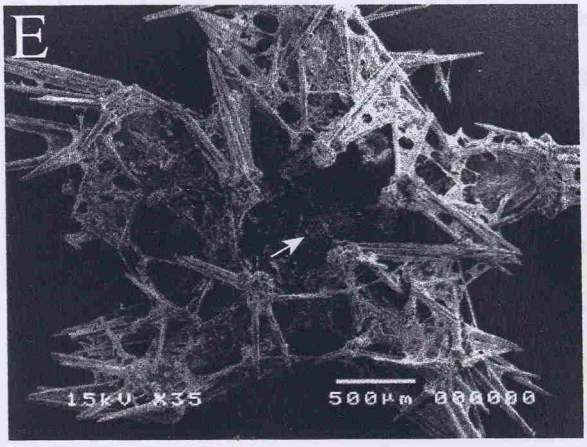
E
15kV X35
500µm 000000

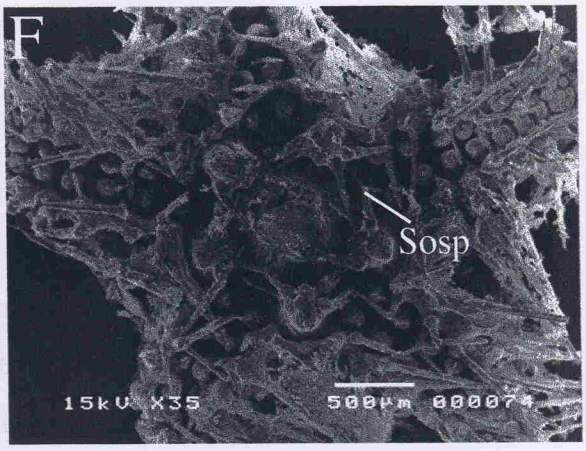
F
Sosp
15kV X35
500µm 000074

At R=2.43 mm (R/r=2.49), a suboral spine is present next to the apical spine, being slightly larger. There are 2 long adambulacral spines on the furrow (Fig. 4.10D and F).

When the animal attains R=16.70 mm, the paxillae bear 3 spines and the oral plates have 4 short and conical marginal and 2 stout suboral spines. Three adambulacral spines are present.

Order Forcipulatida Perrier, 1884

Family Zoroasteridae Sladen, 1889

Zoroaster fulgens Thomson, 1873

Figures 4.11A and 4.11C show 2 individuals of *Zoroaster fulgens* at R=0.53 mm (R/r=1.60) and R=0.58 mm (R/r=1.46), respectively. The specimen in figure 4.11A was critical point dried, which preserved the skin over the skeleton quite well, hiding the plates from view. In this specimen, we note six knobs on the abactinal surface (1 central and 5 interradial) and a terminal plate with 4 stubby spines.

The individual in figure 4.11C was air dried. Using this method, the skin is pulled away, revealing details of the skeleton. In this figure we notice that the 6 knobs are 6 stubby spines placed on the rounded central primary plate and on each interradial plate. The terminals are somewhat spherical and do not meet in the interradial area. Each terminal bears 4 large and thick spinulose spines.

R=0.78 mm (R/r=1.43): the spines on the primary plates are larger in size, and 5 radial plates are present. Some of the radials bear a single small spine. The 1st superomarginal is present on the sides of the terminals, bearing 1 spine (Fig. 4.11E).

R=1.05 mm (R/r=1.79): the central primary plate has a pentagonal shape, and the interradials are polygonal. Adjacent terminals are still separated by the interradials. The proximal margin of the terminals is almost straight and some small spines are present. The 4 primary spines of the terminals are much enlarged (Fig. 4.11F).

R=1.59 mm (R/r=1.95): a large rectangular plate is present between 2 interradials, with no other equivalent on the other radii. The spines of the interradials are very large. The terminals are strongly circular and a row of small spines is visible on their periphery, right above the 4 large spines. Two superomarginals are present, each with a small spine (Fig. 4.11H).

Figure 4.11. *Zoroaster fulgens* juvenile development (A-L). A, C, E, F, H, J and L, abactinal view; B, D, G, I and K, actinal view. A. 0.53 mm; B. 0.54 mm; C. 0.58 mm; D. 0.80 mm; E. 0.78 mm. cp = central plate; inter = interradial plate; J = jaw; rem? = remnants of lecithotrophic egg (?); sens = sensory podium; tf = tube foot. See Fig. 4.1 for further explanation. Sizes represent the arm radius (R).

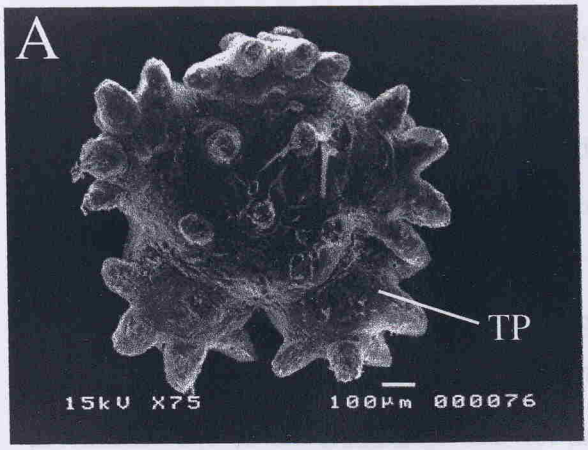
A
TP
15kV X75
100µm 000076

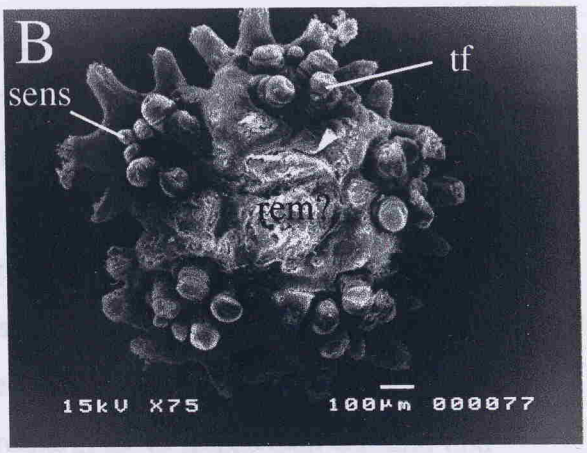
B
sens
tf
rem?
15kV X75
100µm 000077

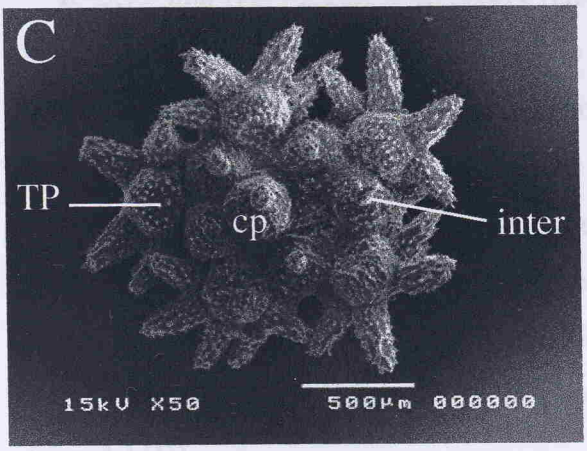
C
TP
cp
inter
15kV X50
500µm 000000

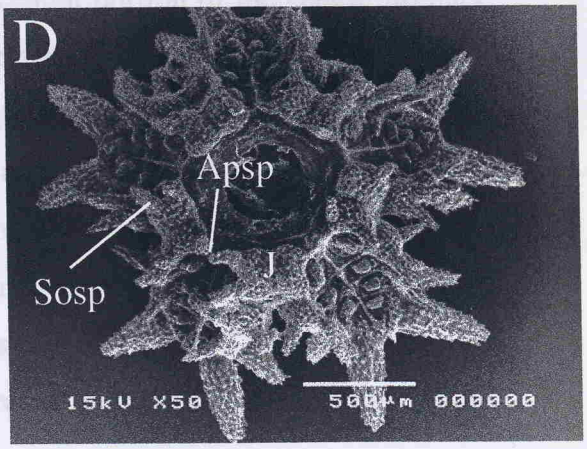
D
Apsp
Sosp
J
15kV X50
500µm 000000

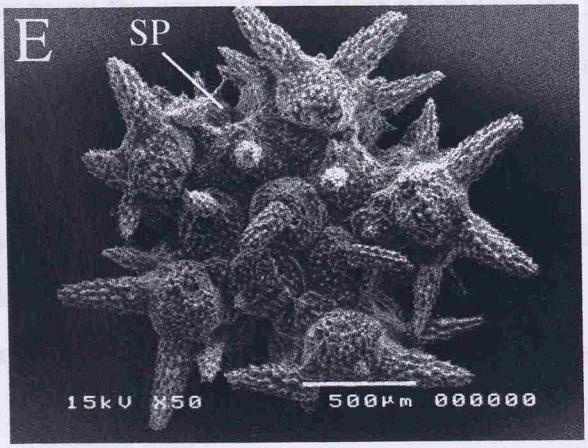
E
SP
15kV X50
500µm 000000

R=2.04 mm (R/r=2.45): the spine of the central primary plate is very large and strong, and it is surrounded by 5 smaller spines (about half the size). The central spine of the interradials is not as large and it is also surrounded by smaller spines. The terminals change in shape from circular to more elongated, with a slightly concave proximal margin. Of the 4 primary spines of the terminals, the 2 internal-most are very enlarged, almost twice as large as the external ones. Smaller spines are present all over the perimeter of the plate. Three small spines are also present on the proximal edge of the terminals. The 1st superomarginal is larger than the 2nd and bears 2 small spines (Fig. 4.11J).

R=3.75 mm (R/r=3.15): a markedly raised central portion of the central primary plate can be seen, where the central spine is inserted. The abactinal plates of the arms form a single row, each bearing 3 spines arranged transversally. A large radial plate on the base of the arm is present with 2 large spines and some smaller ones surrounding them. The terminals are large and their proximal margin is strongly concave. Four superomarginals are present with 2 small spines each (Fig. 4.11L).

On the actinal side, the critical point dried specimens, at R=0.54 mm (R/r=1.41), show no spines. Three pairs of tube feet are present plus the unpaired sensory podia (Fig. 4.11B).

R=0.80 mm (R/r=1.53): the jaw is rectangular in shape and each oral plate bears an apical and a suboral spine on the opposite end, both placed on the adradial corner of the plate. Only 1 adambulacral and 1 subambulacral spines are present. The subambulacral spines point abradially (Fig. 4.11D).

R=1.25 mm (R/r=1.89): the apical spines are larger and 2 fully formed adambulacral plates are present. A 3rd plate is starting to develop on the internal side between the terminal plate and the 2nd adambulacral. A groove is present in the central area of the terminals, probably as a channel for the sensory podia (Fig. 4.11G).

R=2.46 mm (R/r=2.50): the spines of the jaw are larger. The small inferomarginals can be seen next to the adambulacrals, but they do not meet at the interradial area (Fig. 4.11I). *R=3.74 mm (R/r=3.40)*: the suboral spines are much enlarged and are larger than the apical spines. The arms are long and the terminals

Figure 4.11 (cont.). *Zoroaster fulgens* juvenile development. F. 1.05 mm; G. 1.25 mm; H. 1.59 mm; I. 2.46 mm; J. 2.04 mm; K. 3.74 mm; L. 3.75 mm. cp = central plate; odd rad = odd radial plate; rad = radial plate. See Fig. 4.1 for further explanation. Sizes represent the arm radius (R).

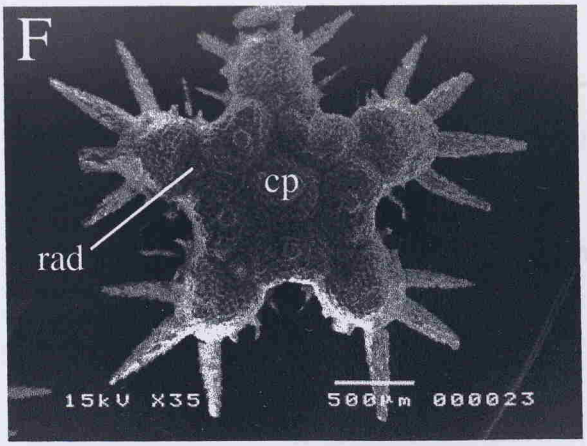
F
cp
rad
15kV X35
500µm 000023

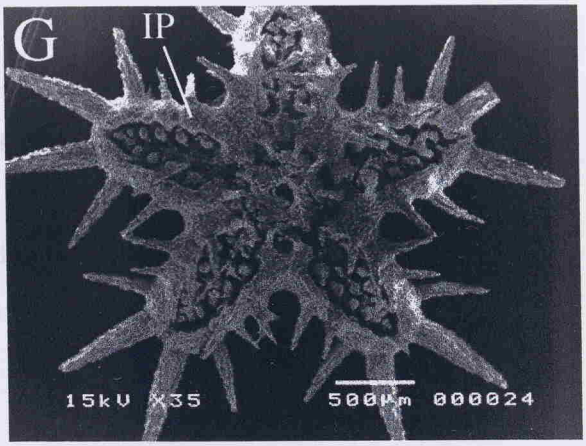
G
IP
15kV X35
500µm 000024

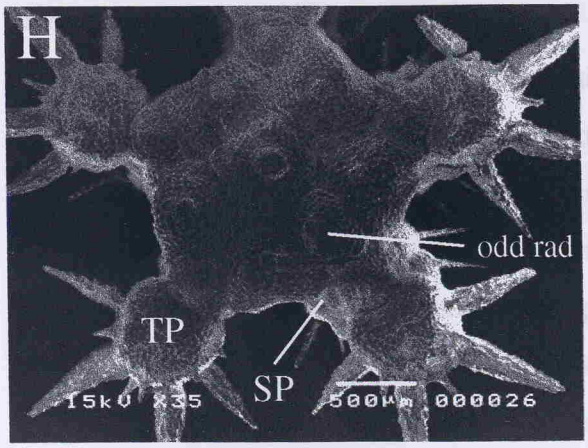
H
odd rad
TP
SP
15kV X35
500µm 000026

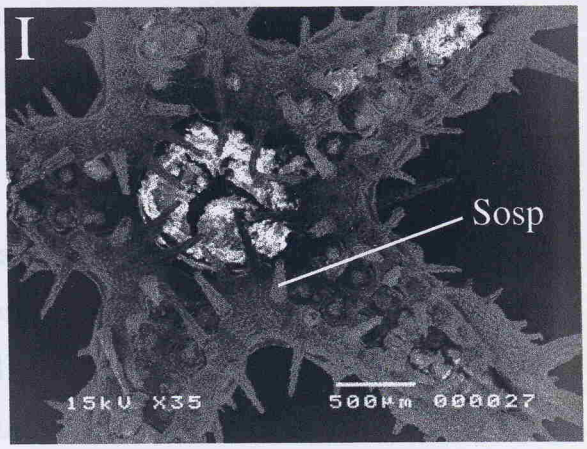
I
Sosp
15kV X35
500µm 000027

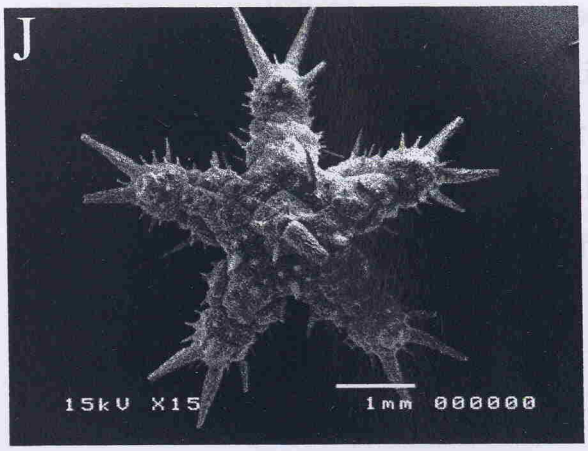
J
15kV X15
1mm 000000

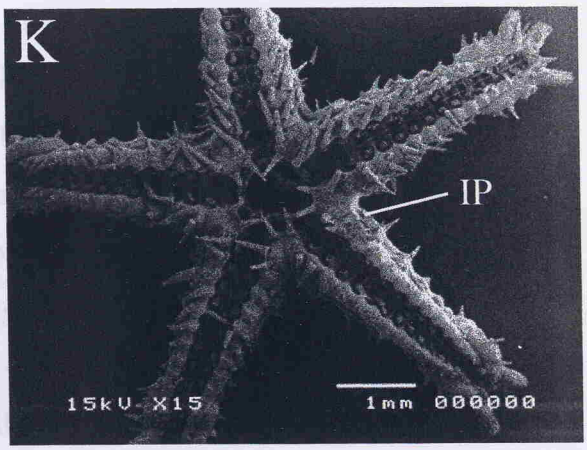
K
IP
15kV X15
1mm 000000

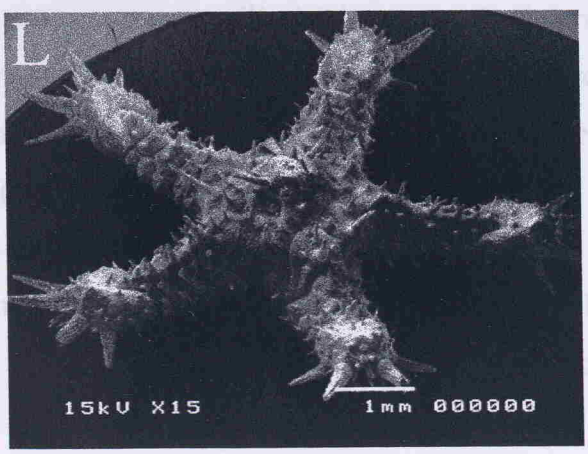
L
15kV X15
1mm 000000

enclose around 4 adambulacral plates. The inferomarginals bear 1 rather large spine (Fig. 4.11K).

Later, animals at R=5.00 mm have 2 adambulacral and 1 subambulacral spines. At R=26.00 mm large duck-billed pedicellariae can be seen on the furrow spines.

Order Brisingida Fisher, 1928

Family Brisingidae G.O. Sars, 1875

Brisingella coronata (G.O. Sars, 1872)

All specimens of *B. coronata* were critical point dried, which made the description of the abactinal plates impossible. The number of arms varied between 8-10 in the specimens described and were usually broken.

The abactinal surface of specimens with disk diameter (D) of 2.08 mm bear 1 large central spine and large interradial spines. Smaller spines can also be seen scattered over the surface (Fig. 4.12A). Crossed pedicellariae are present on the base of the large spines and also on the abactinal surface, close to the base of the arms (Fig. 4.13A).

D=2.27 mm: two large spines can be seen in some interradius. The arms are broader at the bases, tapering towards the tip (Fig. 4.12B). The tip of the arms are bifurcated with 1 spine issuing from each branch (Fig. 4.12C). The abactinal surface of the arms are covered by crossed pedicellariae (Fig. 4.13B). The spines are long and point abradially, having large clusters of crossed pedicellariae at their bases (Fig. 4.13C). The pedicellariae are small (~70 μm long and 24 μm in width) with the distal edge broadened and with a serrated border (Fig. 4.13C).

D=2.40 mm: a ring of small spines is visible around the edge of the disk. A madreporite is present on the edge of the disk in the interradius (Fig. 4.12D).

D=6.81 mm: the large central spine is still visible, as are the interradial spines. Small and abundant spines scattered all over the abactinal surface. The large madreporite is found at the edge of the disk. Crossed pedicellariae are scattered all over the abactinal surface (Fig. 4.12E).

On the actinal side, the oral aperture at D=1.71 mm is very large and circular, with a large oral membrane covering most of the oral aperture. The disk being formed basically by the vertebrae of the arms. On the interradial area a jaw is present with 2

Figure 4.12. *Brisingella coronata* juvenile development (A-I). A, B, D and E, abactinal view; C, lateral view; F-I, actinal view. A. 2.08 mm; B. 2.27 mm; C. 1.50 mm; D. 2.40 mm; E. 6.81 mm. Note the elongated spine in the centre of the disk. See Fig. 4.1 for further explanation. Sizes represent the disk diameter.

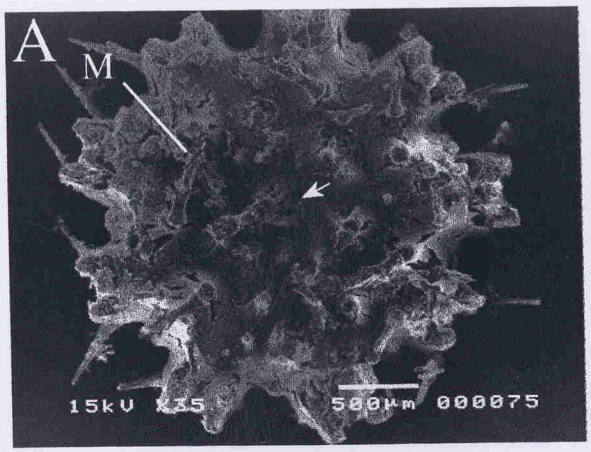
A
M
15kV X35
500µm 000075

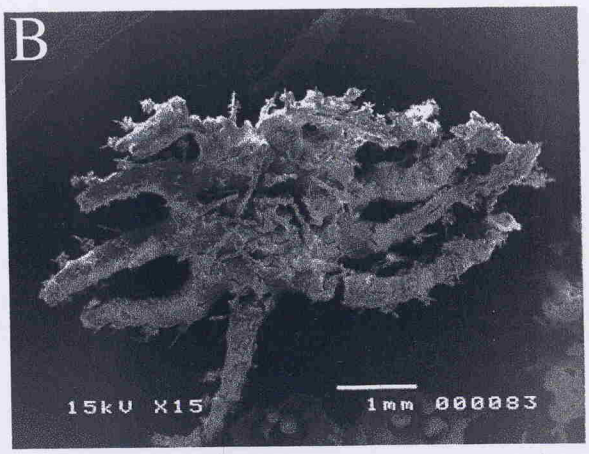
B
15kV X15
1mm 000083

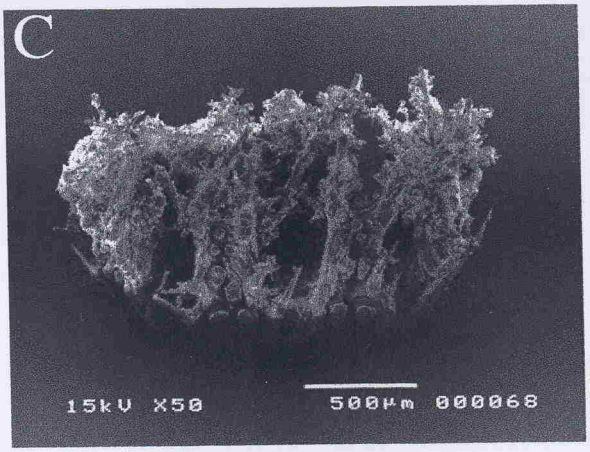
C
15kV X50
500µm 000068

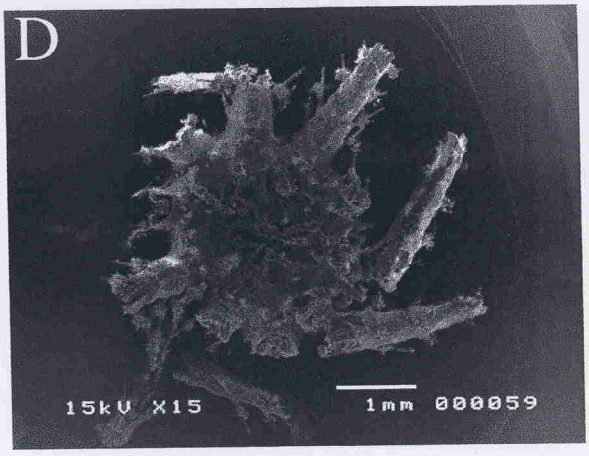
D
15kV X15
1mm 000059

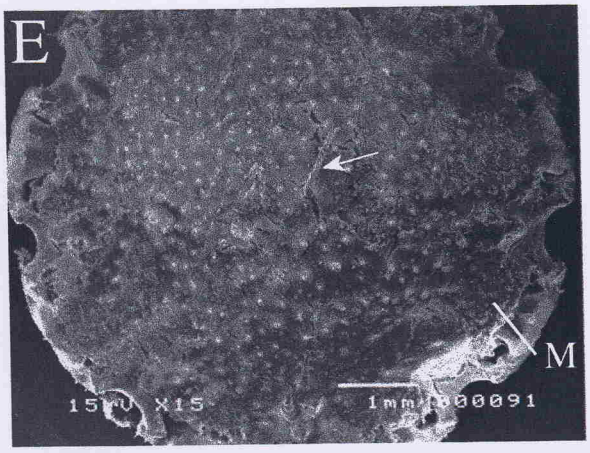
E
M
15kV X15
1mm 000091

Figure 4.12 (cont.). *Brisingella coronata* juvenile development. F. 1.71 mm; G. 2.60 mm; H. 2.66 mm; I. 5.38 mm. mo = mouth; om = oral membrane; sp = spine; tf = tube foot. See Fig. 4.1 for further explanation. Sizes represent the disk diameter.

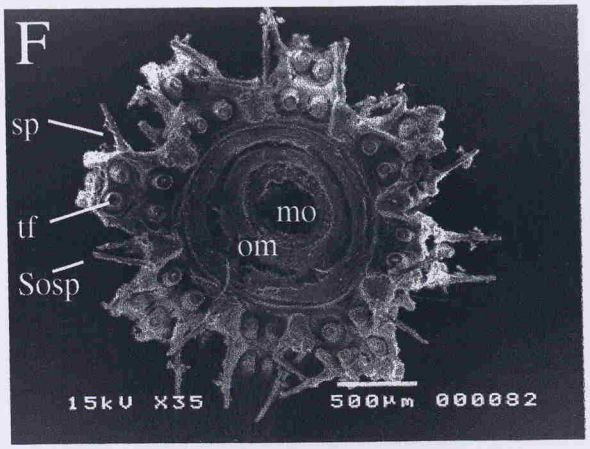
F
sp
tf
Sosp
mo
om
15kV X35
500µm 000082

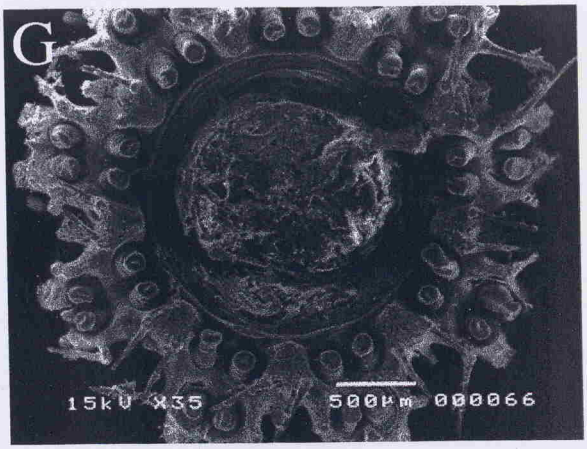
G
15kV X35
500µm 000066

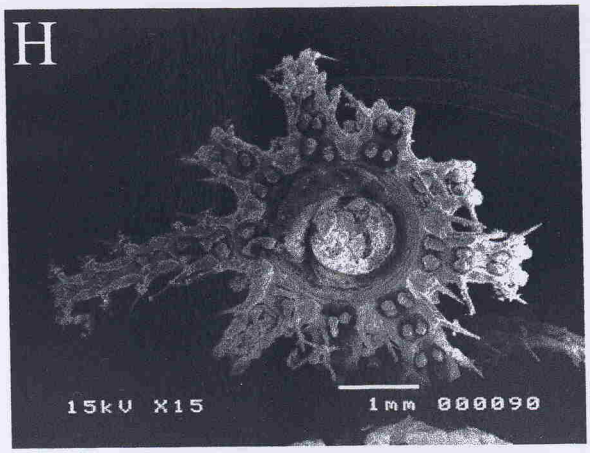
H
15kV X15
1mm 000090

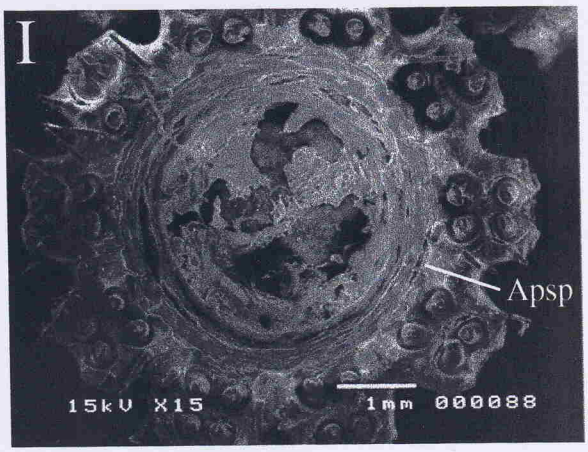
I
Apsp
15kV X15
1mm 000088

Figure 4.13. Pedicellariae of *Brisingella coronata* at 2.4 mm disk diameter (A-C). A. Detail of two arms showing the arm spines bearing tufts of crossed pedicellariae at their bases (arrow). B. Detail of the base of the arm. Note the presence of pedicellariae on the surface of the arm (arrow). C. Detail of the arm spine showing the crossed pedicellariae.

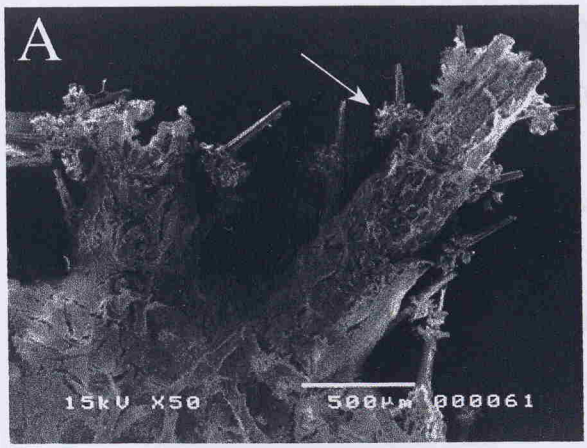
A
15kV X50
500µm 000061

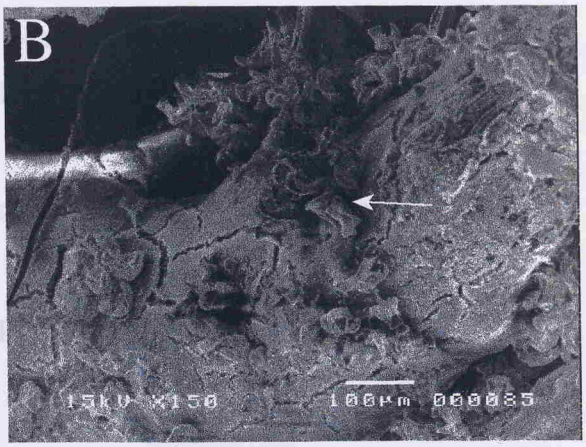
B
15kV X150
100µm 000085

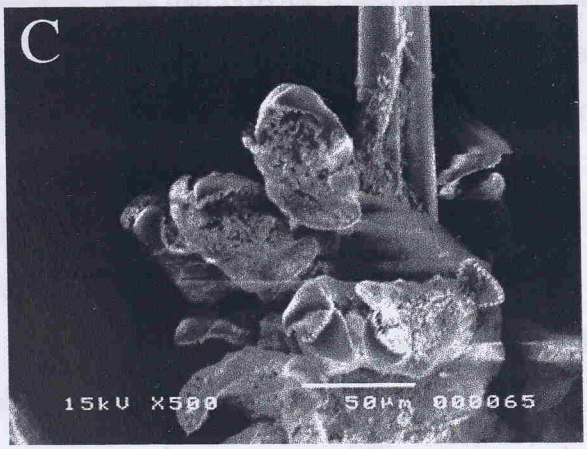
C
15kV X500
50µm 000065

large suboral spines pointing abradially. The adambulacral plates are elongated, bearing 1 long spine on the actinolateral area. Each spine with a cluster of crossed pedicellariae (Fig. 4.12F).

D=2.60 mm: no major changes have occurred (Fig. 4.12G) and figure 4.12H shows the actinal surface of the arm.

D=5.38 mm: two small apical spines are present in the interradial area (Fig. 4.12I).

4.3. Ontogenetic changes in the R/r ratio of asteroids

The R/r ratio in asteroids is a value that provide direct information concerning the shape of the animal. Animals with high R/r ratios show long arms and a relatively small disk, whereas low values represent individuals with an stellate or pentagonal shape.

As mentioned earlier in this chapter, juvenile asteroids can differ in size from conspecific adults in more than two orders of magnitude and the ratio R/r may also be quite different from the adult. Young specimens generally show a more pentagonal shape, with only a terminal plate present in the arms, which generate very low R/r values. However, some species present a different shape altogether, as in *Luidia sarsi*.

I examined the ontogenetic changes in R/r ratios by comparing the changes in both measures taken (R and r). Data for *Hymenaster pellucidus* and *Brisingella coronata* are not available owing to the difficulty in measuring the former species and the absence of sufficient specimens with arms intact in the latter.

The changes in the size R and r in all examined species could be described by a positive linear function of the type:

$$R = \alpha r + \beta \quad (1)$$

where α and β are the regression coefficients from the least squares analysis.

Resolving the equation (1) for R/r we have:

$$\frac{R}{r} = \alpha + \frac{\beta}{r} \quad (2)$$

At any particular time the changes in the ratio R/r will be described by the equation :

$$\frac{d(R/r)}{dt} = -\frac{\beta}{r^2}\frac{dr}{dt} \quad (3)$$

therefore when:

$\beta > 0 \Rightarrow \frac{d(R/r)}{dt} < 0 \Rightarrow$ body grows faster than the arms;

$\beta < 0 \Rightarrow \frac{d(R/r)}{dt} > 0 \Rightarrow$ body grows slower than the arms;

$\beta = 0 \Rightarrow \frac{d(R/r)}{dt} = 0 \Rightarrow$ growth is isometric;

assuming $\frac{dr}{dt}$ is always positive.

Looking at equation (1), α will give a measure of the magnitude of R in relation to r (bearing in mind the constant β). The higher α is, the larger the size R.

In all species examined the arms grow faster than the body during the early stages of life (Figs. 4.14 and 4.15). The changes in the ratio R/r were accentuated in *Luidia sarsi*. The smallest specimen examined (R=1.30 mm) shows a R/r ratio of 2.45. The remaining paxillosidans show a much less accentuated change, with R/r ranging from 1.2 to 2.4. *Psilaster andromeda* (R=4.55 mm) and *Plutonaster bifrons* (R=4.21 mm) showed R/r ratios of 2.2 and 2.4, respectively, whereas in *L. sarsi* at R=4.14 mm the ratio is 4.13 (Fig. 4.14).

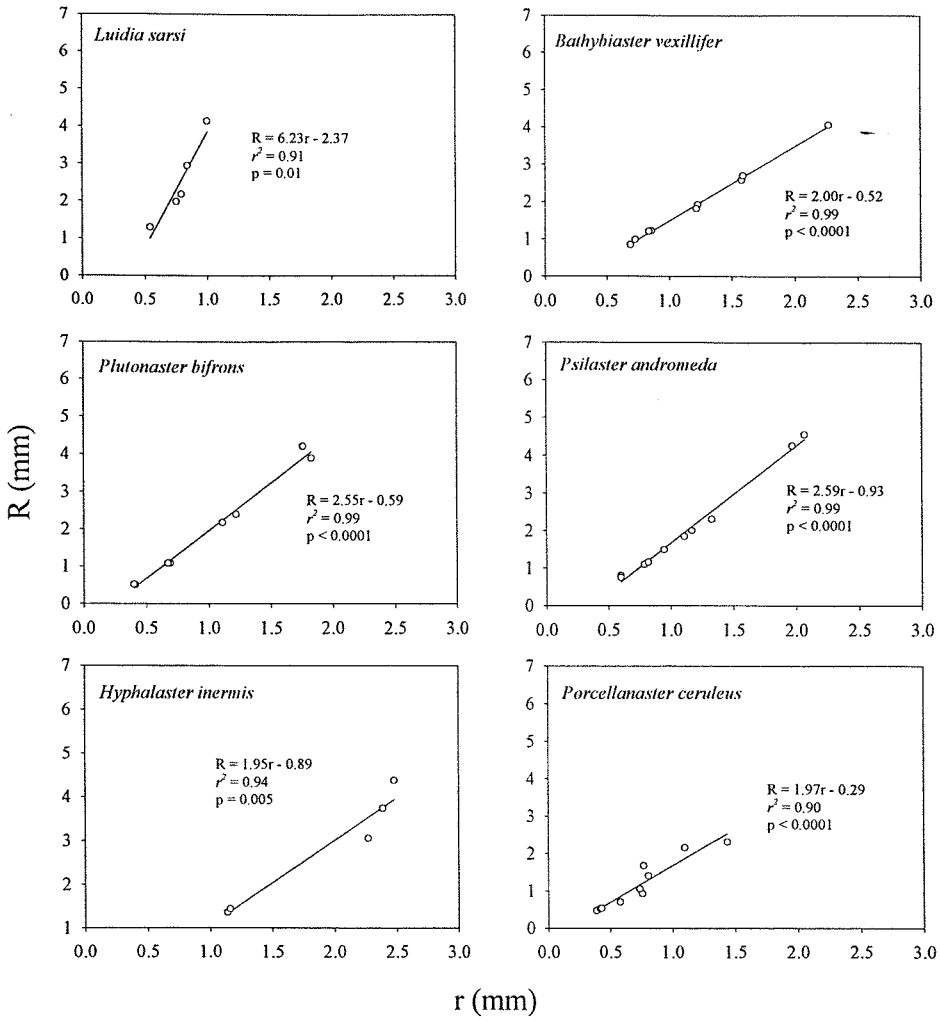

Figure 4.14. Relative changes in size of arm and disk radii with growth in paxillosidans.

In the notomyotids *Benthopecten simplex* and *Pectinaster filholi*, R/r also changes quite rapidly with growth, ranging from 1.4 to 3.6. The same trend occurs in the forcipulatid *Zoroaster fulgens*. In the valvatid *Plinthaster dentatus* the ratio changes very slowly (1.5-1.7) in specimens of sizes between R 1.05 and 3.60 mm (Fig. 4.15).

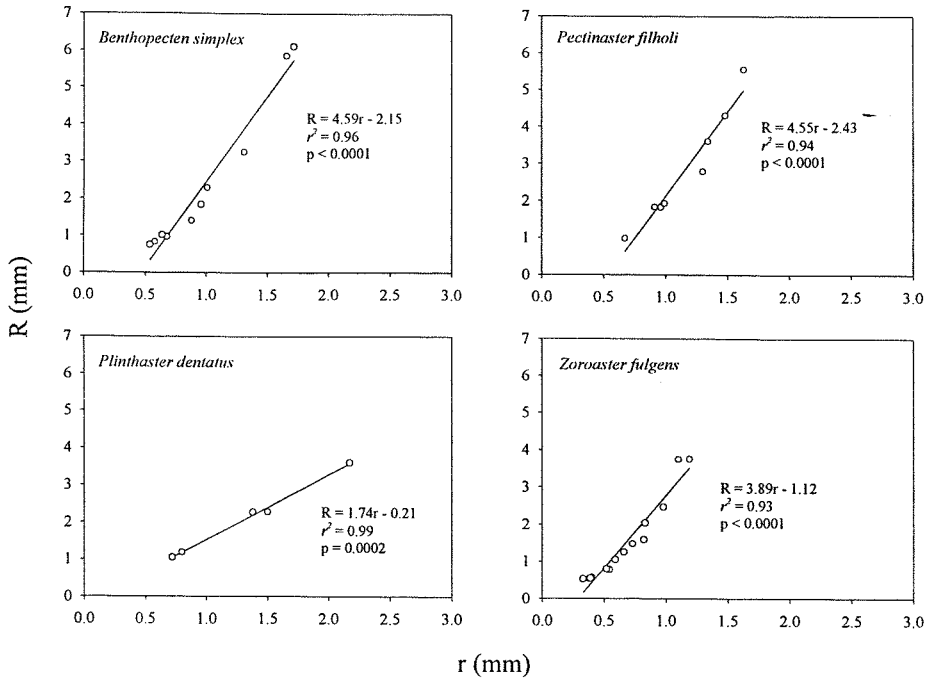

Figure 4.15. Relative changes in size of arm and disk radii with growth in notomyotids (top graphs) and in the goniasterid *Plinthaster dentatus* and the zoroasterid *Zoroaster fulgens* (bottom graphs).

The value of β in equation (3) is related to the relative growth of arms and body. The regression analysis of R against r for the ten species studied generated negative values of β, demonstrating that in all species the arms grow faster than the body. However, for *Porcellanaster ceruleus* and *Plinthaster dentatus*, β values were close to zero. This means that the early growth of these two species is nearly isometric. In general, the larger absolute values of β for the two notomyotids, *Luidia sarsi* and *Zoroaster fulgens* agree with a faster change in the ratio R/r with growth. The three astropectinids and the porcellanasterid *Hyphalaster inermis* show similar β values, intermediate between the two groups mentioned above.

4.4. Juvenile bathymetric distribution in the Porcupine area

A comparison of the juvenile bathymetric distribution with the distribution of conspecific adults in the Porcupine Seabight and Porcupine Abyssal Plain (PAP) was

made. The comparison was based on the known bathymetric distribution of adults of the species examined in the present study (Clark & Downey, 1992), and on the distribution of conspecific adults collected during the same sampling programme (IOS).

The adult range for the asteroids collected during the IOS Programme was always narrower in comparison to that given by Clark & Downey (1992), in part owing to the actual depth range sampled during the former. The IOS Programme sampled depths between 135 and 4850 m, covering mainly the Porcupine Seabight and PAP. A few of the shallower stations were sampled on the Celtic Shelf (from where the shallower record of *Luidia sarsi* was taken). The deepest stations correspond to the approximate maximum depth found in the PAP area (~4850 m).

Juveniles of *Hymenaster pellucidus* and *Brisingella coronata* were found in depths within the upper and lower limits of the distribution of conspecific adults for both ranges given (Fig. 4.16).

Hyphalaster inermis juveniles occurred 490 m shallower than the adults in the same area. However, the juvenile distribution is within the limits known for this species world-wide. The same is found for *Pectinaster filholi* and *Zoroaster fulgens* juveniles, but with the distribution in the Porcupine area being only 50 and 700 m deeper than that of the adults, respectively. In *Porcellanaster ceruleus*, juveniles occurred both shallower (~300 m) and deeper (~500 m) than the respective adult distribution in the area. *Bathybiaster vexillifer* showed the similar results (Fig. 4.16).

The remaining five species showed juvenile distributions deeper than the adults, irrespective of the source. Differences tended to be more accentuated when compared with the data available for the studied area than for the known distribution given by Clark & Downey (1992). Juveniles of *Luidia sarsi*, *Plutonaster bifrons* and *Psilaster andromeda* occurred over 500 m deeper than the lower bathymetric limit of their adult counterparts. *Plinthaster dentatus* juveniles were over 2000 m in excess of adult depths (Fig. 4.16). In *Benthopecten simplex* differences were around 200-300 m when comparing with the known distribution and with that found in the Porcupine area.

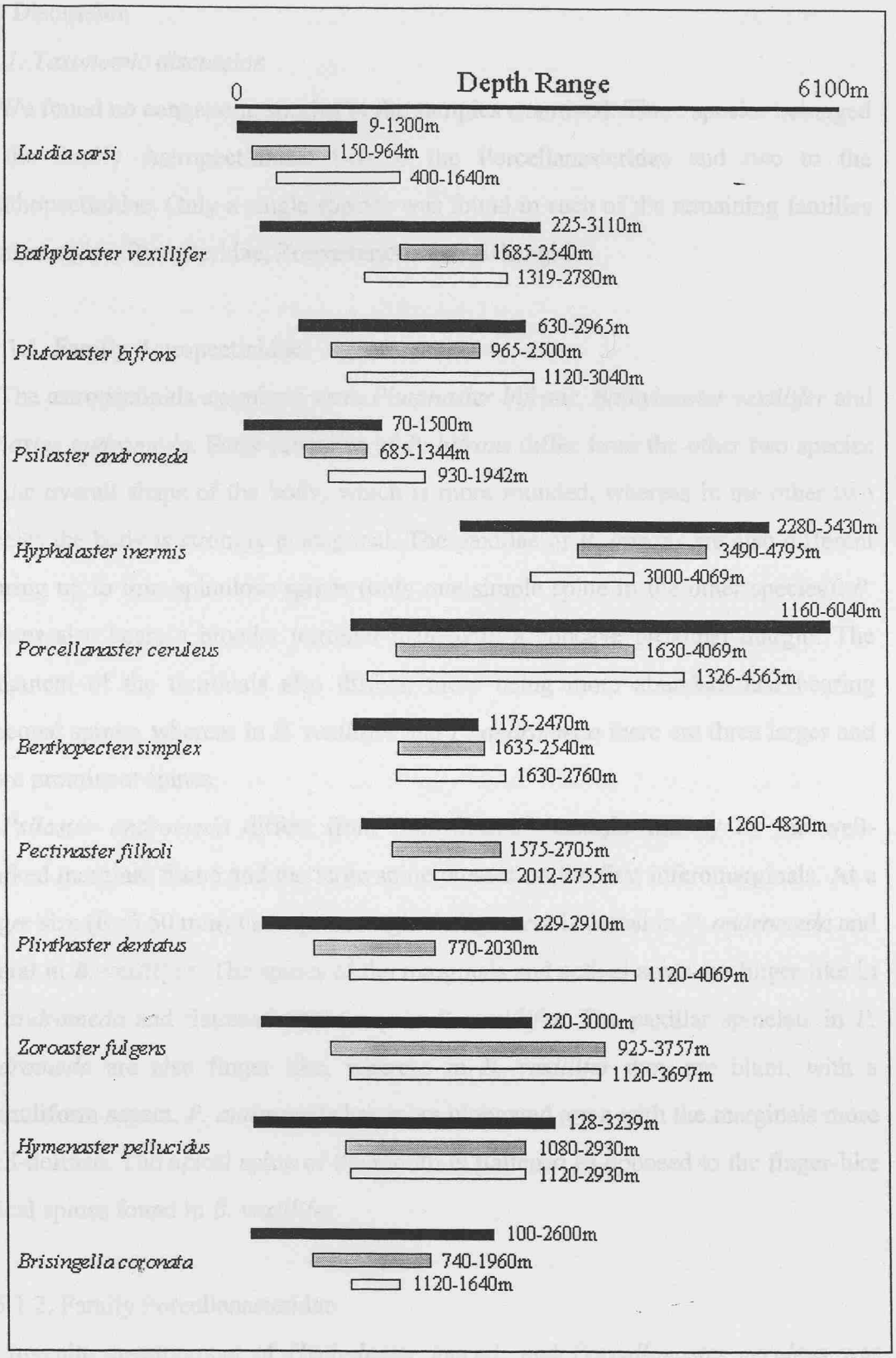

Figure 4.16. General bathymetric distribution of adult asteroids (solid black - Clark & Downey, 1992); of adults collected during the IOS Programme (grey); and of juveniles in the Porcupine area (white).

4.5. Discussion

4.5.1. Taxonomic discussion

We found no congeneric species in the samples examined. Three species belonged to the family Astropectinidae, two to the Porcellanasteridae and two to the Benthopectinidae. Only a single species was found in each of the remaining families Goniasteridae, Pterasteridae, Zoroasteridae and Brisingidae.

4.5.1.1. Family Astropectinidae

The astropectinids examined were *Plutonaster bifrons*, *Bathybiaster vexillifer* and *Psilaster andromeda*. Early juveniles of *P. bifrons* differ from the other two species by the overall shape of the body, which is more rounded, whereas in the other two species the body is strongly pentagonal. The paxillae of *P. bifrons* are also different bearing up to four spinulose spines (only one simple spine in the other species). *P. bifrons* also bears a broader terminal plate with a concave proximal margin. The armament of the terminals also differs, these being more abundant and bearing subequal spines, whereas in *B. vexillifer* and *P. andromeda* there are three larger and more prominent spines.

Psilaster andromeda differs from *Bathybiaster vexillifer* mainly by the well-marked marginal frame and the large spine present on the first inferomarginals. At a larger size (R=5.50 mm) the superomarginal alignment is dorsal in *P. andromeda* and lateral in *B. vexillifer*. The spines of the marginals and actinal areas are finger-like in *P. andromeda* and flattened at the top in *B. vexillifer*. The paxillar spinelets in *P. andromeda* are also finger like, whereas in *B. vexillifer* they are blunt, with a granuliform aspect. *P. andromeda* has more elongated arms with the marginals more well-defined. The apical spine of the mouth is flattened as opposed to the finger-like apical spines found in *B. vexillifer*.

4.5.1.2. Family Porcellanasteridae

Juvenile development of *Hyphalaster inermis* and *Porcellanaster ceruleus* was described by Madsen (1961). However, the smallest specimens described by Madsen (1961) have R>4 mm, whereas in the present chapter descriptions cover individuals from R<1 mm.

Both species can be very easily distinguished. Early juveniles of *Hyphalaster inermis* have a well-marked marginal frame, with a very wide terminal plate forming a strongly pentagonal outline. Each terminal has a moderately small central spine. In *Porcellanaster ceruleus* the marginal frame is not well-marked and there are 3 very large and thin spines on the terminals. Very early juveniles of *P. ceruleus* are also much smaller and bear only 5 interradial plates on the abactinal side, whereas *H. inermis* possesses a much larger number of abactinal plates.

It is interesting to note (although not shown here) that the epiproctal cone probably forms at the same time as the cribriform organs. This could be important for a change in the life style from epibenthic to shallow infaunal. Madsen (1961) shows that individuals of *Hyphalaster inermis* at R=6 mm show both structures already formed. In individuals at R=4 mm an epiproctal cone is not found and the cribriform organs were poorly developed. In *Porcellanaster ceruleus* a well-developed epiproctal cone and cribriform organs were found in specimens at R=4.4 mm.

The difference in the time of appearance of these structures may represent different survival strategies for juveniles of different species. Early juveniles of *Porcellanaster ceruleus* were found to prey upon forams. Possibly, the animals change from a predatory behaviour when small juveniles to the adult mud-swallowing condition (observed) after the cribriform organs and the epiproctal cone are fully developed, allowing the individual to burrow into the sediment. In *P. ceruleus* the furrow and oral spines are initially needle-like, but become flattened with growth, facilitating sediment ingestion and protecting the tube feet from the sediment.

Another interesting point is that the cribriform organs do not always develop at the same rate in the different interradii of the same individual. It was noticed that, in *Porcellanaster ceruleus*, the cribriform organ of the interradius where the madreporite is present is the first to complete development, whereas the others are in an earlier stage of development. Madsen (1981) found that in the species *Styracaster elongatus* the interradius with the madreporite had three cribriform organs, with the central well developed and the outer ones consisting of a single row of papillae on each side. In the cribriform organs of the remaining interradii, however, the development had just begun. The differential development of the cribriform organs

may be related to the need of the individual to ventilate the area of the madreporite, which supplies water for the water vascular system. This may be more important owing to the infaunal life style of these animals.

4.5.1.3. Family Benthopectinidae

The early post-metamorphic stage of both benthopectinid species examined show a similar overall shape and arrangement of the abactinal plates. The abactinal surface is comprised of a central and 5 interradial plates, the latter occupying the whole interradius.

They differ from each other in the pattern of arrangement and relative size of the spines of the terminal plates and on the number and distribution of spines in the primary plates. At a slightly larger size, *Benthopecten simplex* (~R=1.4 mm) develops the odd marginal plate and a large spine on it, typical of this genus. *Pectinaster filholi* does not bear this odd plate.

4.5.2. Phylogenetic considerations

Some interesting features of the post-metamorphic ontogenesis of sea stars were observed. The relative appearance and arrangement of the suboral and subambulacral spines in the early sea star suggest that both structures are homologous. The marginal and adambulacral spines are equally similar in nature and also suggest homology, implying that the oral plate is either an adambulacral ossicle or results from the fusion of two or more adambulacrals. However, Fell (1963) argues that the oral plate in asteroids is derived from the first ambulacral plate, called by Fell (1963) the mouth-angle plate (in the somasteroid genus *Chinianaster*, Fig. 11E). Spencer & Wright (1966) point out that in *Platasterias* (now considered a subgenus of *Luidia*) the mouth-angle plates superficially appear to be enlarged adambulacrals. Indeed Turner & Dearborn (1972) consider the mouth-angle plate as the first ossicle in the adambulacral series. Gale (1987) states, however, that "the origin of the mouth-angle plates (presumably either modified ambulacrals or adambulacrals) remains equivocal in spite of embryological studies". I suggest the oral plates (mouth-angle) may represent fused adambulacrals and consider the suboral and marginal spines as

serially homologous with the subambulacral and adambulacral spines, respectively, since they appear to have the same origin during post-metamorphic ontogeny.

4.5.3. Size at metamorphosis

The descriptions of the early post-metamorphic ontogenesis of the deep-sea asteroids presented in this chapter show the smallest juveniles obtained by the sampling methods applied. However, it is difficult to tell whether those represent the very early stages after metamorphosis, since no data on metamorphosis or culturing of these species are available.

Data available for shallow water species show that recently-metamorphosed individuals usually have two pairs of podia (Strathmann, 1971, 1974*a*; Yamaguchi, 1973; Emlet *et al.*, 1987). Members of the family Luidiidae, however, frequently have a larger number of podia resulting from a large post-larva (Wilson, 1978; Komatsu *et al.*, 1982; Domanski, 1984). Specimens of *Luidia sarsi* examined (not included herein) usually showed over 4 pairs of podia and a large size, in accordance with the formerly cited authors. The lecithotrophic species *Pteraster tesselatus* also develops several pairs of functional podia, which help the attachment in the substratum (McEdward, 1992). Among the studied species, the smallest juveniles of *Plutonaster bifrons*, *Porcellanaster ceruleus*, *Benthopecten simplex* and *Plinthaster dentatus* show only two pairs of tube feet, suggesting they are probably recently-metamorphosed individuals. The same is probably true for *Hyphalaster inermis* and *Pectinaster filholi* which, although the number of podia was not clearly visible, it was probably between 2 and 3. Small individuals of *Bathybiaster vexillifer*, *Psilaster andromeda* and *Zoroaster fulgens* have three pairs of podia and are likely to be early juveniles. *Hymenaster pellucidus* showed 4 pairs of tube feet, but this could be related to the mode of development of this species, which broods the young (Clark & Downey, 1992), producing larger offspring.

Size is another indication of an early-metamorphosed individual. In general, post-larvae of planktotrophic species are less than 1 mm in diameter, whereas those of non-planktotrophic forms are larger than 1 mm in diameter (we can consider the diameter of a sea star as twice the size of the radius R) (Hyman, 1955; Strathmann, 1974*a*). Emlet *et al.* (1987) argue that this could represent a trade-off between the

advantages of survival of a large-sized post-larva and decreased fecundity in non-planktotrophic species. This appears to be true for a species of sea urchin which produces smaller post-larvae when eggs are depleted of their lipid source of energy (Emlet & Hoegh-Guldberg, 1997). Luidiids are, again, exceptions to this statement, producing a large post-larva after planktotrophic development (see above).

The only planktotrophic species examined in the present study was *Plutonaster bifrons*. The smallest post-larvae obtained were R=498 μm, which falls within the expected size. All the remaining species are non-planktotrophs (see introduction) and most juveniles measured over R=800 μm. The only exceptions were *Porcellanaster ceruleus* and *Zoroaster fulgens*. *P. ceruleus* is an asynchronous breeder producing eggs up to 600 μm in diameter (P.A. Tyler, unpublished data) and the smallest juveniles were R=470 μm. In *Z. fulgens*, eggs are up to 950 μm in diameter (Tyler *et al.*, 1984*b*) and juveniles are R=528 μm. These small specimens of *Z. fulgens* even lack a well-formed mouth and show possibly the presence of resorbing larval tissues or maybe remnants of a lecithotrophic egg (Janies & McEdward, 1993) in the mouth region (Fig. 4.11b). Individuals of both these species are at the limit of the usual size at metamorphosis for lecithotrophic species found elsewhere (Strathmann, 1974*a*; Emlet *et al.*, 1987). Other lecithotrophic species, with unusual small juveniles, do occur in nature (Yamaguchi, 1974; Komatsu, 1975).

The sizes encountered in the present work must be interpreted with caution. The lack of knowledge of growth rates and the relative time of appearance of different structures in the early-metamorphosed juvenile make the assessment of the size at metamorphosis speculative. We should also bear in mind that the size at metamorphosis can be influenced by the relative time spent in the plankton (Wilson, 1978; Domanski, 1984) or even by delaying settlement (Yamaguchi, 1974) and the relative feeding state of the larvae (Lucas, 1982). Nevertheless, the present data suggest that the post-metamorphic ontogenesis described include the early stages of growth and consequently the newly-settled individuals.

4.5.4. Changes in the ratio R/r with growth

The analysis of the ratio R/r in asteroids should be taken with caution. A number of factors may cause variation in such measurements. In porcellanasterids this ratio is

affected by the mud-swallowing habit of this group (Madsen, 1961; this chapter). The relative amount of body fluids also was found to have an impact in the disk size of *Odontaster validus* (Pearse, 1965). The ingestion of large prey items, very common among certain groups (*e.g.* astropectinids), may also distort the disk.

Although the data presented herein are scarce and only a few species were analysed, evidence suggests that the changes in the ratio R/r with growth may be similar among related group of species. Species of the families Astropectinidae and Benthopectinidae examined appear to have similar rates of change in R/r with growth within each family. The astropectinids *Bathybiaster vexillifer*, *Plutonaster bifrons* and *Psilaster andromeda* have adults with the mean ratio R/r varying between 4 and 5, whereas in the benthopectinids *Benthopecten simplex* and *Pectinaster filholi* it varies from 5 to 8 (Clark & Downey, 1992). In the juveniles, the ratio of change with growth was more accentuated in the benthopectinids than in astropectinids. If this trend continues throughout the life of the species, one might expect the benthopectinids to attain larger values of R/r in adult life that seems to be the case. Madsen (1961) shows a positive linear relationship between R and r over a wide range of sizes in porcellanasterids, suggesting that changes in R/r are also linear with time.

Porcellanaster ceruleus and *Hyphalaster inermis* show a similar R/r with growth. In the former, however, and also in the goniasterid *Plinthaster dentatus*, growth is nearly isometric during the early stages. The rate of change in R/r with growth in these species is very low. Adult *P. ceruleus* have R/r ratios of up to 3.5 (Madsen, 1961; Clark & Downey, 1992), whereas in *P. dentatus* the ratio is only 1.3 (Clark & Downey, 1992), very close to the ratios found for conspecific juveniles.

The significance of the different changes in the ratio R/r with growth is unknown. Blake (1990) argues that proportions and armour development in asteroids evolved in response to demands of protection, body flexibility, support on soft substrata and internal capacity. Large arms relative to the body may be important in offering a higher motility and flexibility for predator avoidance and/or acquisition (capture and larger area scanned) and manipulation of prey items (reviewed by Blake, 1989). Many sea stars are able to capture motile prey, but the shape of the body varies (Jangoux, 1982). Young sea stars with a carnivorous feeding habit occur in nature

(Sloan, 1980). Evidence of predatory behaviour was found for the three species of Astropectinidae studied. Early juveniles were found to have relatively large prey items such as bivalves, gastropods and forams in the stomach. Although the arms of the studied astropectinids grow faster than the body, this change occurs more gradually than for the benthopectinids. Thus, astropectinids with R similar to that of benthopectinids have relatively larger body (larger r). Astropectinids are intraoral feeders (Jangoux, 1982) and a large disk may allow larger prey to be swallowed (Van Veldhuizen & Oakes, 1981). The size of the prey is important for newly-settled asteroids. Strathmann (1978*b*) stresses that forcipulatid juveniles are about 0.5 mm in diameter at metamorphosis and that newly-metamorphosed bivalves are appropriate prey for them. He argues, however, that barnacle cyprids are maybe too large to be effectively attacked. A rapid increase in disk size could, therefore, confer advantages in selecting a larger variety of prey items. Alternatively, a large size may also be important in providing refuge against predation (Van Veldhuizen & Oakes, 1981).

In the luidiid *Luidia sarsi*, however, which is also an intraoral feeder and carnivore on macroscopic prey (Jangoux, 1982), the relative growth of the body differs from that found for the astropectinids examined. In fact, the ratios R/r in this species are quite high. This suggests that the relationships between body shape and food specialisation are more complex and other different constraints may be involved.

Both species of porcellanasterid studied show little change in R/r ratios with growth. In these species a long arm is probably not needed, since they assume the mud-swallowing habit of the adults quite early in life. However, there is evidence suggesting that very early stages of *Porcellanaster ceruleus* are predators on forams (which are not very active organisms).

Plinthaster dentatus showed a nearly isometric growth with very little change in the ratio R/r. Adult *P. dentatus* feeds on forams, crinoids and solitary corals (Halpern, 1970 in Jangoux, 1982). The feeding habit of the juveniles, however, is not known and may differ from that of the adults.

Some juvenile asteroids have diets completely different from conspecific adults. The coral-eating sea star *Acanthaster planci* has juveniles that feed on coralline algae (Yamaguchi, 1974; Zann *et al.*, 1987; Johnson *et al.*, 1991). This diet changes at a

certain point during development, when animals switch to a non-cryptic life style, feeding on coral during day-time (Zann *et al.*, 1987). Other species also show similar shifts in life style and feeding habit between juveniles and adults (Barker, 1977, 1979; Scheibling, 1980; Barker & Nichols, 1983). This transition in the life history has also been reported for other invertebrate groups (Gosselin, 1997).

Many very early juveniles feed extraorally on the surface film of the sediment (reviewed by Sloan, 1980), including a species of *Luidia* (Birkeland *et al.*, 1971). In this case, the size of the body is not crucial for the ingestion of prey, but large arms may still be advantageous for capturing more motile prey.

It is also possible that shape is phylogenetically constrained. Blake (1989) argues that the same adult feeding habit is shared by morphologically distinct species. In this case, shape has no influence on the feeding habit.

4.5.5. Juvenile bathymetric distribution

It is generally expected that species with planktotrophic development will have a more widespread distribution than species with abbreviated development (either free-living or contained). This view is, however, contradicted by some examples of species with a broad distribution and a non-planktotrophic mode of development (Jackson, 1986; Young & Cameron, 1987; Laegdsgaard *et al.*, 1991). Some lecithotrophic larvae can delay metamorphosis for long periods of time not losing competency (Birkeland *et al.*, 1971), whereas others may show facultative planktotrophy (Kempf & Hadfield, 1985; Emlet, 1986). In the deep-sea, eggs, embryos and larvae of lecithotrophic and planktotrophic species may last a long time in the plankton owing to the lower metabolic levels present in a cold environment (Emlet *et al.*, 1987; Young & Cameron, 1989; Shilling & Manahan, 1994; Young *et al.*, 1996*c*, 1997). This could lead to a higher dispersal potential for these organisms.

The presence of very early juveniles in the sediment is indicative of settlement, suggesting that colonisation by juveniles resulted from the supply of larvae to the area in question. Migration of juveniles is unlikely, since speeds attained by juveniles of *Asterina miniata* are low (Rumrill, 1989), but post-metamorphic dispersal may be important for some species (Chen & Chen, 1992; McEdward, 1992). Therefore, the early stages described in this chapter and their bathymetric distribution probably

reflect the dispersal and settlement patterns of the species involved. Of all the species examined, only 2 showed juvenile distributions within the range of the adults. Among those species, *Hymenaster pellucidus* was the only one that broods young (Clark & Downey, 1992), which leads to a low dispersal capability. The remaining species (*Brisingella coronata*) is probably a lecithotroph (Tyler *et al.*, 1982*c*) and juveniles were relatively rare in the samples.

Despite the presence of species with different modes of development, all the remaining species showed a wider juvenile distribution than the adults. Juveniles occurred within the limits of the adults and also deeper. The porcellanasterids and *Bathybiaster vexillifer* occurred in depths shallower than the adults in the area, but not when compared with the known records for this species (Clark & Downey, 1992). Many juveniles occurred over 500 m deeper than conspecific adults and in some, as *Plinthaster dentatus*, this value was 4 times as large. However, the deepest record for juvenile *P. dentatus* was found for only one juvenile in a single station. All the remaining records of this species fall between 1200-1300 m depth, which makes us suppose that the one odd result was a result of contamination of the sample.

Gage *et al.* (1984) compare the juvenile and adult bathymetric distributions of deep-sea echinoderm species. Among the asteroids analysed, Gage *et al.* (1984) show that, from the most abundant species (in the Rockall Trough area), at least three had wider juvenile than adult bathymetric distributions. It is also known that the ophiuroids *Ophiocten gracilis*, *Ophiura ljungmani* and *Ophiomusium lymani* settle outside the adult range (Gage & Tyler, 1981*a*; Gage *et al.*, 1984; chapter 6). The reason for the absence of adults in the samples at those depths is unknown, but could be related to predation, competition, absence of suitable food for the adults or even pressure.

The development of early embryos of *Plutonaster bifrons* appears to be constrained by pressure (Young *et al.*, 1996*a*). Young *et al.* (1996*a*) point out that pressure tolerances may set up the upper and lower bathymetric limits of the species. The presence of early juveniles in deeper areas suggests that larvae may be tolerant to higher pressures, allowing settlement to occur in such areas. The juvenile resistance to high hydrostatic pressures is not known, but it should be interesting to test the tolerances for this stage of the life history. Early juvenile tolerances to this

environmental variable may be the key to understanding bathymetrical distributions of asteroids in shelf and deep-sea areas.

The fate of the juveniles ending up in deeper areas remains obscure. Predation and competition for food may be important. In shallow water, data on the mortality of juvenile sea stars are divergent. Some studies show that predation and mortality are low in juveniles of some asteroid populations (Barker, 1979; Rumrill, 1989). This may be related to the cryptic attitude taken by juveniles, hiding under boulders or seagrass and macroalgae patches (Yamaguchi, 1973, 1977*a*; Barker, 1977; Scheibling, 1980; Barker & Nichols, 1983).

Nevertheless, Sewell & Watson (1993) found that juvenile mortality could be as high as 99% in *Pisaster ochraceus*. The stress caused by living in the shallow subtidal and intertidal may be important in this case. Zann *et al.* (1987) showed that juveniles of *Acanthaster planci* have a high mortality owing to disease and probably cyclones, but emphasize that predation is probably not an important source of mortality. In deep-sea areas, bioturbation of the sediment and the bulldozing activities of some megafaunal species may be important causes of the mortality of recently-settled individuals. The causes and fate of the allopatric settlement in deeper regions remain unsolved and the importance of pre- and post-settlement processes needs addressing. However, even in shallow water the importance of this is difficult to determine (Keesing *et al.*, 1993).

Chapter Five - Post-larval development of some deep-sea echinoids of the NE Atlantic Ocean

5.1. Introduction

The echinoid fauna of the deep NE Atlantic Ocean comprises species of the orders Cidaroidea, Echinothurioida, Echinoida, Spatangoida and Portalesioidea. The species of the first three orders are conspicuous components of the epibenthic megafauna at slope depths. The remaining two orders comprise the irregular echinoids, many of which burrow into the soft, deep-sea sediments (Gage *et al.*, 1985). Adults of all species present in this region were described during the second half of the nineteenth century and beginning of the twentieth (reviewed by Mortensen, 1928-51). During this time taxonomy dominated the study of echinoderms and other groups. This reflected the need to describe and classify a whole new fauna that was being retrieved from the oceans, particularly by the great expeditions that were taking place at that time. Among those we can cite the voyages of the British Navy ships *Lightning* (1867), *Porcupine* (1868-70) and *Challenger* (1872-76); the French *Travailler* (1881-82) and *Talisman* (1883); the Swedish *Albatross* (1947-48); and the Danish *Galathea* (1950-52), among others (reviewed by Mills, 1983).

Although the echinoid fauna of the NE Atlantic has been sampled for over a century and is relatively well-known, very little is known of the life cycles of particular species. Probably the best known aspect of the life cycle is the reproductive biology of a series of species. The genus *Echinus* has been subjected to several studies. The gametogenesis and population biology is known for *E. affinis* (Tyler & Gage, 1984*a*), *E. acutus* var. *norvegicus* and *E. elegans* (Gage *et al.*, 1986). Together with *E. alexandri* (Mortensen, 1943; Tyler & Gage, 1984*a*) these four species have overlapping distributions on the continental slope of the NE Atlantic and show a similar pattern in reproduction (Tyler *et al.*, 1995*a*). These species have a seasonal cycle in gametogenesis with spawning during the early months of the year (although with a slight variation from species to species). The small egg sizes and high fecundity suggest that they produce a large number of planktotrophic echinoplutei, which feed in the water column. *E. esculentus*, a more coastal species (Comely & Ansell, 1988), can also occur at slope depths (Mortensen, 1903). In

shallower water it also presents seasonality in reproduction (Moore, 1935; Nichols *et al.*, 1985; Comely & Ansell, 1989). In the deep areas of the NE Atlantic it is thought that the seasonal pulse of phytodetritus (Billett *et al.*, 1983) fuel and cue the reproductive cycles of these species (Tyler *et al.*, 1982*c*). Evidence for *E. affinis* suggests that this material is indeed used as a source of energy for both maintenance and body and gonad growth (Campos-Creasey *et al.*, 1994).

Tyler & Gage (1984*b*) studied the gametogenic cycle of two deep-sea cidarid and five echinothurioid species. In all echinothurioids (*Phormosoma placenta*, *Calveriosoma hystrix*, *Araeosoma fenestrum*, *Sperosoma grimaldii* and *Hygrosoma petersii*) and in the cidarid *Poriocidaris purpurata* gametogenesis is asynchronous and the production of relatively large oocytes suggests an abbreviated lecithotrophic development. In *Cidaris cidaris* there was no evidence of seasonality, although a planktotrophic larva is known for this species (Prouho, 1888; Mortensen, 1927*a*).

The reproductive biology of the deep-sea pourtalesiid echinoids *Pourtalesia jeffreysi*, *P. miranda* and *Echinosigra phiale* has been studied in detail by Harvey & Gage (1984). The authors suggest that development in all three species is lecithotrophic, based on egg size and fecundity. In the spatangoid *Brisaster fragilis*, Mortensen (1927*a*) proposes a direct development based on the large yolky eggs this species possesses. In *Hemiaster expergitus* reproduction is probably not seasonal (Gage, 1987).

The larval stages of some of the echinoid species of the NE Atlantic are known. Larvae of *Cidaris cidaris* (above), *Echinus esculentus* and *E. acutus* (Shearer & Lloyd, 1913; Shearer *et al.*, 1914; Hagström & Lønning, 1961) have been cultured. The spatangoid *Spatangus purpureus*, an irregular sea urchin occurring from the lowermost tide limit to upper slope depths, has a known larva (Ohshima, 1921; Mortensen, 1913; Rees, 1953), which is present in the water column during the summer months suggesting seasonality in reproduction (Mortensen, 1927*a*). The larva of the spatangoid *Brissopsis lyrifera* is also well-known (Mortensen, 1920; Rees, 1953). According to Mortensen (1927*a*) the larva of *B. lyrifera* is distinguished from other known spatangoid larvae by the lack of postero-lateral arms.

Despite the very good quality, echinoid taxonomy (and probably general taxonomy) is biased towards the study of adult-based characters (Agassiz, 1872;

Lovén, 1874; Thomson, 1874*b*; Mortensen, 1903, 1907, 1928-51). This reflects the generally more conspicuous nature of the adults and relative ease with which they are sampled in the marine environment, as opposed to larval and early post-larval stages. Larval biology and ecology has received a great deal of attention. However, larval morphology probably contributes little to systematics (Fell, 1948; Wray, 1996; Smith, 1997) and similarity of larval morphology between echinoderm groups appears to be the result of convergent evolution in a completely different environment from post-metamorphic individuals (Raff, 1987; Strathmann, 1988*a*, *b*; Smith *et al.*, 1995*a*).

Post-larvae and juveniles could be treated as "adult miniatures", sharing similar morphological characteristics with conspecific adults, as well as sharing their benthic environment. However, many such characteristics are still developing and the small size makes them experience a completely different physical and biological environment. The study of their morphological state, development and relative time of appearance can be important for taxonomy and evolutionary, ecological and developmental processes. For instance, the time of appearance of the cribriform organ and epiproctal cone in porcellanasterids may represent an important ecological shift in the mode of life of these organisms (see chapter 4).

Because of the secular experience in culturing echinoid larvae, knowledge of the development and metamorphosis of shallow water species is extensive (Müller, 1854; Bury, 1895; MacBride, 1903; Mortensen, 1921, 1927*a*; Ubish, 1927; Mortensen, 1937; Strathmann, 1974*a*, 1978*a*; Cameron & Hinegardner, 1978; Chia & Burke, 1978; Schroeder, 1981; Emlet, 1986; Emlet *et al.*, 1987). However, most of the efforts on these studies were directed towards the study of larval forms and metamorphosis. As a result, only the very early post-metamorphic stages are described (MacBride, 1914; Onoda, 1936, 1938; McPherson, 1968; Hinegardner, 1975; Cameron & Hinegardner, 1978; Amemiya & Tsuchiya, 1979; Emlet, 1988; Olson *et al.*, 1993), with some exceptions where more advanced juvenile stages are shown (Hinegardner, 1969). Detailed description of plates and test development are, nevertheless, lacking in these papers.

The papers devoted to the study of the post-larval morphology and development of echinoids date back to the last century. Many accounts relate to isolated juvenile

stages found scattered among the vast taxonomic literature of the Echinoidea (e.g. Lovén, 1874; Mortensen, 1903, 1907, 1910). Detailed study of the post-larval development was made by Théel (1892) who studied the clypeasteroid *Echinocyamus pusillus*, showing the development of spines, teeth and sphaeridia. Gordon (1926*a*, *b*) described the plate formation and morphology during the post-metamorphic ontogeny of the regular sea urchin *Psammechinus miliaris* (as *Echinus miliaris*, see also Théel, 1902) and the spatangoid *Echinocardium cordatum*, respectively. The post-larval development of cidaroids was addressed by Mortensen (1927*b*). Gordon (1929) studied the plate development in *Arbacia punctulata* and *Echinarachnius parma*. Salas & Hergueta (1994) used the SEM to describe the changes in morphology in the post-larvae of the shallow water sea urchin *Arbaciella elegans* from the Mediterranean coast of Spain.

On the other hand, descriptions of deep-sea species relied (and still do) exclusively on post-larvae sampled from benthic populations. Mortensen (1903, 1907) describes some juvenile features of two deep-sea species, *Phormosoma placenta* and *Hemiaster expergitus* respectively, collected during the Danish Ingolf Expedition. Mortensen (1907) also described the test morphology of *Spatangus purpureus* at 4 mm in length and the post-larval development of another spatangoid, *Brisaster fragilis* (Fig. 5.1). Although both species occur in shallow water, their distributions extend to upper bathyal depths. The post-metamorphic development and morphology of some pourtalesiid sea urchins have been examined in detail by Gage (1984) and Harvey & Gage (1984). The latter authors, however, could not distinguish between two different species at sizes smaller than 3 mm in length.

Biological and ecological aspects of echinoid post-larval life are poorly known in the deep-sea. Most knowledge comes from samples dredged on a seasonal basis, revealing spatio-temporal patterns in settlement and recruitment success (Gage & Tyler, 1985; Flach & Heip, 1996). Gage *et al.* (1985) suggest that recruitment in the genus *Echinus* is variable from year-to-year. In addition, it appears that some echinoid juveniles may have a wider bathymetric distribution than their adult counterparts (Gage *et al.*, 1984), as seen in some ophiuroids (chapter 6) and asteroids (chapter 4). However, the major problem faced by researchers is the identification of such individuals (Tyler & Gage, 1984*a*; Gage & Tyler, 1985; Gage *et al.*, 1985),

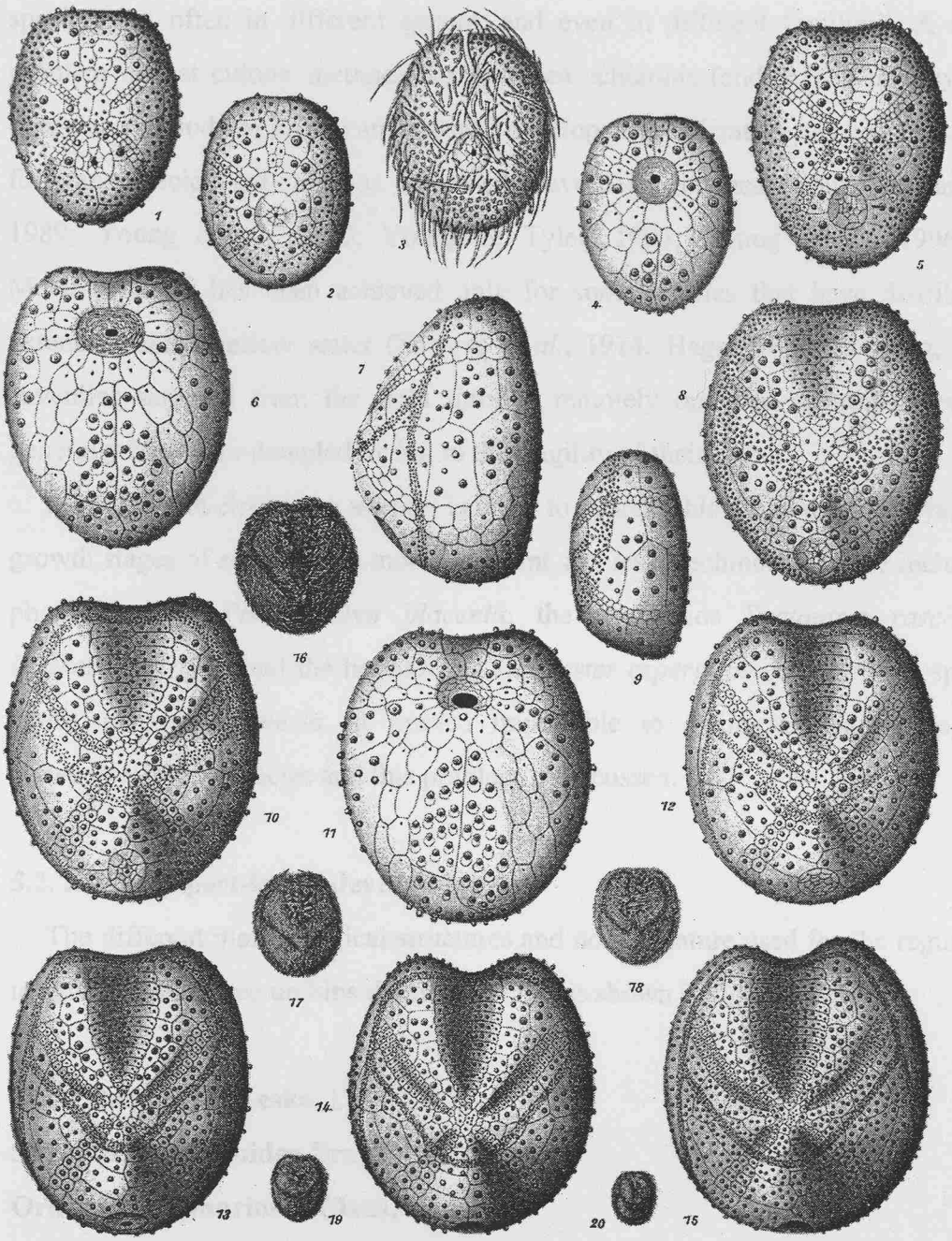

Figure 5.1. Growth stages of *Brisaster fragilis* depicted by Mortensen (1907).

leaving a gap in the understanding of patterns of settlement and recruitment of determinate species.

Agassiz (1869), referring to differences between juveniles and adult echinoids, stresses that "the changes some species undergo are so great that nothing would have been more natural than to place the two extremes of the series not only in different

species, but often in different genera, and even in different families". A further problem is that culture methods for deep-sea echinoids (and indeed for any other deep-sea echinoderm group) are not well developed. Fertilization has been successful for some species and embryos and larvae have been obtained (Young & Cameron, 1989; Young *et al.*, 1989; Young & Tyler, 1993; Young *et al.*, 1996*a*, *b*). Metamorphosis has been achieved only for some species that have distributions extending into shallow water (Shearer *et al.*, 1914; Hagström & Lønning, 1961). Juveniles sampled from the field through remotely operated sampling gears are generally broken or denuded owing to the fragility of their tests.

In the present chapter an attempt is made to address this problem by analysing the growth stages of some of the more abundant species of echinoids. These include the phormosomatid *Phormosoma placenta*, the spatangids *Spatangus raschi* and *Brissopsis lyrifera* and the hemiasterid *Hemiaster expergitus*. For the very speciose genus *Echinus*, however, it proved impossible to distinguish morphologically between different species and this problem is discussed.

5.2. Echinoid post-larval development

The different morphological structures and nomenclature used for the regular and irregular juvenile sea urchins described below is shown in figure 5.2.

Class Echinoidea Leske, 1778

Subclass Euechinoidea Bronn, 1860

Order Echinothurioida Claus, 1880

Family Phormosomatidae Mortensen, 1934

Phormosoma placenta Thomson, 1872

This species is distributed in the North Atlantic from off Iceland and Faroes to the Gulf of Guinea and from Davis Strait to the West Indies (Mortensen, 1927*a*). It occurs in depths of 260 to 2898 m (Harvey *et al.*, 1988) and animals collected with dredges and trawls have generally collapsed tests owing to the imbricating arrangement of the coronal plates.

Juveniles were not abundant in samples and most of the specimens had denuded tests, which made an accurate description of the spines and pedicellariae not possible.

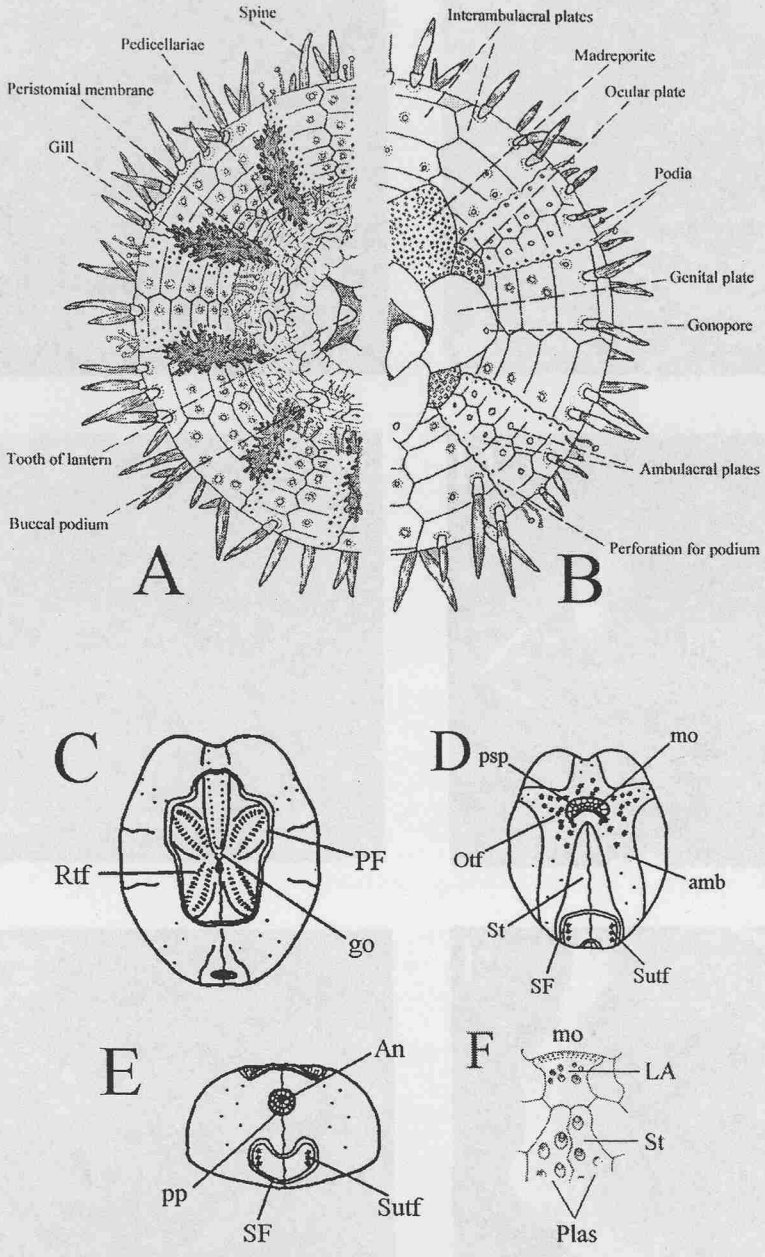

Figure 5.2. Morphological characteristics of regular (A-B) and irregular (C-F) echinoids. A and D. adoral view; B and C. aboral view; E. anal view; F. Detail of plastron of *Echinocardium flavescens*. amb = ambulacrum; An = anus; go = gonopore; LA = labrum; mo = mouth; Otf = oral tube feet; PF = peripetalous fasciole; Plas = plastron; pp = periproct; psp = peristomial plates; Rtf = respiratory tube feet; SF = subanal fasciole; St = sternal plate; Sutf = subanal tube tube feet. A and B modified from Barnes (1968); C-E modified from Nichols (1959); F modified from Hayward & Ryland (1990).

Furthermore, specimens did not yield good SEM micrographs and only a partial description of some early stages is given.

Figure 5.3. *Phormosoma placenta* juvenile development (A-G). A. Aboral view of juvenile at 1.58 mm; B. Detail of the tubercule of the test spine of the specimen of F. Note the large perforation in the centre; C. 3.30 mm, aboral view; D. 3.72 mm, aboral view; E. Detail of periproct of specimen of D showing the anal opening (arrow); F. 2.48 mm, adoral view; G. 3.48 mm. BP = buccal plate; GP = genital plate; IP = interambulacral plate; OP = ocular plate; pp = periproct; T = tooth. Sizes represent the test diameter.

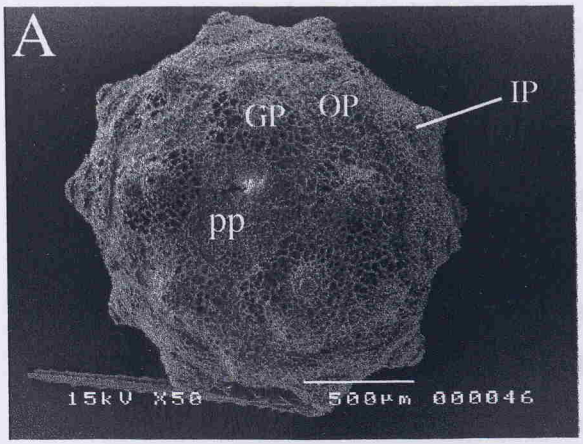
A
GP
OP
IP
pp
15kV X50
500µm 000046

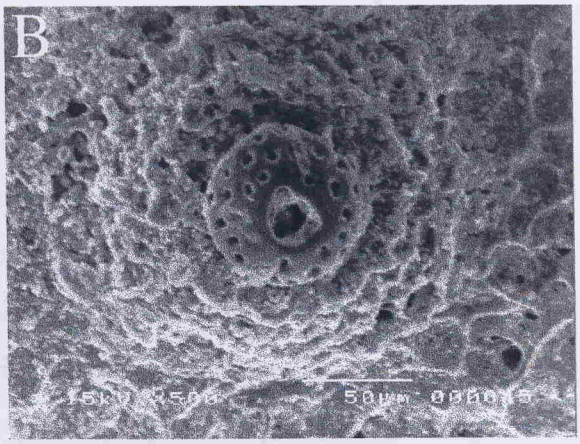
B

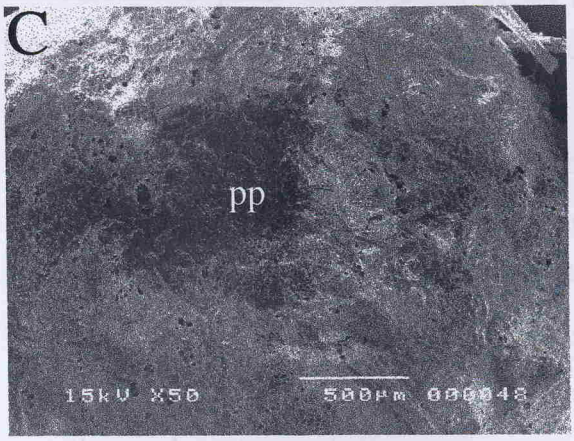
C
pp
15kV X50
500µm 000048

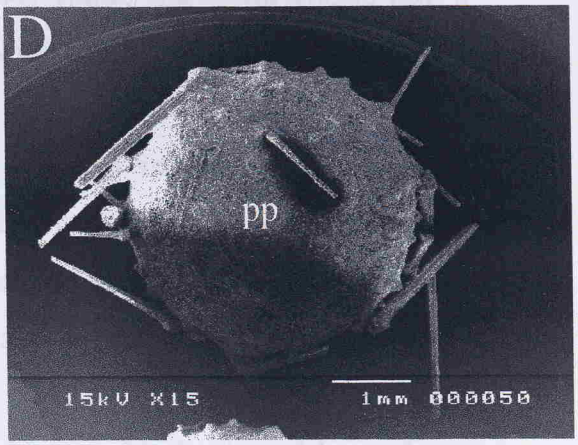
D
pp
15kV X15
1mm 000050

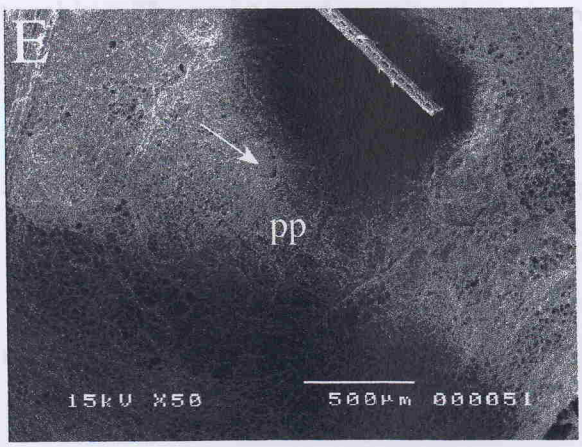
E
pp
15kV X50
500µm 000051

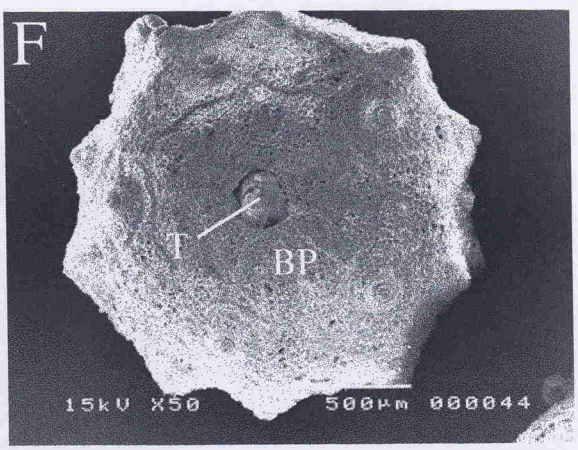
F
T
BP
15kV X50
500µm 000044

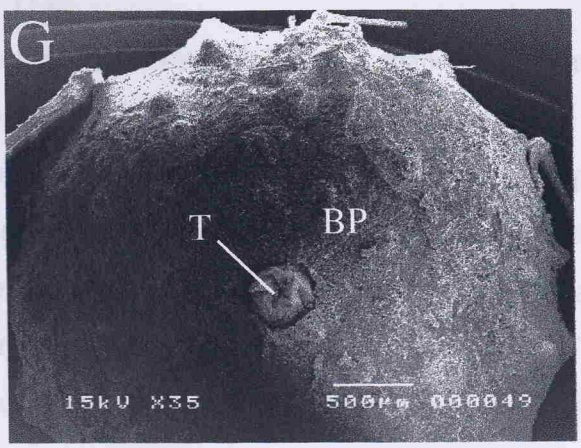
G
T
BP
15kV X35
500µm 000049

The smallest specimens found measured 1.58 mm in diameter. On the aboral surface the periproct is irregular in shape, bearing several small scales. The anal opening is still not formed. Surrounding the periproct there are five polygonal genital plates bearing up to two tubercles, where spines are inserted. The ocular plates are also polygonal in shape and almost as large as the genitals and do not touch the periproct region. Together, the periproct and apical system occupy almost the whole of the aboral surface (Fig. 5.3A). Only one primary spine is present on each interambulacral plate. The tubercles of the primary spines and apical system bear a large foramen in the centre of the mamelon, with small pits surrounding it (Fig. 5.3B).

At 3.30 mm diameter the periproct is much enlarged and circular, but the anal orifice is not formed (Fig. 5.3C). This structure is formed when the animal attains around 3.72 mm in diameter (Fig. 5.3D). At this size the genital plates have up to three tubercles and the proximal tip of the oculars touch the periproct (Fig. 5.3E).

On the adoral side at 2.48 mm diameter the teeth are pointed and arranged in a way that each tooth overlaps its subsequent neighbour, with the tips of the teeth not touching. The peristomial membrane is completely covered by the buccal plates (Fig. 5.3F).

At 3.48 mm diameter the arrangement of the teeth is clearly visible. Some plates are added to the peristomial membrane between the buccal and coronal plates (Fig. 5.3G).

Order Echinoida Claus, 1876

Family Echinidae Gray, 1825

Genus *Echinus* Linnaeus, 1758

Post-larvae of the genus *Echinus* were globular in shape and slightly flattened at the adoral surface (Fig. 5.4A and B). The aboral surface is composed by a large and round central anal plate surrounded by 5 genital plates. The genital plates are large and polygonal, bearing one juvenile spine each (Fig. 5.4A). The juvenile spines bear large branches at the tip. In some specimens, the juvenile spines have only small branches, which may suggest these represent a different species (Fig. 5.4C). The ocular plates are large and polygonal with two juvenile spines each. The ocular plates

Figure 5.4. *Echinus* juveniles (A-C). A. 0.97 mm, aboral view; B. 0.80 mm, adoral view; C. 1.00 mm, adoral view. AP = anal plate; Asp = adult spine; BP = buccal plate; GP = genital plate; Gped = globiferous pedicellaria; IP = interambulacral plate; Jsp = juvenile spine; OP = ocular plate; Oped = ophicephalous pedicellaria; ps = peristome; T = tooth. Sizes represent the test diameter.

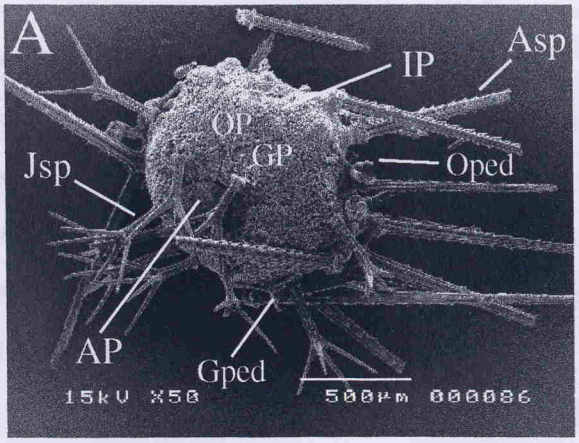
A
IP
Asp
OP
GP
Jsp
Oped
AP
Gped
15kV X50
500µm 000086

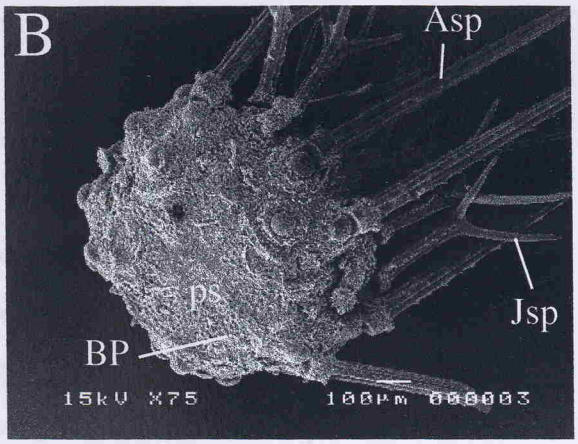
B
Asp
ps
Jsp
BP
15kV X75
100µm 000003

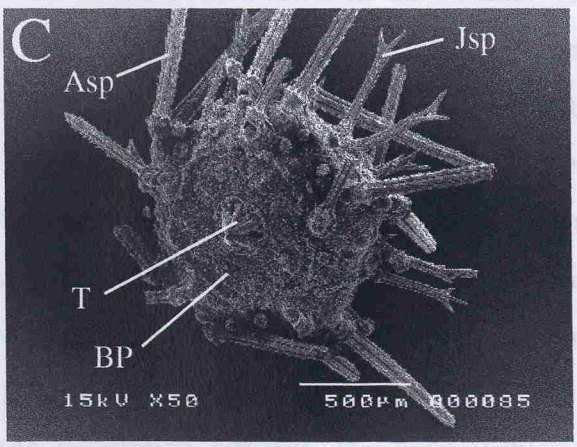
C
Jsp
Asp
T
BP
15kV X50
500µm 000085

surround the genital plates, forming a dicyclic apical system (Fig. 5.4A). Interambulacral plates are present on the ambital and adoral areas, and bear large adult spines (Figs. 5.4A and B).

Ophicephalous pedicellariae are present all over the test surface (Fig. 5.4A), even in very small specimens. Globiferous pedicellariae are rarer and generally appear when individuals are around 1 mm in diameter (Fig. 5.4A).

Individuals at 0.8 mm in diameter do not have the mouth apparatus formed. In the peristomial region only a peristomial membrane is present, which is still not pierced by the mouth, but already bear developing buccal plates (Fig. 5.4B). In some individuals at 1 mm, the Aristotle's lantern is already present and the whole peristomial area is well-developed (Fig. 5.4C).

Order Spatangoida Claus, 1876

Family Hemiasteridae Clark, 1917

Hemiaster expergitus Lovén, 1874

Hemiaster expergitus is a rather conspicuous member of the infauna of deep-sea sediments to the west of the British Isles. In the Rockall Trough this species was recorded from 1047 to 2910 m depth (Gage *et al.*, 1985; Harvey *et al.*, 1988), but the depth range can be larger elsewhere (Mortensen, 1927*a*). Test length (TL) can reach up to 53.5 mm (Mortensen, 1927*a*) and Gage (1987) suggests that it should take around 16 years for an individual to attain a test length of 30 mm.

Post-larval *Hemiaster expergitus* is described by Mortensen (1907) from size of 3 mm TL. The smallest specimen found in the present samples measured 0.91 mm TL. Because of the fragility of the test, very small specimens were always broken, making an accurate description difficult. The most striking feature in these small specimens are the relatively large, broad, leaf-shaped spines present on the adoral surface and on the ambitus of the test. The individuals show no fascioles.

TL=1.10 mm: the test is globular in shape. The mouth is pentagonal and the peristomial membrane already bears several small plates. The mouth opening is already formed. Five adoral spines surround the mouth (peristomial spines), bending over it. The spines differ in shape from those of the test, being much thinner and

Figure 5.5. *Hemiaster expergitus* juvenile development (A-H). A-B, adoral view; C. lateral view; D-H, aboral view. A. 1.10 mm; B. 2.30 mm; C. 4.23 mm. Note the location of the peristome (arrow) and periproct (double arrowhead); D. 0.91 mm; E. 1.47 mm; F. 2.13 mm; G. 4.02 mm; H. Detail of G. amb = ambulacrum; Ftf = frontal tube foot; Gped = globiferous pedicellaria; LA = labrum; PF = peripetalous fasciole; Plsp = plastron spines; pp = periproct; ps = peristome; Pssp = peristomial spine; Ptf = penicillate tube foot; St = sternal plate; Tsp = test spine. Asterisk points the location of a genital plate. Sizes represent the test length.

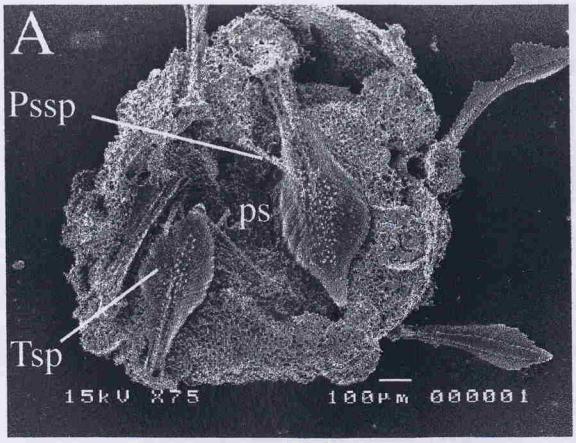
A
Pssp
ps
Tsp
15kV X75
100µm 000001

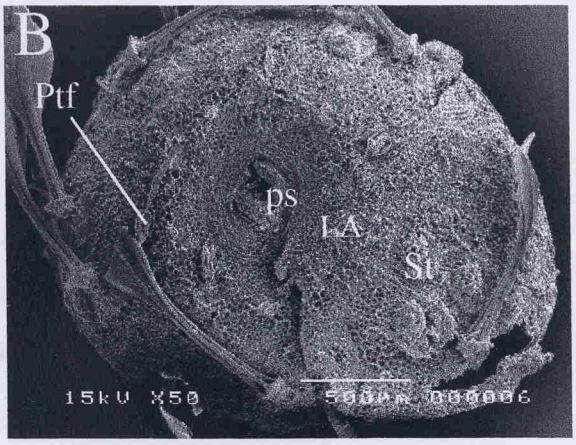
B
Ptf
ps
LA
St
15kV X50
500µm 000006

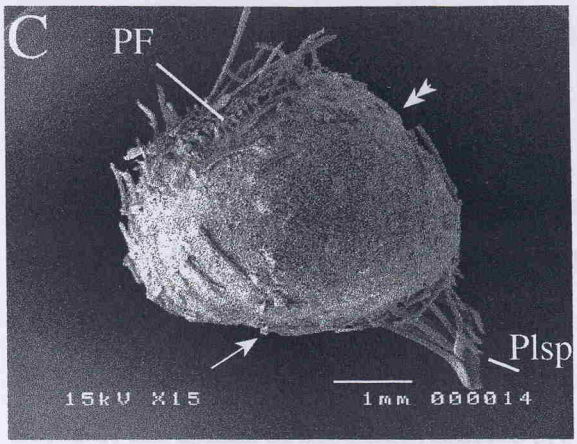
C
PF
Plsp
15kV X15
1mm 000014

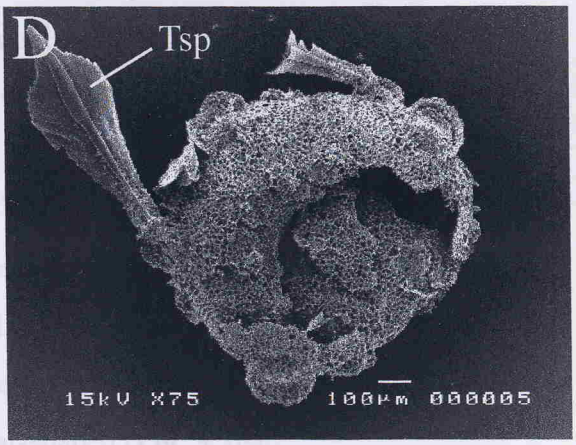
D
Tsp
15kV X75
100µm 000005

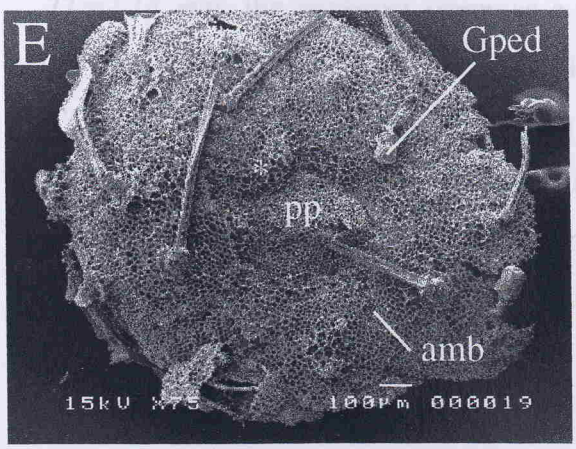
E
Gped
pp
amb
15kV X75
100µm 000019

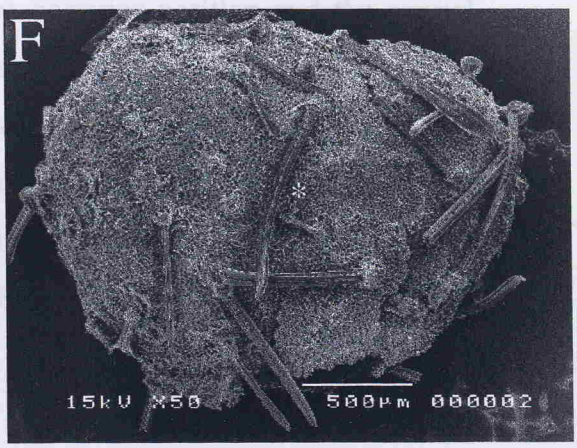
F
15kV X50
500µm 000002

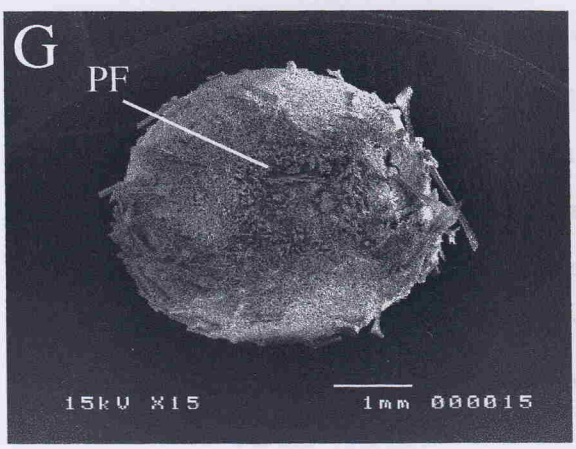
G
PF
15kV X15
1mm 000015

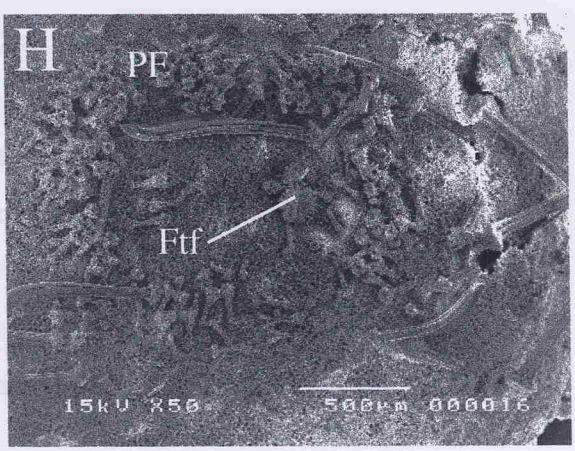
H
PF
Ftf
15kV X50
500µm 000016

smaller. Surrounding the mouth are the penicillate tube feet and sphaeridia (Fig. 5.5A).

TL=2.30 mm: the labrum is square in shape and the sternal plates each bear two large leaf-shaped spines. The ambulacral areas, not clearly visible in figure 5.5B, can be noticed by the presence of the penicillate tube feet (Fig. 5.5B).

TL=4.23 mm: the test is more globular, increasing in height (Fig. 5.5C). The labrum starts to differentiate to form a lip. A cluster of plastron spines is clearly visible towards the rear of the adoral side of the test (Fig. 5.5C).

On the aboral surface at 0.91 mm TL, the anus is already formed, but not clearly visible in figure 5.5D. In those specimens the digestive tract is well-formed and is clearly visible through the transparent test.

TL=1.47 mm: the test begins to elongate. The periproct is clearly visible and formed by five triangular plates. The ambulacra are formed by small plates and appear to end right on the periproct. The genital plates cannot be seen with certainty. At this stage some ophicephalous pedicellariae are present on the interambulacra. Some of the spines of the aboral surface are spear-shaped (Fig. 5.5E).

TL=2.13 mm: the periproct occupies a more posterior position and the genital plates appear to be present right next to it. No fasciole is present (Fig. 5.5F).

TL=4.02 mm: the peripetalous fasciole is present. The spines of the rear end of the test are spoon-shaped, whereas those of the front end are leaf-shaped (Fig. 5.5G). The spines within the peripetalous fasciole are also spoon-shaped (Fig. 5.5H). Two frontal tube feet are present within the fasciole (Fig. 5.5H).

Family Spatangidae Gray, 1825

Spatangus raschi Lovén, 1869

Spatangus raschi is an abundant species to the west of the British Isles. Farran (1913) reported large numbers in the Porcupine Seabight and on the Porcupine Bank (146-1024 m depth). In the Rockall Trough area this species was recorded from 225 to 1020 m depth (Harvey *et al.*, 1988), but the actual depth range for this species appears to be from 150 to 1500 m (Gage *et al.*, 1985).

Small juveniles examined in the present work presented a purple colour, similar to that of the adults. The smallest specimens measured around 0.67 mm TL.

Figure 5.6. *Spatangus raschi* juvenile development (A-N). A-H, aboral view; I. view of the rear portion of the animal; J-N, adoral view. A. 0.69 mm; B. 0.83 mm; C. 0.99 mm; D. 1.26 mm; E. Detail of the spines of the anterior end of the test; F. 1.64 mm. Note the location of the ambulacra (arrows); G. Detail of the anterior end of F; H. Detail of the posterior end of F. Note the double row of pedicellariae in the ambulacrum (arrow). Plsp = plastron spines; ps = peristome; SF = subanal fasciole; Susp = subanal spine; tf = tube foot. Sizes represent the test length.

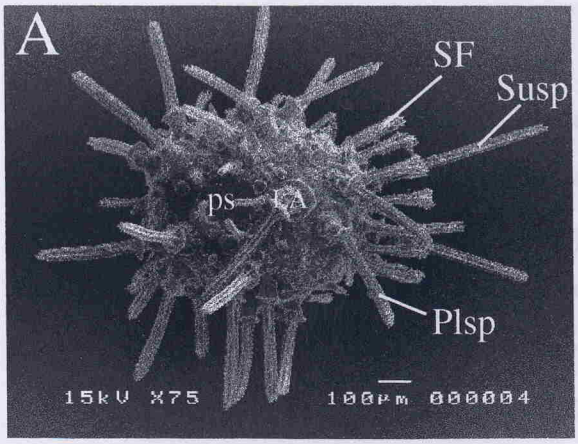
A
SF
Susp
ps
CA
Plsp
15kV X75
100µm 000004

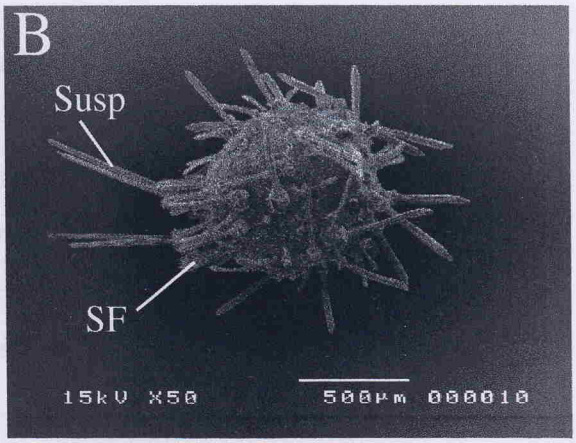
B
Susp
SF
15kV X50
500µm 000010

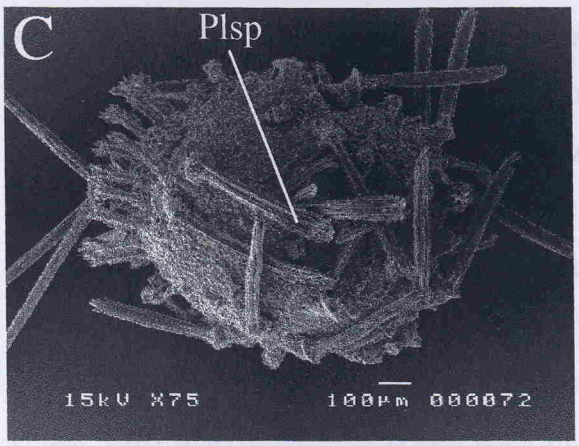
C
Plsp
15kV X75
100µm 000072

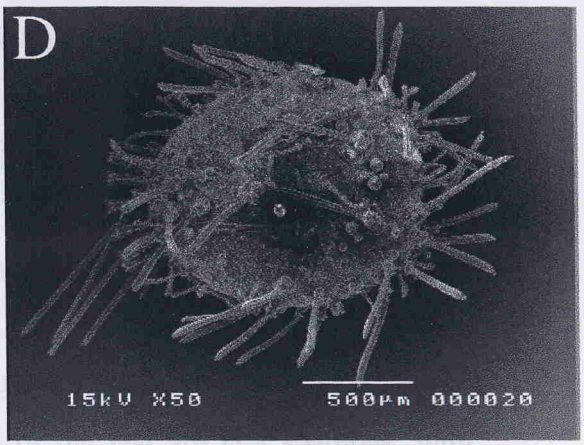
D
15kV X50
500µm 000020

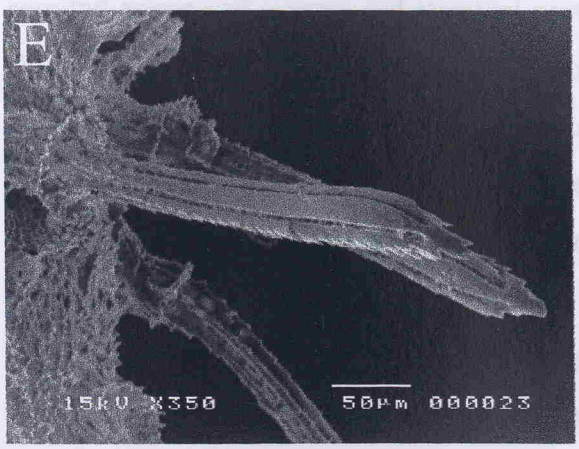
E
15kV X350
50µm 000023

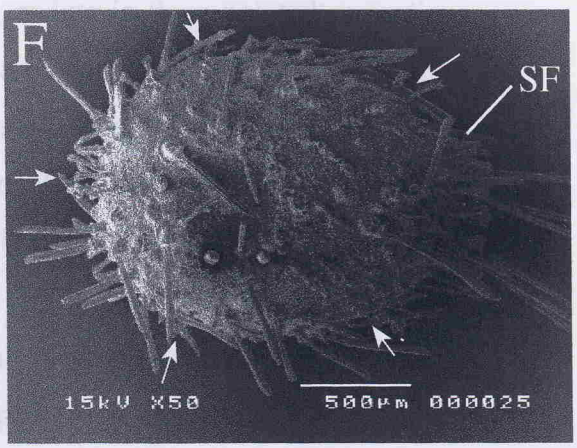
F
SF
15kV X50
500µm 000025

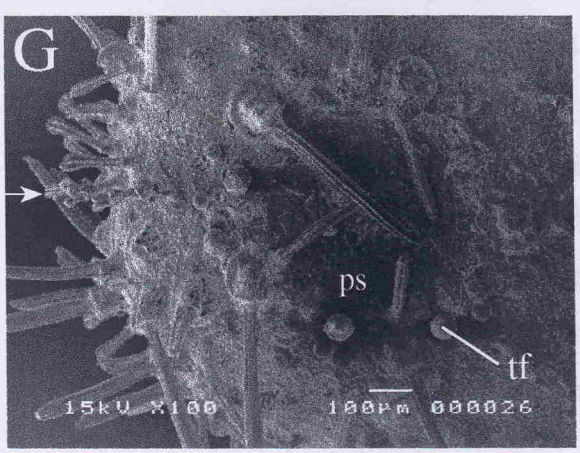
G
ps
tf
15kV X100
100µm 000026

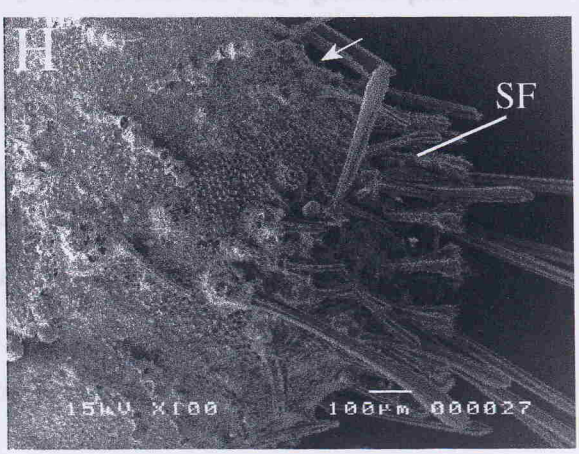
H
SF
15kV X100
100µm 000027

Specimens at 0.69 mm TL showed a rather elongated test with a very conspicuous, closed subanal fasciole, formed by a single row of clavulae arranged in a circle (Fig. 5.6I). The clavulae are quite elongated and widened at the tip. Inside the subanal fasciole, four long, thin subanal spines are present being directed distally (see Figs. 5.6A and I). All the primary spines of the interambulacral plates are slightly curved and finger-like. The labrum possesses a large primary spine and a smaller mouth spine bending over the peristome. Another four peristomial spines are present, each belonging to an interambulacral plate. The two sternal plates are rather small, with only one spine each. The peristomial membrane bearing no plates and with no sign of the perforation for the mouth. Each ambulacrum surrounding the peristome bears two tube feet (one on each plate), not yet penicillate, and one sphaeridium (Fig. 5.7A).

TL=0.83 mm: the spines of the interambulacral areas change in shape. The spines are beginning to become more heavily calcified. In a more advanced stage the spines of the plastron are spatulate, with a rounded posterior end and serrated at the edges (Figs. 5.6B and C). Those of the anterior end of the test are less spatulate, with serrated edges and a narrowed terminal portion, ending in three pointed projections (Figs. 5.6B, C and E). The peristomial spines are somewhat flattened and slightly curved. The peristomial membrane is already pierced with the mouth opening and bears several small plates arranged concentrically (Fig. 5.7B). Ophicephalous pedicellariae are distributed along the adoral side in rows accompanying the ambulacra (Fig. 5.7F).

TL=1.26 mm: the peristome is pentagonal in shape and the plates in the peristomial membrane are much more developed (Figs. 5.6D and 5.7C). On the aboral side, at 1.35 mm TL, the periproct is clearly visible and the large genital plate 2 can be seen (Fig. 5.6K). The dorsal spines are spear-shaped. Those of the posterior end of the test are surrounded by small, club-shaped spines. Inside the subanal fasciole, six long spines are now present (Figs. 5.6J and K).

TL=1.64 mm: the rows of ophicephalous pedicellariae are very conspicuous on the adoral surface (Fig. 5.6F). A closer look at the bivial ambulacra shows that each pedicellaria is attached to a somewhat rounded ambulacral plate, forming a double row (Fig. 5.6H). However, in the trivial ambulacra the pedicellariae appear as a small

Figure 5.6 (cont.). *Spatangus raschi* juvenile development. I. 0.69 mm; J. 1.35 mm; K. Detail of the posterior end of J; L. 3.63 mm; M. Detail of the posterior end of L showing periproct; N. Detail of the posterior end of L showing the secondary club-shaped spines surrounding the primary spines of the rear of the test. Gped = globiferous pedicellaria; pp = periproct; SF = subanal fasciole; Ssp = secondary spine; Susp = subanal spine; Tped = tridentate pedicellaria. Sizes represent the test length.

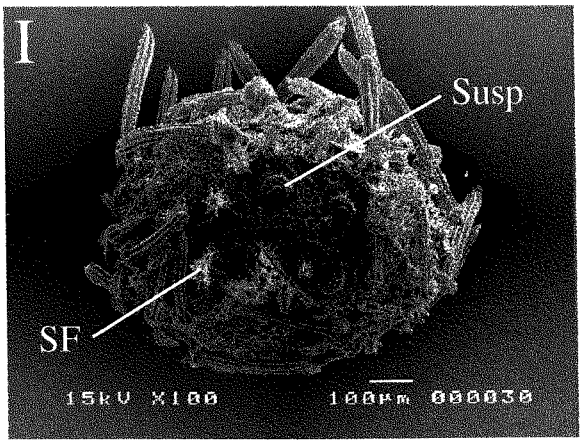
I
Susp
SF
15kV X100
100µm 000030

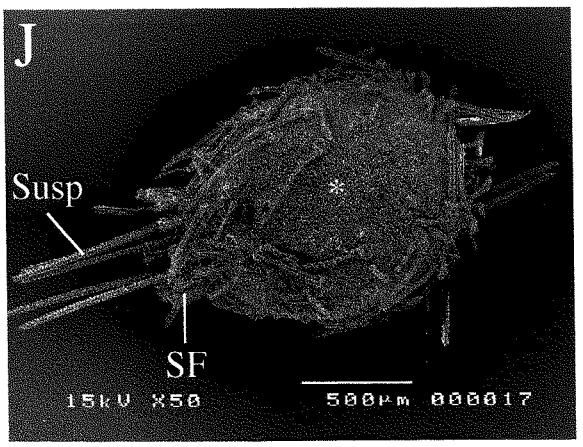
J
Susp
SF
15kV X50
500µm 000017

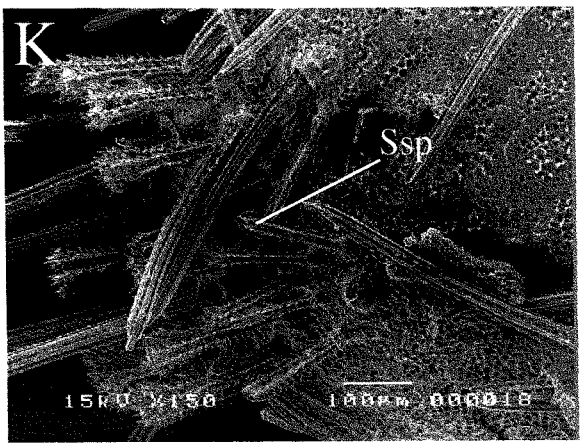
K
Ssp
15kV X150
100µm 000018

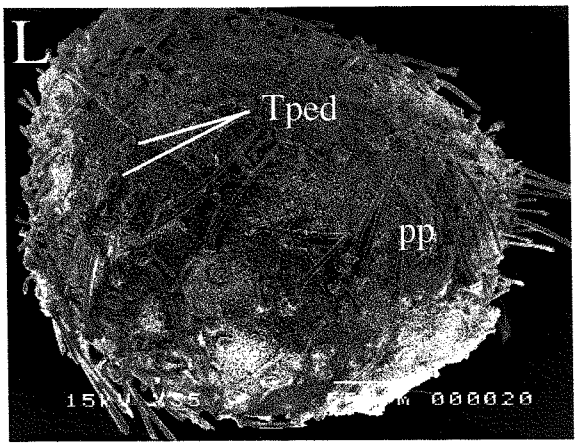
L
Tped
pp
15kV X55
000020

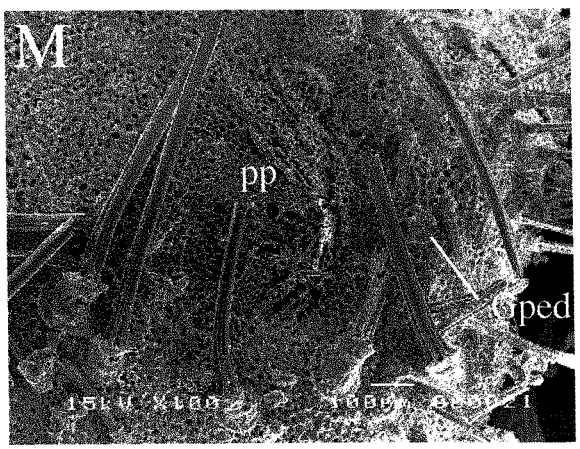
M
pp
Tped
15kV X100

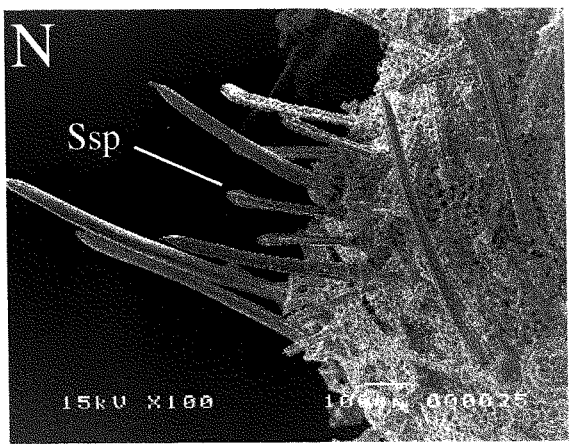
N
Ssp
15kV X100

Figure 5.7. Peristome development of *Spatangus raschi* and pedicellariae (A-F). A. 0.69 mm; B. 0.83 mm; C. 1.26 mm; D. Tridentate pedicellaria; E. Ophicephalous pedicellariae; F. Ophicephalous pedicellariae arranged in double rows along the ambulacrum. LA = labrum; mo = mouth; ps = peristome; psp = peristomial plates; Pssp = peristomial spine; Sph = sphaeridia; Ssp = secondary spine; tf = tube foot. Sizes represent the test length.

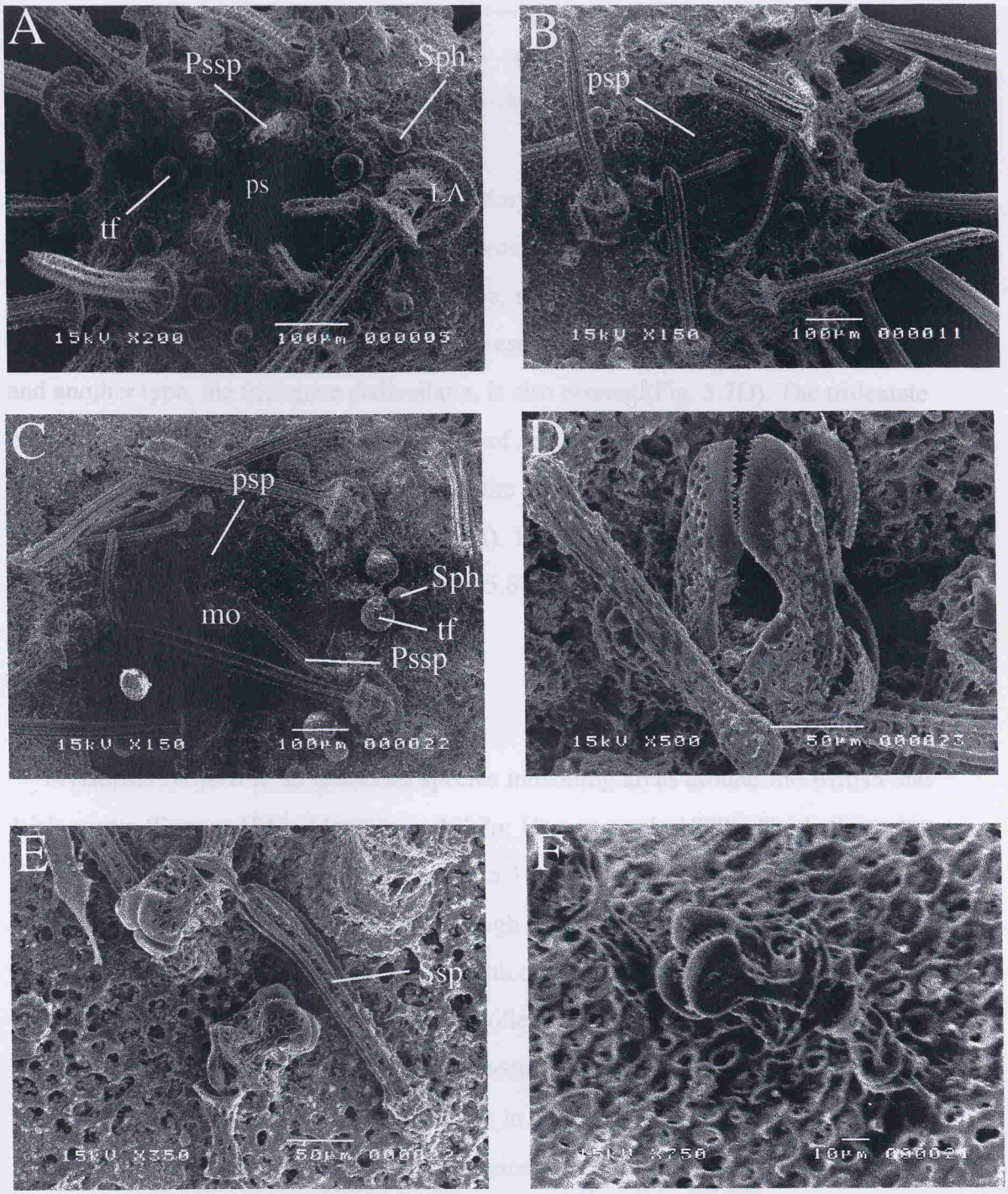
A
Pssp
Sph
ps
LA
tf
15kV X200
100µm 000005
B
psp
15kV X150
100µm 000011
C
psp
Sph
mo
tf
Pssp
15kV X150
100µm 000022
D
15kV X500
50µm 000023
E
Ssp
15kV X350
50µm 000022
F
15kV X750
10µm 000021

single row, probably owing to the smaller size of the ambulacral plates and its arrangement (Fig. 5.6G). Several small, club-shaped spines are present in the front of the test.

Aborally at 1.67 mm TL the small secondary spines are still present in the region between the subanal fasciole and the periproct. At 3.63 mm TL, the shape of the body changes from egg-shape to heart-shape, more similar to the adult (Fig. 5.6L). The ophicephalous pedicellariae are now present on the aboral surface (Fig. 5.7E) and another type, the tridentate pedicellaria, is also present (Fig. 5.7D). The tridentate pedicellaria shows the same characteristics of adult tridentate pedicellariae depicted by Mortensen (1907) for this species. On the aboral side, the pedicellariae are not restricted to the ambulacral areas (Fig. 5.6M). The secondary spines (club-shaped) on the rear end of the test are still present (Fig. 5.6N).

Family Brissidae Gray, 1855

Brissopsis lyrifera (Forbes, 1841)

Brissopsis lyrifera is an abundant species inhabiting areas around the British and Irish coasts (Farran, 1913; Mortensen, 1927*a*; Harvey *et al.*, 1988). The bathymetric distribution of this species ranges from 5 to 1400 m. Harvey *et al.* (1988) report a species of *Brissopsis* from the Rockall Trough area, which they argue is probably *B. lyrifera*, based mainly on the length and width of the anterior and posterior petals and pedicellariae. The present specimens were collected from the Porcupine Seabight and Goban Spur areas, where juveniles of this species were abundant.

The peristomial development is similar to the other spatangoids described. At around 0.50 mm TL, the five peristomial spines are already present. They are small and slightly curved, bending over the site of the future mouth (as to form a dome). On the ambulacral areas, close to the mouth, there is one penicillate tube foot (with its projections starting to be issued) and one sphaeridium (Fig. 5.8A). As the development progresses, the peristomial membrane appears (Fig. 5.8B) and the peristomial spines start to elongate (Fig. 5.8C). At 2.70 mm TL, the mouth has a pentagonal shape and the peristomial membrane is already pierced, forming the mouth opening. The peristomial membrane bears small scales arranged concentrically around the mouth. Three penicillate tube feet are present in each

Figure 5.8. Peristome development of *Brissopsis lyrifera* (A-E). A. 0.50 mm; B. 0.62 mm; C. 0.85 mm; D. 2.70 mm; E. 3.18 mm. LA = labrum; mo = mouth; Ptf = penicillate tube foot; Plsp = plastron spine; ps = peristome; psp = peristomial plates; Pssp = peristomial spine; Sph = sphaeridia. Sizes represent the test length.

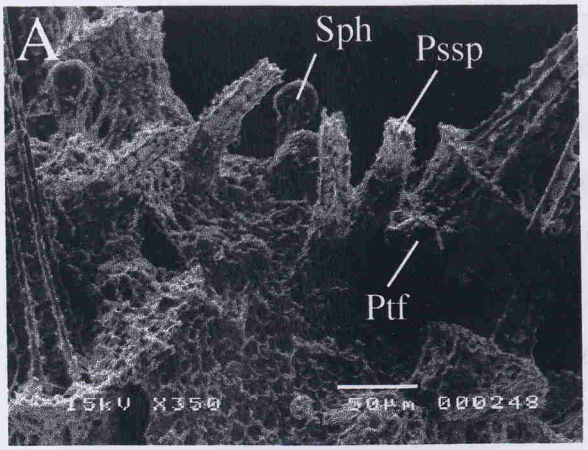
A
Sph
Pssp
Ptf
15kV X350
50µm 000248

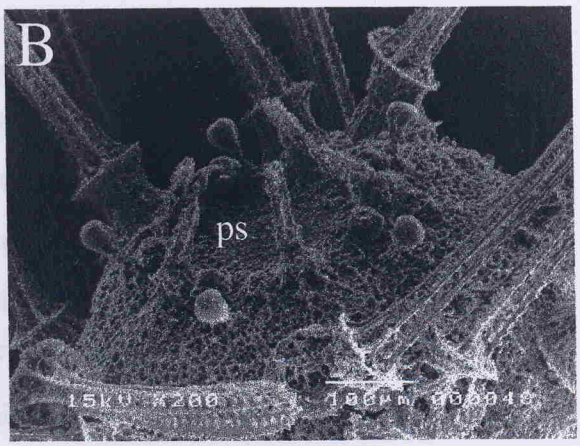
B
ps
15kV X200
100µm 000048

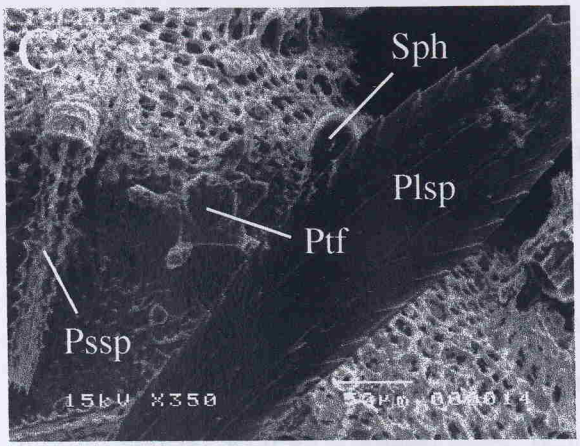
C
Sph
Plsp
Ptf
Pssp
15kV X350
50µm 000014

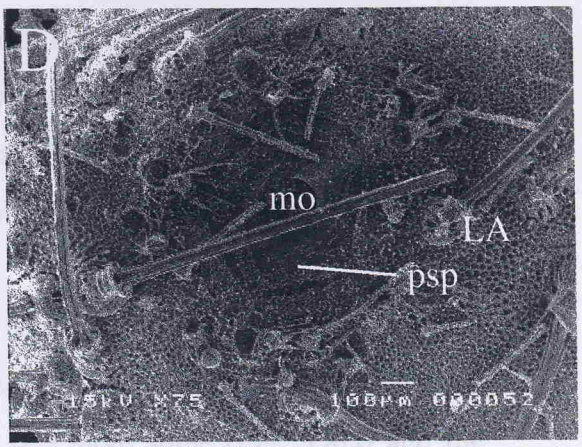
D
mo
LA
psp
15kV X75
100µm 000052

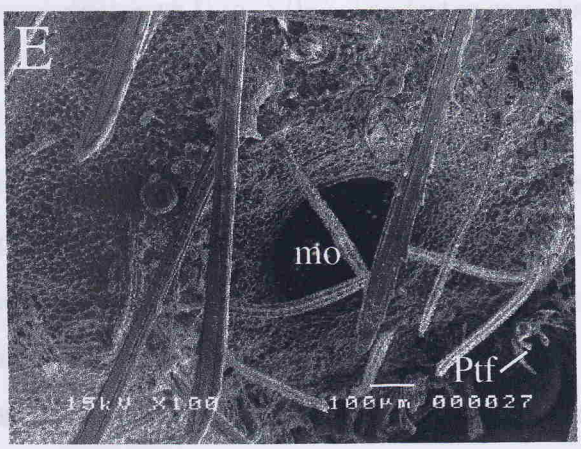
E
mo
Ptf
15kV X100
100µm 000027

ambulacrum, each bearing several elongated rods (Fig. 5.8D). At 3.18 mm TL, the peristomial spines are much elongated and curved (Fig. 5.8E).

The development of the test is described below. At 0.54 mm TL, the test is spherical in shape. The spines of the test, although large, are still quite rudimentary, with the stereom formed by a series of interconnected bridges of calcium carbonate. The spines are slightly curved and finger-like (Fig. 5.9A).

TL=0.60 mm: the stereom structure of the spines begins to change. The distal ends of the spines are more spatulate and a layer of stereom begins to be deposited along the length of the spines (Fig. 5.9B). As a result, the spines change completely in shape and structure, bearing a smooth and ornamented surface when the animal attains 0.85 mm TL (Fig. 5.9C). These spines are distributed on the interambulacral areas on the adoral surface and on the ambitus of the test. The test at this stage is still spherical in shape.

TL=1.26 mm: the test is more elongated and the plastron spines are easily recognized, although the plates are not clearly seen (Fig. 5.9D). At 2.70 mm TL, the labrum can be seen as a square plate, bearing one large spine (Fig. 5.8D) and the sternal plates bearing three spines each (Fig. 5.9E). The test is egg-shaped.

On the aboral surface, at 0.68 mm TL, a very conspicuous juvenile fasciole is present surrounding the whole of the aboral area and the periproct. This fasciole is a circle formed from a single row of clavulae. Each clavula is short, ending in a quite enlarged cone-shaped projection. Inside the fasciolar area, four large spines are present distributed in each corner as to form an imaginary square. The spines are thin and elongated, with a simple stereom structure (Fig. 5.9F).

TL=1.06 mm: the test is more elongated and the juvenile fasciole still surrounds the whole of the aboral surface. The four spines inside the fasciole have a more complex structure, with a smooth surface and a spear-shape. Some secondary, small club-shaped spines are also present. The periproct is formed by several small, triangular plates, with spinulose tips. At the rear of the test four long spines are present (Fig. 5.9G).

TL=1.60 mm: a subanal fasciole is already formed, composed by a single row of clavulae. At 2.30 mm TL, this fasciole is well-developed and a peripetalous fasciole is beginning to form (Fig. 5.9H). The peripetalous fasciole is composed by a single

row of clavulae on the frontal portion of the aboral surface. The clavulae from both subanal and peripetalous fascioles are thin, with a not very pronounced distal end. In this specimen we can note the remains of the juvenile fasciole (which is being resorbed), in which the clavulae have a completely different morphology. Although both clavulae cone-shaped ends, the diameter of the terminal portion of those of the subanal and peripetalous fascioles is around 40 μm, whereas that of the juvenile fasciole is around 90 μm at this stage (Figs. 5.9H and I). All over the aboral surface many small, club-shaped secondary spines can be seen (Fig. 5.9I). The primary spines of the anterior of the test are spear-shaped, whereas those of the posterior end are spoon-shaped (Fig. 5.9H). In this specimen, a small rostrate pedicellaria is present on the ambital region of the test (Fig. 5.10A).

TL=3.18 mm: a tridentate (Fig. 5.10B) and a triphyllous (Fig. 5.10C) pedicellariae are present. In some specimens the labrum starts to project over the mouth.

TL=3.87 mm: the overall shape of the body is ovoid, but the front of the test is straight (Fig. 5.9K). The peripetalous fasciole is somewhat heart-shaped, formed by a double row of clavulae. Within this fasciole two frontal tube feet are present and several small club-shaped and large spear-shaped spines (Fig. 5.9L). At the rear of the test, the very conspicuous subanal fasciole is formed by a large number of clavulae. The primary spines are spoon-shaped. The periproct is rounded and covered by several small scales (Fig. 5.9M).

In larger specimens at around 20.00 mm TL, fully developed rostrate (Fig. 5.10E) and tridentate (Fig. 5.10D) pedicellariae can be found. No globiferous pedicellariae were found.

Figure 5.9. *Brissopsis lyrifera* juvenile development (A-M). A-E, adoral view; H, I and J, lateral view; F, G, K, L and M, aboral view. A. 0.54 mm; B. 0.60 mm; C. 0.85 mm; D. 1.26 mm; E. 2.70 mm. JF = juvenile fasciole; LA = labrum; Plsp = plastron spine; ps = peristome; SF = subanal fasciole; Tsp = test spine. Sizes represent the test length.

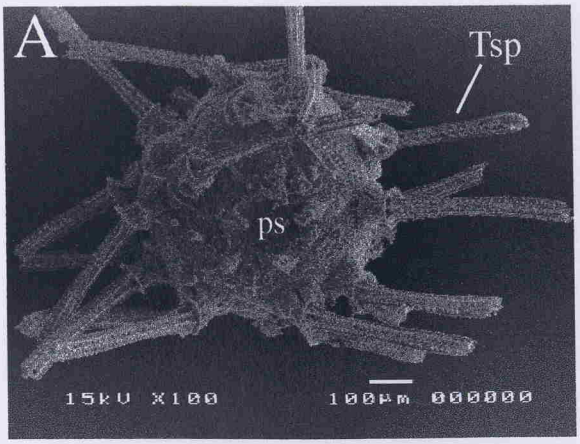
A
Tsp
ps
15kV X100
100µm 000000

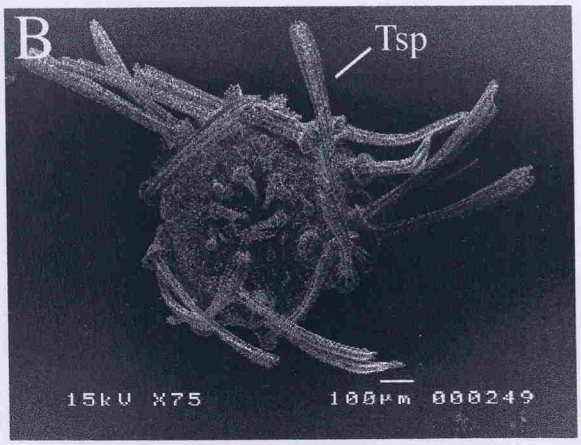
B
Tsp
15kV X75
100µm 000249

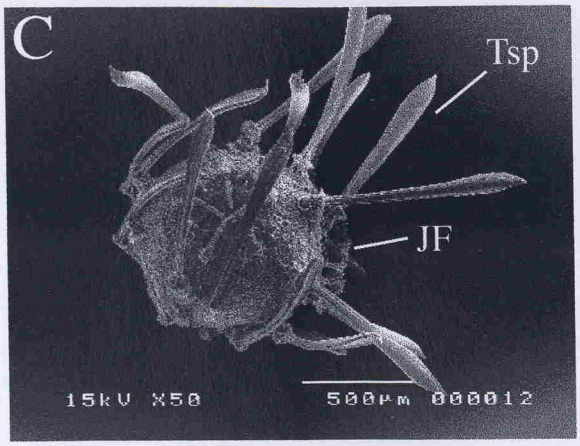
C
Tsp
JF
15kV X50
500µm 000012

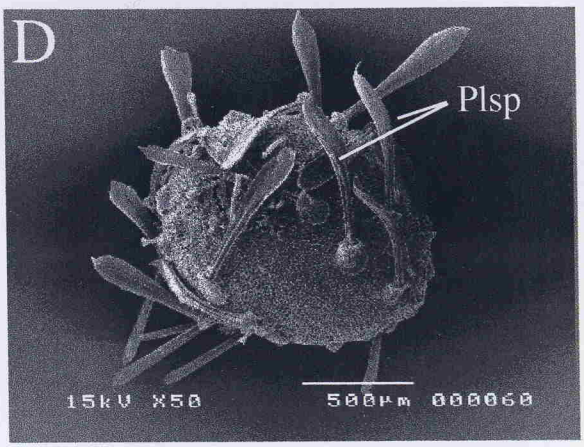
D
Plsp
15kV X50
500µm 000060

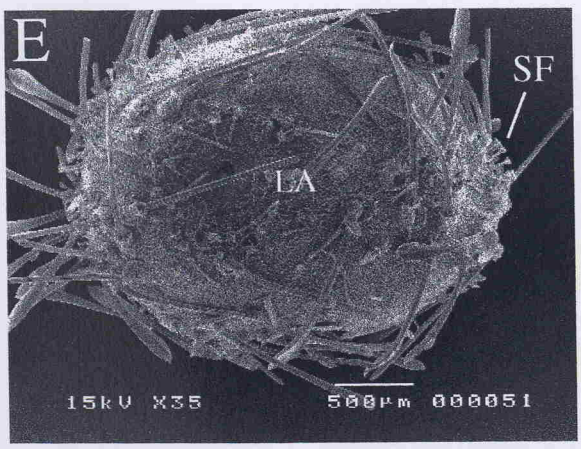
E
SF
LA
15kV X35
500µm 000051

Figure 5.9 (cont.). *Brissopsis lyrifera* juvenile development. F. 0.68 mm; G. 1.06 mm; H. 2.30 mm; I. Detail of H showing the clavulae of the juvenile and peripetalous fascioles and the secondary spines; J. 3.18 mm; K. 3.87 mm; L. Detail of K showing the peripetalous fasciole and the frontal tube feet; M. Detail of K showing the periproct are and the subanal fasciole. Acl = clavula of adult fasciole; Ftf = frontal tube foot; Jcl = clavula of juvenile fasciole; JF = juvenile fasciole; mo = mouth; PF = peripetalous fasciole; pp = periproct; Rped = rostrate pedicellaria; SF = subanal fasciole; Ssp = secondary spine; Tsp = test spine. Sizes represent the test length.

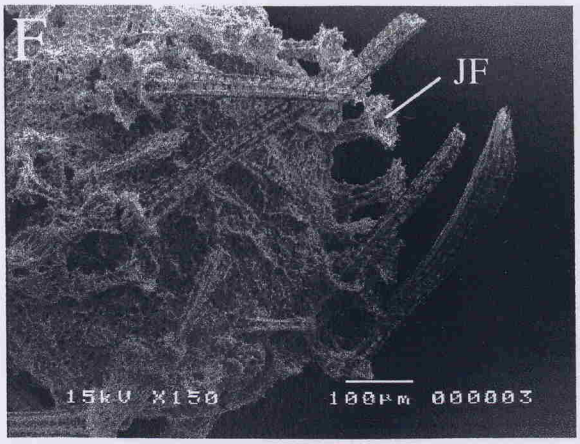
F
JF
15kV X150
100µm 000003

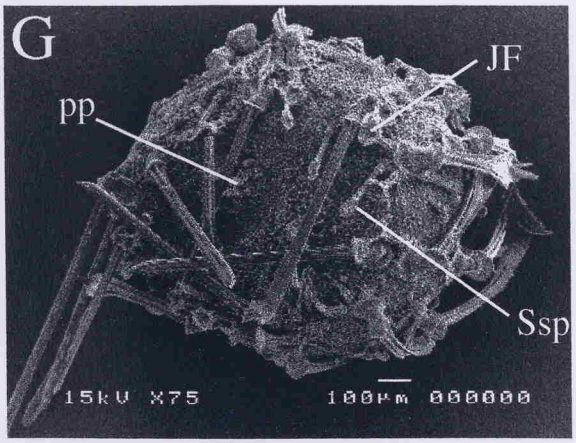
G
JF
pp
Ssp
15kV X75
100µm 000000

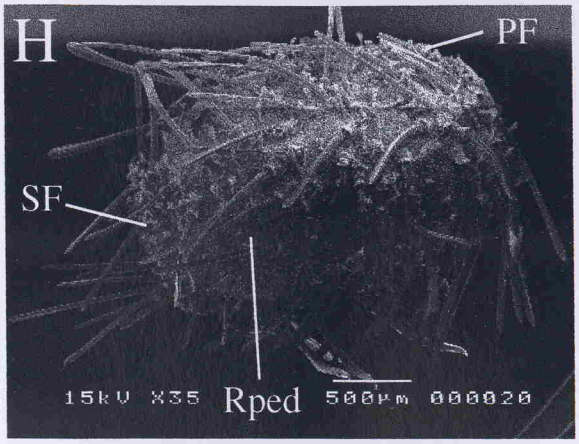
H
PF
SF
15kV X35
Rped
500µm 000020

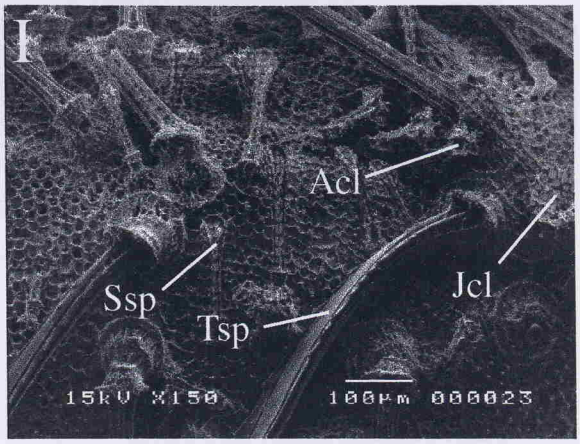
I
Acl
Jcl
Ssp
Tsp
15kV X150
100µm 000023

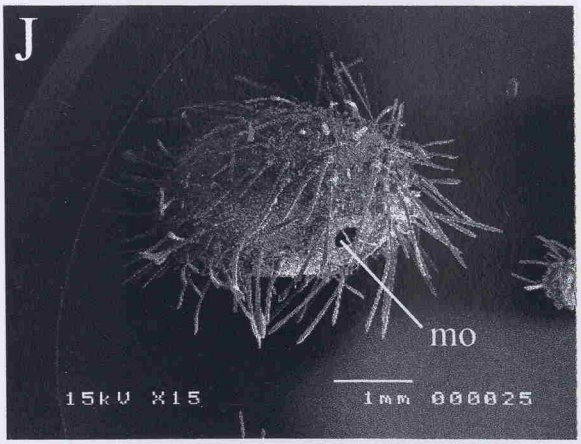
J
mo
15kV X15
1mm 000025

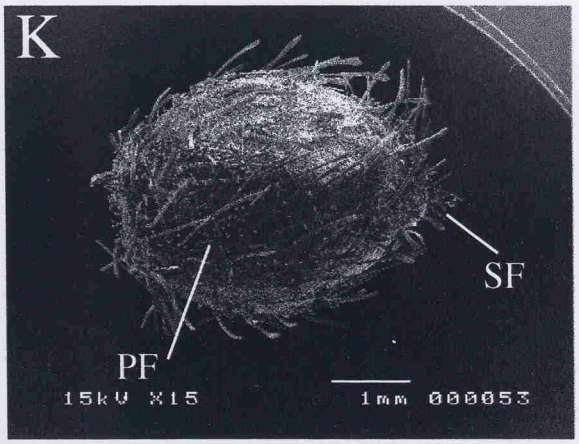
K
SF
PF
15kV X15
1mm 000053

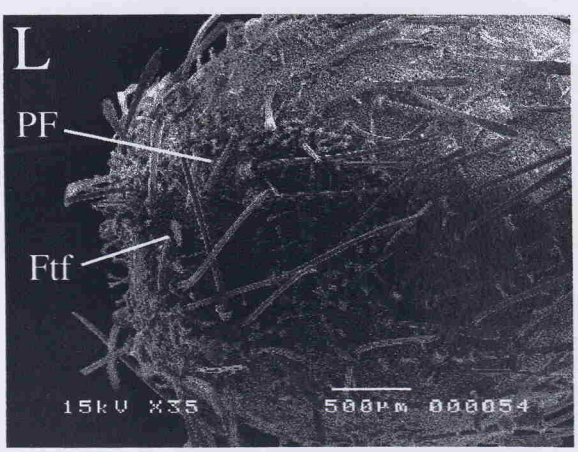
L
PF
Ftf
15kV X35
500µm 000054

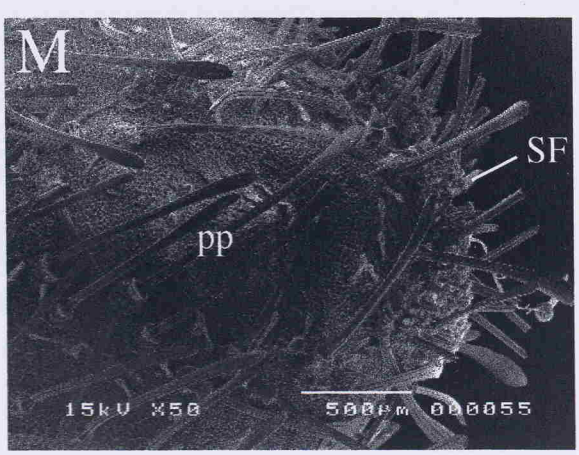
M
SF
pp
15kV X50
500µm 000055

Figure 5.10. Pedicellariae of *Brissopsis lyrifera* (A-E). A. Small rostrate pedicellaria of a 2.30 mm TL specimen; B. Small tridentate pedicellaria of a 3.18 mm TL juvenile; C. Triphyllous pedicellaria of the same juvenile of B; D. Fully developed tridentate pedicellaria of a 20.00 mm TL specimen; E. Fully developed rostrate pedicellaria of the same specimen of D.

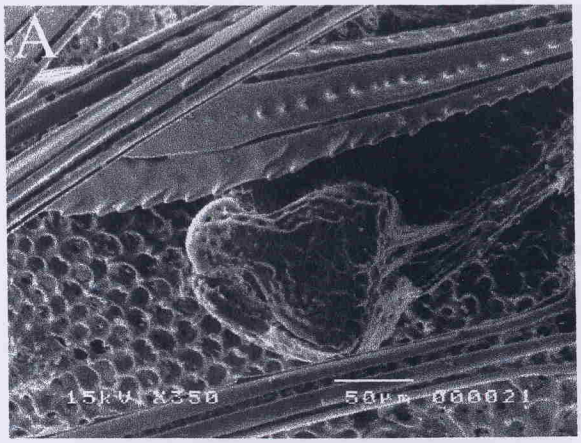
A
15kV X350
50µm 000021

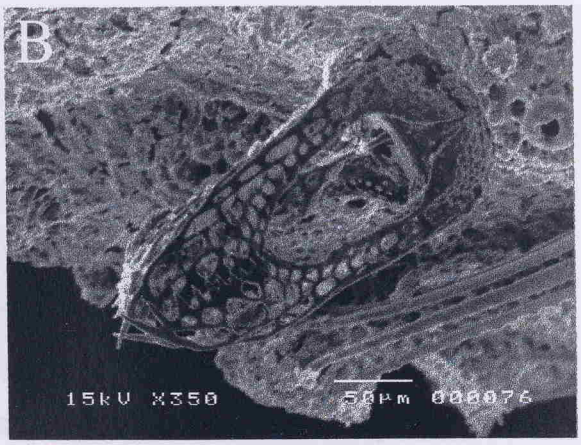
B
15kV X350
50µm 000076

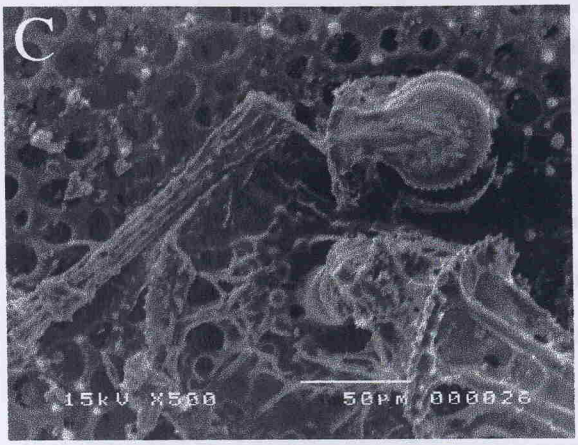
C
15kV X500
50µm 000026

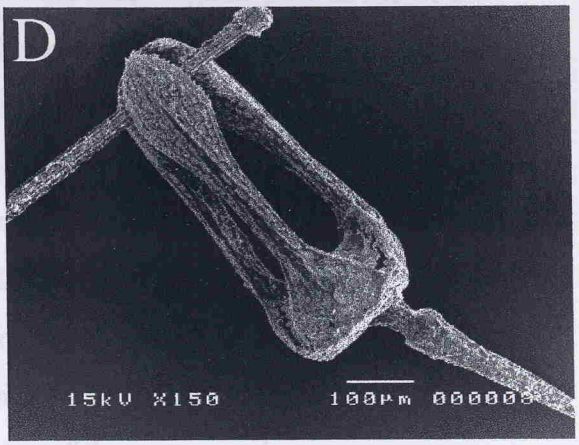
D
15kV X150
100µm 000003

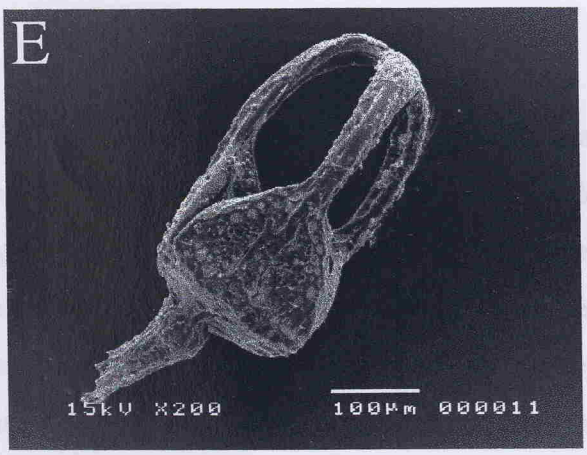
E
15kV X200
100µm 000011

5.3. Discussion

5.3.1. Taxonomic discussion

5.3.1.1. *Phormosoma placenta*

Unfortunately this species was not very abundant in the samples and most specimens presented denuded tests. They also did not yield good SEM pictures owing to the poor contrast achieved during examination. No other juvenile echinothurioid was found in the samples, making any comparison impossible. *Phormosoma placenta* differs, nevertheless, from the other regular post-larvae of the genus *Echinus* by the presence of several small plates in the periproct (a large anal plate is present in *Echinus*; compare figures 5.3A and 5.4A below) and the different stereom structure of the genital and ocular plates (labyrinthic in *P. placenta* and perforate in *Echinus* - see Smith, 1980). The primary tubercles in *P. placenta* have a foramen in the centre (Fig. 5.3B), whereas in *Echinus* they bear very small, regularly distributed holes. On the ventral side they differ in the arrangement of the teeth and buccal plates (see Figs. 5.3F and 5.4C). The apical system in *P. placenta* agrees with that depicted by Mortensen (1903) for a post-larva of the same species.

5.3.1.2. Spatangoids

Three species of spatangoids are described in the present chapter. *Spatangus raschi* belong to the family Spatangidae, *Brissopsis lyrifera* to the Brissidae, and the third, *Hemiaster expergitus*, to the Hemiasteridae. Although all three species showed a similar peristomial structure, with similar arrangement of spines, tube feet and sphaeridia around the peristome, early post-larvae of *H. expergitus* are easily separated from the other two by the complete absence of a fasciole. In this species only a peripetalous fasciole is formed after the animal is over 3 mm TL (Mortensen, 1907) and it is the only fasciole present during all its life. The spines in *H. expergitus* are also very distinctive, being very broad and leaf-shaped.

The other two species are clearly distinguished by the position of the fasciole and the morphology of the clavulae. *Spatangus raschi* bears a subanal fasciole clearly directed to the rear of the test, formed by very elongated clavulae. In *Brissopsis lyrifera* a juvenile fasciole is present surrounding the whole of the aboral surface, including the periproct. The clavulae are relatively shorter, with a much wider

terminal portion in comparison with those of *S. raschi*. Later this fasciole gradually disappears, giving way to the adult peripetalous and subanal fascioles. At these later stages *B. lyrifera* bears two distinct fascioles, whereas *S. raschi* possesses only the subanal fasciole. The plastron spines are also very distinctive, with those of *B. lyrifera* being leaf-shaped and elongated, with pointed tips. In *S. raschi* spines are also spatulate, but with rounded tips.

5.3.2. Development of the apical system and periproct in spatangoids

Gordon (1926*b*) describes, in great detail, the development of the spatangoid *Echinocardium cordatum*. Gordon (1926*b*) shows how the apical system in early juveniles is endocyclic, becoming exocyclic as ontogeny progresses. Although plate development is not as clear in the spatangoids examined, it is clear in *Hemiaster expergitus* that the development of the apical system and periproct is similar to that described for *E. cordatum*. Mortensen (1907) states that in a juvenile of *H. expergitus* examined by him, the periproct is clearly separated from the apical system. Mortensen's specimen, however, is 3 mm TL and the examination of smaller specimens in the present chapter (1.47 mm TL, Fig. 5.5E) shows clearly the endocyclic nature of the apical system, with the periproct later migrating towards the posterior of the test in the interambulacrum 5. The same is probably true for the other two species examined, possibly representing a characteristic of the whole order. Indeed another spatangoid, *Brisaster fragilis*, show a similar trend during ontogenesis (Fig. 5.1; Mortensen, 1907). Fell (1963) argues that there is a tendency for the migration of the periproct out of the apical system to the interambulacrum 5 in certain groups. This is an evidence for the belief that irregular echinoids evolved from a regular echinoid ancestral (Durham, 1966; Littlewood & Smith, 1995; Smith *et al.*, 1995). Perhaps the exocyclic type of apical system evolved through heterochrony from an endocyclic type of apical system. Heterochrony seems to have played an important role in the evolution of echinoids (McNamara, 1982, 1988). McNamara (1987) points out that this ontogenetic and phylogenetic migration of the periproct may have arisen from a localized plate translocation of the periproct and genital plate 5 from the rest of the apical system.

5.3.3. Formation of the mouth and fascioles in spatangoids

The spatangoids examined and the genus *Echinus* (see section 5.3.4 below) probably develop indirectly through a planktotrophic echinopluteus. This is thought to be true either by direct evidence, as in the case of the known larva of *Brissopsis lyrifera* (Mortensen, 1920) and *Echinus esculentus* and *E. acutus* (Shearer & Lloyd, 1913; Shearer *et al.*, 1914; Hagström & Lønning, 1961), or indirectly by looking at egg size (see introduction for species of the genus *Echinus*). Evidence for several echinoid species with larval development suggests that the size of post-larvae at metamorphosis ranges between 0.3-0.6 mm TL (MacBride, 1903, 1914; Mortensen, 1938; Onoda, 1936; Lønning & Wennerberg, 1963; Hinegardner, 1969; Emlet *et al.*, 1987; Emlet, 1988).

It is interesting to note that all *Echinus* specimens examined during the course of this work (discussed later) showed no sign of a mouth at sizes up to almost 1 mm in diameter. The spatangoids, also, did not develop a mouth until they attained around 0.8 mm TL. It is likely that these specimens remain in the sediment without eating for some time until a proper mouth is formed. Olson *et al.* (1993) found that early juveniles of the pencil sea urchin *Phyllacanthus imperialis* do not show any evidence of a mouth until they are 21 days old. *P. imperialis* develops through a lecithotrophic echinopluteus. Olson *et al.* (1993) argue that young urchins meet their nutritional needs from remaining stored nutrients or possibly through the uptake of dissolved organic matter (DOM). Emlet & Hoegh-Guldberg (1997) showed that post-larvae of the lecithotrophic sea-urchin *Heliocidaris erythrogramma* benefit from energy reserves from the egg. Post-larvae that developed from eggs that had been deprived from lipid stores were smaller in size than those developing from normal, lipid-rich eggs (Emlet & Hoegh-Guldberg, 1997). In the case of the planktotrophic species examined here, however, it is possible that uptake of DOM may play an important role, since nutrients are stored in eggs of planktotrophic species are unlikely to last long during development. Larvae of some species are able to take up amino acids from the water (De Burgh & Burke, 1983; Manahan *et al.*, 1983, 1990; Shilling & Manahan, 1994).

The arrangement and shape of the fascioles in the three spatangoids examined showed different patterns, which may represent different life styles once the animal

settles on the sediment. In *Spatangus raschi* a well-developed subanal fasciole is present, probably at metamorphosis, as evidenced by the small specimens collected. Gordon (1926*b*) shows that this fasciole is present in *Echinocardium cordatum* when metamorphosis is completed. Nichols (1959) shows how the subanal fasciole together with the subanal tube feet act to build a sanitary tube in many spatangoids, where all the currents generated on the surface of the test converge. Many spatangoids also build a respiratory funnel. However, according to Nichols (1959) adult *S. raschi* probably does not need these devices, since this species probably ploughs through the substratum with most of its corona exposed above the surface. Nichols (1959) argues that the sanitary device in *S. raschi* is reduced and only concerned with faecal waste. In early post-larvae, the subanal fasciole is much larger relative to the body and large subanal spines are present. It is possible that this fasciole has an important role for circulation of water and cleaning of the juvenile sea urchin, which is likely to have a burrowing life style. Even though we could not find any subanal tube foot, possibly the elongated clavulae and the very long subanal spines are sufficient to form a sanitary tube when juveniles are burrowed.

A very different situation is found in *Brissopsis lyrifera*. This species possesses a juvenile fasciole enclosing the periproct. Adult peripetalous and subanal fascioles develop later during ontogeny. The function of the juvenile fasciole is unknown, but the morphology of the clavulae differs completely from those of the subanal fasciole of *Spatangus raschi* and even from the adult fascioles (subanal and peripetalous) of *B. lyrifera*. The clavulae of the juvenile fasciole is shorter, stubbier and much wider at the tip, whereas those of *S. raschi* and *B. lyrifera* (adult fascioles) are thinner and less widened at the tip. Because of the dorsal position of the juvenile fasciole, it is possible that *B. lyrifera* post-larvae live partially buried, with the aboral region exposed and the fasciole functioning in the circulation of water and cleaning of the faecal products. Later in development, with both adult fascioles present, the animal will show the presence of the respiratory funnel and double sanitary tube described by Nichols (1959).

Hemiaster expergitus is unique among the former two species, since it does not bear any fasciole until the animal has attained 3 mm TL (Mortensen, 1907; present study). Gage *et al.* (1985) report a specimen of *H. expergitus* with 32 mm TL living

in a burrow 12 cm below the surface of the sediment, with a long oblique siphon connecting it to the surface. It is unlikely that early post-larvae can live deep in the sediment mainly because of the size and the absence of the frontal tube feet (important in the construction of a respiratory funnel - see Nichols, 1959; Chesher, 1963) and a peripetalous fasciole. Early post-larvae are likely to be shallow burrowers, burrowing deeper into the sediment as ontogeny progresses (formation of the peripetalous fasciole, frontal tube feet and increase in size).

The spines of the test of all spatangoids studied are spatulate, with those of *Hemiaster expergitus* being the most spatulate. In adults, the spatulate spines of the plastron serve as locomotory appendages. Nichols (1959) noted that these spines were not essential for descending into the substratum in two spatangoid species, *Echinocardium cordatum* and *Spatangus purpureus*. Feber & Lawrence (1976) found that the oar-shaped ventral spines around the plastron of the spatangoid *Lovenia elongata* (this species has a naked plastron) were important during the process of burrowing. In juveniles, the spatulate spines are distributed throughout the adoral and ambital regions of the test and are likely to function as locomotory, as well as digging appendages. However, very early post-larvae of *Spatangus raschi* and *Brissopsis lyrifera* do not have spatulate spines (*H. expergitus* smaller than 1 mm TL were not found). Spatulate spines develop a little later during ontogeny and if these animals are really shallow burrowers this might not be a serious problem.

Another interesting aspect is that the mouth formation and structure are similar in all spatangoids studied. The presence of the peristomial spines bending over the mouth and penicillate tube feet suggest that the mode of feeding in juveniles is similar to that of the adults (Nichols, 1959).

5.3.4. The Echinus *problem*

During the course of this study I have examined a quite large number of recently-metamorphosed specimens of the genus *Echinus*. It was not possible to distinguish between different species, despite some differences found. Adult *Echinus* species are identified based on the characteristics of the test and coronal plates and pedicellariae (Mortensen, 1927*a*).

In juveniles, the shape of the test and the coronal plates differ completely from those of adult specimens. The plates of the apical system (genitals and oculars) occupy most of the aboral surface of the test (Fig. 5.4A). The genitals and oculars also bear juvenile spines, whereas adult spines are present only on the ambitus and adoral surface on the interambulacral plates (Fig. 5.4A). Juvenile spines appear very early during the development of some sea urchins (*e.g.* Gordon, 1926*a*). Emlet (1988) notes that cidaroid juveniles possess a larger number of juvenile spines than euechinoids. The juvenile spines were, in fact, the only structure that differ substantially between specimens. It was found that in some individuals, the ramifications of these spines, which normally bear four branches at their tips, were very long and prominent. In other specimens, however, they were short and poorly developed (compare specimens of Figs. 5.4A and C). It is possible that this may represent different species, but these spines are lost with growth before other distinguishable specific characters are formed, including pedicellariae (see section 5.3.4.1 below).

Most of the remaining characteristics and general morphology of the test and spines were very similar in all specimens, making it impossible to morphologically separate different species.

5.3.4.1. Ontogenetic changes in the morphology of pedicellariae in *Echinus*

Early post-larval specimens of the genus *Echinus* presented a considerable number of ophicephalous pedicellariae on the aboral surface. In slightly larger individuals these were present also on the ambitus of the test (Fig. 5.4A) and on the adoral surface, including the buccal plates. The early presence of ophicephalous pedicellariae is common in many species and in some cases they are present even before metamorphosis takes place (Mortensen, 1921). Despite its early presence, this type of pedicellariae (Fig. 5.11D) has no value for the identification of *Echinus* species, since they show very little interspecific variation (see Mortensen, 1903, 1943). Triphyllous pedicellariae also occur, but are equally of minor importance for taxonomy (Fig. 5.11E).

Pedicellariae which show some interspecific variation among different *Echinus* species include the globiferous and tridentate (Fig. 5.11A, B and C). In general,

Figure 5.11. Pedicellariae of the genus *Echinus* (A-E). A. Adult tridentate pedicellaria of *E. acutus norvegicus*; B. Adult tridentate pedicellaria of *E. alexandri*; C. Globiferous pedicellariae of *E. alexandri*; D. Ophicephalous pedicellaria of a juvenile; E. Triphyllous (Tped) and ophicephalous (Oped) pedicellariae of a juvenile.

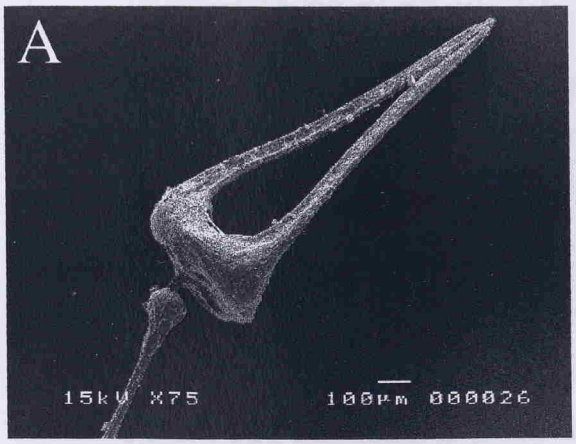
A
15kV X75
100µm 000026

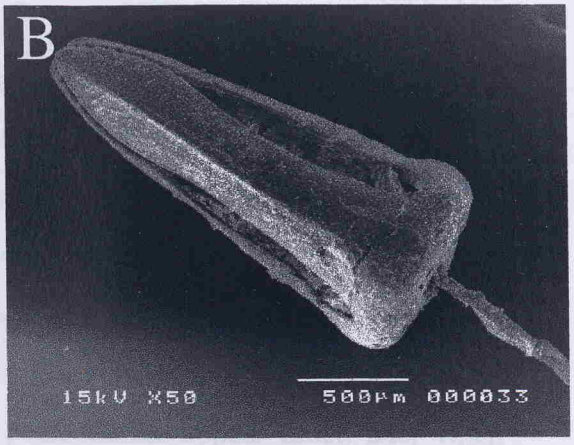
B
15kV X50
500µm 000033

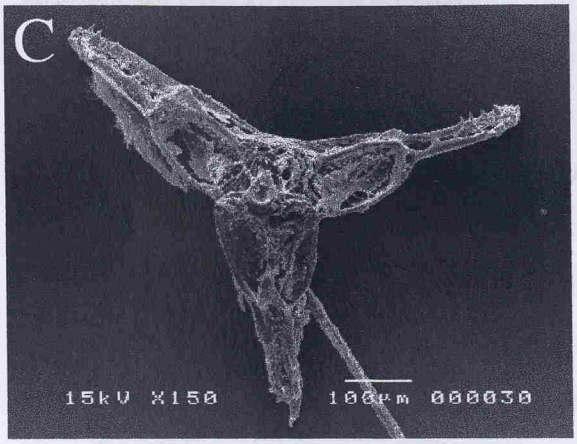
C
15kV X150
100µm 000030

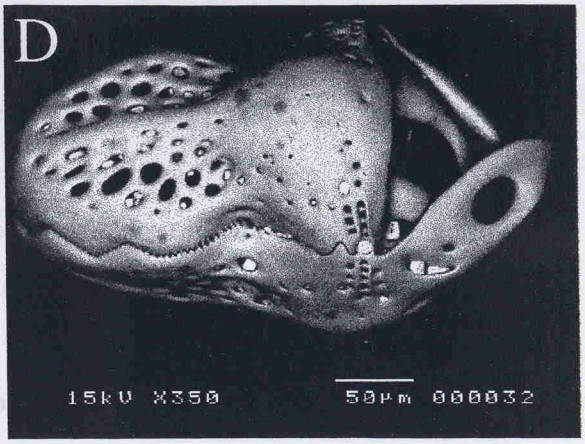
D
15kV X350
50µm 000032

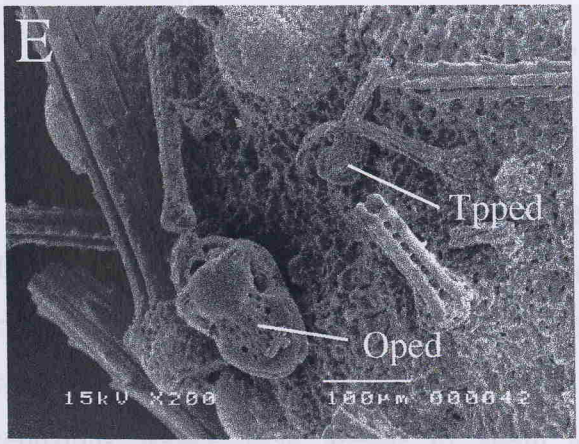
E
Tpped
Oped
15kV X200
100µm 000042

however, a combination of both kinds is needed for identification, since they often show some overlapping characteristics owing to intraspecific morphological variation. For instance, globiferous pedicellariae of *Echinus elegans* bear 2-3 teeth on either side of the blade, whereas those of *E. alexandri* have 3-4, *E. affinis* 2-3 and *E. acutus* var. *norvegicus*, 1-2 teeth (Mortensen, 1903). In juveniles, globiferous pedicellariae appear generally when the animal is around 1 mm in diameter and are not very numerous (Fig. 5.10A). Tridentate pedicellariae appear much later when animals are over 15 mm in diameter.

A further problem concerning the use of pedicellariae for the identification of juvenile *Echinus* is that evidence suggests that these structures undergo ontogenetic changes concomitantly with the development of the test. Table 5.1 shows that globiferous pedicellariae increase in size as ontogeny progresses. The same appears to be true for the ophicephalous pedicellariae. In the globiferous type, however, pedicellariae appear to be increasing in size continuously and, even in individuals with a test diameter of 15 mm, these pedicellariae do not appear to have attained full size. In adults, globiferous pedicellariae appear to reach larger sizes (Mortensen, 1903, 1928-51). Figure 5.12 shows that not only the size, but also other characteristics may change with growth. In smaller globiferous pedicellariae, the blade is shorter and only one tooth is present on each side (Fig. 5.12A). In larger individuals, the blade is longer and one or two teeth may be present in the same individual (Fig. 5.12B and C). The ontogenetic changes in the morphology of globiferous pedicellariae suggest these structures are not reliable indicators of taxonomic affinities at least in juveniles of the genus *Echinus*.

In contrast, ophicephalous pedicellariae appear to show more ontogenetic variation in size than in the overall shape. In addition, these structures probably attain full size earlier than the globiferous type. An *Echinus* juvenile at 6.5 mm in diameter showed ophicephalous pedicellariae measuring 245 μm in length, whereas an individual at 15 mm in diameter had pedicellariae measuring only 255 μm in length.

Table 5.1. Size of globiferous and ophicephalous pedicellariae in *Echinus* juveniles.

Test Diameter (mm)	Globiferous Length (μm)*	Test Diameter (mm)	Ophicephalous Length (μm)**
1.00	100	0.78	65
1.20	125	1.00	84
1.43	104	1.00	95
3.80	200	6.50	245
6.50	230	15.00	255
15.00	470	---	---

* Total length of one valve
** Length of the blade, not including the handle at the base of the pedicellaria

5.3.4.2. Possible reasons for the similarity among *Echinus* post-larvae

As already mentioned earlier in this chapter, the NE Atlantic Ocean around the British Isles is shared by five species of the genus *Echinus*, with overlapping distributions on the shelf and slope. All species show seasonality in reproduction, with the production of a planktotrophic echinopluteus. There appears to be, however, a different time of spawning for some species (Tyler *et al.*, 1995*a*). Nevertheless, it seems likely that juveniles of such species co-occur in the sediment. The study of the post-larval morphology revealed a high morphological similarity among all individuals examined, with only slight differences in the shape of juvenile spines. Why then are all juveniles so similar to each other?

The number of different species of *Echinus* examined in the samples cannot be determined. However, it seems that at least two were present. The difficulty in distinguishing these post-larvae is great even in specimens with very well-known life cycles. MacBride (1903) stresses that he could not identify with certainty small sea urchins dredged in the Plymouth Sound. This was not possible even though they belong to different genera (*Echinus esculentus* and *Psammechinus miliaris*, as *Echinus miliaris*).

A further problem to this question is that some species of *Echinus* are known to form hybrids (Shearer *et al.*, 1914; Hagström & Lønning, 1961). Shearer *et al.* (1914) show that post-metamorphosed hybrids of *E. esculentus* and *E. acutus flemingii* have intermediate morphological characteristics. Deep-sea species like *E. alexandri*, *E.*

Figure 5.12. Valves of globiferous pedicellariae of juveniles of the genus *Echinus*. Note the difference in size and the variability on teeth number. B and C from the same specimen.

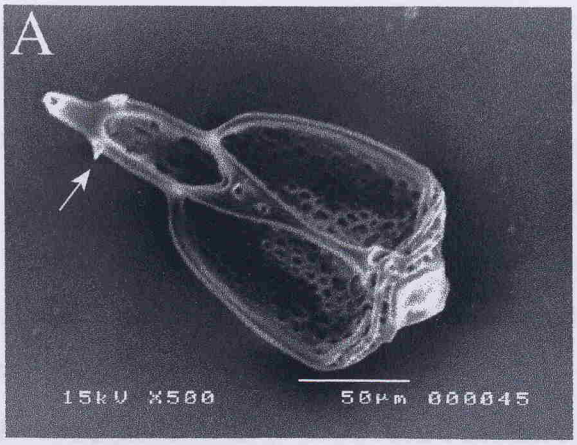
A
15kV X500
50µm 000045

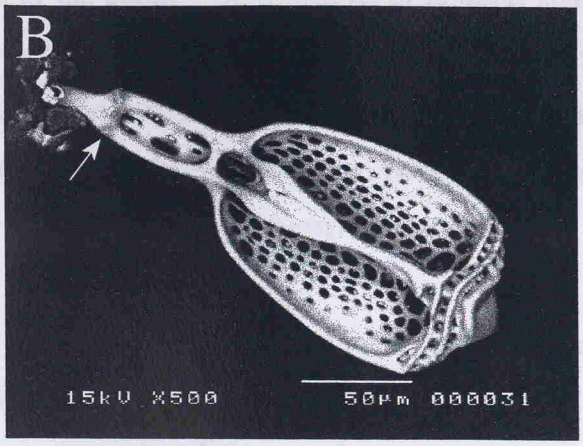
B
15kV X500
50µm 000031

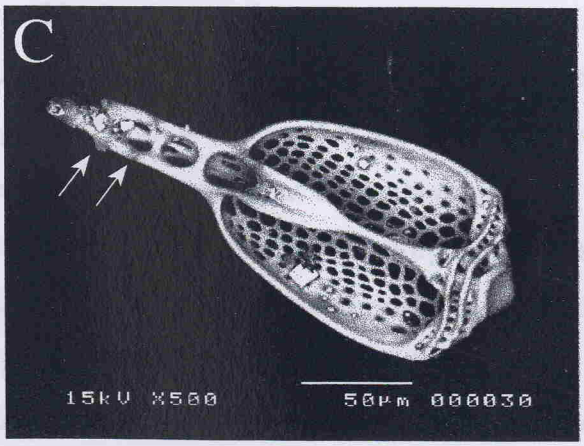
C
15kV X500
50µm 000030

elegans and *E. acutus norvegicus* spawn during similar periods and may form hybrids. This would compound yet more problems for the identification of juveniles. It is interesting that, despite having differentiated morphologically, some of the *Echinus* species of the British Isles did not evolve any kind of reproductive barrier, like for instance, the gamete incompatibility found in the Indo-Pacific sea urchins of the genus *Echinometra* (Metz *et al.*, 1991).

The similarity among juvenile stages may also be related to the probably relative recent speciation of the genus. Fossil records of *Echinus* start appearing in Pliocene deposits (c.a. 2-5 mya) (Mortensen, 1943). Tyler *et al.* (1995*a*) suggest that the cosmopolitan distribution of the genus is related to the variation in hydrographic events associated with the glacial/interglacial periods. The absence of a reproductive barrier for some species (discussed above) also points to the closer relations among these species (in the NE Atlantic).

Tyler *et al.* (1995*a*) argue that the distribution and speciation in the North Atlantic (centre of distribution of the genus - Clark, 1912; Mortensen, 1943) may be related to the pressure adaptation of embryos, enabling the genus to invade deeper areas. Evidence suggests this process is taking place in the species *E. acutus*, generating a shallow and a deep water forms, with larvae exhibiting different pressure tolerances (Tyler & Young, 1998). It is likely that the selective pressures acting on the speciation of the genus are operating at the embryonic/larval and/or adult period. It seems clear also that the early post-larval morphology has been preserved as a "winning combination", essential for the survival in the sediment during the early stages of life. A similar result was reported by Dixon & Dixon (1996) for hydrothemal vent shrimps. Dixon & Dixon (1996) could not distinguish between three genera of vent shrimp post-larvae morphologically despite being genetically different. This may reflect the need of a particular set of morphological characteristics in order to be successful in a particular environment.

We cannot, however, rule out the possibility of changes in the physiology of post-larval stages enabling them to survive in deeper areas. Studies on the pressure tolerances of early post-larvae would be interesting to test whether their tolerance would prevent or not the colonization of deep-sea areas. Embryos of a number of echinoid species seem to resist high hydrostatic pressures (Marsland, 1938, 1950;

Young, 1996) and Young *et al.* (1995) point out that larvae would not be prevented from invading depths as great as 2000 m (see also Young *et al.*, 1997*a*; Tyler & Young, 1998). At the same time, pressure tolerances of larvae of some species appear to set the bathymetric range of conspecific adults (Young & Tyler, 1993; Young *et al.*, 1996*a*). If evolution in the genus *Echinus* is operating as a way of preserving the early morphology, this would explain why different species have such similar early post-metamorphic morphologies.

Chapter Six - Reproduction, dispersal, settlement and carbon demands of the bathyal ophiuroid Ophiocten gracilis *in the NE Atlantic*

6.1. Introduction

Five species of the brittle star genus *Ophiocten* are found in the North Atlantic, Mediterranean and Arctic Ocean. Early confusion in the taxonomy of this genus was clarified by Paterson *et al.* (1982). *O. sericeum* is an Arctic species, in predominantly shallow water, but occurring as deep as 2000 m. *O. abyssicolum* is present from the Mediterranean Sea at depths below 100 m to south-west Ireland where it has been found between 300-1000 m depth. *O. hastatum* inhabits the deeper part of the eastern Atlantic from 1130 to 4700 m depth whilst *O. centobi* is known from the Bay of Biscay at 2420 m depth (Paterson *et al.*, 1982). The most common deep water species is *O. gracilis*, which occupies upper slope depths in the temperate North Atlantic.

Ophiocten gracilis is a small brittle star (max. disk diameter ca. 12 mm) probably present throughout the North Atlantic at depths of 600-1200 m. It was formerly considered a 'warm water' variety of *O. sericeum* (*O. sericeum gracilis*) (Grieg, 1903; Mortensen, 1933; Semenova *et al.*, 1964), but its specific status was clearly stated by Paterson *et al.* (1982), based on morphological characteristics and geographical and bathymetric distribution.

Populations of *Ophiocten gracilis* are well-developed on the eastern side of the North Atlantic at depths between 800-1000 m, where densities can be as high as 800 m^{-2} (Piepenburg & von Juterzenka, 1994; Lamont & Gage, 1998). The larva, *Ophiopluteus ramosus* (Tyler & Gage, 1982*b*), occurs in the North Atlantic during spring and summer months. Geiger (1963) reported *O. ramosus* east of Newfoundland and Flemish Cap during the spring whilst Semenova *et al.* (1964) found *O. ramosus* in the Norwegian and Barents Seas. A slightly longer period of occurrence of this larva is reported by Tyler & Gage (1982*b*), extending from February to September in the Rockall Trough area. Post-larvae of *Ophiocten gracilis* have been shown to settle over a wide bathymetric range, even in the deeper areas of the Rockall Trough, where the juveniles do not survive to the next year (Gage & Tyler, 1981*a*). This mortality represents a large wastage of dispersal stages for this

species.

The events occurring after the settlement of *Ophiocten gracilis* post-larvae, as well as for most (if not all) other deep-sea invertebrate juvenile stages, are virtually unknown, as the assessment of mortality and other ecological parameters often require studies at time scales of days or less (Stoner, 1990; Rowley, 1990; Gosselin & Qian, 1996). This is very difficult in deep-sea areas. In fact, most studies reporting the ecology of juvenile stages were undertaken in the intertidal zone or shallow subtidal (see Gosselin & Qian, 1997 for review). However, knowledge of rates of mortality and growth are of great importance for recruitment studies and the maintenance of populations in specific areas. The early post-metamorphic stages in some species are known to suffer a dramatic mortality during the first day of benthic life (Gosselin & Qian, 1997; Hunt & Scheibling, 1997).

Individuals of *Ophiocten gracilis* settle as small juveniles after metamorphosis in the water column. Therefore, processes occurring during the early benthic life must have a large impact in the distribution and abundance of the adult populations. This might explain the preclusion of this species in deeper areas where the supply of post-larvae is common. Despite their presence in the water column and sediments during spring and summer months (Gage & Tyler, 1981*a*; Tyler & Gage, 1982*b*; Piepenburg & von Juterzenka, 1994; Flach & Heip, 1996), very little is known about the biology and ecology of juvenile stages of this species. The post-metamorphic ontogenesis of *O. gracilis* is described in chapter 3. The presence of larval and post-larval stages in the water column during specific months denotes a seasonality in the reproduction. However, gametogenesis of *O. gracilis* has not been described previously.

In this chapter we describe the gametogenesis of *Ophiocten gracilis* and analyse the growth of newly-settled post-larvae, based on individuals collected with sledges and trawls, and weekly samples taken by sediment traps, respectively. Sediment trap samples provided an unique opportunity to estimate the carbon demands required during the early growth after settlement, together with a visual analysis of the stomach contents of individuals. The recruitment and possible causes of the widespread allopatric settlement are discussed.

6.2. Reproductive biology

Both males and females showed a similar pattern in gonad development (Fig. 6.1). The animals were ripe in February presenting well-developed gonads. In April all the animals started to develop gonads, probably after a major spawning period. Gonads continued to mature during mid-spring through autumn. These data show a distinctive seasonal pattern in reproduction, with a synchronous spawning occurring in the early months of the year.

Examination of early post-larval stages showed that developing gonads were found in individuals as small as 1.4 mm dd. In these animals even the sex could be determined. Germinal cells were recognised in a post-larva only 1 mm dd.

Fecundity values were similar for 3 of the 4 brittle stars examined, with the highest value of 50,820 eggs ind^{-1} (Table 6.1). The fourth individual presented the lowest value of 23,166 eggs ind^{-1} and was also the animal with the smallest disk diameter. The mean fecundity for all the females measured was 40,356 eggs ind^{-1} (SD=11,997). All the individuals measured were at the same reproductive stage III and showed similar egg sizes (Table 6.1). At this stage the oocytes start to accumulate yolk and present a pale cytoplasm with a large eccentric germinal vesicle (Tyler, 1977).

Table 6.1. Fecundity and egg size of specimens of *Ophiocten gracilis*.

DD (mm)	Fecundity (total No eggs)	Mean egg size (μm)	Max. egg size (μm)	Stage of Development (M.I)
6.72	23166	56.55 (*SD=12.52*)	82.38	III
7.53	45165	***	***	III
8.19	42273	49.86 (*SD=12.09*)	80.02	III
8.24	50820	58.61 (*SD=9.15*)	77.5	III

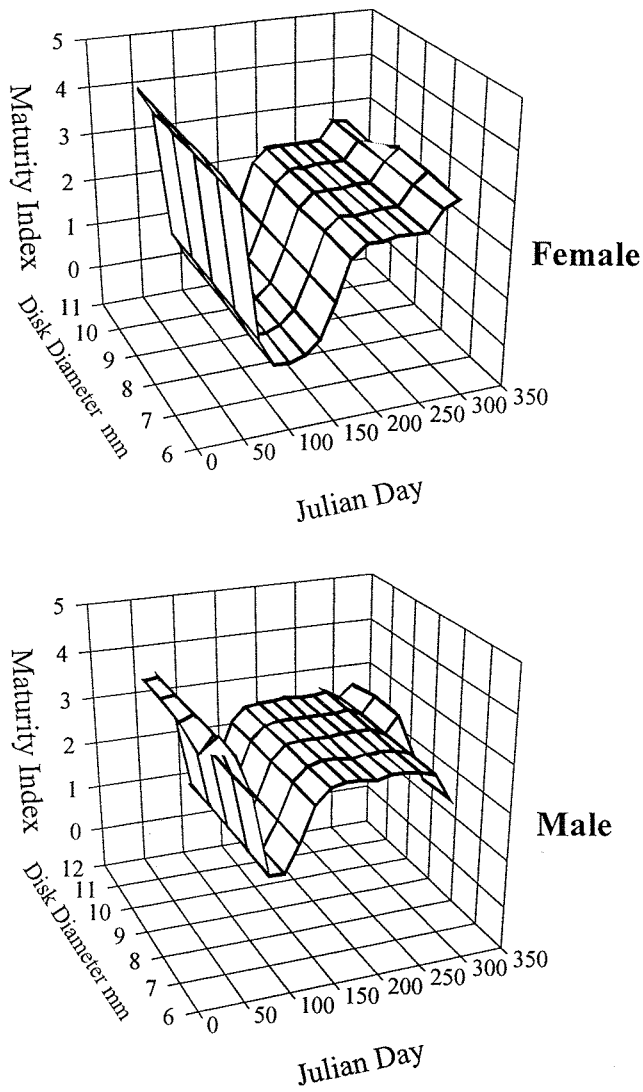

Figure 6.1. Changes in the maturity index of the gonads of *Ophiocten gracilis* with time of both males (n=33) and females (n=32) of different sizes.

6.3. Growth of the early post-larva

Settlement occurred in both traps during mid-May. The mean disk diameter was 0.66 mm (SD=0.06) for the 1000 m trap and 0.69 mm (SD=0.08) for the 1400 m trap (Fig. 6.2). It is assumed that a large number of post-larvae settled in the cone and in the baffle of the trap and grew during the period of collection and, from time to time, a number of individuals fell into the cup, being immediately killed by the

preservative present. Therefore, the increasing mean disk diameter observed during the period reflects the growth of the organisms in the cone and/or baffle. Several lines of evidence suggest growth on the traps (see section 6.7.2).

In order to test differences in mean disk diameter in the two traps, a t-test was applied. For days 149.5 and 156.5 a Mann-Whitney U-test was employed since the data did not pass the Kolmogorov-Smirnov test for normality and the test for homogeneity of variances. The mean disk diameter of the organisms collected during day 142.5 (mid-point of the sampling interval) was not statistically different for both traps at 1000 and 1400 m depth ($t=-0.78$, $p=0.44$, $n_1=4$, $n_2=345$). However, those values were significantly different for days 149.5 ($U'=18530$, $p=<0.0001$, $n_1=195$, $n_2=1156$), 156.5 ($U'=76$, $p=<0.0001$, $n_1=64$, $n_2=84$) and 212.5 ($t=4.92$, $p=<0.0001$, $n_1=11$, $n_2=10$), being smaller in the deeper trap. Values for day 198.5 ($t=0.75$, $p=0.47$, $n_1=11$, $n_2=4$) were not significantly different, whereas for days 170.5 and 177.5 only two and one individuals were collected in the 1400 m trap, respectively. For the rest of the sampling period (days 163.5, 184.5, 191.5 and 205.5) comparison was not possible owing to the lack of data on either trap.

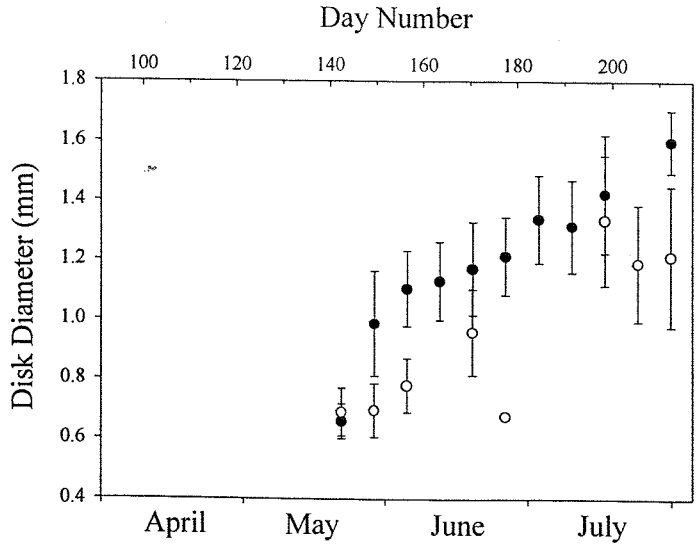

Figure 6.2. Mean changes in disk diameter of post-larval *Ophiocten gracilis* collected in the sediment traps. Numbers collected during each sampling period are listed in Table 6.6. Filled circles are 1000 m trap; open circles are 1400 m trap. Error bars are standard deviation.

6.4. Settling rates

The results of the single analysis of variance (ANOVA) to test differences in settling times of different size post-larvae showed that for 2°C, 10°C and 15°C no significant differences were found (Table 6.2). For 5°C however, results were significantly different with animals at 0.91 mm dd settling faster (558.84 m day^{-1}) than the 2 smaller size classes individuals (497.30 and 474.92 m day^{-1}) (Tables 6.2 and 6.4; Fig. 6.3).

Table 6.2. One-way analyses of variance testing differences in settling times of different size post-larvae of *Ophiocten gracilis* (0.63, 0.79 and 0.91 mm feret dd) at 4 temperatures.

Temperature (°C)	Source of variation	d.f.	SS	MS	*F*	p
2	Between groups	2	14796.84	7398.421	2.218	0.134
	Within groups	21	70058.8	3336.133		
5	Between groups	2	23662.05	11831.02	3.390	0.052
	Within groups	22	76782.64	3490.12		
10	Between groups	2	1630.744	815.372	0.299	0.745
	Within groups	23	62754.22	2728.444		
15	Between groups	2	6521.625	3260.812	1.084	0.355
	Within groups	23	69214.99	3009.347		

The comparison of the settling rates of each size class at different temperatures showed mixed results. No difference was found in the 0.63 mm mean feret diameter size class (Table 6.3). This group presented a high variance in settling times and the mean settling rate (pooled data) was of 524.02 m day^{-1} (SD=75.56, n=40).

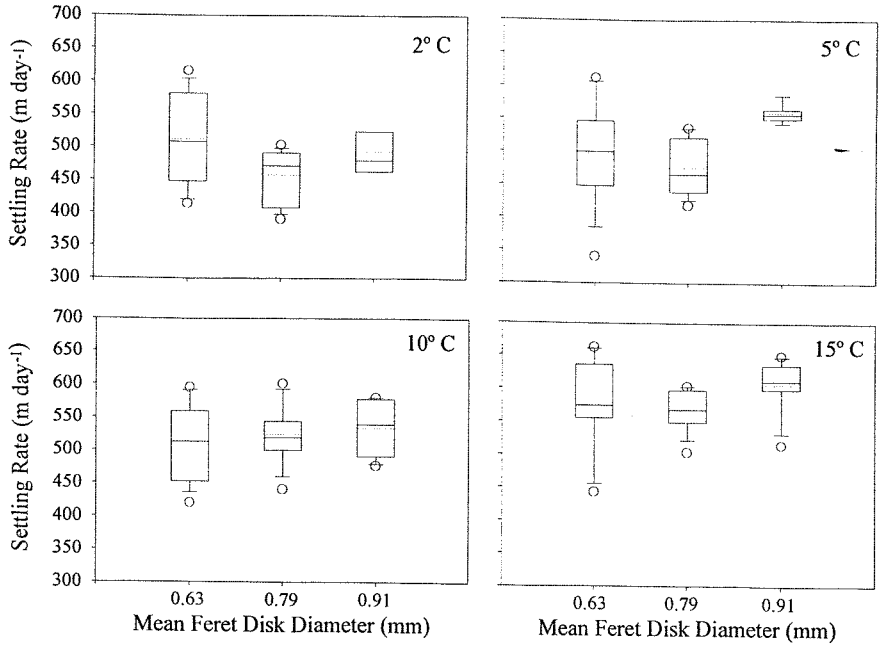

Figure 6.3. Settling rates of post-larvae of *Ophiocten gracilis* at different temperatures. Each box encloses the middle 50% of measurements. The median value is marked by a horizontal continuous line and the mean by a dashed line within the box. Bars above and below each box enclose the 95th and 5th percentiles. Measurements lying outside the 5th and 95th percentiles are plotted as small, open circles.

Table 6.3. One-way analyses of variance testing differences in settling times of post-larvae of *Ophiocten gracilis* at 4 temperatures (2, 5, 10 and 15°C).

Mean Feret Disk Diameter (mm)	Source of variation	d.f.	SS	MS	F	p
0.63	Between groups	3	34997.66	11665.89	2.238	0.101
	Within groups	36	187687.7	5213.547		
0.79	Between groups	3	69560.93	23186.98	13.399	6.2E-06
	Within groups	34	58833.08	1730.385		
0.91	Between groups	3	36780.48	12260.16	7.214	0.002
	Within groups	19	32289.88	1699.468		

A significant difference in settling rates was observed for the 0.79 and 0.91 mm mean feret dd size classes (Table 6.3; Fig. 6.4). In these groups there was observed a decrease in settling rates with increasing water temperatures. For the 0.79 mm feret dd size class, the mean settling rate was 457.28 (SD=41.60, n=10, 2°C), 474.92 (SD=43.88, n=10, 5°C), 523.48 (SD=47.14, n=9, 10°C) and 567.13 m day^{-1} (SD=31.91, n=9, 15°C). In the 0.91 mm size class, the values were 493.15 (SD=48.17, n=4, 2°C), 558.84 (SD=15.95, n=5, 5°C), 533.25 (SD=45.26, n=7, 10°C) and 605.88 m day^{-1} (SD=44.75, n=7, 15°C) (Table 6.4; Fig. 6.4).

Table 6.4. Mean settling rates (± SD) of *Ophiocten gracilis* of different sizes at different temperatures.

Mean Feret Disk Diameter (mm)	Temperature (°C)	*n*	Settling Rate ± SD (m day^{-1})
0.63	2	10	511.19 ± 72.66
	5	10	497.30 ± 80.58
	10	10	513.47 ± 60.26
	15	10	574.12 ± 73.83
0.79	2	10	457.28 ± 41.60
	5	10	474.92 ± 43.88
	10	9	523.48 ± 47.14
	15	9	567.13 ± 31.91
0.91	2	4	493.15 ± 48.17
	5	5	558.84 ± 15.95
	10	7	533.25 ± 45.26
	15	7	605.88 ± 44.75

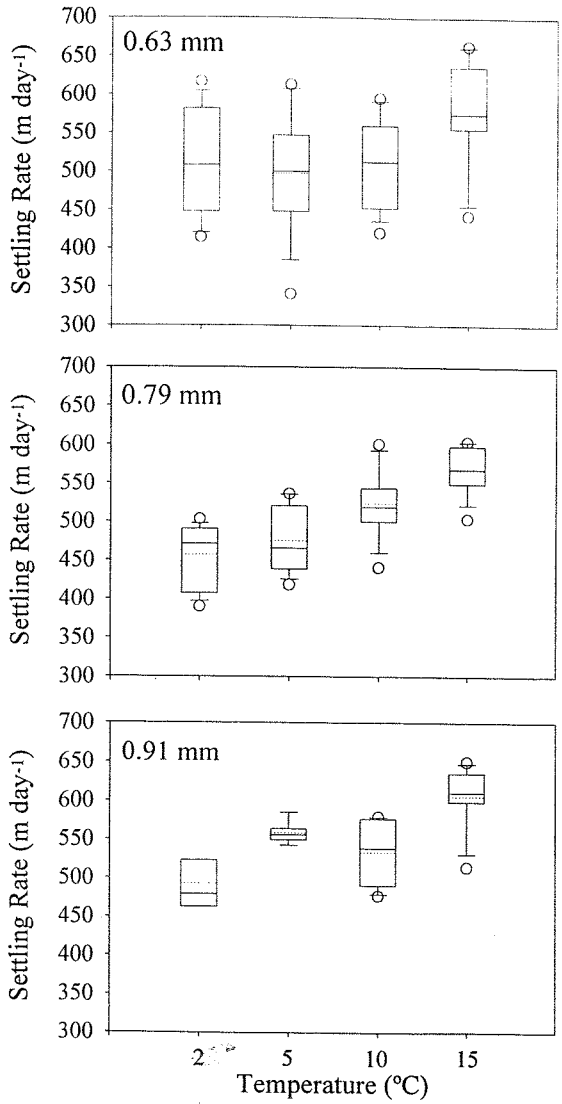

Figure 6.4. Settling rates of post-larvae of *Ophiocten gracilis* of different sizes at 2, 5, 10 and 15°C. See figure 6.3 for explanation.

6.5. Stomach contents

The qualitative analysis of the stomach contents of post-larvae of *Ophiocten gracilis* collected in the two sediment traps revealed the predominance of detritus and foraminifera among the specimens. The number of animals showing empty stomachs was also very high (Table 6.5), but this may have been partially caused by regurgitation. Note that the presence of forams and detritus was not mutually exclusive and a large number of animals presented both items in the stomach. Large

forams were probably more easily removed from the stomach by the regurgitation action than detritic material.

The number of individuals with stomachs containing detritus varied from none (days 142.5 and 149.5) to more than 80% (day 212.5) in the 1000 m trap. In the 1400 m trap, the percentage of organisms with detritus in the stomach was also higher during the later sampling periods (Table 6.5; Fig. 6.5).

In the 1000 m trap, the number of organisms with forams present in the stomach was always higher than 15%, with a maximum of around 55% in day 156.5. The average number in this trap was around 32%. In the 1400 m trap, an average of about 16% of the organisms had forams in their stomachs, with a maximum of 25% (Table 6.5).

In both traps, between 50 and 60% of the animals on average had empty stomachs, with the larger values present in the earlier sampling periods. In some samples the numbers were as high as 85% (Fig. 6.5).

Table 6.5. Percentage of the collected post-larvae of *Ophiocten gracilis* presenting a particular kind of food. Numbers in parentheses are total number of organisms with the specific food type. NI = Not Identified material.

1000m Trap											
Day Number	**142.5**	**149.5**	**156.5**	**163.5**	**170.5**	**177.5**	**184.5**	**191.5**	**198.5**	**205.5**	**212.5**
Forams	25.00 (1)	35.90 (70)	54.69 (35)	42.86 (15)	36.36 (8)	49.12 (28)	16.67 (1)	20.83 (10)	18.18 (2)	---	18.18 (2)
Detritus			32.81 (21)	31.42 (11)	72.73 (16)	50.88 (29)	50.00 (3)	47.92 (23)	45.45 (5)	---	81.82 (9)
Empty	75.00 (3)	72.31 (141)	60.94 (39)	62.86 (22)	27.27 (6)	49.12 (28)	50.00 (3)	52.08 (25)	54.55 (6)	---	18.18 (2)
Polychaeta	---	0.51 (1)	---	---	---	---	---	2.08 (1)	---	---	---
Eggs	---	0.51 (1)	---	---	---	---	---	---	---	---	---
NI	---	1.54 (3)	---	---	---	---	---	---	---	---	---
No Total ind.	4	195	64	35	22	57	6	48	11	---	11
1400m Trap											
Day Number	**142.5**	**149.5**	**156.5**	**163.5**	**170.5**	**177.5**	**184.5**	**191.5**	**198.5**	**205.5**	**212.5**
Forams	25.22 (87)	12.11 (140)	15.48 (13)	---	---	---	---	---	---	---	10.00 (1)
Detritus	28.69 (99)	17.73 (205)	8.33 (7)	---	50.00 (1)	100.00 (1)	---	---	75.00 (3)	60.00 (3)	50.00 (5)
Empty	65.80 (227)	79.50 (919)	85.71 (72)	---	50.00 (1)	---	---	---	25.00 (1)	40.00 (2)	50.00 (5)
Polychaeta	0.29 (1)	---	1.19 (1)	---	---	---	---	---	---	---	---
NI	0.29 (1)	---	---	---	---	---	---	---	---	---	---
No Total ind.	345	1156	84	---	2	1	---	---	4	5	10

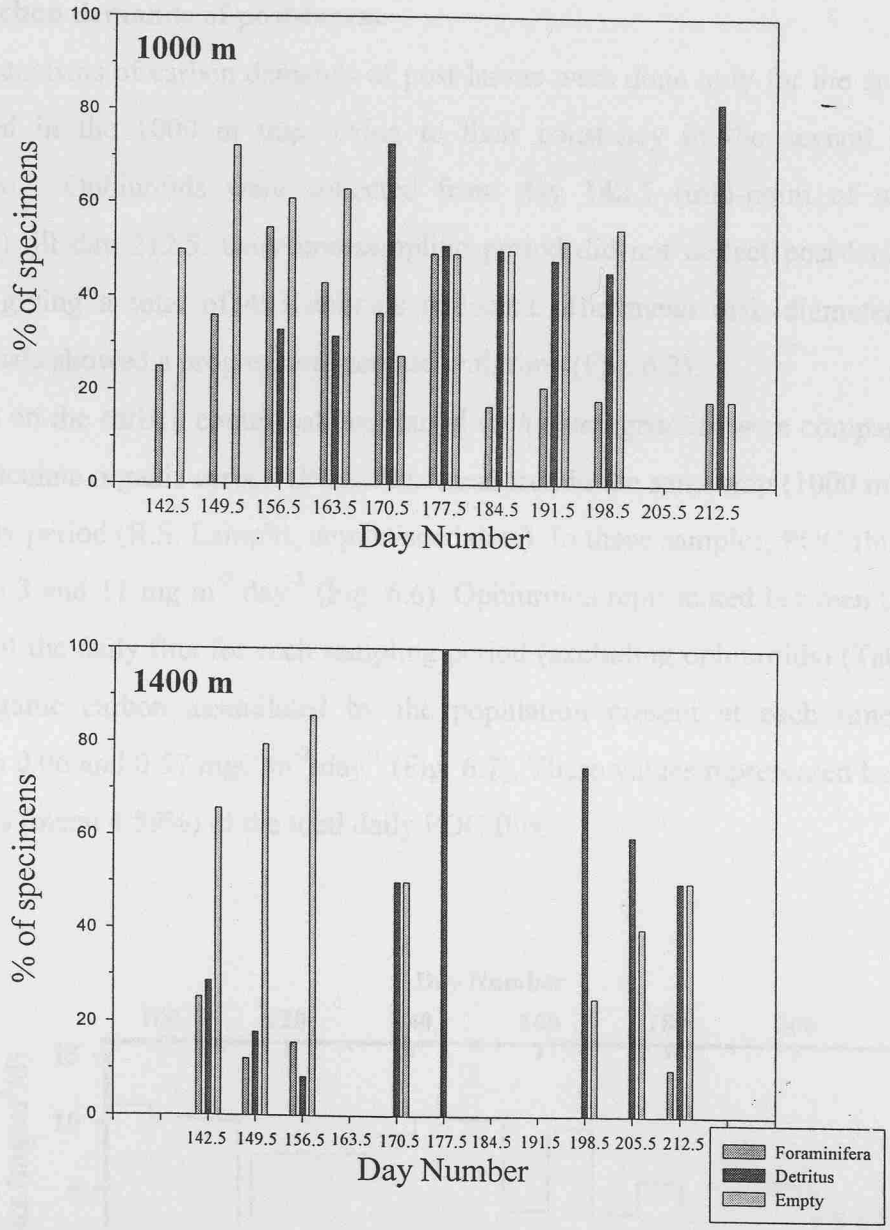

Figure 6.5. Percentage of the total number of *Ophiocten gracilis* post-larvae collected in each sampling interval with a determinate type of food within the stomach for the top and bottom sediment traps.

From all the animals examined, a few presented stomach contents other than forams and detritus or material not identified. These include 5 post-larvae with a

polychaete and 1 post-larva with eggs of an unknown species.

6.6. Carbon demands of post-larvae

The analysis of carbon demands of post-larvae were done only for the specimens collected in the 1000 m trap owing to their constancy in the several samples collected. Ophiuroids were collected from day 142.5 (mid-point of sampling interval) till day 212.5. Only one sampling period did not collect post-larvae (day 205.5) giving a total of 453 animals collected. The mean disk diameter of the individuals showed a progressive increase with time (Fig. 6.2).

Data on the carbon content of post-larval *Ophiocten gracilis* were compared with the particulate organic carbon (POC) flux measured in the same trap (1000 m) during the study period (R.S. Lampitt, unpublished data). In these samples, POC flux varied between 3 and 11 mg m^{-2} day^{-1} (Fig. 6.6). Ophiuroids represented between 0.07 and 7.32% of the daily flux for each sampling period (excluding ophiuroids) (Table 6.6). The organic carbon assimilated by the population present at each time varied between 0.06 and 0.57 mgC m^{-2} day^{-1} (Fig. 6.7). These values represented between 1 and 11% (mean 4.59%) of the total daily POC flux.

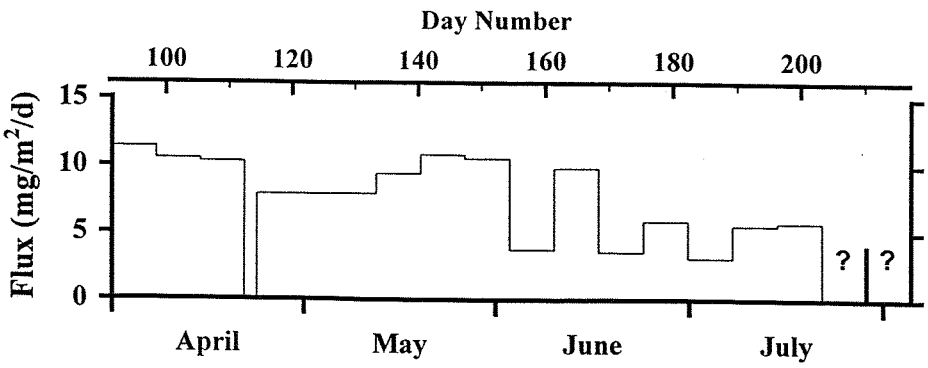

Figure 6.6. Flux of Particulate Organic Carbon (POC) during the study period for the 1000 m trap. Data for the last 2 sampling periods are not available (R.S. Lampitt, unpublished data).

Table 6.6. Percentage of the POC flux (only for the 1000 m trap) consumed by post-larval *Ophiocten gracilis* assuming (1) 3/7 P/R ratio and (2) observed mean changes in AFDW. dd is the disk diameter. Note also the number of specimens collected in the 1400 m trap.

Day Number	POC Flux ($mgC\ day^{-1}$) (1000 m)	Number specimens (1000 m)	Number specimens (1400 m)	Mean dd ± SD (mm)	% Flux Represented by Ophiuroids	% Flux Used by Ophiuroids (1)	% Flux Used by Ophiuroids (2)
142.5	10.78	4	345	0.66±0.06	0.07	3.34	8.24
149.5	10.52	195	1156	0.99±0.18	6.59	5.42	9.79
156.5	3.75	64	84	1.10±0.13	7.32	10.13	16.72
163.5	9.79	35	***	1.13±0.13	1.61	2.96	4.77
170.5	3.56	22	2	1.17±0.16	3.02	7.3	11.19
177.5	5.84	57	1	1.21±0.13	5.09	3.77	5.78
184.5	3.11	6	***	1.34±0.15	1.26	4.82	7.01
191.5	5.52	48	***	1.31±0.16	5.51	2.54	3.61
198.5	5.74	11	4	1.42±0.20	1.5	1.05	1.26
205.5	***	***	5	***	***	***	***
212.5	***	11	10	1.60±0.10	***	***	***

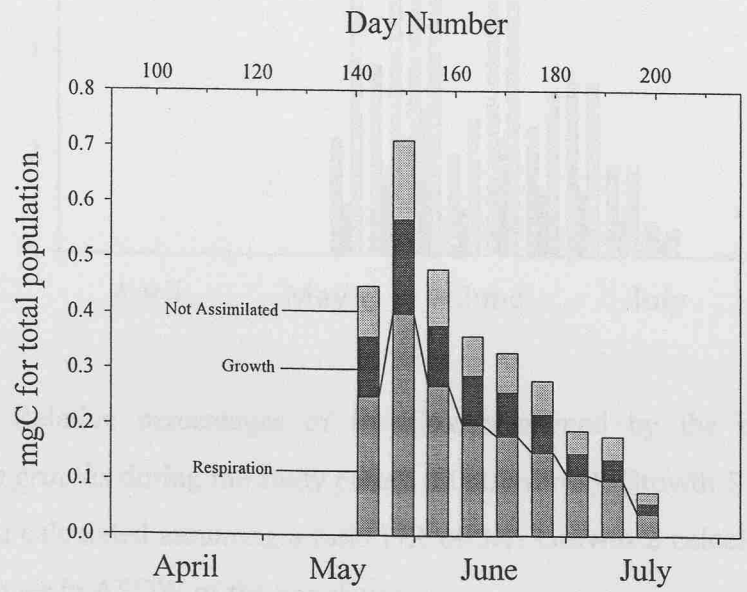

Figure 6.7. Estimates of the total amount of carbon consumed by the *Ophiocten gracilis* population assuming a ratio P/R of 3/7 and assimilation efficiency of 80%. The respiration component represents a real loss of organic carbon within the trap (1000 m).

Results based on the calculation of somatic production from changes in AFDW yield different results. The change in mean AFDW with time is described by a linear regression with equation:

AFDW = 0.0014 DN - 0.1706 (r^2 = 0.9416), where DN=Day Number.

The results showed that a higher demand for carbon is necessary for the animals in order to attain the weights found in the samples, than that calculated based on weight-specific respiration rates (Fig. 6.7). In fact, between around 1 and 17% (mean 7.60%) of the carbon flux would be necessary to account for the changes in AFDW of the population (Table 6.6).

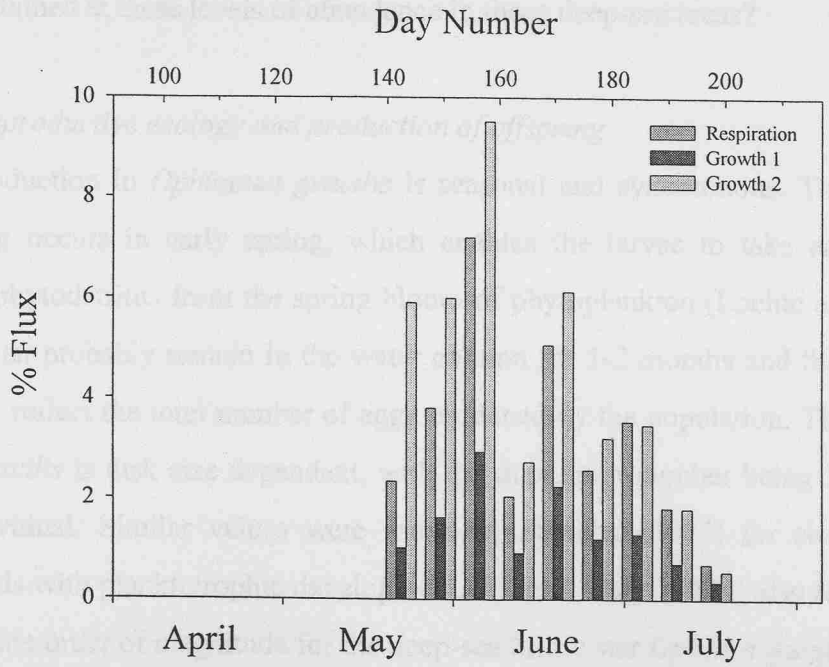

Figure 6.8. Relative percentages of the flux consumed by the post-larvae of *Ophiocten gracilis* during the study period (1000 m trap). Growth 1 represents the production calculated assuming a ratio P/R of 3/7. Growth 2 calculated based on mean changes in AFDW of the population.

6.7. Discussion

Populations of *Ophiocten gracilis* are well-developed at depths of around 800-1000 m on the upper slope of the North Atlantic. Off the east coast of the USA and Canada, this species was described as *Ophioglypha signata* (Verrill, 1882), but it was

later assigned as *Ophiocten gracilis* (Paterson *et al.*, 1982). The Flemish Cap, off Newfoundland, appears to be the source population for the larvae and post-larvae collected in the plankton by Geiger (1963) and Semenova *et al.* (1964).

On the east side of the North Atlantic at upper slope depths of the Rockall Trough area, the population density of *Ophiocten gracilis* reaches 800 ind m^{-2} (Lamont & Gage, 1998). Piepenburg & von Juterzenka (1994) estimated a maximum density of 497 ind m^{-2} in the Kolbeinsey Ridge, north of Iceland, and biomasses up to 120 mg AFDW m^{-2}. Such an abundance and biomass imply this species as one of the most conspicuous members of the megabenthos and, probably, with no less importance for the structure of the benthic community. The main question is how such populations are maintained at these levels of abundance in those deep-sea areas?

6.7.1. Reproductive ecology and production of offspring

Reproduction in *Ophiocten gracilis* is seasonal and synchronous. The period of spawning occurs in early spring, which enables the larvae to take advantage of sinking phytodetritus from the spring bloom of phytoplankton (Lochte *et al.*, 1993). Larvae can probably remain in the water column for 1-2 months and their numbers probably reflect the total number of eggs produced by the population. The fecundity of *O. gracilis* is disk size dependent, with the maximum number being 50,820 eggs per individual. Similar values were found by Hendler (1975) for shallow water ophiuroids with planktotrophic development. Tyler & Gage (1980) also report values of the same order of magnitude for the deep-sea brittle star *Ophiura ljungmani*. If the *O. gracilis* mean fecundity per individual (Table 6.1) is multiplied by population density (800 ind m^{-2}, Lamont & Gage, 1998), assuming a sex ratio of 1:1, a total population fecundity of ~16 million eggs m^{-2} is achieved. The high abundance and, therefore, the close proximity between individuals would probably lead to a high rate of fertilization success (Pennington, 1985), with a large production of embryos and larvae.

Ophioplutei (*Ophiopluteus ramosus*) and post-larval *Ophiocten gracilis* are common in the surface plankton of the North Atlantic during spring and summer months (Mortensen, 1901; Geiger, 1963; Semenova *et al.*, 1964; Tyler & Gage 1982*b*). Semenova *et al.* (1964) reported densities up to 1000 larvae m^{-3}, representing

around 80% of all the zooplankton sampled. The upward vertical migration to surface waters seems to pose no obstacles to these animals. Spawning in this species occurs early in spring which may be an adaptation for the larvae to reach the surface layers before seasonal stratification of the water column. Young *et al.* (1996*c*) suggest that long vertical migrations for deep-sea urchin larvae are more likely to be limited by physiological tolerances than by energy stores. Ascending in a cooler water column would also conserve energy through a lower metabolic rate (Young *et al.*, 1996*c*). Other larvae of deep-sea benthic invertebrates are known to perform such a migration (Killingley & Rex, 1985; Bouchet & Warén, 1994).

6.7.2. Metamorphosis and settlement: revisiting the non-viable settlement of Ophiocten gracilis

Metamorphosis takes place in the water column and post-larvae will probably settle randomly affected by advective processes in the subsurface water column. The high abundance of the larval stage were also observed for post-larvae. In sediment traps, densities reached 3,214 post-larvae m^{-2}, during a single settlement period. Although mortality is likely to be high during these stages, the high population fecundity is reflected in terms of numbers settling on the bottom.

However, not all post-larvae settle close to the adult population and many benthic post-larvae settle outside the depth range of the species (Gage & Tyler, 1981*a*). Post-larval *O. gracilis* were collected in a trap moored at 4500 m depth in the Porcupine abyssal plain (not included herein). Early juveniles were also collected at shelf depths round the Faroe Islands (Chapter 3; Tyler *et al.*, *in prep.*). These data show that post-larvae are spread not only over a large bathymetric range, but also over a large geographical area. We do not know the source population for these post-larvae, but we cannot rule out the possibility of larvae being carried by the Gulf Stream from populations in the western side of the Atlantic. These animals were indeed collected far offshore by Geiger (1963) and Semenova *et al.* (1964). If this holds true, it may be significant in maintaining the gene flow between populations of the two sides of the Atlantic.

Settlement of post-larvae occurred during mid-May, but data in the literature suggests that it can be extended until September (Gage & Tyler, 1981*a*). Post-larvae

start settling on the bottom probably when they have attained around 0.60 mm dd and 5-6 arm segments. Hendler (1975) points out that planktotrophic post-larvae settle with 0-8 arm segments and that they have normally high arm length/dd ratios. Hendler argues that this could enhance dispersal and could even confer advantages in feeding and locomotion. It is likely that up to a size of 0.6 mm dd, the larger number of arm segments will be important for flotation, however this was not quantified in the present study. For larger sizes, the larger number of arm segments was probably outweighed by the increase in weight. In fact, larger animals sank faster even with longer arms.

The measured settling rates suggests that they sink rapidly (~500 m day^{-1}). This rate is up to 5 times the sinking rates of marine snow (Lampitt, 1985; Alldredge & Gotschalk, 1988; Lampitt *et al.*, 1993*b*; Turley *et al.*, 1995). However, it should be kept in mind that the experiments presented in this chapter were done in a very small scale and in still water using dead animals. In the open ocean many hydrodynamic features may keep those animals in suspension or take them to the bottom. During the period between metamorphosis and settlement is was observed that in some individuals collected (including *Ophiocten gracilis* and *Ophiura ljungmani*) in additional samples (not included herein) the degree of calcification was much smaller. Nevertheless, we do not know whether this represents a real feature or only an artefact of preservation. If this is real, then this could be an essential feature which allows post-metamorphic individuals to remain afloat, enhancing the dispersal potential. Larval arms are present after metamorphosis in *O. gracilis* (J.D. Gage, personal communication) and may also help in keeping post-larvae afloat. Nevertheless, no post-larvae collected in either the sediments or sediment traps had larval arms still attached, suggesting that larval arms are only present at smaller sizes (<0.5 mm).

Gage & Tyler (1981*a*) argued that post-larvae settling in deeper waters do not survive to the following year. The causes of the non-viability of such a settlement remain unclear. Competition for resources, predation and lack of suitable food may be involved. Effects of pressure may also prevent colonization of deeper areas by shallow water organisms. Somero (1992) notes that vertical distribution patterns of species in aquatic habitats may be established by differences in tolerance of pressure.

However, larvae of a series of shallow water species are tolerant to high hydrostatic pressures (Tyler & Young, 1998).

If larvae of shallower water animals are capable of withstanding pressures higher than those faced by conspecific adults, pressure may have a deleterious effect on others stages of the life history, such as metamorphosis or the early post-metamorphic life. In the two traps examined in the present study, post-larval *Ophiocten gracilis* were collected. The 1000 m depth trap was placed at the right depth range of the species and the post-larvae appear to have had a 'normal' growth, attaining a considerable size and even started to develop gonads. In the deeper trap (1400 m), which was outside the depth range of the species, growth was limited and at days 149.5 and 156.5 presented a much smaller size than the animals of the shallower trap at the same dates. It is clear that animals settled at the same time and size in both traps, but the subsequent growth was different. Pressure may be an important factor affecting the growth of post-larvae and the underlying cause precluding the development of this species in deeper water.

The smaller sizes in the lower trap could also be explained by the arrival of newly-settled post-larvae, but why then was this not recorded by the upper trap? Food supply cannot be responsible since the flux of organic carbon was quantitatively similar for both traps during the study period (section 6.6; R.S. Lampitt, personal communication). The difference in temperature between the upper and lower traps was about 3°C. This could have caused the lower growth rate observed in the deeper trap, since temperatures were lower at 1400 m. Whatever the reasons may be, they are certainly related to events occurring during the early benthic life, since post-larvae collected in deeper water probably do not grow much further from the size at settlement (Gage & Tyler, 1981*a*). In such a case, post-larvae will form an ephemeral pseudopopulation (Mileikovsky, 1961) at these sites, serving as additional sources of food for the benthic community. In the Hebridean Slope, post-larvae of *Ophiocten gracilis* represented more than 7% of the total POC flux at times (Table 6.6).

6.7.3. Juvenile ecology

The early benthic life is probably of great importance (see above) and subsequent growth probably play an important role for survival. Fast growth may be essential for

avoiding predation. During the early phase of benthic life post-larvae face a completely different set of predators and prey, and overall environmental conditions, than the adults. Hunt & Scheibling (1997) point out that recently settled echinoderms are preyed upon mainly by small predators. Larger size has been shown to provide protection against predators in many invertebrates (Smith & Herrnkind, 1992; Gosselin & Qian, 1997). However, this is not always the case (see Hunt & Scheibling, 1997 for review).

The time these animals will take to recruit to the adult population will depend on the definition given to this episode. The definition of recruitment often varies in different fields of research (*e.g.* fisheries and benthic ecology). If we consider recruits as the smallest sized animals that can be censused in the samples, which is many times used in benthic ecology studies, then we could consider recruitment as occurring at the time of settlement of *Ophiocten gracilis*. However, Hunt & Scheibling (1997) question this definition of recruitment and emphasise that a probably more meaningful definition is the time when individuals are added to the breeding population. If we consider recruitment according to this second definition, *O. gracilis* individuals probably recruit around 5 to 9 months after settlement, considering a settlement period from May to September and reproduction in February/March. At this time animals would probably have attained a size of 2-3 mm in disk diameter. These data are based on the exponential growth of post-larvae examined and on the relative fast development of the gonads, which would ensures that individuals could join the reproducing populations in the reproductive season immediately following settlement. It is clear that individuals of *O. gracilis* will spend a considerable period of time as macrofauna, even after recruitment has happened. During this period evidence on stomach contents suggests these animals are omnivores and opportunistic carnivores, predating on forams and polychaetes, and probably on other groups as opportunity arises. This shows that recruitment to the adult population not always ensure a fully change from juvenile to adult life and, therefore, the term recruitment should be used with care in ecological studies.

Recruitment is likely to be relatively constant in the Rockall Trough area. Examination of the samples collected during the long-term programme in this deep-sea area by the Scottish Association for Marine Science suggests that post-larvae of

Ophiocten gracilis have a quite constant presence in summer month samples (J.D. Gage, personal communication). Gage (1995), based on growth models, concluded that variations in the size structure of populations of *Ophiura ljungmani* are likely to be affected by interannual variations in recruitment success. *Ophiocten gracilis* share many features of the life cycle of *Ophiura ljungmani*, including seasonal breeding and planktotrophic larvae. If the model proposed by Gage (1995) is right and recruitment is constant, it is expected that the population size structure of *Ophiocten gracilis* is constant over time. The widespread settlement that this species presents supports this idea.

Populations of *Ophiocten gracilis* in the Hebridean slope will likely be maintained by the huge fecundity of the population, which is helped by the early recruitment to the reproducing population. Also these animals probably live for maybe 10 years and are, of course, well adapted to the conditions in the upper slope. This fecundity will be converted into a large number of post-larvae settling regularly which, although a probably large larval and post-larval mortality and wastage of post-larvae do occur, will maintain the population at such high abundance.

The whole life cycle of *Ophiocten gracilis* and mainly the production of larvae and the settlement back to the benthic environment must be of great importance for the bentho-pelagic coupling and the exchange of carbon between these two compartments. As stated in section 6.6, the total number of post-larvae settling onto the bottom of the Hebridean slope can represent a considerable fraction of the total carbon flux in the region. The supply of post-larvae to deeper water can also represent a important source of food for populations living at such depths. Furthermore, eggs and embryos produced at the bottom are transferred to the surface layers where they will interact, consuming part of the primary production as larvae and be consumed by other organisms.

6.7.4. Significance of the growth of post-larval O. gracilis *for sediment trap measurements*

6.7.4.1. Problems with the sediment trap technique

Sediment traps have often been used to measure downward flux of POC and there is a considerable body of complementary data to indicate that they function in a quantitative way (*e.g.* Gardner *et al.*, 1997 and references cited therein) and a picture is now emerging of the global trends and the relationship between deep water particle flux and primary production in the euphotic zone (Lampitt & Antia, 1997). However, there are a number of features of the trapping technique, both physical and biological, which suggest that a degree of caution is required.

The most important physical problem associated with the sediment trap technique is that the effects of ambient currents are poorly understood, but almost certainly have a significant effect on trapping efficiency (Hargraves & Burns, 1979, Gardner, 1980*a*, *b*, Butman, 1986, Baker *et al.*, 1988). Other problems include solubilization of carbon (Knauer *et al.*, 1984), bacterial degradation (Iturriaga, 1979, Gardner *et al.*, 1983), resuspension (Gardner & Richardson, 1992) and the presence of swimmers (Coale, 1979, Lee *et al.*, 1988, Karl & Knauer, 1989, Michaels *et al.*, 1990, Hansell & Newton, 1994).

An aspect which has not been considered to date is the settlement of benthic organisms onto the cone and/or baffle of those traps which have such a design.

6.7.4.2. Evidence for growth in the trap

In section 6.6 we presented data on post-larval brittle stars supposedly growing in a deep-sea sediment trap. However, before discussing the carbon demands of the population of brittle stars we should consider whether there is evidence that growth occurred within the trap. Although they were not actually seen growing or dwelling in the trap, a number of lines of evidences suggest this was the case. The first one is the progressive increase in size of individuals collected throughout the study period (Figure 6.2). The growth of these organisms appears to be similar to the growth of conspecific adults (J.D. Gage, personal communication).

The large disk diameters observed in later samples are also unique. Evidence collected in the present study and elsewhere (Gage & Tyler, 1981*a*; J.D. Gage, personal communication) suggests that post-metamorphic *Ophiocten gracilis* individuals settle with a size around 0.6 mm dd and 5-6 arm segments. Post-larvae of planktotrophic brittle stars normally possess up to 8 arm segments (Hendler, 1975). Some post-larvae collected in the traps were around 1.8 mm dd with over 20 arm segments. To our knowledge, there is no evidence showing that these organisms (or any other post-larval ophiuroid) can attain such sizes while still in the water column. Resupension of juveniles from the bottom and subsequent collection by the trap is very unlikely, since the trap in question was almost 500 m above the bottom. Despite the presence of Intermediate Nepheloid Layers in the area (Fig. 6.9), these were carrying only very small particles and at very slow speeds (R.S. Lampitt, personal communication). Therefore, this increase of around 3 fold in disk diameter was assumed to have been caused by growth within the sediment trap.

The analysis of the stomach contents revealed the presence of foraminifera, unidentified detritus and even polychaete worms (section 6.5). This suggests that organisms were eating the particulate material reaching the trap, since there is no evidence to date showing that post-larval ophiuroids are able to feed while afloat in the water column. This hypothesis is also supported by the large percentage of animals with empty stomachs found during the early periods of sampling (at settlement). Mileikovsky (1968) emphasises that larvae of ophiuroids are limited in their range of dispersal because of their inability to remain afloat a long time after metamorphosis and because of the lack of suitable food conditions for post-larvae in the plankton. However, Strathmann (1974*a*) points out that metamorphosed ophiuroids collected from the plankton exhibit no signs of starvation and argues that maybe further evidence would show that these animals either can feed or do not spend much energy while in the plankton. This evidence, however, has still to be obtained.

The results presented above suggest that growth occurred in the trap after a major settlement event. This occurred during mid-May and it is reinforced by the appearance of post-larvae of similar sizes in the 1400 m trap. No evidence could be

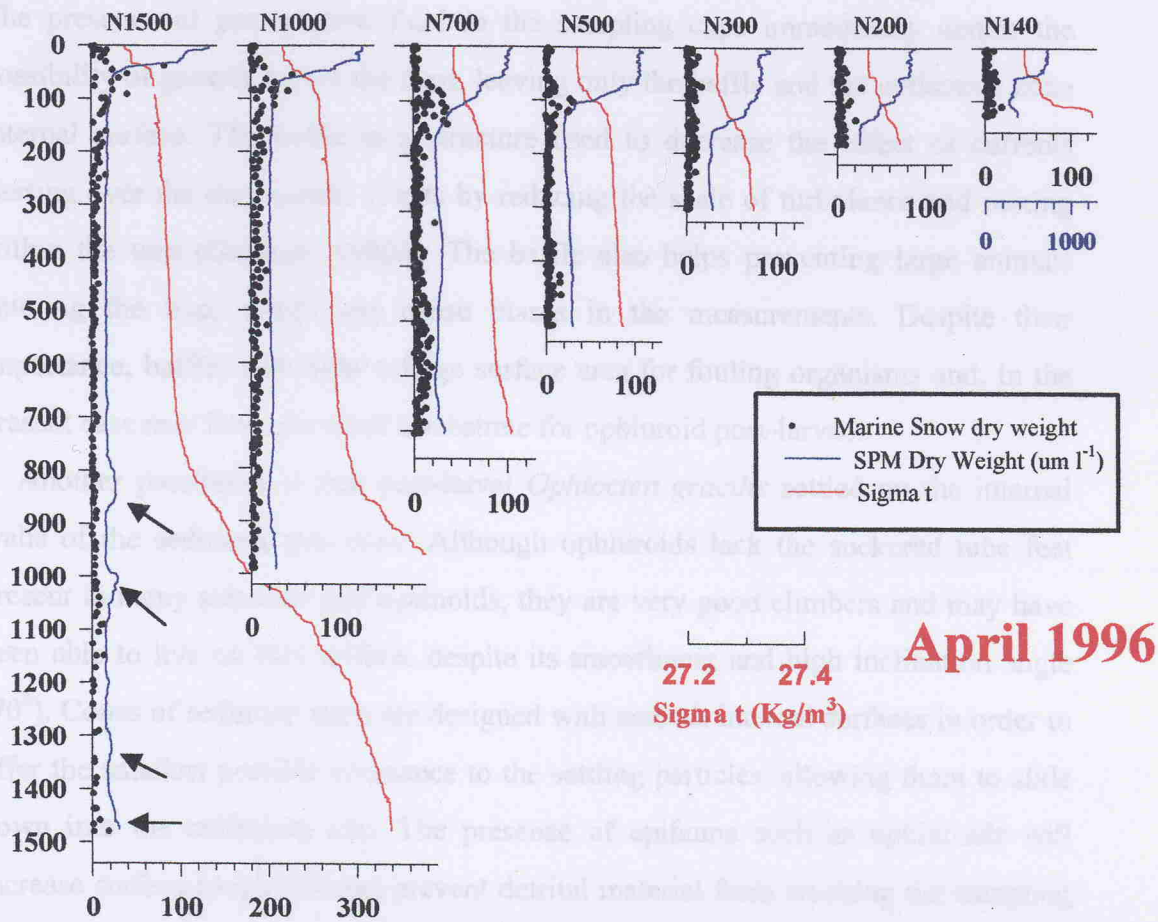

Figure 6.9. Across-slope depth profiles showing the amount of suspended particulate matter (SPM) present in the Hebridean Slope area during the study period. Note the presence of Intermediate and Benthic Nepheloid Layers (INL and BNL - arrows) on the N1500 profile.

found of a second settlement in the traps, from which we conclude that the specimens collected were all from a single cohort.

Assuming the animals are growing in the traps and eating the settling organic material, the second question is where and how did those animals survive in the trap? The presence of preservative fluid in the sampling cups immediately denies the possibility of growth within the cups, leaving only the baffle and the collection cone internal surface. The baffle is a structure used to decrease the effect of currents passing over the trap mouth. It acts by reducing the scale of turbulence and mixing within the trap (Gardner, 1980*b*). The baffle also helps preventing large animals entering the trap, which can cause biases in the measurements. Despite their importance, baffles also offer a large surface area for fouling organisms and, in the present case may have provided a substrate for ophiuroid post-larvae.

Another possibility is that post-larval *Ophiocten gracilis* settled on the internal walls of the sediment trap cone. Although ophiuroids lack the suckered tube feet present in many asteroids and echinoids, they are very good climbers and may have been able to live on that surface, despite its smoothness and high inclination angle (70^{o}). Cones of sediment traps are designed with smooth internal surfaces in order to offer the smallest possible resistance to the settling particles, allowing them to slide down into the collection cup. The presence of epifauna such as ophiuroids will increase surface roughness and prevent detrital material from reaching the sampling cup. This could generate a microenvironment where POC would be ultimately consumed by ophiuroids and possibly other organisms ("swimmers", etc.) and also degraded by bacteria (Iturriaga, 1979, Gardner *et al.*, 1983). Recovery of Parflux traps is carried out without a sampling cup under the cone and it is possible that some epifauna on the trap walls do not fall into the cups but are nevertheless washed off and lost during recovery. If all the specimens were on the cone wall, a rough calculation indicates that up to 0.95% of the surface of the cone would have been covered by the ophiuroids during the present study.

6.7.4.3. Carbon demands of post-larvae

The third question to be posed here is whether the results of carbon demands are valid, bearing in mind a number of uncertainties in the error. Estimated values are based on the numbers of post-larvae collected during the period of study, which will represent a minimum estimate of the total living in the trap.

Measurements of weight-specific respiration rates also carry an intrinsic error, since the relationship of size to respiration was derived from a variety of different species from invertebrates to fishes (Mahaut *et al.*, 1995). In fact the calculation of growth based on the increase in the population biomass over time showed higher values. This could represent a higher allocation of resources to growth than that assumed here (P/R=3/7). Our results suggest a P/R ratio of around 1. Furthermore, P/R ratios are highly variable among different species and life stages (Humphreys, 1979) and one would expect some variation from the assumed 3/7 ratio. Although errors may be large, they represent a minimum which is still a sizeable proportion of the primary flux. Consumption of carbon for growth should not be considered a direct loss provided animals are included in the flux. However, growth within the trap can transfer the settling organic carbon to different periods in time biasing the results obtained.

The serious problem for the sediment trap technique described above will not be experienced in all regions of the ocean. Although ophiuroids are found throughout the marine environment, including shallow and deep water (Piepenburg & von Juterzenka, 1994), populations of a number of species are particularly abundant at slope depths in many different areas (Gage & Tyler, 1981*a*, Fujita & Ohta, 1989, 1990, Shin & Koh, 1993). Post-larval ophiuroids result from normally abundant planktotrophic larvae present in the plankton, which take advantage of seasonal increases in primary production as an energy source. Planktotrophy is a very common mode of development among brittle stars and the settlement of post-metamorphosed ophiuroids in heavily populated areas are likely to occur in order to maintain the high levels of abundance in source populations (Gage & Tyler, 1981*a*, present study). These areas may be considered as potentially problematic during certain periods of the year when these animals are breeding and care should be taken.

Post-larval ophiuroids, whenever found in traps, should be considered as part of the total flux of carbon and be included in the calculation. The losses of organic carbon through remineralisation are a direct loss from the primary flux and in future, results from sediment trap studies should be enhanced to take such losses into account.

Chapter Seven - General discussion

In deep-sea benthic organisms reproduction and dispersal act together to assure a supply of recruits to the next generations and, in many instances, they have to be in synchrony with the short and, in some places, variable food resources (Tyler *et al.*, 1994*a*). Although still fragmentary, the knowledge of the reproductive and larval ecology have benefitted a great deal from indirect studies based on preserved samples (see Table 1.1). Experimental work carried out with larvae during the past 10 years is an important contribution (Young & Cameron, 1989; Young *et al.*, 1989; Young & Eckelbarger, 1994).

Post-larval biology and ecology are probably the least known aspects of the life cycle of deep-sea invertebrates. As already stressed in previous chapters, the early events occurring in the sediments are probably of crucial importance to recruitment to the adult population (Gosselin & Qian, 1997; Hunt & Scheibling, 1997). The post-larval development of thirty species of deep-sea echinoderms was described in the present thesis. The adults of most of these species have been known since the last century, but not much is known about their juvenile biology and ecology. The present thesis represents the first step to the understanding of the early post-metamorphic life of deep-sea echinoderms, allowing an accurate identification and inferences about the life style. Because those species comprise possibly most of the more common echinoderm species in the North-east Atlantic and juveniles are usually found in samples, it was intended to produce a 'guide' to help the identification of such stages. Chapter six examines the life history of *Ophiocten gracilis* and serves as a case study, showing the importance and some ecological aspects of post-larval life. The approach used, describing growth series based on morphology, is probably the most feasible way of treating the problem of identification in view of the difficulties with culture methods. However, the use of molecular techniques may come to play an important role for the identification of such stages (Metz *et al.*, 1991; Miller *et al.*, 1991; Medeiros-Bergen *et al.*, 1995).

7.1. The importance of morphological studies of post-larval echinoderms

Despite the prospect of the use of molecular techniques for the identification of post-larval stages, morphological studies are still needed to understand development. A comprehensive view of the morphological development allows the study of functional morphology, which may lead to many important inferences about the ecology of very early stages. Some asteroid species examined in the present study appears to undergo an ecological transition during the juvenile life. Such shifts in diet and habitat occur during the juvenile period of other aquatic animals (Werner & Gilliam, 1984; Gosselin, 1997), but were unknown for deep-sea species. This approach is crucial for deep-sea species, which are mostly remotely sampled and preserved, because of the difficulty of *in situ* or laboratory work on live animals.

Another important aspect of the study of ontogenesis is that it provides clues to evolutionary processes (Gould, 1977; McKinney & McNamara, 1991). Klingenberg (1998) stresses that ontogeny and evolution are intimately and reciprocally interrelated, since evolutionary changes in morphological characters require changes in the developmental processes that produce the structures of interest. Many of such modifications during the evolution of ontogenesis are thought to occur through heterochrony (McKinney & Gittleman, 1995). Heterochrony may be defined as changes in the relative time of appearance and rate of development of characters already present in ancestors (Gould, 1977; McNamara, 1986; McKinney & McNamara, 1991). A good example is the migration of the periproct away from the apical system during the evolution of spatangoid echinoids (see section 5.3.2; McKinney, 1988). Heterochronal changes appear to have also played an important role during the early development of echinoderms (Wray, 1995).

Beside providing clues to processes that may have generated evolutionary novelties and, consequently, speciation, post-larval morphology may provide data on the taxonomic and phylogenetic affinities among extant species. Morphological affinities were found among early stages of ophiuroids analysed in chapter three, being important for the assignment of a different generic status of an ophiuroid. Furthermore, morphology of post-larvae may strengthen phylogenetic schemes through the addition of new characters, in the same fashion as the relatively recent

introduction of DNA data in phylogenetic analysis (Littlewood & Smith, 1995; Lafay *et al.*, 1995; Smith *et al.*, 1995; Littlewood *et al.*, 1997).

7.2. Post-larvae and the colonization of the deep-sea

At different spatial and temporal scales, dispersal is thought to influence gene flow between populations; increase species longevity; facilitate the location of temporally or spatially variable resources and the coexistence with disturbance; allow colonization of new areas and maintain local population structure and diversity (Scheltema, 1974; Strathmann, 1974*b*; Hansen, 1978; Sebens, 1981; Palmer & Strathmann, 1981; Todd & Doyle, 1981; Scheltema, 1986; Wilson & Hessler, 1987; Carlon & Olson, 1993; Young *et al.*, 1997*b*). Dispersal may also have disadvantageous effects, carrying individuals to areas unsuitable to survival (Gage & Tyler, 1981*a*; Strathmann *et al.*, 1981). Etter & Caswell (1994) suggest that, at low levels of disturbance, both long and short dispersal are advantageous, but at intermediate levels, long distance dispersal appears to be better.

In benthic marine invertebrates with complex life cycles, dispersal is carried out mostly by larval stages. The extent of the dispersal potential has been associated with the type of larva produced (Scheltema, 1986). In general, planktotrophic larvae are long-lived and, therefore, have a larger dispersal power (Scheltema, 1986). Lecithotrophic larvae, on the other hand, depend on food reserves stored in the egg, which are depleted during the larval development and metamorphosis. Because of the limited energy content of lecithotrophic eggs and inability of larvae to feed, larval life is shorter, with a lower dispersal potential (Millar, 1971). Nevertheless, such generalizations are not completely true. Planktotrophic larvae may show a high variability in the length of planktonic life and, consequently, dispersal potential (Strathmann, 1978*a*). Lecithotrophic larvae, likewise, may show unexpectedly long life and dispersal potential (Olson, 1985; Scheltema, 1986). Shilling & Manahan (1994) point out that some Antarctic echinoderms with lecithotrophic larvae may live for months to years and relate this with the lower temperatures and uptake of dissolved organic matter (DOM). It is expected that, in the deep-sea, the cold temperatures would have similar effects on the physiology, increasing the longevity of lecithotrophic larvae (Young *et al.*, 1996*c*). Indeed, Young *et al.* (1997*b*) argue

that lecithotrophic development does not necessarily constrain dispersal in the deep-sea.

In the present thesis, it was found that a common phenomenon is a wider bathymetric distribution of juveniles than adults, for both planktotrophic (chapter 6; Gage & Tyler, 1981*a*; Tyler & Gage, 1984*a*) and lecithotrophic (chapter 4; Gage *et al.*, 1984) species. The dispersal into deeper areas by shallow water fauna may have been the key factor for the colonization of the deep-sea and subsequent speciation in that environment (Tyler & Young, 1998). Tyler & Young (1998) found that the sea urchin *Echinus acutus* var. *norvegicus* has two forms, a shallower and a deeper water types, which have larvae with different resistance to pressure. Tyler & Young (1998) suggest that these two types may be in the process of speciation. The gradual increase in the bathymetric ranges through widespread dispersal may have played an important role for the selection of pressure-adapted animals and, consequently, speciation in a different environment.

At present, it seems that recently-metamorphosed individuals advected to deeper areas do not survive to full adulthood, although some initiate gametogenesis (chapter 6). Physical and biological processes, as *e.g.* pressure, competition and predation, may be acting as key factors for the mortality of such stages. Post-larvae of the ophiuroid *Ophiura ljungmani* and the echinoid *Brissopsis lyrifera* appear to be predated upon by juveniles of the asteroid species *Brisingella coronata* and *Psilaster andromeda*, respectively (personal observations). In the case of *Ophiocten gracilis*, dispersal of post-larval stages appears to be random (chapter 6). Some ophiuroid species retain active larval arms after metamorphosis, probably being able of some substratum selection through the use of the juvenile podia (Burke, 1983). Although larval arms were not found attached to recently-metamorphosed benthic *O. gracilis* post-larvae, post-larvae collected in the water column show evidence of residual larval arms (J.D. Gage, personal communication). It is more likely, however, that settlement of *O. gracilis* is driven by hydrography, as evidence from the widespread settlement and settlement in sediment traps suggests.

On the other hand, many asteroid larvae have the ability to test the substratum, delaying metamorphosis if needed (Strathmann, 1974*a*). In this case, settlement in unsuitable areas may not be entirely related to environmental variables, unless

currents carry larvae too far away from the adult range and metamorphosis occurs after a long delay in settlement. This suggests that biological processes occurring during the juvenile phase may be playing an important role in the zonation of echinoderms and maintenance of local population structure and diversity.

Over larger time scales, however, changes in the community structure driven by different processes (*e.g.* glaciation or catastrophic events such as sediment slides) may create or vacate a niche by removing a stronger competitor or predator and/or by altering the physical conditions, allowing such stages to establish themselves and speciate.

References

Agassiz, A. 1869. Preliminary report on the Echini and star-fishes dredged in deep water between Cuba and the Florida Reef. *Bull. Mus. Comp. Zool.* **1**: 253-308.

Agassiz, A. 1872. Revision of the Echini. *Mus. Comp. Zool. No 7.* 762 pp.

Aldred, RG; Thurston, MH; Rice, AL & Morley, DR. 1982. An acoustically monitored opening and closing epibenthic sledge. *Deep-Sea Res.* **23**: 167-174.

Aldredge, AL & Gotschalk, CC. 1988. In situ settling behaviour of marine snow. *Limnol. Oceanogr.* **33**: 339-351.

Aldredge, AL & Silver, MW. 1988. Characteristics, dynamics and significance of marine snow. *Prog. Oceanog.* **20**: 41-82.

Aller, JY. 1989. Quantifying sediment disturbances by bottom currents and its effect on benthic communities in a deep-sea western boundary zone. *Deep-Sea Res. I* **36**: 901-934.

Aller, JY. 1997. Benthic community response to temporal and spatial gradients in physical disturbance within a deep-sea western boundary region. *Deep-Sea Res. I* **44**: 39-69.

Arhan, M; Colin de Verdière, A & Mémery, L. 1994. The eastern boundary of the subtropical North Atlantic. *J. Phys. Oceanog.* **24**: 1295-1316.

Amemiya, S & Tsuchiya, T. 1979. Development of the echinothurid sea urchin *Asthenosoma ijimai*. *Mar. Biol.* **52**: 93-96.

Baker, ET; Milburn, HB & Tennant, DA. 1988. Field assessment of sediment trap efficiency under varying flow conditions. *J. Mar. Res.* **46**: 573-592.

Ballard, RD. 1977. Notes on a major oceanographic find. *Oceanus* **20**: 35-44.

Barker, MF. 1977. Observations on the settlement of the brachiolaria larvae of *Stichaster australis* (Verrill) and *Coscinasterias calamaria* (Gray) (Echinodermata: Asteroidea) in the laboratory and on the shore. *J. Exp. Mar. Biol. Ecol.* **30**: 95-108.

Barker, MF. 1979. Breeding and recruitment in a population of the New Zealand starfish *Stichaster australis* (Verrill). *J. Exp. Mar. Biol. Ecol.* **41**: 195-211.

Barker, MF & Nichols, D. 1983. Reproduction, recruitment and juvenile ecology of the starfish, *Asterias rubens* and *Marthasterias glacialis*. *J. Mar. Biol. Ass. U.K.* **63**: 745-765.

Barnes, H & Powell, HT. 1951. The growth-rate of juvenile *Asterias rubens* L. *J. Mar. Biol. Ass. U.K.* **30**: 381-385.

Barnes, RD. 1968. *Invertebrate Zoology*. 2nd ed. W.B. Saunders, Philadelphia. 743 pp.

Berg, CJ, Jr. 1985. Reproductive strategies of mollusks from abyssal hydrothermal vent communities. *Bull. Biol. Soc. Was.* **6**: 185-197.

Berg, CJ, Jr & Van Dover, CL. 1987. Benthopelagic macrozooplankton communities at and near deep-sea hydrothermal vents in the eastern Pacific Ocean and the Gulf of California. *Deep-Sea Res. I* **34**: 379-401.

Billett, DSM; Lampitt, RS; Rice, AL & Mantoura, RFC. 1983. Seasonal sedimentation of phytoplankton to the deep-sea benthos. *Nature* **302**: 520-522.

Birkeland, C; Chia, FS & Strathmann, RR. 1971. Development, substratum selection, delay of metamorphosis and growth in the seastar, *Mediaster aequalis* Stimpson. *Biol. Bull.* **141**: 99-108.

Blake, DB. 1989. Asteroidea: Functional morphology, classification and phylogeny. *Echinoderm Studies* **3**: 179-223.

Blake, DB. 1990. Adaptive zones of the class Asteroidea (Echinodermata). *Bull. Mar. Sci.* **46**: 701-718.

Bouchet, P & Warén, A. 1979*a*. Planktotrophic larval development in deep-water gastropods. *Sarsia* **64**: 37-40.

Bouchet, P & Warén, A. 1979*b*. The abyssal molluscan fauna of the Norwegian Sea and its relation to the other faunas. *Sarsia* **64**: 211-243.

Bouchet, P & Warén, A. 1994. Ontogenetic migration and dispersal of deep-sea gastropod larvae. *In*: Young, CM & Eckelbarger, KJ (eds.). *Reproduction, larval biology biology and recruitment of deep-sea benthos*. Columbia Univ. Press, New York. p. 98-117.

Brattegard, T & Fosså, JH. 1991. Replicability of an epibenthic sampler. *J. Mar. Biol. Ass. U.K.* **71**: 153-166.

Bronsdon, SK; Tyler, PA; Rice, AL & Gage, JD. 1993. Reproductive biology of two epizoic anemones from the deep North-Eastern Atlantic Ocean. *J. Mar. Biol. Ass. U.K.* **73**: 531-542.

Bubnov, VA. 1968. Boundaries of intermediate water masses in the North Atlantic. *Oceanology* **19**: 322-326.

Burke, RD. 1983. The induction of metamorphosis of marine invertebrate larvae: stimulus and response. *Can. J. Zool.* **61**: 1701-1719.

Bury, H. 1895. The metamorphosis of echinoderms. *Q. J. Mic. Sci.* **38**: 45-135.

Butman, CA. 1986. Sediment trap biases in turbulent flows: results from a laboratory flume study. *J. Mar. Res.* **44**: 601-644.

Byrne, M. 1991. Reproduction, development and population biology of the Caribbean ophiuroid *Ophionereis olivacea*, a protandric hermaphrodite that broods its young. *Mar. Biol.* **111**: 387-399.

Cameron, RA & Hinegardner, RT. 1978. Early events in sea urchin metamorphosis, decription and analysis. *J. Morph.* **157**: 21-32.

Cameron, JL; McEuen, FS & Young, CM. 1988. Floating lecithotrophic eggs from the bathyal echinothuriid sea urchin *Araeosoma fenestratum*. *In*: Burke, RD; Mladenov, PV; Lambert, P & Parsley, RL. (eds.). *Echinoderm biology*. Balkema, Rotterdam. p. 177-180.

Campbell, AS. 1922. Preliminary notes on growth stages in brittle-stars. *J. Ent. Zool.* **14**: 37-44.

Campos-Creasey, LS; Tyler, PA; Gage, JD & John, AWG. 1994. Evidence for coupling the vertical flux of phytodetritus to the diet and seasonal life-history of the deep-sea echinoid *Echinus affinis*. *Deep-Sea Res. I* **41**: 369-388.

Cann, J; Van Dover, CL; Walker, C; Dando, P & Murton, B. 1994. Diversity of vent ecosystems (DOVE). *Bridge Workshop Report n° 4*. p. 1-31.

Carlon, DB & Olson, RR. 1993. Larval dispersal distance as an explanation for adult spatial pattern in two Caribbean reef corals. *J. Exp. Mar. Biol. Ecol.* **173**: 247-263.

Cary, SC; Felback, H & Holland, ND. 1989. Observations on the reproductive biology of the hydrothermal vent tubeworm *Riftia pachyptila*. *Mar. Ecol. Prog. Ser.* **52**: 89-94.

Chen, B-Y & Chen, C-P. 1992. Reproductive cycle, larval development, juvenile growth and population dynamics of *Patiriella pseudoexigua* (Echinodermata: Asteroidea) in Taiwan. *Mar. Biol.* **113**: 271-280.

Cherbonnier, G & Sibuet, M. 1973. Résultats scientifique de la campagne Noratlante: Astérides et ophiures. *Bull. Mus. Hist. Nat., Paris, 3e sér., n° 102, Zool.* **76**: 1333-1394.

Chesher, RH. 1963. The morphology and function of the frontal ambulacrum of *Moira atropos* (Echinoidea: Spatangoida). *Bull. Mar. Sci. Gulf Caribb.* **13**: 549-573.

Chia, FS & Burke, RD. 1978. Echinoderm metamorphosis: fate of larval structure. *In*: Chia, FS & Rice, M. (eds.). *Settlement and metamorphosis of marine invertebrate larvae*. Elsevier, Amsterdam. p. 219-234.

Clark, AM. 1981. Notes on Atlantic and other Asteroidea. 1. Family Benthopectinidae. *Bull. Br. Mus. Nat. Hist. (Zool.)* **41**: 91-135.

Clark, AM. 1982. Notes on Atlantic Asteroidea. 2. Luidiidae. *Bull. Br. Mus. Nat. Hist.* **42**: 157-184.

Clark, AM. 1984. Notes on Atlantic Asteroidea. 4. Families Poraniidae and Asteropseidae. *Bull. Br. Mus. Nat. Hist. (Zool.)* **47**: 19-51.

Clark, AM & Courtman-Stock, J. 1976. *The echinoderms of Southern Africa*. British Museum (Natural History), London. 277 pp.

Clark, AM & Downey, ME. 1992. *Starfishes of the Atlantic*. Chapman & Hall, London. 794 pp.

Clark, HL. 1912. Hawaiian and other Pacific Echini. *Mem. Mus. Comp. Zool.* **34**(3): 205-383.

Clark, HL. 1914. Growth changes in brittlestars. *Publs. Carnegie. Instn. Was.* **5**: 93-125.

Coale, KH. 1990. Labyrinth of doom: a device to minimize the "swimmer" component in sediment trap collections. *Limnol. Oceanog.* **35**: 1376-1380.

Colman, JG & Tyler, PA. 1988. Observations on the reproductive biology of the deep-sea trchid *Calliotropis ottoi* (Philippi). *J. Moll. Stud.* **54**: 239-242.

Colman, JG; Tyler, PA & Gage, JD. 1986*a*. Larval development of deep-sea gastropods (Prosobranchia: Neogastropoda) from the Rockall Trough. *J. Mar. Biol. Ass. U.K.* **66**: 951-965.

Colman, JG; Tyler, PA & Gage, JD. 1986*b*. The reproductive biology of *Colus jeffreysianus* (Gastropoda: Prosobranchia) from 2200 m in the N.E. Atlantic. *J. Moll. Stud.* **52**: 45-54.

Comely, CA & Ansell, AD. 1988. Population density and growth of *Echinus esculentus* L. on the Scottish west coast. *Estuar. Coast. Shelf Sci.* **27**: 311-334.

Comely, CA & Ansell, AD. 1989. The reproductive cycle of *Echinus esculentus* L. on the Scottish west coast. *Estuar. Coast. Shelf Sci.* **29**: 385-407.

Copley, JTC. 1998. *Ecology of deep-sea hydrothermal vents*. Unpublished PhD Thesis, University of Southampton. 204 pp.

Cosson, N; Sibuet, M & Galeron, J. 1997. Community structure and spatial heterogeneity of the deep-sea macrofauna at three contrasting stations in the tropical northeast Atlantic. *Deep-Sea Res. I* **44**: 247-269.

De Burgh, ME & Burke, RD. 1983. Uptake of dissolved amino acids by embryos and larvae of *Dendraster excentricus* (Eschscholtz) (Echinodermata: Echinoidea). *Can. J. Zool.* **61**: 349-354.

Desbruyères, D & Laubier, L. 1991. Systematics, phylogeny, ecology and distribution of the Alvinellidae (Polychaeta) from deep-sea hydrothermal vents. *Ophelia Supplement* **5**: 31-45.

Deuser, WG. 1986. Seasonal and interannual variations in deep water particle fluxes in the Sargasso Sea and their relation to surface hydrography. *Deep-Sea Res. I* **33**: 225-246.

Deuser, WG & Ross, EH. 1980. Seasonal change in the flux of organic carbon to the deep Sargasso Sea. *Nature* **283**: 364-365.

Deuser, WG; Ross, EH & Anderson, RF. 1981. Seasonality in the supply of sediment to the deep Sargasso Sea and implications to the rapid transfer of matter to the deep ocean. *Deep-Sea Res. I* **28**: 495-505.

Dixon, DR & Dixon, LRJ. 1996. Results of DNA analyses conducted on vent-shrimp postlarvae collected above the Broken Spur vent field during the CD95 cruise, August 1995. *BRIDGE Newsletter* (11): 9-15.

Domanski, PA. 1984. Giant larvae: prolonged planktonic larval phase in the asteroid *Luidia sarsi*. *Mar. Biol.* **80**: 189-195.

Dooley, HD & Meincke, J. 1981. Circulation and water masses in the Faroese channels during Overflow'73. *Deuts. Hydrog. Zeit.* **34**: 41-54.

Durham, JW. 1966. Evolution among the Echinoidea. *Biol. Rev.* **41**: 368-391.

Ellett, DJ & Martin, JHA. 1973. The physical and chemical oceanography of the Rockall Channel. *Deep-Sea Res.* **20**: 585-625.

Ellett, DJ & Roberts, DG. 1973. The overflow of Norwegian Sea Deep Water across the Wyville-Thomson Ridge. *Deep-Sea Res.* **20**: 819-835.

Ellett, DJ; Edwards, A & Bowers, R. 1986. The hydrography of the Rockall Channel - an overview. *Proc. R. Soc. Edinb.* **88B**: 61-81.

Emlet, RB. 1986. Facultative planktotrophy in the tropical echinoid *Clypeaster rosaceus* (Linnaeus) and a comparison with obligate planktotrophy in *Clypeaster subdepressus* (Gray) (Clypeasteroidea: Echinoidea). *J. Exp. Mar. Biol. Ecol.* **95**: 183-202.

Emlet, RB. 1988. Larval form and metamorphosis of a "primitive" sea urchin, *Eucidaris thouarsi* (Echinodermata: Echinoidea: Cidaroida), with implications for developmental and phylogenetic studies. *Biol. Bull.* **174**: 4-19.

Emlet, RB & Hoegh-Guldberg, O. 1997. Effects of egg size on postlarval performance: experimental evidence from a sea urchin. *Evolution* **51**: 141-152.

Emlet, RB; McEdward, LR & Strathmann, R. 1987. Echinoderm larval ecology viewed from the egg. *Echinoderm Studies* **2**: 55-136.

Emson, RH; Tyler, PA & Nørrevang, A. 1994. Distribution of bathyal ophiuroids round the Faroes in relation to the local hydrodynamic regime. *In*: David, B; Guille, A; Féral, JP & Roux, M (eds). *Echinoderms through time*. Balkema, Rotterdam. p. 411-418.

Etter, RJ & Caswell, H. 1994. The advantages of dispersal in a patchy environment: effects of disturbance in a cellular automation model. *In*: Young, CM & Eckelbarger, KJ (eds.). *Reproduction, larval biology and recruitment of the deep-sea benthos*. Columbia University Press, New York. P. 284-305.

Farran, GP. 1913. The deep-water Asteroidea, Ophiuroidea and Echinoidea of the west coast of Ireland. *Scientific Investigations, 1912. Fisheries Branch, Dept. of Agriculture Ireland, Dublin* **6**: 1-66.

Faugeres, JC; Gonthier, E; Grousset, F & Poutiers, J. 1981. The Feni Drift: the importance and meaning of slump deposits on the eastern slope of the Rockall Bank. *Mar. Geol.* **40**: M49-M57.

Feber, I & Lawrence, JM. 1976. Distribution, substratum preference and burrowing behaviour of *Lovenia elongata* (Gray) (Echinoidea: Spatangoida) in the Gulf of Elat ('Aqaba), Red Sea. *J. Exp. Mar. Biol. Ecol.* **22**: 207-225.

Feder, HM. 1970. Growth and predation by the ochre sea star, *Pisaster ochraceus* (Brandt), in Monterey Bay, California. *Ophelia* **8**: 161-185.

Fell, HB. 1941. The direct development of a New Zealand ophiuroid. *Q. J. Microsc. Sci.* **82**: 377-441.

Fell, HB. 1948. Echinoderm embryology and the origin of chordates. *Biol. Rev.* **23**: 81-107.

Fell, HB. 1963. The phylogeny of sea-stars. *Phil. Trans. R. Soc. Lond. B* **246**: 381-485.

Fenaux, L. 1970. Maturation of the gonads and seasonal cycle of the planktonic larvae of the ophiuroid *Amphiura chiajei* Forbes. *Biol. Bull.* **138**: 262-271.

Fewkes, JW. 1887. On the development of the calcareous plates of *Amphiura*. *Bull. Mus Comp. Zool.* **18**(4): 107-150.

Flach, E & Heip, C. 1996. Seasonal variations in faunal distributions and activity across the continental slope of the Goban Spur area (NE Atlantic). *J. Sea Res.* **36**: 203-215.

Forbes, E. 1844. Report on the Mollusca and Radiata of the Aegean Sea, and their distribution, considered as bearing on Geology. *Report (1843) to the 13th Meeting of the British Association for the Advancement of Science*. p. 30-193.

France, SC; Hessler, RR & Vrijenhoek, RC. 1992. Genetic differentiation between spatially-disjunct populations of the deep-sea, hydrothermal vent-endemic amphipod *Ventiella sulfuris*. *Mar. Biol.* **11**: 551-559.

Fujita, T & Ohta, S. 1989. Spatial structure within a dense bed of the brittle star *Ophiura sarsi* (Ophiuroidea: Echinodermata) in the bathyal zone off Otsuchi, Northeastern Japan. *J. Oceanog. Soc. Japan Nihon Kaiyo Gakkai* **45**: 289-300.

Fujita, T & Ohta, S. 1990. Size structure of dense populations of the brittle star *Ophiura sarsi* (Ophiuroidea: Echinodermata) in the bathyal zone around Japan. *Mar. Ecol. Prog. Ser.* **64**: 1-2.

Gage, JD. 1984. On the status of the deep-sea echinoids, *Echinosigra phiale* and *E. paradoxa*. *J. Mar. Biol. Ass. U.K.* **64**: 157-170.

Gage, JD. 1986. The benthic fauna of the Rockall Trough: regional distribution and bathymetric zonation. *Proc. R. Soc. Edinb.* **88B**: 159-174.

Gage, JD. 1987. Growth of the deep-sea irregular sea urchins *Echinosigra phiale* and *Hemiaster expergitus* in the Rockall Trough (N.E. Atlantic Ocean). *Mar. Biol.* **96**: 19-30.

Gage, JD. 1991. Biological rates in the deep-sea: a perspective from studies on processes in the benthic boundary layer. *Reviews in Aquatic Sciences* **5**: 49-100.

Gage, JD. 1994. Recruitment ecology and age structure of deep-sea invertebrate populations. *In:* Young, CM & Eckelbarger, KJ (eds). *Reproduction, larval biology biology and recruitment of deep-sea benthos*. Columbia University Press, New York. p.223-242.

Gage, JD. 1995. Demographic modelling in the analysis of population dynamics of deep-sea macrobenthos. *Int. Revue ges. Hydrobiol.* **80**: 171-185.

Gage, JD & Tyler, PA. 1981*a*. Non-viable seasonal settlement of larvae on upper bathyal brittle star *Ophiocten gracilis* in the Rockall Trough Abyssal. *Mar. Biol.* **64**: 153-161.

Gage, JD & Tyler, PA. 1981*b*. Re-appraisal of age composition, growth and survivorship of the deep-sea brittle star *Ophiura ljungmani* from size structure in a sample time series from the Rockall Trough. *Mar. Biol.* **64**: 163-172.

Gage, JD & Tyler, PA. 1982*a*. Growth strategies in deep-sea ophiuroids. *In:* Lawrence, JM (ed). *International Echinoderms Conference, Tampa Bay*. Balkema, Rotterdam. p.305-311.

Gage, JD & Tyler, PA. 1982*b*. Depth-related gradients in size structure and the bathymetric zonation of deep-sea brittle stars. *Mar. Biol.* **71**: 299-308.

Gage, JD & Tyler, PA. 1982*c*. Growth and reproduction of the deep-sea brittlestar *Ophiomusium lymani* Wyville Thomson. *Oceanol. Acta* **5**: 73-83.

Gage, JD & Tyler, PA. 1985. Growth and recruitment of the deep-sea urchin *Echinus affinis*. *Mar. Biol.* **90**: 41-53

Gage, JD & Tyler, PA. 1991. *Deep-sea biology. A natural history of organisms at the deep-sea floor*. Cambridge University Press, Cambridge. 504 pp.

Gage, JD; Tyler, PA & Nichols, D. 1986. Reproduction and growth of *Echinus acutus* var. *norvegicus* Düben & Koren and *E. elegans* Düben & Koren on the continental slope off Scotland. *J. Exp. Mar. Biol. Ecol.* **101**: 61-83.

Gage, JD; Billett, DSM; Jensen, M & Tyler, PA. 1985. Echinoderms of the Rockall Trough and adjacent areas. 2. Echinoidea and Holothuroidea. *Bull. Brit. Mus. Nat. Hist. (Zool.)* **48**: 173-213.

Gage, JD; Lightfoot, RH; Pearson, M & Tyler, PA. 1980. An introduction to a sample time-series of abyssal macrobenthos: methods and principle sources of variability. *Oceanol. Acta* **3**: 169-176.

Gage, JD; Pearson, M; Clark, AM; Paterson, GLJ & Tyler, PA. 1983. Echinoderms of the Rockall Trough and adjacent areas. I. Crinoidea, Asteroidea and Ophiuroidea. *Bull. Br. Mus. Nat. Hist. (Zool.)* **45**: 263-308.

Gage, JD; Pearson, M; Billett, DSM; Clark, AM; Jensen, M; Paterson, GLJ & Tyler, PA. 1984. Echinoderm zonation in the Rockall Trough (NE Atlantic). *In*: Keegan, BF & O'Connor, BDS (eds.). *Proceedings of the fifth international echinoderm conference, Galway*. Balkema, Rotterdam. p. 31-36.

Gale, AS. 1987. Phylogeny and classification of the Asteroidea (Echinodermata). *Zool. J. Linn. Soc.* **89**: 107-132.

Gardner, WD. 1980*a*. Sediment trap dynamics and calibration: a laboratory evaluation. *J. Mar. Res.* **38**: 17-39.

Gardner, WD. 1980*b*. Field calibration of sediment traps. *J. Mar. Res.* **38**: 41-52.

Gardner, WD & Richardson, MJ. 1992. Particle export and resuspension fluxes in the western North Atlantic. *In*: Rowe, GT & Pariente, V (eds.). *Deep-Sea Food Chains and the Global Carbon Cycle*. Kluwer Academic Publisher, Dordrecht. p. 339-364.

Gardner, WD; Biscaye, PE & Richardson, MJ. 1997. A sediment trap experiment in the Vema Channel to evaluate the effect of horizontal particle fluxes on measured vertical fluxes. *J. Mar. Res.* **55**: 995-1028.

Gardner, WD; Hinga, KR & Marra, J. 1983. Observations on the degradation of biogenic material in the deep ocean with implications on the accuracy of sediment trap fluxes. *J. Mar. Res.* **41**: 195-214.

Geiger, SR. 1963. *Ophiopluteus ramosus* between Iceland and Newfoundland. *Nature* **198**: 908-909.

George, RY & Menzies, RJ. 1967. Indication of cyclic reproductive activity in Abyssal organisms. *Nature* **215**: 878.

George, RY & Menzies, RJ. 1968. Further evidence for seasonal breeding cycles in deep-sea. *Nature* **220**: 80-81.

German, CR; Baker, ET & Klinkhammer, G. 1995. Regional setting of hydrothermal activity. *In*: Parson, LM; Walker, CL & Dixon, DR (eds.). *Hydrothermal vents and processes*. The Geological Society of London Special Publication n° 87. p. 3-15.

Gordon 1926*a*. The development of the calcareous test of *Echinus miliaris*. *Phil. Trans. R. Soc. Lond. B* **214**: 259-312.

Gordon, I. 1926*b*. The development of the calcareous test of *Echinocardium cordatum*. *Phil. Trans. R. Soc. Lond. B* **215**: 255-313.

Gordon, I. 1929. Skeletal development in *Arbacia*, *Echinarachnius* and *Leptasterias*. *Phil. Trans. R. Soc. Lond. B* **217**: 289-334.

Gosselin, LA. 1997. An ecological transition during juvenile life in a marine snail. *Mar. Ecol. Prog. Ser.* **157**: 185-194.

Gosselin, LA & Qian, PY. 1996. Early post-settlement mortality of an intertidal barnacle: A critical period for survival. *Mar. Ecol. Prog. Ser.* **135**: 69-75.

Gosselin, LA & Qian, PY. 1997. Juvenile mortality in benthic marine invertebrates. *Mar. Ecol. Prog. Ser.* **146**: 265-282.

Gould, SJ. 1977. *Ontogeny and phylogeny.* Belknap Press/Harvard University Press, Cambridge. 501 pp.

Gross, TF; Williams, AJ, III & Nowell, ARM. 1988. A deep-sea sediment transport storm. *Nature* **331**: 518-521.

Gustafson, RG & Lutz, RA. 1994. Molluscan life history traits at deep-sea hydrothermal vents and cold methane/sulfide seeps. *In*: Young, CM & Eckelbarger, KJ (eds.). *Reproduction, larval biology and recruitment of deep-sea benthos.* Columbia University Press, New York. p. 76-97.

Hagström, BE & Lønning, S. 1961. Morphological and experimental studies on the genus *Echinus*. *Sarsia* **4**: 21-31.

Hancock, DA. 1958. Notes on an Essex oyster bed. *J. Mar. Biol. Ass. U.K.* **37**: 565-589.

Hansel, DA & Newton, JA. 1994. Design and evaluation of a "swimmer"-segregating particle interceptor trap. *Limnol. Oceanog.* **39**: 1487-1495.

Hansen, B. 1975. Systematics and biology of the deep-sea holothurians. Part 1. Elasipoda. *Galathea Reports* **13**: 1-262.

Hansen, B. 1985. The circulation of the northern part of the Northeast Atlantic. *Rit Fiskid.* **9**: 110-126.

Hansen, TA. 1978. Larval dispersal and species longevity in Lower Tertiary gastropods. *Science* **199**: 885-887.

Hargrave, BT & Burns, NM. 1979. Assessment of sediment trap collection efficiency. *Limnol. Oceanog.* **24**: 1124-1136.

Harvey, JG. 1982. Θ-S relationships and water masses in the eastern North Atlantic. *Deep-Sea Res.* **29**: 1021-1033.

Harvey, R & Gage, JD. 1984. Observations on the reproduction and postlarval morphology of pourtalesiid sea urchins in the Rockall Trough area (N.E. Atlantic Ocean). *Mar. Biol.* **82**: 181-190.

Harvey, R; Gage, JD; Billett, DSM; Clark, AM & Paterson, GLJ. 1988. Echinoderms of the Rockall Trough and adjacent areas. 3. Additional records. *Bull. Br. Mus. Nat. Hist. (Zool.)* **54**: 153-198.

Hayward, PJ & Ryland, JS (eds.). 1990. *The marine fauna of the British Isles and North-west Europe. Vol. 2. Molluscs and Chordates.* Clarendon Press, Oxford. 996 pp.

Hecker, B. 1985. Fauna from a cold sulfur-seep in the Gulf of Mexico: comparison with hydrothermal vent communities and evolutionary implications. *Bull. Biol. Soc. Was.* **6**: 465-473.

Hendler, G. 1975. Adaptational significance of the patterns of ophiuroid development. *Am. Zool.* **15**:

691-715

Hendler, G. 1978. Development of *Amphioplus abditus* (Verrill) (Echinodermata: Ophiuroidea). II. Description and discussion of ophiuroid skeletal ontogenies and homologies. *Biol. Bull.* **154**: 79-95.

Hendler, G. 1988. Ophiuroid skeleton ontogeny reveals homologies among skeletal plates of adults: a study of *Amphiura filiformis*, *Amphiura stimpsonii* and *Ophiophragmus filograneus* (Echinodermata). *Biol. Bull.* **174**: 20-29.

Hendler, G. 1998. Implications of the remarkable ontogenetic changes in some deep-sea brittle stars. *In*: Mooi, R & Telford, M (eds.). *Echinoderms: San Francisco*. Balkema, Rotterdam. p. 353-358.

Hessler, RR & Sanders, HL. 1967. Faunal diversity in the deep-sea. *Deep-Sea Res.* **14**: 65-78.

Hinegardner, RT. 1969. Growth and development of the laboratory cultured sea urchin. *Biol. Bull.* **137**: 465-475.

Hinegardner, RT. 1975. Morphology and genetics of sea urchin development. *Amer. Zool.* **15**: 679-689.

Humphreys, WF. 1979. Production and respiration in animal populations. *J. Anim. Ecol.* **48**: 427-453.

Hunt, HL & Scheibling, RE. 1997. Role of early post-settlement mortality in recruitment of benthic marine invertebrates. *Mar. Ecol. Prog. Ser.* **155**: 269-301.

Hyman, LH. 1955. *The invertebrates: Echinodermata. The coelomate Bilateria.* Vol. IV. McGraw-Hill, New York. 763 pp.

Iturriaga, R. 1979. Bacterial activity related to sedimenting particulate matter. *Mar. Biol.* **55**: 157-169.

Jackson, JBC. 1986. Modes of dispersal of clonal benthic invertebrates: consequences for species' distributions and genetic structure of local populations. *Bull. Mar. Sci.* **39**: 588-606.

Jaeckle, WB. 1995. Variation in the size, energy content, and biochemical composition of invertebrate eggs: correlates to the mode of larval development. *In*: McEdward, L (ed.). *Ecology of marine invertebrate larvae*. CRC Press, Boca Raton. p. 49-77.

Jangoux, M. 1982. Food and feeding mechanisms: Asteroidea. *In*: Jangoux, M & Lawrence, JM (eds.). *Echinoderm nutrition. Balkema, Rotterdam*. p. 117-159.

Janies, DA & McEdward, LR. 1993. Highly derived coelomic and water-vascular morphogenesis in a starfish with pelagic direct development. *Biol. Bull.* **185**: 56-76.

Jannasch, HW & Wirsen, CO. 1979. Chemosynthetic primary production at East Pacific sea floor spreading centres. *Bioscience* **29**: 592-598.

Jenkins, CJ & Keene, JB. 1992. Submarine slope failures of the southeast Australian continental slope: A thinly sedimented margin. *Deep-Sea Res. I* **39**: 121-136.

Johnson, CR; Sutton, DC; Olson, RR & Giddins, R. 1991. Settlement of crown-of-thorns starfish: role of bacteria on surfaces of coralline algae and a hypothesis for deepwater recruitment. *Mar. Ecol. Prog. Ser.* **71**: 143-162.

Jones, ML & Gardiner, SL. 1985. Light and scanning electron microscopic studies of spermatogenesis in the vestimentiferan tube worm *Riftia pachyptila* (Pogonophora: Obturata). *Trans. Am. Soc. Microsc.* **104**: 1-18.

Kanatani, H; Shirai, H; Nakanishi, K & Kurokawa, T. 1969. Isolation and identification of meiosis inducing substance in starfish *Asterias amurensis*. *Nature* **221**: 273-274.

Karl, DM & Knauer, GA. 1989. Swimmers: a recapitulation of the problem and a potential solution. *Oceanography* **2**: 32-35.

Keesing, JK & Halford, AR. 1992. Importance of post-settlement processes for the population dynamics of *Acanthaster planci* (L.). *Aust. J. Mar. Fresh. Res.* **43**: 635-651.

Keesing, JK; Cartwright, CM & Hall, KC. 1993. Measuring settlement intensity of echinoderms on coral reefs. *Mar. Biol.* **117**: 399-407.

Kempf, SC & Hadfield, MG. 1985. Planktotrophy by lecithotrophic larvae of a nudibranch, *Phestilla sibogae* (Gastropoda). *Biol. Bull.* **169**: 119-130.

Kennicutt, MC II; Brooks, JM; Bidigare, RR; Fay, RR; Wade, BL & McDonald, TJ. 1985. Vent-type taxa in a hydrocarbon seep region on the Louisiana slope. *Nature* **317**: 351-352.

Kidd, RB & Huggett, QJ. 1981. Rock debris on abyssal plains in the Northeast Atlantic: a comparison of epibenthic sledge hauls and photographic surveys. *Oceanol. Acta* **4**: 99-104.

Killingley, JS & Rex, MA. 1985. Mode of larval development in some deep-sea gastropods indicated by oxygen-18 values of their carbonate shells. *Deep-Sea Res.* **32**: 809-818.

Kim, SL; Mullineaux, LS & Helfrich, KR. 1994. Larval dispersal via entrainment into hydrothermal vent plumes. *J. Geophys. Res.* **99**(C6): 12655-12665.

Klingenberg, CP. 1998. Heterochrony and allometry: the analysis of evolutionary change in ontogeny. *Biol. Rev.* **73**: 79-123.

Knauer, GA; Karl, DM; Martin, JH & Hunter, CN. 1984. In situ effects of selected preservatives on total carbon, nitrogen and metals collected in sediment traps. *J. Mar. Res.* **42**: 445-462.

Koehler, R. 1897. Resultats scientifiques de la Campagne du Caudan dans le Golfe de Gascogne. Echinodermes. *Annls. Univ. Lyon* **26**: 33-122.

Komatsu, M. 1975. On the development of the sea-star, *Astropecten latespinosus* Meissner. *Biol. Bull.* **148**: 49-59.

Komatsu, M; Oguro, C & Kano, YT. 1982. Development of the sea-star, *Luidia quinaria* von Martens. *In*: Lawrence, JM (ed.). *International Echinoderms Conference, Tampa Bay.* Balkema, Rotterdam. p. 497-503.

Kontar, EA & Sokov, AV. 1994. A benthic storm in the northeastern tropical Pacific over the fields of manganese nodules. *Deep-Sea Res. I* **41**: 1069-1089.

Laegdsgaard, P; Byrne, M & Anderson, DT. 1991. Reproduction of sympatric populations of *Heliocidaris erythrogramma* and *H. tuberculata* (Echinoidea) in New South Wales. *Mar. Biol.* **110**: 359-374.

Lafay, B; Smith, AB & Christen, R. 1995. A combined morphological and molecular approach to the phylogeny of asteroids (Asteroidea: Echinodermata). *Syst. Biol.* **44**: 190-208.

Lamont, PA & Gage, JD. 1998. Dense brittle star population on the Scottish continental slope. *In*: Mooi, R & Telford, M (eds.). *Echinoderms: San Francisco*. Balkema, Rotterdam.

Lampitt, RS. 1985. Evidence for the seasonal deposition of detritus to the deep-sea floor and its subsequent resuspension. *Deep-Sea Res.* **32**: 885-897.

Lampitt, RS & Antia, AN. 1997. Particle flux in deep-seas: regional characteristics and temporal variability. *Deep-Sea Res. I* **44**: 1377-1403.

Lampitt, RS; Billett, DSM & Rice, AL. 1986. Biomass of the invertebrate megabenthos from 500 to 4100 m in the northeast Atlantic Ocean. *Mar. Biol.* **93**: 69-81.

Lampitt, RS; Hillier, WR & Challenor, PG. 1993*a*. Seasonal and diel variation in the open ocean concentration of marine snow aggregates. *Nature* **362**: 737-739.

Lampitt, RS; Wishner, KF; Turley, CM & Angel, MV. 1993*b*. Marine snow studies in the Northeast Atlantic Ocean: distribution, composition and role as a food source for migrating plankton. *Mar. Biol.* **116**: 689-702.

Laubier, L & Monniot, C. 1985. *Peuplements profounds du Golfe de Gascogne campagnes BIOGAS*. IFREMER, Brest. 629 pp.

Laubier, L & Sibuet, M. 1979. Ecology of the benthic communities of the deep North East Atlantic. *Ambio Spec. Rep.* (6): 37-42.

Le Danois, E. 1948. *Les profondeurs de la mer*. Payot, Paris.

Lee, A & Ellett, DJ. 1965. On the contribution of overflow water from the Norwegian Sea to the hydrographic structure of the North Atlantic Ocean. *Deep-Sea Res.* **12**: 129-142.

Lee, C; Wakeham, SG & Hedges, JI. 1988. The measurement of oceanic particles flux - are 'swimmers' a problem? *Oceanography* **1**: 34-36.

Lightfoot, RH; Tyler, PA & Gage, JD. 1979. Seasonal reproduction in deep-sea bivalves and brittlestars. *Deep-Sea Res. I* **26**: 967-973.

Linck, JH. 1733. *De Stellis Marinis, xxiv*. Lipsiae. 107 pp.

Linnaeus, C. 1758. *Systema Naturae*. Ed. 10. Holmiae. 824 pp.

Littlewood, DTJ & Smith, AB. 1995. A combined morphological and molecular phylogeny for sea urchins (Echinoidea: Echinodermata). *Phil. Trans. R. Soc. Lond. B* **347**: 213-234.

Littlewood, DTJ; Smith, AB; Clough, KA & Emson, RH. 1997. The interrelationships of the echinoderm classes: morphological and molecular evidence. *Biol. J. Linn. Soc.* **61**: 409-438.

Lochte, K; Ducklow, HW; Fasham, MJR & Stienen, C. 1993. Plankton succession and carbon cycling at 47°N 20°W during the JGOFS North Atlantic Bloom Experiment. *Deep-Sea Res. II* **40**: 91-114.

Lønning, S & Wennerberg, C. 1963. Biometric studies of echinoderm eggs. *Sarsia* **11**: 25-27.

Lonsdale, P & Hollister, CD. 1979. A near-bottom traverse of Rockall Trough: hydrographic and geologic inferences. *Oceanol. Acta* **2**: 91-105.

Loosanoff, VL. 1964. Variations in time and intensity of settling of the starfish, *Asterias forbesi*, in Long Island Sound during a twenty-five-year period. *Biol. Bull.* **126**: 423-439.

Lovén, S. 1874. Études sur les Échinoidées. *Kongl. Svensk. Vet. -Akad. Handl.* **11**(7): 1-91.

Lucas, JS. 1982. Quantitative studies of feeding and nutrition during larval development of the coral reef asteroid *Acanthaster planci* (L.). *J. Exp. Mar. Biol. Ecol.* **65**: 173-193.

Ludwig, H. 1899. Jugendformen von Ophiuren. *Sber. Preuss. Akad. Wiss.* **14** (1): 210-235.

Lutz, RA. 1988. Dispersal of organisms at deep-sea hydrothermal vents: a review. *Oceanologica Acta, Special Volume*, n° 8. p. 23-29.

Lutz, RA; Fritz, LW & Cerrato, RM. 1988. A comparison of bivalve (*Calyptogena magnifica*) growth at two deep-sea hydrothermal vents in the eastern Pacific. *Deep-Sea Res.* **35**: 1793-1810.

Lutz, RA; Jablonski, D & Turner, RD. 1984. Larval development and dispersal at deep-sea hydrothermal vents. *Science* **226**: 1451-1454.

Lutz, RA; Jablonsky, D; Rhoads, DC & Turner, RD. 1980. Larval dispersal of a deep-sea hydrothermal vent bivalve from the Galapagos Rift. *Mar. Biol.* **57**: 127-133.

Lyman, T. 1882. Report on the Ophiuroidea. *Rep. Sci. Res. Voy. H.M.S. Challenger 1873-1876, Zool.* **5**: 1-387.

MacBride, EW. 1903. The development of *Echinus esculentus*, together with some points in the development of *E. miliaris* and *E. acutus*. *Phil. Trans. R. Soc. Lond. B* **195**: 285-327.

MacBride, EW. 1914. The development of *Echinocardium cordatum*. Part I. The external features of the development. *Q. J. Mic. Sci.* **59**: 471-486.

Madsen, FJ. 1961. The Porcellanasteridae. A monograph revision of an abyssal group of sea-stars. *Galathea Rep.* **4**: 33-174.

Madsen, FJ. 1981. Records of a porcellanasterid, *Styrachaster elongatus* (Echinodermata: Asteroidea), from the Caribbean, with remarks on growth and notes on some other species of the genus. *Steenstrupia* **7**: 309-319.

Mahaut, ML; Sibuet, M & Shirayama, Y. 1995. Weight-dependent respiration rates in deep-sea organisms. *Deep-Sea Res.* **42**: 1575-1582.

Manahan, DT; Davis, JP & Stephens, GC. 1983. Bacteria-free sea urchin larvae: selective uptake of neutral amino acids from seawater. *Science* **220**: 204-206.

Marsland, DA. 1938. The effects of high hydrostatic pressure upon cell division in *Arbacia* eggs. *J. Cell. Comp. Physiol.* **12**: 57-70.

Marsland, DA. 1950. The mechanisms of cell division: temperature-pressure experiments on the cleaving eggs of *Arbacia punctulata*. *J. Cell. Comp. Physiol.* **36**: 205-227.

Mauritzen, C. 1996. Production of dense overflow waters feeding the North Atlantic across the Greenland-Scotland Ridge. Part 1: Evidence for a revised circulation scheme. *Deep-Sea Res. I* **43**: 769-806.

McCartney, MS & Talley, LD. 1982. The Subpolar Mode Water of the North Atlantic Ocean. *J. Phys. Oceanog.* **12**: 1169-1188.

McEdward, LR. 1992. Morphology and development of a unique type of pelagic larva in the starfish *Pteraster tesselatus* (Echinodermata: Asteroidea). *Biol. Bull.* **182**: 177-187.

McHugh, D. 1989. Population structure and reproductive biology of two sympatric hydrothermal vent polychaetes, *Paralvinella pandorae* and *P. palmiformis*. *Mar. Biol.* **103**: 95-106.

McHugh, D & Tunnicliffe, V. 1994. Ecology and reproductive biology of the hydrothermal vent polychaete *Amphysamytha galapagensis* (Ampharetidae). *Mar. Ecol. Prog. Ser.* **106**: 111-120.

McKinney, ML. 1988. Roles of allometry and ecology in echinoid evolution. *In*: Paul, CRC & Smith, AB (eds.). *Echinoderm phylogeny and evolutionary biology*. Clarendon Press, Oxford. p. 165-173.

McKinney, ML & Gittleman, JL. 1995. Ontogeny and phylogeny: tinkering with covariation in life history, morphology, and behaviour. *In*: McNamara, KJ (ed.). *Evolutionary change and heterochrony*. John Wiley & Sons, Chichester. p. 21-47.

McKinney, ML & McNamara, KJ. 1991. *Heterochrony: the evolution of ontogeny*. Plenum Press, New York.

McNamara, KJ. 1982. Heterochrony and phylogenetic trends. *Paleobiology* **8**: 130-142.

McNamara, KJ. 1986. A guide to the nomenclature of heterochrony. *J. Paleont.* **60**: 4-13.

McNamara, KJ. 1987. Plate translocation in spatangoid echinoids: its morphological, functional and phylogenetic significance. *Paleobiology* **13**: 312-325.

McNamara, KJ. 1988. Heterochrony and the evolution of echinoids. *In*: Paul, CRC & Smith, AB (eds.). *Echinoderm phylogeny and evolutionary biology*. Clarendon Press, Oxford. p. 149-163.

McPherson, 1968. Contributions to the biology of the sea urchin *Eucidaris tribuloides*. *Bull. Mar. Sci.* **18**: 408-443.

Medeiros-Bergen, DE. 1996. On the stereom microstructure of ophiuroid teeth. Ophelia **45**: 211-222.

Medeiros-Bergen, DE; Olson, RR; Conroy, JA & Kocher, TD. 1995. Distribution of holothurian larvae determined with species-specific genetic probes. *Limnol. Oceanogr.* **40**: 1225-1235.

Metz, EC; Yanagimachi, H & Palumbi, SR. 1991. Gamete compatibility and reproductive isolation of closely related Indo-Pacific sea urchins, genus *Echinometra*. *In*: Yanagisawa; Yasumasu; Oguro; Suzuki & Motokawa (eds.). *Biology of Echinodermata*. Balkema, Rotterdam. p. 131-137.

Michaels, AF; Silver, MW; Gowing, MM & Knauer, GA. 1990. Cryptic zooplankton "swimmers" in the upper ocean sediment traps. *Deep-Sea Res.* **37**: 1285-1296.

Mileikovsky, SA. 1961. Character and nature of deep-water populations of eurybathic benthic forms of invertebrates with pelagic larvae taking as an example the Polychaeta *Euphrosyne borealis* Oersted 1843 from the North Atlantic. *Okeanologiya* **1**: 679-687.

Mileikovsky, SA. 1968. Some common features in the drift of pelagic larvae and juvenile stages of bottom invertebrates with marine currents in temperate regions. *Sarsia* **34**: 209-216.

Mileikovsky, SA. 1971. Types of larval development in marine bottom invertebrates, their distribution and ecological significance: a re-evaluation. *Mar. Biol.* **10**: 193-213.

Millar, RH. 1971. The biology of ascidians. *Adv. Mar. Biol.* **9**: 1-100.

Miller, KM; Jones, P & Roughgarden, J. 1991. Monoclonal antibodies as species-specific probes in oceanographic research: Examples with intertidal barnacle larvae. *Mol. Mar. Biol. Biotechnol.* **1**: 35-47.

Mills, EL. 1983. Problems of deep-sea biology: a historical perspective. *In*: Rowe, GT (ed.). *Deep-sea biology*. The Sea. Vol. 8. John Wiley & Sons, New York. p. 1-79.

Moore, HB. 1935. A comparison of the biology of *Echinus esculentus* in different habitats. Part II. *J. Mar. Biol. Ass. U.K.* **20**: 109-128.

Mortensen, T. 1901. Die Echinodermen-larven. *K. Brandt's Nordisches Plankton (Kiel & Leipzig) No 9*: 1-30.

Mortensen, T. 1903. Echinoidea (Part 1). *Dan. Ingolf-Exped.* **4**(1): 1-193.

Mortensen, T. 1907. Echinoidea (Part 2). *Dan. Ingolf-Exped.* **4**(2): 1-200.

Mortensen, T. 1910. The Echinoidea of the Swedish South-polar expedition. *Wissensch. Ergebn. Schwed. Südpolar Exped. 1901-1903* **6**(4): 1-114.

Mortensen, T. 1912. Über *Asteronyx loveni. M. Tr. Zeits f. w. Zool.* **101**:264-289.

Mortensen, T. 1913. On the development of some British echinoderms. *J. Mar. Biol. Ass. U.K.* **10**: 1-18.

Mortensen, T. 1920. Notes on the development and the larval forms of some Scandinavian echinoderms. *Vidensk. Medd. Dansk natur. Foren. Kjøbenhavn* **71**: 133-160.

Mortensen, T. 1921. Studies of the development and larval forms of echinoderms. *G.E.C. Gad., Copenhagen*. p. 1-261.

Mortensen, T. 1927*a*. *Handbook of the echinoderms of the British Isles*. Oxford University Press, London. 471 pp.

Mortensen, T. 1927*b*. On the postlarval development of some cidaroids. *Kgl. Dan. Vidensk. Selsk. Sber. Naturvid. Math. Ser. 8* **11**(5): 368-387.

Mortensen, T. 1928-51. *A monograph of the Echinoidea*. C.A. Reitzel, Copenhagen. 5 Vols.

Mortensen, T. 1933. Echinoderms of South Africa (Asteroidea and Ophiuroidea). *Vidensk. Medd. Dansk natur. Foren. Kjøbenhavn.* **93**: 215-400.

Mortensen, T. 1936. Echinoidea and Ophiuroidea. '*Discovery' Rep.* **12**: 199-348.

Mortensen, T. 1937. Contributions to the study of the development and larval forms of echinoderms III. *Kgl. Dan. Vidensk. Selsk., Skr. Naturvid. Math. Afd. (9)* **7**(1): 1-65.

Mortensen, T. 1938. Contributions to the study of the development and larval forms of echinoderms IV. *Kgl. Dan. Vidensk. Selsk., Skr. Naturvid. Math. Afd. (9)* **7**(3): 1-59.

Mortensen, T. 1943. *A monograph of the Echinoidea. Vol. III(3). Camarodonta. 2. Echinidae, Strongylocentrotidae, Parasaleniidae, Echinometridae*. C.A. Reitzel, Copenhagen. 446 pp.

Muirhead, A; Tyler, PA & Thurston, MH. 1986. Reproductive biology and growth of the genus *Epizoanthus* (Zoanthidea) from the North-East Atlantic. *J. Mar. Biol. Ass. U.K.* **66**: 131-143.

Müller, J. 1854. Über die gattungen de seeigellarven, siebenk abhandlung über die metamorphose der echinodermen. *Abh. Konig. Akad. Wiss. Berlin* **1854**: 1-55.

Mullineaux, LS. 1994. Implications of mesoscale flows for dispersal of deep-sea larvae. *In*: Young, CM & Eckelbarger, KJ (eds.). *Reproduction, larval biology biology and recruitment of deep-sea benthos*. Columbia Univ. Press, New York. p. 201-222.

Mullineaux, LS; Wiebe, PH & Baker, ET. 1995. Larvae of benthic invertebrates in hydrothermal vent plumes over Juan de Fuca Ridge. *Mar. Biol.* **122**: 585-596.

Mullineaux, LS; Kim, SL; Pooley, A & Lutz, RA. 1996. Identification of archaeogastropod larvae from a hydrothermal vent community. *Mar. Biol.* **124**: 551-560.

Muus, K. 1981. Density and growth of juvenile *Amphiura filiformis* (Ophiuroidea) in the Øresund. *Ophelia* **20**: 153-168.

Newton, PP; Lampitt, RS; Jickells, TD; King, P & Boutle, C. 1994. Temporal and spatial variability of biogenic particle fluxes during the JGOFS northeast Atlantic process studies at 47°N, 20°W. *Deep-Sea Res. I* **41**: 1617-1642.

Nichols, D. 1959. Changes in the chalk heart-urchin *Micraster* interpreted in relation to living forms. *Phil. Trans. R. Soc. Lond. B* **242**: 347-437.

Nichols, D & Barker, MF. 1984. Growth of juvenile *Asterias rubens* L. (Echinodermata: Asteroidea) on an intertidal reef in Southwestern Britain. *J. Exp. Mar. Biol. Ecol.* **78**: 157-165.

Nichols, D; Bishop, GM & Sime, AAT. 1985. Reproductive and nutritional periodicities in populations of the European sea-urchin, *Echinus esculentus* (Echinodermata: Echinoidea) from the English Channel. *J. Mar. Biol. Ass. U.K.* **65**: 203-220.

Nørrevang, A; Brattegard, T; Josefson, AB; Sneli, JA & Tendal, OS. 1994. List of Biofar stations. *Sarsia* **79**: 165-180.

Oguro, C; Komatsu, M & Kano, YT. 1976. Development and metamorphosis of the sea-star, *Astropecten scoparius* Valenciennes. *Biol. Bull.* **151**: 560-573.

Ohshima, H. 1921. Notes on the larval skeleton of *Spatangus purpureus*. *Q. J. Mic. Sci.* **65**: 479-492.

Olson, RR. 1985. The consequences of short-distance larval dispersal in a sessile marine invertebrate. *Ecology* **66**: 30-39.

Olson, RR; Cameron, JL & Young, CM. 1993. Larval development (with observations on spawning) of the pencil urchin *Phyllacanthus imperialis*: a new intermediate larval form? *Biol. Bull.* **185**: 77-85.

Onoda, K. 1936. Notes on the development of some Japanese echinoids, with special reference to the structure of the larval body. *Jpn. J. Zool.* **6**: 637-654.

Onoda, K. 1938. Notes on the development of some Japanese echinoids, with special reference to the structure of the larval body. Rep. III. *Jpn. J. Zool.* **8**: 1-13.

Orton, JH. 1920. Sea temperature, breeding, and distribution in marine animals. *J. Mar. Biol. Ass. U.K.* **12**: 339-366.

Orton, JH & Fraser, JH. 1930. Rate of growth of the common starfish, *Asterias rubens*. *Nature* **126**: 567.

Pain, SL; Tyler, PA & Gage, JD. 1982*a*. The reproductive biology of *Hymenaster membranaceus* from the Rockall Trough, North-East Atlantic Ocean, with notes on *H. gennaeus*. *Mar. Biol.* **70**: 41-50.

Pain, SL; Tyler, PA & Gage, JD. 1982*b*. The reproductive biology of the deep-sea asteroids *Benthopecten simplex* (Perrier), *Pectinaster filholi* Perrier and *Pontaster tenuispinus* Düben & Koren (Phanerozonia: Benthopectinidae) from the Rockall Trough. *J. Exp. Mar. Biol. Ecol.* **65**: 195-211.

Palmer, AR & Strathmann, RR. 1981. Scale of dispersal in varying environments and its implications for life histories of marine invertebrates. *Oecologia* **48**: 308-318.

Patent, DH. 1969. The reproductive cycle of *Gorgonocephalus caryi* (Echinodermata: Ophiuroidea). *Biol. Bull.* **136**: 241-252.

Paterson, GLJ. 1985. The deep-sea Ophiuroidea of the North Atlantic Ocean. *Bull. Brit. Mus. Nat. Hist. (Zool.)* **49**: 1-162.

Paterson, GLJ & Lambshead, PJD. 1995. Bathymetric patterns of polychaete diversity in the Rockall Trough, northeast Atlantic. *Deep-Sea Res. I* **42**: 1199-1214.

Paterson, GLJ; Tyler, PA & Gage, JD. 1982. The taxonomy and zoogeography of the genus *Ophiocten* (Echinodermata: Ophiuroidea) in the North Atlantic Ocean. *Bull. Br. Mus. nat. Hist. (Zool.)* **43**: 109-128.

Pearse, JS. 1965. Reproductive periodicities in several contrasting populations of *Odontaster validus* Koehler, a common antarctic asteroid. *Biology of the Antarctic Seas II* **5**: 39-85.

Pearse, JS. 1994. Cold-water echinoderms break "Thorson's Rule". *In*: Young, CM & Eckelbarger, KJ (eds.). *Reproduction, larval biology, and recruitment of deep-sea benthos*. Columbia Univ. Press, New York. p. 26-43.

Pennington, JT. 1985. The ecology of fertilization of echinoid eggs: the consequences of sperm dilution, adult aggregation, and synchronous spawning. *Biol. Bull.* **169**: 417-430.

Piepenburg, D & Schmid, MK. 1997. A photographic survey of the epibenthic megafauna of the Arctic Laptev Sea shelf: distribution, abundance, and estimates of biomass and organic carbon demand. *Mar. Ecol. Prog. Ser.* **147**: 63-75.

Piepenburg, D & von Juterzenka, K. 1994. Abundance, biomass and spatial distribution patterns of brittle stars (Echinodermata: Ophiuroidea) on the Kolbeinsey Ridge north of Iceland. *Polar Biol.* **14**: 185-194.

Prouho, H. 1888. Recherches sur le *Doriocidaris papillata* et quelques autres échinides de la Méditerranée. *Arch. Zool. expér. et génér.* (2) **v. 1888**: 213-380.

Raff, RA. 1987. Constraint, flexibility, and phylogenetic history in the evolution of direct development in sea urchins. *Develop. Biol.* **119**: 6-19.

Rees, CB. 1953. The larvae of the Spatangidae. *J. Mar. Biol. Ass. U.K.* **32**: 477-490.

Rex, MA & Warén, A. 1982. Planktotrophic development in deep-sea prosobranch snails from the Western North Atlantic. *Deep-Sea Res. I* **29**: 171-184.

Rice, AL; Thurston, MH & Bett, BJ. 1994. The IOSDL DEEPSEAS programme: introduction and photographic evidence for the presence and absence of a seasonal input of phytodetritus at contrasting abyssal sites in the northeastern Atlantic. *Deep-Sea Res. I* **41**: 1305-1320.

Rice, AL; Tyler, PA & Paterson, GJL. 1992. The Pennatulid *Kophobelemnon stelliferum* (Cnidaria: Octocorallia) in the Porcupine Seabight (North-East Atlantic Ocean). *J. Mar. Biol. Ass. U.K.* **72**: 417-434.

Rice, AL; Billett, DSM; Thurston, MH & Lampitt, RS. 1991. The Institute of Oceanographic Sciences biology programme in the Porcupine Seabight: background and general introduction. *J. Mar. Biol. Ass. U.K.* **71**: 281-310.

Rice, AL; Billett, DSM; Fry, J; John, AWG; Lampitt, RS; Mantoura, RFC & Morris, RJ. 1986. Seasonal deposition of phytodetritus to the deep-sea floor. *Proc. R. Soc. Edinb.* **88B**: 265-279.

Richardson, MJ; Weatherly, GL & Gardner, WD. 1993. Benthic storms in the Argentine Basin. *Deep-Sea Res. II* **40**: 975-987.

Roberts, DG. 1975. Marine geology of the Rockall Plateau and Trough. *Phil. Trans. R. Soc. Lond. A* **278**: 447-509.

Roberts, DG; Hunter, PM & Laughton, AS. 1979. Bathymetry of the northeast Atlantic: continental margin around the British Isles. *Deep-Sea Res. I* **26**: 417-428.

Rokop, FJ. 1974. Reproductive patterns in the deep-sea benthos. *Science* **186**: 743-745.

Rokop, FJ. 1977. Patterns of reproduction in the deep-sea benthic crustaceans: a re-evaluation. *Deep-Sea Res.* **24**: 683-691.

Rowe, GT (ed.). 1983*a*. *Deep-sea biology*. The sea, Vol. 8. John Wiley & Sons, New York.

Rowe, GT. 1983*b*. Biomass and production of the deep-sea macrobenthos. *In*: Rowe, GT (ed.). *Deep-sea biology*. The sea, Vol. 8. John Wiley & Sons, New York. p. 97-121.

Rowley, RJ. 1990. Newly settled sea urchins in a kelp bed and urchin barren ground: a comparison of growth and mortality. *Mar. Ecol. Prog. Ser.* **62**: 229-240.

Rumrill, SS. 1989. Population size-structure, juvenile growth, and breeding periodicity of the sea star *Asterina miniata* in Barkley Sound, British Columbia. *Mar. Ecol. Prog. Ser.* **56**: 37-47.

Salas, C & Hergueta, E. 1994. Early growth stages and ecology of *Arbaciella elegans* Mortensen (Echinodermata, Echinoidea) in Southern Spain. *P.S.Z.N. I: Mar. Ecol.* **15**: 255-265.

Salonen, K; Sarlava, J; Hakala, I & Viljanen, ML. 1976. The relation of energy and organic carbon in aquatic invertebrates. *Limnol. Oceanog.* **21**: 724-730.

Sanders, HL; Hessler, RR & Hampson, GR. 1965. An introduction to the study of deep-sea benthic faunal assemblages along the Gay Head-Bermuda transect. *Deep-Sea Res.* **12**: 845-867.

Sars, GO. 1875. *I. On some remarkable forms of animal life from the great deeps off the Norwegian coast. II. Researches on the structure and affinities of the genus* Brisinga, *based on the study of a new species,* B. coronata. Christiania: University Thesis. 111 pp.

Scheibling, RE. 1980. Abundance, spatial distribution, and size structure of populations of *Oreaster reticulatus* (Echinodermata: Asteroidea) in seagrass beds. *Mar. Biol.* **57**: 95-105.

Scheltema, RS. 1974. Biological interactions determining larval settlement of marine invertebrates. *Thal. Jugosl.* **10**: 263-296.

Scheltema, RS. 1986. On dispersal and planktonic larvae of benthic invertebrates: an eclectic overview and summary of problems. *Bull. Mar. Sci.* **39**: 290-322.

Scheltema, RS. 1994. Adaptations for reproduction among deep-sea benthic molluscs: an appraisal of the existing evidence. *In*: Young, CM & Eckelbarger, KJ (eds.). *Reproduction, larval biology and recruitment of deep-sea benthos*. Columbia University Press, New York. p. 44-75.

Schoener, A. 1967. Post-larval development of five deep-sea ophiuroids. *Deep-Sea Res.* **14**: 645-660.

Schoener, A. 1968. Evidence for reproductive periodicity in the deep-sea. *Ecology* **49**(1): 81-87.

Schoener, A. 1969. Atlantic ophiuroids: some post-larval forms. *Deep-Sea Res.* **16**: 127-140.

Schoener, A. 1972. Fecundity and possible mode of development of some deep-sea ophiuroids. *Limnol. Oceanogr.* **17**: 193-199.

Schroeder, TE. 1981. Development of a 'primitive' sea urchin (*Eucidaris tribuloides*): irregularities in the hyaline layer, micromeres, and primary mesenchyme. *Biol. Bull.* **161**: 141-151.

Sebens, KP. 1981. Recruitment in a sea anemone population: juvenile substrate becomes adult prey. *Science* **213**: 785-787.

Semenova, TN; Mileikovsky, SA & Nesis, KN. 1964. The morphology, distribution, and seasonal incidence of the ophiura larva *Ophiocten sericeum* (Forbes) S.L. in the North West Atlantic, Norwegian Sea, and Barents Sea plankton. *Okeanologiya* **4**: 669-683.

Sewell, MA & Watson, JC. 1993. A "source" for asteroid larvae?: recruitment of *Pisaster ochraceus*, *Pycnopodia helianthoides* and *Dermasterias imbricata* in Nootka Sound, British Columbia. *Mar. Biol.* **117**: 387-398.

Shearer, C & Lloyd, J. 1913. On methods of producing artificial parthenogenesis in *Echinus esculentus* and rearing of the pathenogenetic plutei through metamorphosis. *Q. J. Mic. Sci.* **58**: 523-551.

Shearer, C; DeMorgan, W & Fuchs, HM. 1914. On the experimental hybridization of echinoids. *Phil. Trans. Roy. Soc. B.* **204**: 255-362, 7 pls.

Shilling, FM & Manahan, DT. 1994. Energy metabolism and amino acid transport during early development of Antarctic and temperate echinoderms. *Biol. Bull.* **187**: 398-407.

Shin, HC & Koh, CH. 1993. Distribution and abundance of ophiuroids on the continental shelf and slope of the East Sea (Southwestern Sea of Japan), Korea. *Mar. Biol.* **115**: 393-399.

Sibuet, M. 1977. Repartition et diversité des Echinodermes (Holothurides - Astérides) en zone profonde dans le Golfe de Gascogne. *Deep-Sea Res.* **24**: 549-563.

Sibuet, M. 1979. Distribution and diversity of asteroids in Atlantic abyssal basins. *Sarsia* **64**: 85-91.

Sibuet, M. 1984. Quantitative distribution of echinoderms (Holothuroidea, Asteroidea, Ophiuroidea, Echinoidea) in relation to organic matter in the sediment, in deep sea basins of the Atlantic Ocean. *In*: Keegan, BF & O'Connor, BDS (eds.). *Proceedings of the fifth international echinoderm conference, Galway*. Balkema, Rotterdam. p. 99-108.

Sibuet, M & Cherbonnier, G. 1972. Description de stades juvéniles de *Plutonaster bifrons* (Wyville Thomson). *C. R. Acad. Sc. Paris* **275**: 2515-2518.

Sibuet, M; Floury, L; Alayse-Danet, AM; Echardour, A; LeMoign, T & Perron, R. 1990. *In situ* experimentation at the water/sediment interface in the deep-sea: 1. Submersible experimental instrumentation developed for sampling and incubation. *Prog. Oceanog.* **24**: 161-167.

Sladen, WP. 1889. The Asteroidea. *Rep. Scient. Res. Voy. Challenger (Zool.)* **30**: 1-935.

Sloan, NA. 1980. Aspects of the feeding biology of asteroids. *Oceanogr. Mar. Biol. Annu. Rev.* **18**: 57-124.

Smith, AB. 1980. Stereom microstructure of the echinoid test. *Spec. Pap. Palaeont.* (25): 1-81.

Smith, AB. 1997. Echinoderm larvae and phylogeny. *Annu. Rev. Ecol. Syst.* **28**: 219-241.

Smith, AB; Littlewood, DTJ & Wray, GA. 1995*a*. Comparing patterns of evolution: larval and adult life history stages and ribosomal RNA of post-Palaeozoic echinoids. *Phil. Trans. R. Soc. Lond. B* **349**: 11-18.

Smith, AB; Paterson, GLJ & Lafay, B. 1995*b*. Ophiuroid phylogeny and higher taxonomy: morphological, molecular and paleontological perspective. *Zool. J. Linn. Soc.* **114**: 213-243.

Smith, KN & Herrnkind, WF. 1992. Predation on early juvenile spiny lobsters *Panulirus argus* (Latreille): influence of size and shelter. *J. Exp. Mar. Biol. Ecol.* **157**: 3-18.

Soltwedel, T; Pffannkuche, O & Thiel, H. 1996. The size structure of deep-sea meiobenthos in the north-eastern Atlantic: Nematoda size spectra in relation to environmental variables. *J. Mar. Biol. Ass. U.K.* **76**: 327-344.

Somero, GN. 1992. Adaptations to high hydrostatic pressure. *Annu. Rev. Physiol.* **54**: 557-577.

Southward, EC. 1988. Development of the gut and segmentation of newly settled stages of *Ridgeia* (Vestimentifera): implications for relationship between Vestimentifera and Pogonophora. *J. Mar. Biol. Ass. U.K.* **68**: 465-487.

Southward, EC & Coates, KA. 1989. Spermatophores and sperm transfer in a vestimentiferan, *Ridgeia piscesae* Jones, 1985 (Pogonophora: Obturata). *Can. J. Zool.* **67**: 2776-2781.

Spencer, WK & Wright, CW. 1966. Asterozoans. *In*: Moore, RC (ed.). *Treatise on invertebrate paleontogy. Vol. 1. Part U. Echinodermata 3*. The Geological Society of America, New York. p. U4-U107.

Stancyk, SE. 1973. Development of *Ophiolepis elegans* (Echinodermata: Ophiuroidea) and its implications in estuarine environment. *Mar. Biol.* **21**: 7-12.

Stoner, DS. 1990. Recruitment of a tropical colonial ascidian: relative importance of pre-settlement vs. post-settlement processes. *Ecology* **71**: 1682-1690.

Strathmann, RR. 1971. The feeding behavior of planktotrophic echinoderm larvae: mechanisms, regulation, and rates of suspension-feeding. *J. Exp. Mar. Biol. Ecol.* **6**: 109-160.

Strathmann, RR. 1974*a*. Introduction to function and adaptation in echinoderm larvae. *Thal. Jugosl.* **10**: 321-339.

Strathmann, RR. 1974*b*. The spread of sibling larvae of sedentary marine invertebrates. *Am. Nat.* **108**: 29-44.

Strathmann, RR. 1978*a*. Length of pelagic period in echinoderms with feeding larvae from the northeast Pacific. *J. Exp. Mar. Biol. Ecol.* **34**: 23-27.

Strathmann, RR. 1978*b*. Larval settlement in echinoderms. *In*: Chia, FS & Rice, ME (eds.). *Settlement and metamorphosis of marine invertebrate larvae.* Elsevier, Amsterdam. p. 235-246.

Strathmann, RR. 1988*a*. Larvae, phylogeny and von Baer's Law. *In*: Paul, CRC & Smith, AB (eds.). *Echinoderm phylogeny and evolutionary biology.* Clarendon Press, Oxford. p. 53-68.

Strathmann, RR. 1988*b*. Functional requirements and evolution of developmental patterns. *In*: Burke, RD; Mladenov, PV; Lambert, P & Parsley, RL (eds.). *Echinoderm biology.* Balkema, Rotterdam. p. 55-61.

Strathmann, RR; Branscomb, ES & Vedder, K. 1981. Fatal errors in set as a cost of dispersal and the influence of intertidal flora on set of barnacles. *Oecologia* **48**: 13-18.

Talley, LD & McCartney, MS. 1982. Distribution and circulation of Labrador Sea Water. *J. Phys. Oceanog.* **12**: 1189-1205.

Théel, H. 1892. On the development of *Echinocyamus pusillus*. *Nova Acta Reg. Soc. Upsala Ser. 3* **15**(6): 1-57.

Théel, H. 1902. Development of *Echinus miliaris* L. *Bih. Svensk. Akad.* **28, IV**(7): 1-11.

Thiel, H; Pffannkuche, O; Schriever, G; Lochte, K; Gooday, AJ; Hemleben, C; Mantoura, RFG; Turley, CM; Patching, JW & Riemann, F. 1988. Phytodetritus on the deep-sea floor in a central oceanic region of the Northeast Atlantic. *Biol. Oceanog.* **6**: 203-239.

Thomson, W. 1874*a*. *The depths of the sea.* MacMillan & Co., London. 527 pp.

Thomson, W. 1874*b*. On the Echinoidea of the 'Porcupine' Deep-sea Dredging-Expeditions. *Phil. Trans. R. Soc. Lond. B* **164**: 719-756.

Thorson, G. 1936. The larval development, growth and metabolism of Arctic marine bottom invertebrates - compared with those of other seas. *Medd. Groenland.* **100** (6): 1-155.

Thorson, G. 1950. Reproductive and larval ecology of marine bottom invertebrates. *Biol. Rev.* **25**: 1-45.

Todd, CD & Doyle, RW. 1981. Reproductive strategies of marine benthic invertebrates: a settlement-timing hypothesis. *Mar. Ecol. Prog. Ser.* **4**: 75-83.

Tunnicliffe, V. 1991. The biology of hydrothermal vents: ecology and evolution. *Oceanogr. Mar. Biol. Ann. Rev.* **29**: 319-407.

Turley, CM; Lochte, K & Lampitt, RS. 1995. Transformations of biogenic particles during sedimentation in the northeastern Atlantic. *Phil Trans. R. Soc. B* **348**: 179-189.

Turner, RD; Lutz, RA & Jablonsky, D. 1985. Modes of molluscan larval development at deep-sea hydrothermal vents. *Bull. Biol. Soc. Was.* **6**: 167-184.

Turner, RL. 1974. Post-metamorphic growth of the arms in Ophiophragmus filograneus (Echinodermata: Ophiuroidea) from Tampa Bay, Florida (USA). *Mar. Biol.* **24**: 273-277.

Turner, RL & Dearborn, JH. 1972. Skeletal morphology of the mud star, *Ctenodiscus crispatus* (Echinodermata: Asteroidea). *J. Morph.* **138**: 239-262.

Turner, RL & Dearborn, JH. 1979. Organic and inorganic composition of pos-metamorphic growth stages of *Ophionotus hexactis* (E.A. Smith) (Echinodermata: Ophiuroidea) during intraovarian incubation. *J. Exp. Mar. Biol. Ecol.* **36**: 41-51.

Turner, RL & Miller, JE. 1988. Pos-metamorphic recruitment and morphology of two sympatric brittlestars. *In*: Burke, RD; Mladenov, PV; Lambert, P & Parsley, RL (eds.). *Echinoderm biology*. Balkema, Rotterdam. p. 493-502.

Tyler, PA. 1977. Seasonal variation and ecology of gametogenesis in the genus *Ophiura* (Ophiuroidea: Echinodermata) from the Bristol Channel. *J. Exp. Mar. Biol. Ecol.* **30**: 185-197.

Tyler, PA. 1988. Seasonality in the deep-sea. *Oceanogr. Mar. Biol. Ann. Rev.* **26**: 227-258.

Tyler, PA. 1995. Conditions for the existence of life at the deep-sea floor: an update. *Oceanogr. Mar. Biol. Annu. Rev.* **33**: 221-244.

Tyler, PA & Billett, DSM. 1987. The reproductive ecology of elasipodid holothurians from the N.E. Atlantic. *Biol. Oceanog.* **5**: 273-296.

Tyler, PA & Fenaux, L. 1994. Cherchez la femme: Is the upper bathyal ophiuroid *Ophiura carnea* the adult of *Ophiopluteus compressus*? *Sarsia* **79**: 45-52.

Tyler, PA & Gage, JD. 1979. Reproductive ecology of deep-sea ophiuroids from the Rockall Trough. *In*: Naylor, E & Hartnoll, RG (eds.). *Cyclic phenomena in marine plants and animals*. Pergamon Press, Oxford. p. 215-222.

Tyler, PA & Gage, JD. 1980. Reproduction and growth of the deep-sea brittlestar *Ophiura ljungmani* (Lyman). *Oceanol. Acta* **3**: 177-185.

Tyler, PA & Gage, JD. 1982*a*. The reproductive biology of *Ophiacantha bidentata* (Echinodermata: Ophiuroidea) from the Rockall Trough. *J. Mar. Biol. Ass. U.K.* **62**: 45-55.

Tyler, PA & Gage, JD. 1982*b*. *Ophiopluteus ramosus*, the larval form of *Ophiocten gracilis* (Echinodermata: Ophiuroidea). *J. Mar. Biol. Ass. U.K.* **62**: 485-486.

Tyler, PA & Gage, JD. 1983. The reproductive biology of *Ypsilothuria talismani* (Holothuroidea: Dendrochirota) from the N.E. Atlantic. *J. Mar. Biol. Ass. U.K.* **63**: 609-616.

Tyler, PA & Gage, JD. 1984*a*. Seasonal reproduction of *Echinus affinis* (Echinodermata: Echinoidea) in the Rockall Trough, northeast Atlantic Ocean. *Deep-Sea Res.* **31**: 387-402.

Tyler, PA & Gage, JD. 1984*b*. The reproductive biology of echinothuriid and cidarid sea urchins from the deep-sea (Rockall Trough, North-East Atlantic Ocean). *Mar. Biol.* **80**: 63-74.

Tyler, PA & Lampitt, RS. 1988. Submersible observations of echinoderms at bathyal depths in the N.E. Atlantic. *In*: Burke, RD; Mladenov, PV; Lambert, P & Parsley, RL. (eds.). *Echinoderm biology*. Balkema, Rotterdam. p.431-434.

Tyler, PA & Pain, SL. 1982*a*. The reproductive biology of *Plutonaster bifrons*, *Dytaster insignis* and *Psilaster andromeda* (Asteroidea: Astropectinidae) from the Rockall Trough. *J. Mar. Biol. Ass. U.K.* **62**: 869-887.

Tyler, PA & Pain, SL. 1982*b*. Observations of gametogenesis in the deep-sea asteroids *Paragonaster subtilis* and *Pseudarchaster parelli* (Phanerozonia: Goniasteridae). *Int. J. Invert. Rep.* **5**: 269-272.

Tyler, PA & Young, CM. 1998. Temperature and pressure tolerances in dispersal stages of the genus *Echinus* (Echinodermata: Echinoidea): prerequisites for deep-sea invasion and speciation. *Deep-Sea Res. II* **45**: 253-277.

Tyler, PA & Zibrowius, H. 1992. Submersible observations of the invertebrate fauna on the continental slope southwest of Ireland (NE Atlantic Ocean). *Oceanologica Acta* **15**: 211-226.

Tyler, PA; Billett, DSM & Gage, JD. 1987. The ecology and reproductive biology of *Cherbonniera utriculus* and *Molpadia blakei* from the N.E. Atlantic. *J. Mar. Biol. Ass. U.K.* **67**: 385-397.

Tyler, PA; Billett, DSM & Gage, JD. 1990. Seasonal reproduction in the seastar *Dytaster grandis* from 4000 m in the North-East Atlantic Ocean. *J. Mar. Biol. Ass. U.K.* **70**: 173-180.

Tyler, PA; Campos-Creasey, LS & Giles, LA. 1994*a*. Environmental control of quasi-continuous and seasonal reproduction in deep-sea benthic invertebrates. *In*: Young, CM & Eckelbarger, KJ (eds.). *Reproduction, larval biology and recruitment of deep-sea benthos*. Columbia University Press, New York. p. 158-178.

Tyler, PA; Eckelbarger, K & Billett, DSM. 1994*b*. Reproduction in *Bathyplotes natans* (Holothurioidea: Synallactidae) from bathyal depths in the North-East and Western Atlantic. *J. Mar. Biol. Ass. U.K.* 74: 383-402.

Tyler, PA; Gage, JD & Billett, DSM. 1985*a*. Life-history biology of *Peniagone azorica* and *P. diaphana* (Echinodermata: Holothurioidea) from the North-east Atlantic Ocean. *Mar. Biol.* **89**: 71-81.

Tyler, PA; Gage, JD & Billett, DSM. 1991. Reproduction and recruitment in deep-sea invertebrate populations in the NE Atlantic Ocean: a review of the options. *In:* Colombo, G; Ferrari, I; Ceccherelli, VU & Rossi, R (eds). *Marine eutrophication and population dynamics*. Olsen & Olsen, Denmark. p. 257-262.

Tyler, PA; Muirhead, A & Colman, J. 1985*b*. Observations on continuous reproduction in large deep-sea epibenthos. *J. Mar. Biol. Ass. U.K. Supplement.*

Tyler, PA; Pain, SL & Gage, JD. 1982*a*. The reproductive biology of the deep-sea asteroid *Bathybiaster vexillifer*. *J. Mar. Biol. Ass. U.K.* **62**: 57-69.

Tyler, PA; Pain, SL & Gage, JD. 1982*b*. Gametogenic cycles in deep-sea phanerozoan asteroids from the N.E. Atlantic. *In*: Lawrence, JM (ed.). *Echinoderms: Proceedings of the International Conference, Tampa Bay. Balkema*, Rotterdam. p. 431-434.

Tyler, PA; Young, CM & Serafy, K. 1995*a*. Distribution, diet and reproduction in the genus *Echinus*: Evidence for recent diversification? *In*: Emson, RH; Smith, AB & Campbell, AC (eds.). *Echinoderm research 1995*. Balkema, Rotterdam. p. 29-35.

Tyler, PA; Bronsdon, SK; Young, CM & Rice, AL. 1995*b*. Ecology and gametogenic biology of the genus *Umbellula* (Pennatulacea) in the North Atlantic Ocean. *Int. Revue ges. Hydrobiol.* **80**: 187-199.

Tyler, PA; Gage, JD; Paterson, GJL & Rice, AL. 1993. Dietary constraints on reproductive periodicity in two sympatric deep-sea astropectinid seastars. *Mar. Biol.* **115**: 267-277.

Tyler, PA; Grant, A; Pain, SL & Gage, JD. 1982*c*. Is annual reproduction in deep-sea echinoderms a response to variability in their environment? *Nature* **300**: 1-3.

Tyler, PA; Harvey, R; Giles, LA & Gage, JD. 1992. Reproductive strategies and diet in deep-sea nuculanid protobranchs (Bivalvia: Nuculoidea) from the Rockall Trough. *Mar. Biol.* **114**: 571-580.

Tyler, PA; Muirhead, A; Billett, DSM & Gage, JD. 1985*c*. Reproductive biology of the deep-sea holothurians *Laetmogone violacea* and *Benthogone rosea* (Elasipoda: Holothurioidea). *Mar. Ecol. Prog. Ser.* **23**: 269-277.

Tyler, PA; Muirhead, A; Gage, JD & Billett, DSM. 1984*a*. Gametogenic strategies in deep-sea echinoids and holothurians from the N.E. Atlantic. *In: Proceedings of the fifth International Echinoderm Conference, Galway*. p. 135-140.

Tyler, PA; Pain, SL; Gage, JD & Billett, DSM. 1984*b*. The reproductive biology of deep-sea forcipulate seastars (Asteroidea: Echinodermata) from the N.E. Atlantic Ocean. *J. Mar. Biol. Ass. U.K.* **64**: 587-601.

Tyler, PA; Paterson, GLJ; Sibuet, M; Guille, A; Murton, BJ & Segonzac, M. 1995*c*. A new genus of ophiuroid (Echinodermata: Ophiuroidea) from hydrothermal mounds along the Mid-Atlantic Ridge. *J. Mar. Biol. Ass. U.K.* **75**: 977-986.

Ubish, L von. 1927. Über die symmetrieverhältnisse von larvae und imago bei regulären und irregulären seeigeln. *Zeitscha. f. wissenschaftl. Zool.* 129 Bd., 4 Heft. p. 541-566.

Ursin, E. 1960. A quantitative investigation of the Echinoderm fauna of the Central North Sea. *Meddelelser fra Kommissionen for Danmarks Fiskeri-og Havundersøgelser* **2**: 1-204.

Van Aken, HM & Becker, G. 1996. Hydrography and through-flow in the north-eastern North Atlantic Ocean: the NANSEN project. *Prog. Oceanog.* **38**: 297-346.

Van Dover, CL. 1995. Ecology of Mid-Atlantic Ridge hydrothermal vents. *In*: Parson, LM; Walker, CL & Dixon, DR (eds.). *Hydrothermal vents and processes.* The Geological Society of London Special Publication n° 87. p. 257-294.

Van Dover, CL & Fry, B. 1994. Microorganisms as a food resource at deep-sea hydrothermal vents. *Limnol. Oceanogr.* **39**: 51-57.

Van Dover, CL; Berg, CJ, Jr & Turner, RD. 1988. Recruitment of marine invertebrates to hard substrates at deep-sea hydrothermal vents on the East Pacific Rise and Galapagos spreading center. *Deep-Sea Res. I* **35**: 1833-1849.

Van Dover, CL; Factor, JR; Williams, AB & Berg, CJ, Jr. 1985. Reproductive patterns of decapod crustaceans from hydrothermal vents. *Bull. Biol. Soc. Was.* **6**: 223-227.

Van Praët, M. 1990. Gametogenesis and the reproductive cycle in the deep-sea anemone *Paracalliactis stephensoni* (Cnidaria: Actiniaria). *J. Mar. Biol. Ass. U.K.* **70**: 163-172.

Van Praët, M; Rice, AL & Thurston, MH. 1990. Reproduction in two deep-sea anemones (Actiniaria); *Phelliactis hertwigi* and *P. robusta*. *Prog. Oceanog.* **24**: 207-222.

Van Veldhuizen, HD & Oakes, VJ. 1981. Behavioral responses of seven species of asteroids to the asteroid predator *Solaster dawsoni*. *Oecologia* **48**: 214-220.

Verrill, AE. 1882. Notice of the remarkable marine fauna occupying the outer bank of the southern coast of New England. Nos 3 & 4. *Am. J. Sci.* (3) **23**: 216-225.

Vevers, HG. 1949. The biology of *Asterias rubens* L.: growth and reproduction. *J. Mar. Biol. Ass. U.K.* **28**: 165-187.

Walenkamp, JHC. 1976. The asteroids of the coastal waters of Surinam. *Zool. Verhan.* (147): 1-91.

Warén, A & Bouchet, P. 1993. New records, species, genera and a new family of gastropods from hydrothermal vents and hydrocarbon seeps. *Zool. Scrip.* **22**: 1-90.

Weatherly, GL & Kelley, EA. 1985. Storms and flow reversals at the HEBBLE site (High Energy Benthic Boundary Layer Experiment; Nova Scotian Rise). *Mar. Geol.* **66**: 205-218.

Webb, CM & Tyler, PA. 1985. Post-larval development of the common north-west European brittle stars *Ophiura ophiura*, *O. albida* and *Acrocnida brachiata* (Echinodermata: Ophiuroidea). *Mar. Biol.* **89**: 281-292.

Werner, EE & Gilliam, JF. 1984. The ontogenetic niche and species interactions in size-structured populations. *Annu. Rev. Ecol. Syst.* **15**: 393-425.

Wiebe, PH; Copley, N; Van Dover, CL; Tamse, A & Manrique, F. 1988. Deep-water zooplankton of the Guaymas Basin hydrothermal vent field. *Deep-Sea Res. I* **35**: 985-1013.

Williams, AB & Chace, FA. 1982. A new caridean shrimp of the family Bresiliidae from thermal vents of the Galapagos Rift. *J. Crust. Biol.* **2**: 136-147.

Wilson, GDF & Hessler, RR. 1987. Speciation in the deep-sea. *Annu. Rev. Ecol. Syst.* **18**: 185-207.

Wilson, DP. 1978. Some observations on bipinnariae and juveniles of the starfish genus *Luidia*. *J. Mar. Biol. Ass. U.K.* **58**: 467-478.

Wray, GA. 1995. Causes and consequences of heterochrony in early echinoderm development. *In*: McNamara, KJ (ed.). *Evolutionary change and heterochrony*. John Wiley & Sons, Chichester. p. 197-223.

Wray, GA. 1996. Parallel evolution of nonfeeding larvae in echinoids. *Syst. Biol.* **45**: 308-322.

Yamaguchi, M. 1973. Early life histories of coral reef asteroids, with special reference to *Acanthaster planci* (L.). *In*: Jones, OA & Endean, R (eds.). *Biology and geology of coral reefs*. Vol. 2. Biology 1. Academic Press, New York. p. 369-387.

Yamaguchi, M. 1974. Growth of the juvenile *Acanthaster planci* (L.) in the laboratory. *Pacif. Sci.* **28**: 123-138.

Yamaguchi, M. 1977*a*. Population structure, spawning, and growth of the coral reef asteroid *Linckia laevigata* (Linnaeus). *Pacif. Sci.* **31**: 13-30.

Yamaguchi, M. 1977*b*. Estimating length of the exponential growth phase: growth increment observations of the coral-reef asteroid *Culcita novaguineae*. *Mar. Biol.* **39**: 57-59.

Young, CM. 1991. Episodic recruitment and cohort dominance in echinoid populations at bathyal depths. *In*: Colombo, G *et al.* (eds). *Marine eutrophication and population dynamics.* Olsen & Olsen, Denmark. p. 239-246.

Young, CM. 1994. A tale of two dogmas: the early history of deep-sea reproductive biology. *In*: Young, CM & Eckelbarger, KJ (eds.). *Reproduction, larval biology and recruitment of deep-sea benthos.* Columbia University Press, New York. p. 1-25.

Young, CM & Cameron, JL. 1987. Laboratory and *in situ* flotation rates of lecithotrophic eggs from the bathyal echinoid *Phormosoma placenta. Deep-Sea Res.* **34**: 1629-1639.

Young, CM & Cameron, JL. 1989. Developmental rate as a function of depth in the bathyal echinoid *Linopneustes longispinus. In*: Ryland, JS & Tyler, PA (eds.). *Reproduction, genetics and distribution of marine organisms.* Olsen & Olsen, Fredensborg. p. 225-231.

Young, CM & Eckelbarger, KJ (eds.). 1994. *Reproduction, larval biology, and recruitment of deep-sea benthos.* Columbia Univ. Press, New York. 336 pp.

Young, CM & Tyler, PA. 1993. Embryos of the deep-sea echinoid *Echinus affinis* require high pressure for development. *Limnol. Oceanogr.* **38**: 178-181.

Young, CM; Cameron, JL & Eckelbarger, KJ. 1989. Extended pre-feeding period in the planktotrophic larvae of the bathyal echinoid *Aspidodiadema jacobyi. J. Mar. Biol. Ass. U.K.* **69**: 695-702.

Young, CM; Tyler, PA & Emson, RH. 1995. Embryonic pressure tolerances of bathyal and littoral echinoids from the tropical Atlantic and Pacific Oceans. *In*: Emson, RH; Smith, AB & Campbell, AC (eds.). *Echinoderm Research 1995.* Balkema, Rotterdam. p. 325-331.

Young, CM; Tyler, PA & Fenaux, L. 1997*a*. Potential for deep-sea invasion by Mediterranean shallow water echinoids: pressure and temperature as stage-specific dispersal barriers. *Mar. Ecol. Prog. Ser.* **197**: 197-209.

Young, CM; Tyler, PA & Gage, JD. 1996*a*. Vertical distribution correlates with pressure tolerances of early embryos in the deep-sea asteroid *Plutonaster bifrons. J. Mar. Biol. Ass. U.K.* **76**: 749-757.

Young, CM; Sewell, MA; Tyler, PA & Metaxas, A. 1997*b*. Biogeographic and bathymetric ranges of Atlantic deep-sea echinoderms and ascidians: the role of larval dispersal. *Biodiversity and Conservation* **6**: 1507-1522.

Young, CM; Tyler, PA; Cameron, JL & Rumrill, SG. 1992. Seasonal breeding aggregations in low-density populations of the bathyal echinoid *Stylocidaris lineata. Mar. Biol.* **113**: 603-612.

Young, CM; Vázquez, E; Metaxas, A & Tyler, PA. 1996*b*. Embryology of vestimentiferan tube worms from deep-sea methane/sulphide seeps. *Nature* **381**: 514-516.

Young, CM; Devin, MG; Jaeckle, WB; Ekaratne, SUK & George, SB. 1996*c*. The potential for ontogenetic migration by larvae of bathyal echinoderms. *Oceanologica Acta* **19**: 263-271.

Zal, F; Jollivet, D; Chevaldonné, P & Desbruyères, D. 1995. Reproductive biology and population structure of the deep-sea hydrothermal vent worm *Paralvinella grasslei* (Polychaeta: Alvinellidae) at 13°N on the East Pacific Rise. *Mar. Biol.* **122**: 637-648.

Zann, L; Brodie, J; Berryman, C & Naqasima, M. 1987. Recruitment, ecology, growth and behavior of juvenile *Acanthaster planci* (L.) (Echinodermata: Asteroidea). *Bull. Mar. Sci.* **41**: 561-575.

Zottoli, R. 1983. *Amphisamytha galapagensis*, a new species of Ampharetid polychaete from the vicinity of abyssal hydrothermal vents in the Galapagos Rift, and the role of this species in rift ecosystems. *Proc. Biol. Soc. Was.* **96**: 379-391.

SOUTHAMPTON UNIVERSITY LIBRARY

USER'S DECLARATION

AUTHOR: Sumida, P. Y. G.

TITLE: "Post-larval development in deep-sea echinoderms"

DATE: 1998

I undertake not to reproduce this thesis, or any substantial portion of it, or to quote extensively from it without first obtaining the permission, in writing, of the Librarian of the University of Southampton.

To be signed by each user of this thesis

DATE	SIGNATURE	ADDRESS